Origins of *Pseudomonas cepacia* lipase enantioselectivity towards chiral primary alcohols

by

Alessandra Mezzetti

A thesis submitted to the Faculty of Graduate Studies and Research of McGill University in partial fulfillment of the requirements of the degree of Doctor of Philosophy.

Department of Chemistry
McGill University
Montréal, Québec
Canada

August 2003

Your file Votre référence
ISBN: 0-612-98327-7
Our file Notre référence
ISBN: 0-612-98327-7

...per me la chimica rappresentava una nuvola indefinita di potenze future, che avvolgeva il mio avvenire di nere volute lacerate da bagliori di fuoco, simile a quella che occultava il monte Sinai. Come Mosé, da quella nuvola attendevo la mia legge, l'ordine in me, attorno a me e nel mondo. ... Guardavo gonfiare le gemme in primavera, luccicare la mica nel granito, le mie stesse mani, e dicevo dentro di me: "Capirò anche questo, capirò tutto..."

...for me chemistry represented an indefinite cloud of future potentialities which enveloped my future in black volutes torn by fiery flashes, like those which had hidden Mount Sinai. Like Moses, from that cloud I expected my law, the principle of order in me, around me and in the world. ... I would watch the buds swell in spring, the mica glint in the granite, my own hands, and I would say to myself: "I will understand this, too, I will understand everything..."

Primo Levi, *Il sistema periodico*, 1975.

Abstract

Pseudomonas cepacia lipase (PCL) is a highly enantioselective catalyst in the hydrolysis or formation of esters. It shows high enantioselectivity towards esters of chiral primary alcohols. Several scientists have tried to explain this enantioselectivity *via* modelling studies, however their results are in disagreement.

To explain PCL enantioselectivity towards chiral primary alcohols, we coupled structural studies and modelling of PCL-transition state analogue complexes containing pure enantiomers of chiral primary alcohols as alcohol moieties.

We first elucidate the different enantiospecificity of the enzyme for primary and secondary alcohols showing that primary alcohols do not bind to PCL like secondary alcohols. We then show that PCL enantioselectivity towards 3-methyl-2-phenyl-1-propanol, a chiral primary alcohol without oxygen at the stereocentre, rests on the better hydrogen bond of the fast enantiomer with catalytic histidine and that there are only subtle binding differences between the two alcohol enantiomers within the catalytic pocket of PCL.

Next, we show that PCL enantioselectivity towards chiral primary alcohols having oxygen at the stereocentre depends mainly on the interaction of the oxygen at the stereocentre with PCL residues Leu17 and Thr18, which may favour or disfavour one enantiomer depending on its structural features. This explains why a simple empirical rule cannot be reliably applied to this class of substrates.

We then exploit PCL interfacial activation and the use of a solvent that stabilises the active open form of the enzyme to increase its enantioselectivity towards esters of 2-methyl-3-phenyl-1-propanol and 2-phenoxy-1-propanol from 16 to $\geq$190 and from 17 to 70.

Last, we try to increase the enantioselectivity of *Bacillus thermocatenulatus* lipase (BTL2) towards solketal-*n*-octanoate and some other chiral primary alcohols by structure-guided saturation mutagenesis. However most of the mutants were inactive and we did not find a more enantioselective BTL2 mutant.

Overall, we have shown that lipase enantioselectivity towards chiral primary alcohols is always based on subtle enzyme-substrate interactions, hence the difficulty to

increase lipases enantioselectivity towards these substrates by substrate and protein engineering.

Résumé

La lipase *Pseudomonas cepacia* (LPC) est un catalyseur très sélectif pour l'hydrolyse ou la formation des esters. Elle montre une grande énantiosélectivité vis-à-vis des esters des alcools primaires chiraux. Plusieurs chercheurs ont essayé d'expliquer cette énantiosélectivité avec la modélisation, mais leurs résultats sont en désaccord.

Nous avons utilisé des études structurales et la modélisation moléculaire des complexes LPC-analogues de l'état de transition, contenant les énantiomères d'alcools primaires chiraux comme moities alcooliques, pour expliquer l'énantiosélectivité de la LPC envers les alcools primaires chiraux

Nous avons d'abord démontré que les alcools primaires ne se lient pas à la LPC de la même façon que les alcools secondaires, ce qui explique la différente spécificité de l'enzyme envers les alcools primaires et secondaires chiraux. Nous avons ensuite montré que l'énantiosélectivité de la LPC vis-à-vis le substrat 3-methyl-2-phenyl-1-propanol, un alcool primaire sans oxygène au centre chiral, est basée sur une meilleure liaison hydrogène entre l'oxygène de l'énantiomère favori et l'histidine catalytique. Nous avons également montré qu'il y a seulement de très subtiles différences entre les liaisons des deux alcools énantiomères avec le site actif de l'enzyme.

Nous avons montré que l'énantiosélectivité de la LPC envers les alcools primaires ayant un oxygène au centre chiral dépend surtout de l'interaction entre l'oxygène au centre chiral et les résidus Leu17 et Thr18 de la LPC. Ces derniers peuvent favoriser ou non un énantiomère selon ses caractéristiques structurales. Ça explique pourquoi on ne peut pas appliquer une règle empirique très simple à cette classe de composés.

Nous avons aussi exploité l'activation de la LPC en présence d'interfaces organiques et nous avons utilisé un solvant qui stabilise la forme ouverte et active de l'enzyme pour augmenter son énantiosélectivité envers les esters de 2-methyl-3-phenyl-1-propanol de 16 à ≥190 et de 2-phenoxy-1-propanol de 17 à 70.

Nous avons également essayé d'augmenter l'énantiosélectivité de la lipase issue du *Bacillus thermocatenulatus* (LBT2) vis-à-vis solketal-*n*-octanoate et quelques autres alcools primaires chiraux avec la mutagenèse par saturation. Néanmoins la plupart des mutants étaient inactifs et nous n'avons pas identifié un mutant plus énantiosélectif que la LBT2.

En conclusion, nous avons montré que l'énantiosélectivité des lipases envers les alcools primaires chiraux est toujours basée sur des interactions très subtiles entre l'enzyme et le substrat, d'où la difficulté d'augmenter l'énantiosélectivité des lipases envers ces composées, que ce soit par la modification du substrat ou de la protéine elle-même.

Acknowledgements

There are many people I wish to thank for their help during the past five years. First of all, I wish to express my gratitude to my supervisor, Professor Romas J. Kazlauskas, for his support and encouragement during all these years. I am also grateful to Professor Karl Hult for his guidance during the three months I spent in his beautiful laboratory at the Royal Institute of Technology (KTH) in Stockholm, Sweden and to Johanna C. Rotticci-Mulder for showing me my way around in molecular biology. I am especially indebted to Professor Michael A. Whitehead and to Cécile Malardier-Jugroot for their irreplaceable help in the modelling parts of Chapters 2 and 3 and their constant optimism. I also wish to thank Felaniaina Rakotodradani for very interesting discussions on computational chemistry. Special thanks to Dr. Joseph Schrag of the Biotechnology Research Institute for his hard work on the crystallography part of this thesis. I am also indebted to Mr. Nadim Saadé for obtaining the mass spectra of the compounds I synthesised and to Dr. Fred Morin for his help with the JEOL. Many thanks to Prof. Karine Auclair for proofreading and commenting on this work. In addition, I am grateful to FCAR (Les Fonds Québécois sur la Nature et les Technologies) for financial support.

I am as well indebted to Anna, Feli and Michel for their sincere friendship and their support in the most difficult moments of the past few years. To my lab mates, past and present, especially Lana, Christine, Arnaud, Ebru, Agneta, Eniko, Vladimir, Chris, Paul, Jeremy, Krista and Tobie, thanks, it has been fun!

Last, I am grateful to my parents, for their support during all these years and to André, for making me believe that this was possible.

Thesis Formatting

The following text, concerning the inclusion of manuscripts in a thesis, is reproduced from the "Guidelines for Thesis Preparation".

"As an alternative to the traditional thesis format, the dissertation can consist of a collection of papers of which the student is an author or co-author. These papers must have a cohesive, unitary character making them a report of a single program of research. The structure for the manuscript-based thesis must conform to the following:

1. Candidates have the option of including, as part of the thesis, the text of one or more papers submitted, or to be submitted, for publication, or the clearly duplicated text (not the reprints) of one or more published papers. These texts must conform to the "Guidelines for Thesis Preparation" with respect to font size, line spacing and margin sizes and must be bound together as an integral part of the thesis. (Reprints of published papers can be included in the appendices at the end of the thesis.)

2. The thesis must be more than a collection of manuscripts. All components must be integrated into a cohesive unit with a logical progression from one chapter to the next. In order to ensure that the thesis has continuity, connecting texts that provide logical bridges preceding and following each manuscript are mandatory.

3. The thesis must conform to all other requirements of the "Guidelines for Thesis Preparation" in addition to the manuscripts.

The thesis must include the following:

1. a table of contents;
2. a brief abstract in both English and French;
3. an introduction which clearly states the rational and objectives of the research;
4. a comprehensive review of the literature (in addition to that covered in the introduction to each paper);
5. a final conclusion and summary;

6. a thorough bibliography;
7. appendix containing an ethics certificate in the case of research involving human or animal subjects, microorganisms, living cells, other biohazards and/or radioactive material.

4. As manuscripts for publication are frequently very concise documents, where appropriate, additional material must be provided (e.g., in appendices) in sufficient detail to allow a clear and precise judgement to be made of the importance and originality of the research reported in the thesis.

5. In general, when co-authored papers are included in a thesis the candidate must have made a substantial contribution to all papers included in the thesis. In addition, the candidate is required to make an explicit statement in the thesis as to who contributed to such work and to what extent. This statement should appear in a single section entitled "Contributions of Authors" as a preface to the thesis. The supervisor must attest to the accuracy of this statement at the doctoral oral defence. Since the task of the examiners is made more difficult in these cases, it is in the candidate's interest to clearly specify the responsibilities of all the authors of the co-authored papers.

6. When previously published copyright material is presented in a thesis, the candidate must include signed waivers from the publishers and submit these to the Graduate and Postdoctoral Studies Office with the final deposition, if not submitted previously. The candidate must also include signed waivers from any co-authors of unpublished manuscripts.

7. Irrespective of the internal and external examiners reports, if the oral defence committee feels that the thesis has major omissions with regard to the above guidelines, the candidate may be required to resubmit an amended version of the thesis.

8. In no case can a co-author of any component of such a thesis serve as an external examiner for that thesis."

Contribution of authors

This thesis comprises one introduction and four drafts. The four drafts (Chapters 2 to 4) will be submitted for publication shortly. All the work described in these manuscripts, apart from the study of PCL interfacial activation described at the beginning of Chapter 4, has been carried out as part of my research for the degree of Doctor of Philosophy.

Although these manuscripts have co-authors, I have been the first author in all of them. I wrote the manuscripts in their entirety under the supervision of Professor Romas J. Kazlauskas, apart from parts of Chapter 4, which he wrote. Other co-authors did not write the manuscripts but proofread them.

Co-authorship of manuscripts

Professor Romas J. Kazlauskas, supervisor throughout my doctoral degree, is a co-author for each manuscript.

Chapters 2 and 3: Dr. Chang Seong Cheong first synthesised the inhibitors and prepared pure enantiomers of two of the three alcohols used. Dr. Joseph D. Schrag crystallised all the protein-inhibitor complexes, collected diffraction data and solved the structures. Dr. Mirek Cygler helped in the interpretation of the structures. Mrs. Cécile Maladier-Jugroot helped with the modelling and Prof. Michael A. Whitehead helped interpreting the modelling results. I synthesised the inhibitors, determined kinetic constants, interpreted the crystal structures, performed the modelling and interpreted the results.

Chapter 4: Mr. Curtis Keith studied PCL interfacial activation and Prof. Romas J. Kazlauskas wrote the relative parts of the chapter. I carried out the syntheses of the substrates, the kinetic resolutions, the characterisation of starting materials and products and the determination of the enantioselectivity.

Chapter 5: Dr. Johanna C. Rotticci-Mulder helped design the histidine tag of the BTL2 gene and optimise the production of BTL2. Prof. Karl Hult supervised this first part of the research. Miss Agneta Eriksson screened BTL2 mutants towards three substrates. Prof. Romas J. Kazlauskas performed the PCL-BTL2 alignment used for generating the

first homology-modelled structure of BTL2. I carried out all the experiments for his-tagging the BTL2 gene and for the optimisation of the lipase production. I chose the positions to be mutated and I performed the saturation mutagenesis, screened the mutants libraries towards solketal-*n*-octanoate and the double mutants towards solketal-*n*-octanoate and two other substrates that I synthesised.

Table of contents

Glossary of symbols and abbreviations

α	separation factor
ACN	Acetonitrile
AchE	acetylcoline esterase
AL	*Achromobacter* sp. lipase
Ala	alanine
AMBER	Assisted Model Building with Energy Refinement
AOP	*Aspergillus orizae* proteinase
Asp	aspartic acid
BES	*N,N*-bis[2-hydroxyethyl]-2-aminoethanesulphnic acid
bp	base pair
BTL2	*Bacillus thermocatenulatus* lipase 2
c	conversion
C	Celsius
CAL-B	*Candida antarctica* lipase B
CE	cholesterol esterase
CEase	pancreatic cholesterol esterase
CI	chemical ionisation
CPW	carboxypeptidase II
CRL	*Candida rugosa* lipase
CVL	*Chromobacterium viscosum* lipase
Cys	cysteine
d	doublet (NMR)
D	dextrorotatory
δ	chemical shift
3D	three-dimensional
Da	Dalton
DHL	dienelactone hydrolase
DIEA	di-isopropyl ethyl amine
ΔG	Gibbs free energy change
ΔH	enthalpy difference
ΔS	entropy difference
ε	extinction coefficient ($M^{-1}cm^{-1}$)
E	enantiomeric ratio
	enzyme
EC	Enzyme Classification
EDTA	ethylendiaminetetraacetic acid
ee	enantiomeric excess
EI	electron ionisation
F	phenylalanine
g	gram
G	Gibbs free energy
	glycine
GC	gas chromatography
Gln	glutamine

GLP	*Geotrichum candidum* lipase
Glu	glutammic acid
Gly	glycine
h	hour
H	histidine
HAL	haloalkane dehalogenase
His	histidine
HLE	horse-liver esterase
HPLC	high performance liquid chromatography
Hz	hertz
IDH	isocitrate dehydrogenase
IL	ionic liquid
IMAC	immobilisation affinity chromatography
J	coupling constant (in NMR)
k	kilo (10^3)
k'	capacity factor
k_{cat}	enzyme turnover number
K_M	Michaelis-Menten constant
K_S	dissociation constant
K_{TS}	hypothetic dissociation constant
$K_{cat}^{\ddagger}$	pseudoequilibrium constant for enzyme-catalysed reaction
$K_{un}^{\ddagger}$	pseudoequilibrium constant for non-catalysed reaction
l	pathlength
L	large substituent
	liter
L	lævorotatory
Leu	leucine
m	meter
µ	micro (10^{-6})
M	medium substituent
	molar
MD	molecular dynamics
min	minute
MM	molecular mechanics
MO	molecular orbitals
mol	mole(s)
MPa	mega Pascal
MPP	2-methyl-3-phenyl-1-propanol
MPP-C_7	2-methyl-3-phenyl-1-propyl heptanoate
MS	mass spectroscopy
m/z	mass-to-charge ratio
n	nano (10^{-9})
n.a.	not available
n.d.	not determined
NMR	nuclear magnetic resonance
n.r.	no reaction
Nu	nucleophile

OB	OmpA-BTL2
OBH	OmpA-His_8BTL2
O_l	alcohol oxygen
%	percent (parts per hundred)
p	para
P	partition coefficient
	product
	proline
pC	pCYTEXP1
PCL	*Pseudomonas cepacia* lipase
pCOB	pCYTEXP1-OmpA-BTL2
pCOBH	pCYTEXP1-OmpA-His_8BTL2
PCR	Polymerase Chain Reaction
PEG-DH	polyethylene alcohol dehydrogenase
PFE	*Pseudomonas fluorescens* esterase
PFL	*Pseudomonas fluorescens* lipase
pH	negative logarithm of hydrogen ion concentration
Phe	phenylalanine
pKa	negative logarithm of equilibrium constant for association
PGL	*Pseudomonas glumae* lipase
PM3	Parameterisation Method 3
PNP	*para*-nitrophenol
PNPA	*para*-nitrophenyl acetate
POP	2-phenoxy-1-propanol
POP-C_7	2-phenoxy-1-propyl heptanoate
PPE	porcine pancreatic elastase
PPL	porcine pancreatic lipase
q	quartet (in NMR)
Q	product (other than P)
QH-EDH	quinohaemoprotein alcohol dehydrogenase
QM	quantum mechanics
R	alkyl or aryl group
RDL	*Rhizopus delamar* lipase
R_f	retention factor
RML	*Rhizomucor miehei* lipase
r.m.s.	root mean square
ROL	*Rhizopus oryzae* lipase
s	singlet (in NMR)
S	substrate
	serine
SDS-PAGE	Sodium Dodecyl Sulfate PolyAcrylamide Gel Electrophoresis
sec	second
Ser	serine
Sm	small amino acid
SsMcm	systematic search + Monte carlo minimisation
t	triplet (in NMR)
T	threonine

Taq	*Thermus aquaticus*
t-BME	*tert*-butyl methyl ether
T_d1	first tetrahedral intermediate
T_d2	second tetrahedral intermediate
THF	tetrahydrofuran
Thr	threonine
TLC	thin-layer chromatography
T_{rac}	racemic temperature
TRIS	tris(hydroxymethyl)-aminomethane
Tyr	tyrosine
U	unit
U/mg	μmol of ester hydrolyzed per minute per mg protein.
v	initial rate
V	valine
Val	valine
V_{max}	maximum velocity
Y	tyrosine

Chapter 1

Introduction

"A human being should be able to change a diaper, plan an invasion, butcher a hog, con a ship, design a building, write a sonnet, balance accounts, build a wall, set a bone, comfort the dying, take orders, give orders, cooperate, act alone, solve equations, analyze a new problem, pitch manure, program a computer, cook a tasty meal, fight efficiently, die gallantly. Specialization is for insects."

Robert Heinlein, *Time enough for love - Excerpts from the Notebooks of Lazarus Long,* **1973.**

1.1 A chiral world

The term "chiral", as well as "chirality", derives from the Greek "χειρ", which means "hand". An object is chiral if it is non-superimposable to its mirror image. Such objects lack symmetry elements that include reflection that is, mirror planes, inversion centres, or improper rotational axes.

The concept of chirality is directly related to the one of left and right. We live in a society built for right-handed people: many objects and actions are designed for them, like bottle openers, scissors etc. Left-handed people, belonging to the so-called "sinistral minority",[1] find it difficult or at least awkward to use these chiral objects and tools. Many of the objects common to everyday life are chiral. Gloves and shoes are chiral and fit only one hand or foot. The right hand will not fit in a glove tailored for the left one like the right foot will not fit in the left shoe (Figure 1). Screws, bolts, books and even clothes are chiral.

Figure 1 – Shoes are chiral non-superimposable objects.

Sometimes only one enantiomeric (from the Greek "εναντιοσ" = opposite, and "μερε" = part) form is abundant in nature, while the other is rare or even absent. Most snails have a right-handed spiral,[2] but a few are left-handed, such as *Neptunea contraria*,

Pyrolofusus deformis, *Busycon perversum*, *Busycon contrarium* and *Triphora perversa*. There is no apparent advantage in having a right-handed or left-handed shell. Because left-handed shells are very rare, the Hindu god Vishnu is represented holding a ceremonial trumpet made from a left-handed chank shell of the *Turbinellinae* family.

Climbing plants usually twist in a specific direction.[1,3] For example, the hop plants and the woodbine climb in a counter clockwise spiral, while the honeysuckle and beans do so in a clockwise one. This phenomenon has fascinated even poets. William Shakespeare in "A midsummer-night's dream" writes:

> *"Sleep thou, and I will wind thee in my arms. ... So doth the woodbine the sweet honeysuckle gently entwist..."* [4]

In the microscopic world, the DNA double helix is right handed, proteins contain α-amino acids whose configurations are all *L* with a few exceptions, they fold in right-handed α-helices and sugars have all *D* configuration.

Despite our macroscopic asymmetric world, chirality at the microscopic level was discovered only in the 1800s even though scientists in the 1600s believed that the macroscopic appearance of a solid and its microscopic structure were related. A turning point in the discovery of chirality and molecular structure was the discovery of polarized light by Malus in 1808. Jean Baptiste Biot in 1815 observed that not only crystals but also solutions of organic compounds could rotate the plane of polarized light either to the left or to the right, depending on the compound. He called this property "optical activity".[5] This phenomenon for the organic solutions had to depend on their molecular structure.

Practical and economical problems existing at the beginning of the 1800s also contributed to the development of modern stereochemistry. Mr. Kestner, the owner of a tartaric acid factory in the town of Thann in Alsace, a region of France, found another acid in the preparations of tartaric acid, which he called tannic acid. Gay Lussac, who renamed this substance "racemic acid" from the Latin "*racemes*" = raisin, discovered that its elemental composition was identical to tartaric acid. However while tartaric acid deviated the plane of polarised light, Biot observed that racemic acid did not. Around 1844 scientists had realised that both acids had the same crystalline form but they could not explain the differences in optical activity between them.[3] Louis Pasteur in 1848

crystallised a diluted solution of sodium ammonium racemate and noticed that the crystals were hemihedral (only half the number of faces needed to be symmetrical), therefore they did not possess mirror symmetry (Figure 2). He manually separated them and discovered that the ones that were identical to the crystals of sodium ammonium tartrate also deviated the plane of polarised light by the same amount and in the same direction. The others too rotated the plane of polarised light by the same extent, but in the opposite direction. He called "lævorotatory" isomer (*l* or -) (from the Latin word "lævo" = to the left) the isomer that rotated the plane polarized light to the left and "dextrorotatory" (*d* or +)(from the Latin word "dextro" = to the right) the isomer that rotated it to the right.[6,7] Pasteur also proposed that the properties of the two crystalline forms of racemic acid reflected the different symmetry of the molecules that constituted it, and that racemic acid was in fact composed by equal amounts of two mirror-image forms.[8] He was the first to link molecular structure and optical activity.[8,9]

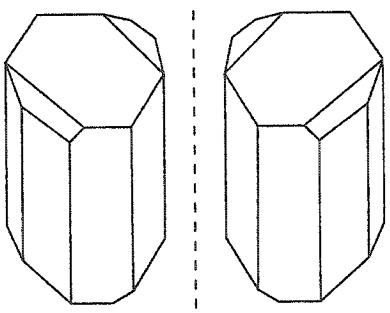

Figure 2 – Drawing of hemihedral crystals of sodium ammonium tartrate. On the left the lævorotatory crystal, on the right the dextrorotatory.

In 1874 two chemists, van't Hoff and Le Bel,[10] independently proposed that the four valences of the carbon atom are not planar but directed in space according to the vertices of a tetrahedron. Thus a compound containing a carbon bearing four different substituents can exist in two non-superimposable forms. Van't Hoff called such carbon atoms "asymmetrisch koolstofatoom" = asymmetric carbon atom.[11] It was the birth of stereochemistry.

1.2 Enantiopure compounds

Enantiopure compounds are mainly (>98%) one enantiomer. Since biological systems are chiral, only one enantiomer (or eutomer) of a racemic drug will be effective while the other enantiomer (or distomer) may not be effective or may even be harmful (Table 1). While (*R*, *R*)-chloramphenicol is an antibacterial agent, its enantiomer has no effect. In other cases enantiomers may have different flavours. (*R*)-carvone has a spearmint flavour while its enantiomer has a caraway aroma (Table 1).

Table 1 - The different effects of the two enantiomers of the same compound.

Compound name	Absolute configuration	Biological effect
asparagine[12,13,14]	*R*	sweet
	S	bitter
carvone[13]	*R*	spearmint flavour
	S	caraway flavour
1-chloropropane-2,3-diol[12]	*R*	toxic
	S	antifertility activity
chloramphenicol[13]	*R, R*	antibacterial
	S, S	inactive
deltamethrin[15,16]	1*R*, 3*R*	potent insecticide
	1*S*, 3*S*	inactive
dextropropoxyphene[17]	2*R*, 3*S*	analgesic
levopropoxyphene	2*S*, 3*R*	antitussive
dopa	*R*	granulocytopenia
(3,4-dihydroxyphenylalanine)[18]	*S*	anti-Parkinson
ethambutol[19]	*S, S*	tuberculostatic
	R, R	optical neuritis/ blindness
2-ethylhexanoic acid[20]	*R*	highly teratogenic
	S	not teratogenic
ketamine[21]	*R*	hallucinogen
	S	anaesthetic
pactobutrazol[22]	2*R*, 3*R*	fungicide
	2*S*, 3*S*	plant growth regulator
penicillamine[23]	*R*	mutagen
	S	antiarthritic
propranolol[13]	*R*	contraceptive
	S	antihypertensive, antiarrhythmic

Some drugs are still administered as racemates even if the distomer shows negative side effects. One such drug is the anaesthetic ketamine, its (*R*) isomer causing

hallucinations.[i,21] Others are sold as single enantiomer drugs, like the non-steroidal anti-inflammatory drug naproxen, its (*R*) isomer being a liver toxin.

The U.S. Food and Drug Administration (FDA) policy statement for the development of new stereoisomeric drugs issued in 1992 and revised in 1997[24] expresses a clear concern regarding the development of racemic mixtures. Manufacturers must measure the activity of each enantiomer *in vivo* at the early stages of drug development. Racemates can only be developed when both enantiomers have similar activity. This policy increased the number of enantiopure drugs. The sales of single-enantiomer drugs amounted to $115 billion (32% of worldwide sales of all final formulation product) in 1999, $133 billion (34%) in 2000, $147 billion (36%) in 2001 and they are forecast to continue rising to $172 billion by 2005.[25]

---

[i]Ketamine is used in minor orthopaedic surgery, minor dental procedures, gynaecological surgery and for a number of examinations under anaesthesia. In the USA, its use as club drug is increasing. Because of its anaesthetic properties, it is considered a "date-rape drug" which can be slipped into someone's drink to provoke unconsciousness (NIDA, National Institute of Drug Abuse, USA).

1.2.1 Synthesis of enantiopure compounds

One of the most used approaches to make enantiopure compounds is the "chiral pool synthesis", where a natural chiral scaffold such as an amino acid, sugar etc. is modified into the final desired chiral product. An example is the synthesis of (2*S*, 4*R*)-4-hydroxyornithine, a non-proteogenic amino acid found in nature, from L-aspartic acid[26] (Scheme 1).

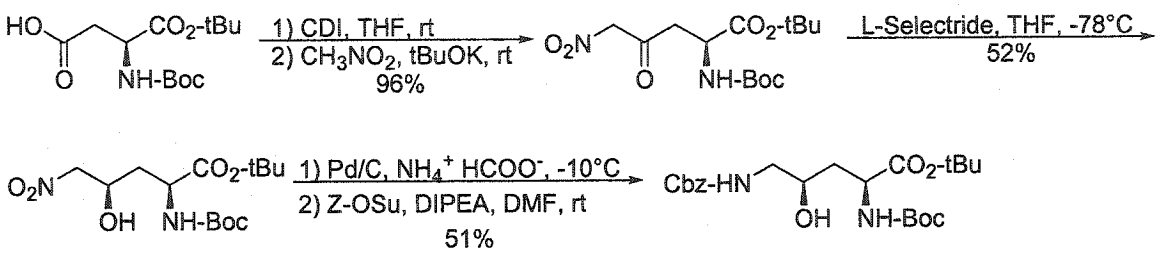

Scheme 1 – Chiral pool synthesis of protected (2*S*, 4*R*)-4-hydroxyornithine (CDI = carbonyl diimidazole, THF = tetrahydrofuran, DIPEA = N,N-diisopropylethylamine, DMF = N,N-dimethylformamide, Z-OSu = Nα-(benzyloxycarbonyloxy)succinimide).

Asymmetric synthesis, another popular approach to the synthesis of enantiopure compounds, involves the transformation of an achiral molecule into a chiral one by means of a catalyst or chiral auxiliary. Isoflavanones, naturally occurring compounds with interesting antifungal and antibacterial activities, are obtained from natural sources as racemates.[27] To study their structure-activity relationships pure enantiomers are needed. Vicario *et al.* prepared isoflavanones by using (*S*, *S*)-(+)-pseudoephedrine as chiral auxiliary (Scheme 2).

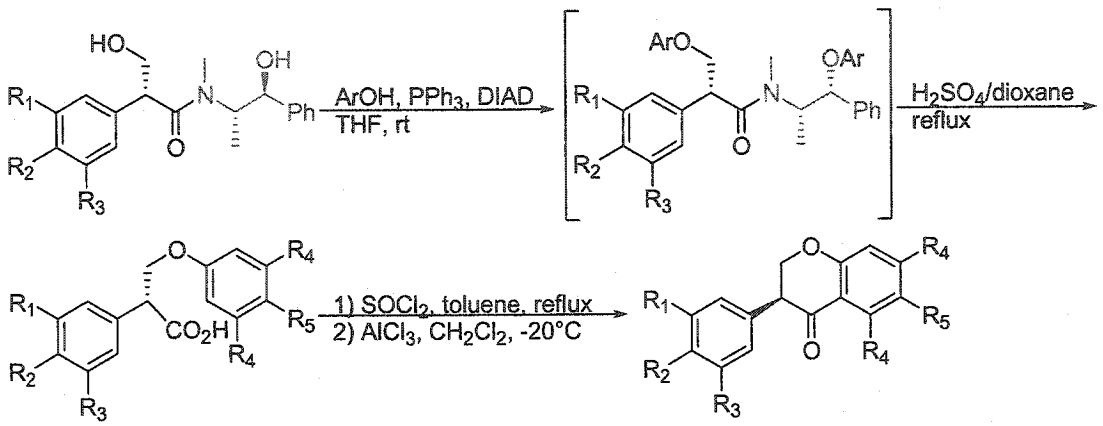

R_1,R_2 = OCH_3, OCH_2O; R_3, R_4, R_5 = H, OCH_3

Scheme 2 – Synthesis of isoflavanones; the chiral auxiliary (*S*, *S*)-(+)-pseudoephedrine is in red (DIAD = diisopropyl azodicarboxylate; THF = tetrahydrofuran, Ar = substituted phenyl containing groups R_4 and R_5).

Another possibility to prepare enantiopure compounds is the resolution of a racemic mixture, where the enantiomers are separated from the mixture. This method dates back to the early days of stereochemistry, when in 1848 Pasteur[6] performed the first resolution of a racemate *via* crystallisation and manual separation of the two different crystalline forms. Other methods employed to resolve racemates are the separation of diastereoisomers[ii] and kinetic resolutions.

Kinetic resolutions occur when one enantiomer reacts faster in a reaction catalysed by a chiral catalyst, i.e. a metal complex or an enzyme that act as resolving agents. Besides the first resolution by crystallisation, Pasteur also performed the first kinetic resolution in 1858[28] when he resolved tartaric acid with *Penicillium glaucum*. He says, in a note relative to *Penicillium glaucum* and to the molecular dissymmetry of natural organic products:

> *"Je dissous dans l'eau du paratartrate acide d'ammoniaque pur et des quantités fort minimes de phosphates; puis je sème dans la liqueur quelques spores de pennicillium glaucum. Ces spores se développent, et reproduisent la plante mère, dont le poids augmente peu à peu d'une*

[ii]Diastereoisomers are stereoisomers not related as mirror images. They have different physical and chemical properties.

manière notable, empruntant sa nourriture à l'oxygène de l'air et aux éléments minéraux et organiques de la solution. En même temps que la plante grandit, l'acide tartrique droit disparaît et l'acide tartrique gauche reste dans la liqueur, d'où il est facile de l'isoler." [29,iii]

Captopril is an antihypertensive agent whose potency depends on the configuration of the mercaptoalkanoyl moiety (red in Scheme 3). Captopril containing the 3-mercapto-(2*S*)-methylpropionic acid moiety is 100 times more potent than captopril containing the (*R*) enantiomer. Kinetic resolution of racemic 3-mercapto-2-methylpropionic acid by lipase PS-30 catalysed hydrolysis yields 3-mercapto-(2*S*)-methylpropionic acid in 95% ee, 24% yield (Scheme 3),[30] which can be used to synthesise captopril.

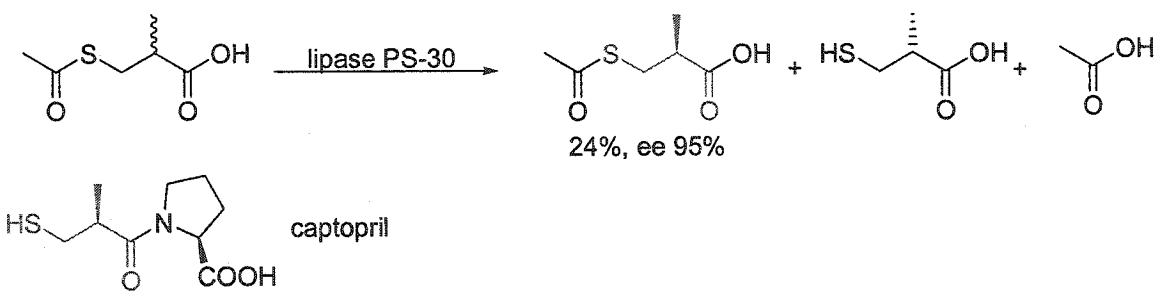

Scheme 3 - Synthesis of captopril side chain

The drawback of kinetic resolutions is the 50% maximum yield of the desired enantiomer. This is often not satisfactory, especially if only one enantiomer is needed. More recent procedures, called dynamic kinetic resolutions, involve on one hand the reaction of only one enantiomer with the chiral catalyst, on the other hand the racemisation of the leftover starting material. This increases the maximum yield to 100% if the racemisation rate is faster than the reaction rate of the fast enantiomer with the catalyst.

[iii]"I dissolve in water some pure ammonium paratartrate and minimal quantities of phosphates; then I seed in the mixture a few spores of *Penicillium glaucum*. These spores grow, replicating themselves, thanks to the oxygen in the air and the mineral and organic elements present in the solution. At the same time the right-handed tartaric acid disappears while the left-handed tartaric acid remains in the solution, from which it is easily separated".

Some researchers have made use of transition metal catalysts to racemise starting materials in dynamic kinetic resolutions. Bäckvall's group[31,32] was the first to couple the ruthenium-catalysed racemisation of secondary alcohols to lipase-catalysed transesterifications to perform dynamic kinetic resolutions. They resolved a number of secondary alcohols with yields ranging from 63% to 88% and ee from 79% to > 99%. For example, they resolved their model substrate, 1-phenylethanol, in 80% yield and ee > 99%, Scheme 4.

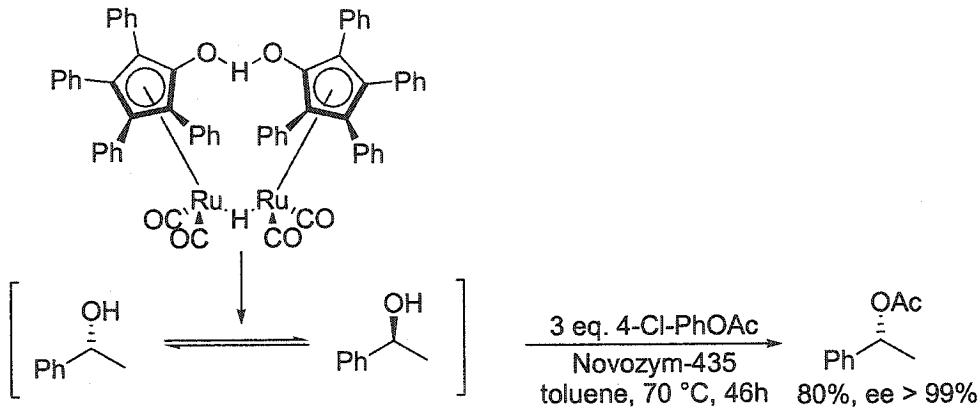

Scheme 4 - Dynamic kinetic resolution of 1-phenylethanol *via* enzyme coupled with a ruthenium catalyst.[31,32] Novozym-435 is an immobilised form of *Candida antarctica* lipase B.

Choi *et al.*[33] recently reported an improvement of the above reaction. They increased the yield of (*S*)-1-phenylethyl acetate from 80% to 97% using a different ruthenium catalyst, aminocyclopentadienyl ruthenium chloride, and vinyl acetate at room temperature.

1.3 Enzymatic kinetic resolutions

Enzymes are widely used in kinetic resolutions. They can be handled like any other chemical, can be very stable, work in organic solvents and accelerate the rate of a reaction, compared to non-enzymatic processes, by a factor of 10^8-10^{10}.[34] Furthermore, the amount of enzyme needed in a kinetic resolution ranges from 10^{-3} to 10^{-4}% mole fraction, while for a chemical catalyst this range is about 0.1 to 1% mole fraction.[34] Also, enzymes usually work under mild conditions (pH 5 to 8, temperatures from 20°C to

40°C), which can minimise problems with the substrate and/or product such as isomerisation, rearrangement, racemisation and decomposition.[34] They can have a large substrate tolerance, accepting also non-natural substrates and they can catalyse a large number of reactions (there is an enzymatic equivalent to almost every organic reaction) (Table 2). Moreover, enzymes are chiral catalysts[iv] that exhibit chemo-, regio-, diastereo- and enantioselectivity.[34]

Table 2 –Enzyme catalysed reactions[34]

Enzyme family	**Reaction**
Hydrolases	Hydrolysis/formation of esters, amides, lactones, lactams, anhydrides, epoxydes, nitriles, glycosides.
Oxydoreductases	Oxydation/reduction of alkanes, alkenes, aromatics, alcohols, aldehydes, ketones, sulfides, sulfoxides.
Lyases	Addition/elimination of water, ammonia and hydrogen cyanide on C=C, C=N and C=O bonds
Ligases	Formation/cleavage of C-O, C-S, C-N, C-C bonds and triphoshate cleavage
Isomerases	Isomerisation
Transferases	Transfer of groups such as aldehydic, ketonic, acyl …

If we consider an enzyme-catalysed reaction like the hydrolysis of an ester, we can describe it in terms of Michaelis-Menten mechanism[35] (equation 1.1):

$$E + S \underset{k_{-1}}{\overset{k_1}{\rightleftharpoons}} ES \xrightarrow{k_2} E + P \qquad (1.1)$$

where E is the enzyme, S the substrate, ES the enzyme-substrate complex, P the product of the reaction and k_1, k_{-1} and k_2 are the kinetic constants that describe the reaction. While during the first, reversible step no chemical changes occur, the second step is irreversible. If the substrate concentration [S] is much higher than that of the enzyme ([S] >> [E]), which is very likely since the enzyme acts as a catalyst, then the rate of change of the concentration of the intermediate ES is much smaller than the one of the reagents. The intermediate is said to be in a *steady-state* and it is possible to write:

[iv]Enzymes building blocks are *L*-amino acids, therefore enzymes are chiral catalysts.

$$\frac{d[ES]}{dt} = k_1[E][S] - k_{-1}[ES] - k_2[ES] = 0 \qquad (1.2)$$

If $k_{-1} >> k_2$, equation (1.2) becomes:

$$\frac{[E][S]}{[ES]} = \frac{k_{-1} + k_2}{k_1} = K_d = K_M \qquad (1.3)$$

where K_d is the dissociation constant of the substrate, in this case ($k_{-1} >> k_2$) equivalent to the Michaelis constant K_M, and the substrate-enzyme complex is known as the *Michaelis complex* in honour of the scientist that first described it. k_2, the first order rate constant that describes the second step of equation (1.1) becomes equivalent to k_{cat}, the turnover number.[v]

The reaction velocity, since the first step occurs with no chemical change and it is assumed to be faster than the second one, can be simplified as:

$$v = k_2[ES] = k_{cat}[ES] \qquad (1.4)$$

At any time during the reaction the enzyme concentration [E], assuming no product inhibition, is given by equation (1.5):

$$[E] = [E_0] - [ES] \qquad (1.5)$$

where E_0 is the initial enzyme concentration. From equation (1.5) and equation (1.3) it follows that:

$$[ES] = \frac{[E_0][S]}{[S] + K_M} \qquad (1.6)$$

---

[v] k_{cat} represents the maximum number of substrate molecules that the enzyme transforms into product per active site per unit of time.

and the reaction velocity can be written as:

$$v = \frac{[E_0][S]k_{cat}}{[S]+K_M} \tag{1.7}$$

Equation (1.7) describes a hyperbola. At low substrate concentration the rate increases linearly with [S] and the velocity can by approximated by:

$$v = \frac{V_{max}[S]}{K_M} \tag{1.8}$$

while at saturating concentrations of substrate the rate tends to an asymptotic value called V_{max} (Figure 3), which is equal to the product of the initial enzyme concentration $[E_0]$ and the turnover number of the enzyme k_{cat}. K_M is the concentration of substrate at half reaction rate (Figure 3).

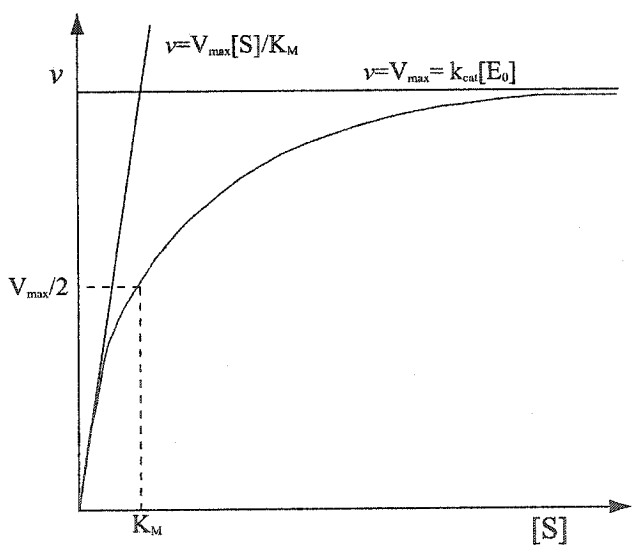

Figure 3 - Plot of reaction rate versus substrate concentration [S].

1.4 Enzyme enantioselectivity E

To express the enantiomeric purity organic chemists typically use the enantiomeric excess (ee), which is calculated from the concentration of both enantiomers as:

$$ee = \frac{|[R]-[S]|}{[R]+[S]} \tag{1.9}$$

where [*R*] is the concentration of the *R* enantiomer and [*S*] is the concentration of the *S* enantiomer. ee_R indicates the enantiomeric excess of the *R* enantiomer and ee_S the enantiomeric excess of the *S* enantiomer.

To describe enzymatic kinetic resolutions, Hein and Neimann[36] introduced the ratio of the enzyme specificity constants (k_{cat}/K_M) for the two enantiomers as a measure of the enzyme selectivity. k_{cat} and K_M are kinetic constants that describe the reaction of each enantiomer with the enzyme. The ratio of the specificity constants, the enantioselectivity E (equation 1.10), describes the preference of the enzyme for one enantiomer.

$$E = \frac{\left(\frac{k_{cat}}{K_M}\right)_R}{\left(\frac{k_{cat}}{K_M}\right)_S} \tag{1.10}$$

This ratio allows comparing the performance of different enzymes in a kinetic resolution and is very often used in biocatalysis.

Equation (1.10) can be derived by considering that, in an enzymatic kinetic resolution, the two enantiomeric substrates compete for the same active site of the enzyme:

$$\begin{aligned} E + R &\underset{}{\overset{(K_M)_R}{\rightleftharpoons}} ER \xrightarrow{(k_{cat})_R} E + P \\ E + S &\underset{}{\overset{(K_M)_S}{\rightleftharpoons}} ES \xrightarrow{(k_{cat})_S} E + Q \end{aligned} \tag{1.11}$$

In this case, by simply considering the initial rate of the reaction that leads to the formation of P and Q, we obtain:

$$v_R = \frac{d[R]}{dt} = (k_{cat})_R[ER] \quad \text{and} \quad v_S = \frac{d[S]}{dt} = (k_{cat})_S[ES] \tag{1.12}$$

Replacing [ER] and [ES] in the above expressions with their expression from equation (1.3):

$$v_R = \left(\frac{k_{cat}}{K_M}\right)_R [E][R] \quad \text{and} \quad v_S = \left(\frac{k_{cat}}{K_M}\right)_S [E][S] \tag{1.13}$$

and from the ratio of the initial rates v_R and v_S, considering equal amounts of the two enantiomers in a racemic mixture, we obtain Equation 1.10.

A more convenient way of measuring the enantioselectivity of an enzyme consists in determining the enantiomeric excess ee of either the product or the substrate at a certain substrate conversion. Chen *et al.*[37] developed formulas that relate the extent of conversion and the enantiomeric purity of reagents or products to the enantiomeric ratio E.

If we write the ratio of the above equations (1.13) and we integrate it, we obtain:

$$\frac{v_R}{v_S} = \left(\frac{k_{cat}}{K_M}\right)_R \left(\frac{K_M}{k_{cat}}\right)_S \frac{[R]}{[S]} \tag{1.14}$$

$$\frac{\ln([R]/[R_0])}{\ln([S]/[S_0])} = \frac{(k_{cat}/K_M)_R}{(k_{cat}/K_M)_S} = E \tag{1.15}$$

Where R_0 and S_0 are the R and S enantiomer at time 0. Expressing the extent of conversion c and the enantiomeric excess of substrates (ee_S) and products (ee_P) as:

$$c = 1 - \frac{[R]+[S]}{[R_0]+[S_0]} \qquad ee_S = \frac{[R]-[S]}{[R]+[S]} \qquad ee_P = \frac{[P]-[Q]}{[P]+[Q]} \tag{1.16}$$

the enantioselectivity E can be rewritten as a logarithmic function of c and ee_S, of c and ee_P or of ee_S and ee_P (equation 1.17):

$$E = \frac{\ln[1-c(1+ee_P)]}{\ln[1-c(1-ee_P)]} = \frac{\ln[(1-c)(1-ee_S)]}{\ln[(1-c)(1+ee_S)]} = \ln\left(\frac{1-ee_S}{1+ee_S/ee_P}\right) \Big/ \ln\left(\frac{1+ee_S}{1+ee_S/ee_P}\right) \tag{1.17}$$

The E values calculated by means of one of the first two forms of equation (1.17) are usually reliable except for very high or very low reaction conversion c, when large errors may be introduced in the manipulation of the samples. In such circumstances the third expression for determining E, devoid of reaction conversion, should be used.[34]

Once the enantioselectivity of an enzyme for the substrate of interest is known, plots of ee% versus c% (Figure 4) are useful to determine which conversion of substrates should be attained for obtaining a desired optical purity of reagents or products.

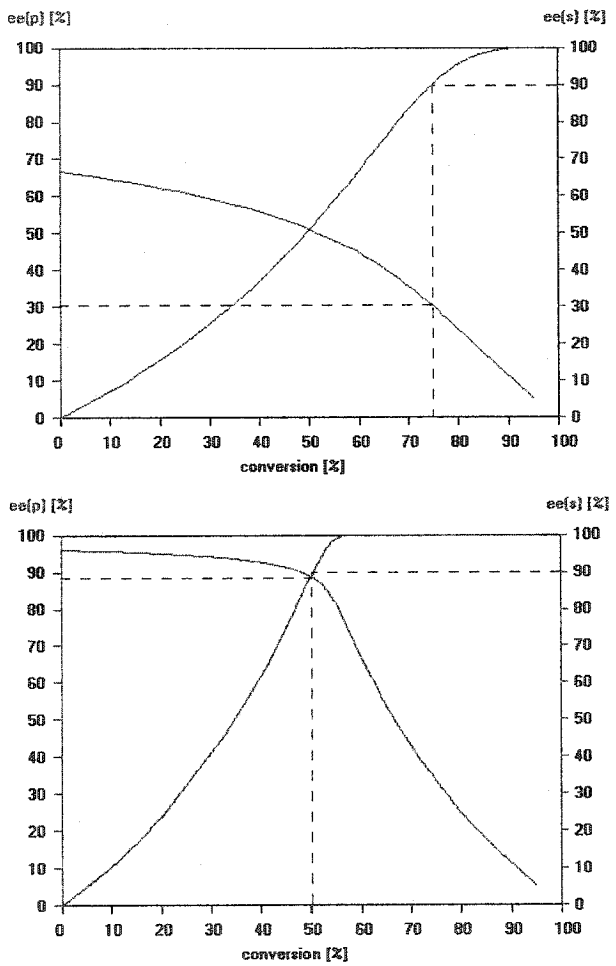

Figure 4 - Dependence of optical purity on conversion. Top: E = 5; bottom: E = 50. Adapted from the program "Enantiomeric Ratio".[vi]

For example, if the enzyme E is 5 to obtain 90% ee_s one has to stop at 75% conversion. In this case ee_p = 30% is obtained. When the enzyme enantioselectivity is 50 it is possible to achieve 90% ee_s at 50% conversion, with ee_p = 88.5%.

[vi] © Doz. Dr. Kurt Faber & AO. Univ. Prof. Dr. Helmut Hönig, Institute of Organic Chemistry, Technical University of Graz, Austria.

The enantioselectivity can also be expressed as the difference in activation energy $\Delta\Delta G^{\ddagger}$ between the two transition states of the two enantiomers during the enzyme-catalysed reaction (equation 1.18)[38]:

$$\Delta\Delta G^{\ddagger} = \Delta G^{\ddagger}_{R} - \Delta G^{\ddagger}_{S} = -RT \ln E \qquad (1.18)$$

Chiral molecules bound to enzymes give rise to diastereoisomeric transition states. The energy of each diastereoisomeric transition state is different. The enzyme-catalysed reaction proceeds *via* the lowest energy path, therefore the favourite enantiomer is the one with the lowest energy transition state (Figure 5).

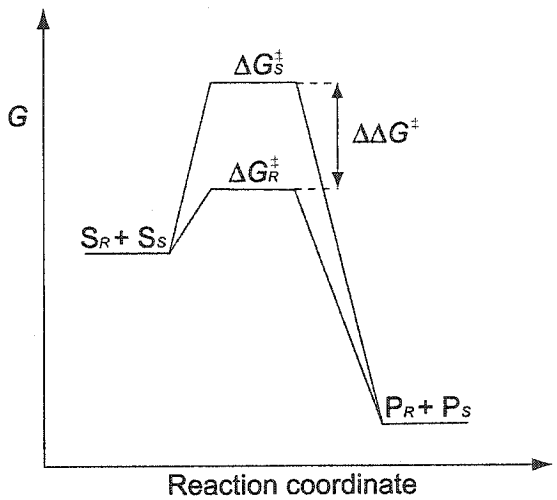

Figure 5 - Energy profile of an enantioselective kinetic resolution. S_R and S_S are the starting material, P_R and P_S are the products. $\Delta G^{\ddagger}_S$ and $\Delta G^{\ddagger}_R$ represent the activation energies for the reaction of the enzyme with the two enantiomers of the substrate. The enantioselectivity originates from the difference in activation energy ($\Delta\Delta G^{\ddagger}$) between the two enantiomeric transition states.

1.5 Lipases

Lipases, triacylglycerol hydrolases (EC 3.1.1.3)[vii], catalyse the hydrolysis of triglycerides into glycerol and fatty acids in many organisms. Triglycerides cannot be

[vii] EC 3.-.-.- represents hydrolases; EC 3.1.-.- represents hydrolases acting on ester bonds; EC 3.1.1.- represents carboxylic ester hydrolases; EC 3.1.1.3 represents triacylglycerol lipases.

directly absorbed into the cells but must first be hydrolysed by lipases into free fatty acids and monoglycerols. Thus triglyceride lipases are essential for transporting fats into cells for storage or for conversion into energy. Lipases are widely distributed in the flora and fauna of our planet, in particular in bacteria, fungi and yeasts. Furthermore they are found in human and pig pancreas and in some plants such as *Ricinus communis* (castor bean) and *Brassica napus* (rapeseed).[39] The most commonly used lipases in biotechnological applications come from microbes, especially *Candida*, *Pseudomonas* and *Rhizopus* species.

Lipases are necessary elements to the food industry. They have been involved in cheese making for millennia. Homer's "Ilias", dating back to earlier than 400 B.C., talks about the use of lamb stomach to make cheese. The typical taste of blue cheeses, mainly due to short-chain fatty acids, was once produced by the action of lipases present in rennet pastes prepared from the stomachs of lambs or calves, which were added during the preparation of the cheeses. Nowadays the dairy industry has replaced the rennet pastes with lipases derived from microorganisms. Lipases are used in baking for "dough conditioning", which gives whiter bread with better organoleptic characteristics. Lipases hydrolyse lipids that are normally contained in wheat flour and bound to gluten. This modifies the lipids-gluten interaction and results in a larger loaf volume and a significantly improved crumb structure. Because the crumb cells obtained with this process are smaller than usual, they give a silkier texture and a whiter colour to the bread.

The fat and oil industry uses lipases to the produce new triglycerides. The position of the fatty acid in the glycerol backbone, its length as well as its degree of insaturation determinine not only the physical properties of the triglyceride, but also its nutritional and sensory value. Lipases are used to change one or more fatty acids with different ones in the glyceride by transesterification. For example *Rhizomucor miehei* lipase (RML) is used to replace palmitic acid of palm oil with stearic acid at positions *sn*-1 and *sn*-3 of the triglyceride, yielding a cocoa butter equivalent.[40]

Lipases have been used for the processing of skin and hides into leather for centuries. Before tanning hides and skins, protein and fat between the collagen fibres must be removed, to render the leather pliable, in a process called "bating". Dog and pigeon droppings were used in this process until the early 1900s, when Otto Röhm

patented the first standardized "bate" containing pancreatic enzymes. While proteases are used in the soaking, bating and hair removal steps, lipases are used in the degreasing step since they hydrolyse fat on the flesh side and inside the skin structure. The use of lipases reduces the need for organic solvents and surfactants, resulting in a more environmentally friendly process.

Lipases are added to detergents as fat removers. Key characteristics of these lipases are: (a) low substrate specificity (they can hydrolyse several types of fats), (b) ability to tolerate harsh conditions such as high pH (10 to 11), (c) capacity to resist to surfactants such as linear alkylbenzene sulfonates and proteases. Such lipases are usually obtained by protein engineering. The first lipase to be employed in a detergent formulation was Lipolase® by Novo Nordisk. It can remove lipstick, frying fats, butter, oil, sauces and stains on collars and cuffs that contain residues of human sebum.[41]

1.5.1 Lipases are α/β hydrolases

Murzin *et al.*[42] have classified proteins taking into account both evolutionary and structural relationships. The SCOP[43] (Structural Classification of Proteins) database groups families (proteins that share a minimum of 30% sequence identity or proteins with less sequence identity but quite similar structure and function), superfamilies (families of proteins that, although sharing low sequence identity, possess structural features that suggest a common origin) and classes (different folds based on the secondary structure elements that they possess). There are five major classes of folds:

- all alpha – mainly α-helices
- all beta – mainly β-sheets
- alpha and beta – interspersed α-helices and β-sheets (α/β)
- alpha plus beta – segregated α-helices and β-sheets
- multi-domain.

Analysis of the known protein three-dimensional structures shows that proteins with a sequence identity greater or equal to 30% always adopt similar tertiary folds. Nevertheless, proteins that share no obvious sequence similarity often adopt similar folds. One such fold is the α/β hydrolase fold (alpha and beta), which is adopted by several lipases with low sequence identity.[44]

Lipases belong to the α/β hydrolases superfamily and to the α/β hydrolase fold, identified by Ollis *et al.*[45] from the comparison of five different enzymes, possessing different characteristics: acetylcholinesterase (AChE), carboxypeptidase II (CPW), dienelactone hydrolase (DHL), *Geotrichum candidum* lipase (GLP) and haloalkane dehalogenase (HAL).

The core of the fold is an almost parallel β sheet. Lipases active site is similar to the one of serine proteases but the order of amino acids differs. The linear sequence is nucleophile-acid-histidine for lipases while it is acid-histidine-nucleophile for subtilisins, nucleophile-histidine-acid in the papain family and histidine-acid-nucleophile in the trypsin family. The nucleophile (Ser or Cys) is part of a highly conserved pentapeptide, Sm-X-Ser-X-Sm (Sm = Gly or Ala, X = any residue) and is located in a sharp turn (Φ usually around 50° to 60°, Ψ usually around -115° to -135°) between strand β5 and helix C, Figure 6. The catalytic acid (Asp or Glu) is situated on a loop that follows strand β7 and catalytic His is at the end of strand β8.

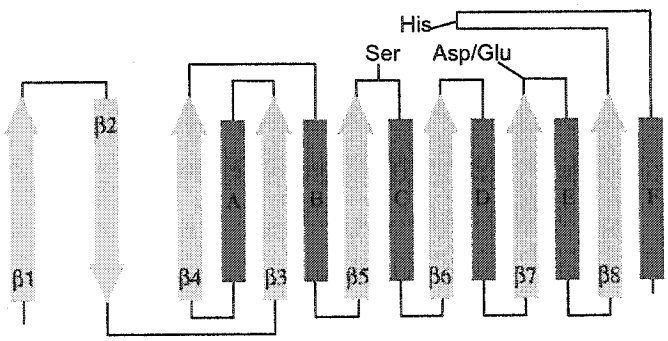

Figure 6 - The typical α/β hydrolase fold.

1.5.2 Interfacial activation in lipases

Most lipases are activated by lipid interfaces. This property, which allows them to handle water-insoluble substrates, distinguishes them from esterases and serine proteases that react only with soluble substrates. While esterase activity depends directly on the substrate concentration and follows normal Michaelis-Menten kinetics, lipases show a modest activity until the substrate concentration is increased beyond its solubility limit in the reaction media. Past this point there is a sharp increase in the lipase activity[46] (Figure 7).

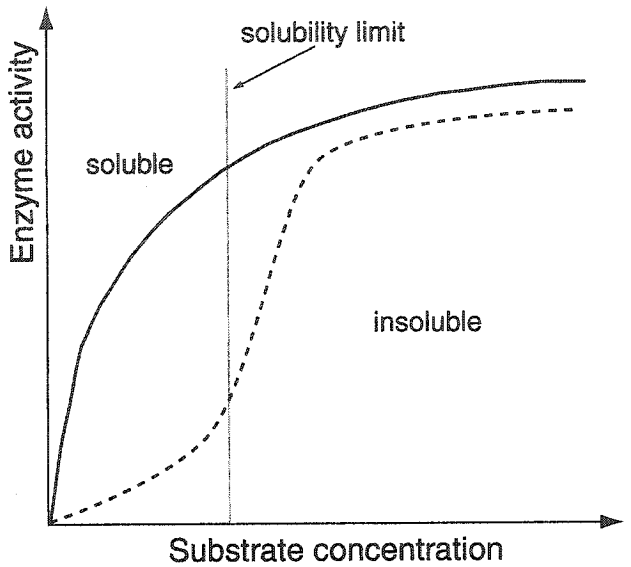

Figure 7 - While esterases display a normal Michaelis-Menten type of kinetics (continuous line), lipases show interfacial activation (dashed line).

On a molecular level, Brzozowski *et al.*[47] and Derewenda *et al.*[48] were the first to observe the conformational change brought about a lipase by a lipid substrate. A comparison of the X-ray crystal structures of *Rizomucor mehei* lipase (RML) complexed with two different inhibitors with the structure of the free enzyme[49] showed the movement of a "lid" composed of 15 amino acids such that some residues moved by about 12 Å. This movement and the change in some dihedral angles exposed a hydrophobic region of ~ 800 $Å^2$, representing ~ 7% of the enzyme surface. In the absence of a water/lipid interface the catalytic triad is hidden behind a short amphipatic helix (Figure 8, left). When bound to an interface, its conformation changes to expose the active site of the lipase. The hydrophobic side of the lid comes in contact with the lipid interface, which increases the hydrophobic interactions between enzyme and interface (Figure 8, right).

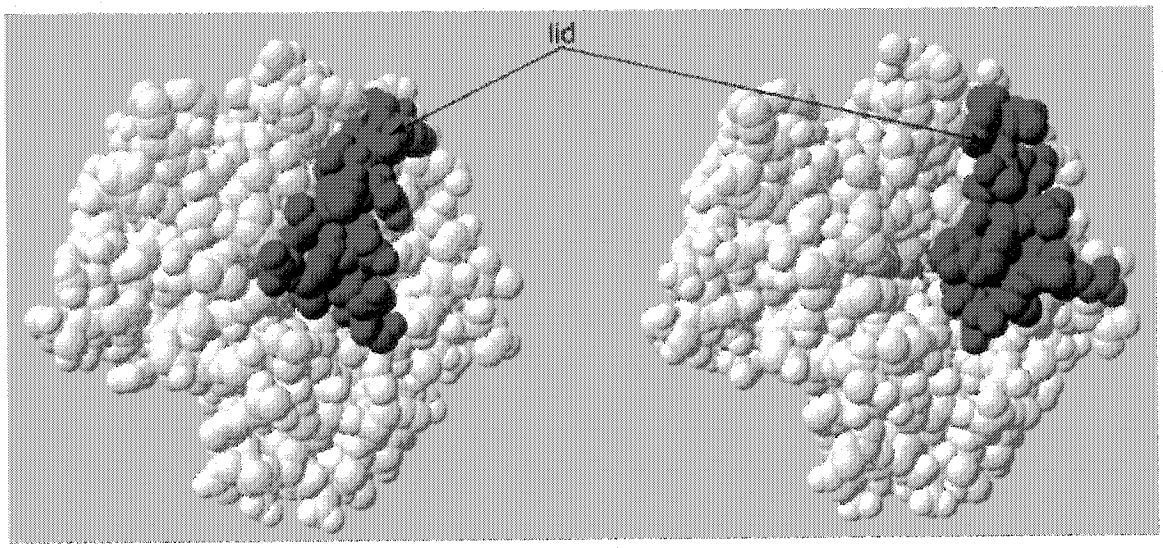

Figure 8 – The closed (left) and open (right) form of RML (PDB ID: 3TGL[50] and 4TGL[48]). The catalytic triad residues Ser144 (orange) and His257 (light blue) are uncovered by the lid opening (left). The inhibitor E600 is in CPK colours. Figure made with Swiss PdbViewer v. 3.7.[51]

Molecular dynamic simulations on RML complexed with either a substrate or a product of the reaction, in the presence of lipid aggregates, have shown[52] that in aqueous solution the lid displacement is thermodynamically unfavourable since it would expose a large hydrophobic surface to water. The process is however favourable in the presence of lipid structures such as aggregates that can stabilize the opening of the lid.

Not all lipases show interfacial activation. For example, *Candida antarctica* lipase B (CAL-B), with and without a bound inhibitor, does not show major differences in the features near the active site. The two helices that border the entrance to the active site contain 5 and 20 amino acids and are very mobile. They may be a lid for the enzyme active site.[53] Although there may be some rearrangement nearby the active site in the presence of a triglyceride, kinetic experiments on the activity of CAL-B did not show any interfacial activation towards *p*-nitrophenyl acetate nor towards *p*-nitrophenyl butyrate in the presence of an interface and the authors concluded that CAL-B behaviour is more typical of an esterase than a lipase.[54]

1.5.3 Reaction mechanism of lipases

The catalytic mechanism of lipases is analogous to the one of serine proteases[55,56] (Figure 9). The first step is the nucleophilic attack of the catalytic serine hydroxyl group

on the carbonyl carbon of the non-covalently bonded substrate (ester). The attack leads to the formation of the first tetrahedral intermediate T_d1. The incipient formation of a hydrogen bond with catalytic histidine activates the catalytic serine towards this attack.

Upon formation of T_d1 the hydrogen is transferred from serine to histidine. It is believed that the proton is both hydrogen bonded to catalytic serine Oγ and substrate alcohol oxygen,[57,58] thus facilitating the release of the alcohol upon collapse of T_d1. Catalytic aspartate stabilises the positively charged imidazole ring of catalytic histidine. Two residues form the oxyanion hole and stabilise the negatively charged oxygen in the tetrahedral intermediate, by forming two hydrogen bonds with their backbone amide hydrogens. Collapse of T_d1 forms the acyl enzyme. Nucleophilic attack of the acyl enzyme by water or another nucleophile present in the reaction medium forms a second tetrahedral intermediate T_d2. This intermediate possesses the same kind of hydrogen bonding network of T_d1. Its breakdown regenerates the free enzyme and releases the acyl group of the substrate as carboxylic acid. All the steps of the reaction mechanism are equilibria. The collapse of the first tetrahedral intermediate is the rate-determining step of the reaction[59] and in section 1.9 its role in determining the enantioselectivity of the lipase towards alcohols is discussed.

Hu *et al.*[60] used *ab initio* methods to locate the transition states and the intermediates in the reaction of ester hydrolysis catalysed by serine hydrolases. They modelled the reaction mechanism by replacing catalytic aspartate, histidine and serine by formate ion, imidazole and methanol. Two water molecules mimicked the oxyanion hole, to shorten computational times while their H-bonds still resembled the typical acidity of NHs in peptides. Their calculations confirm the role of the oxyanion hole and the catalytic aspartate in cooperatively lowering the activation energy for the formation of the first transition state and especially the first tetrahedral intermediate. They also studied the second step of the catalytic mechanism, the deacylation of the enzyme, which has activation energy of about 4 kcal/mol lower than the acylation step. This confirms the formation of the acyl enzyme as being the rate-determining step of the reaction.

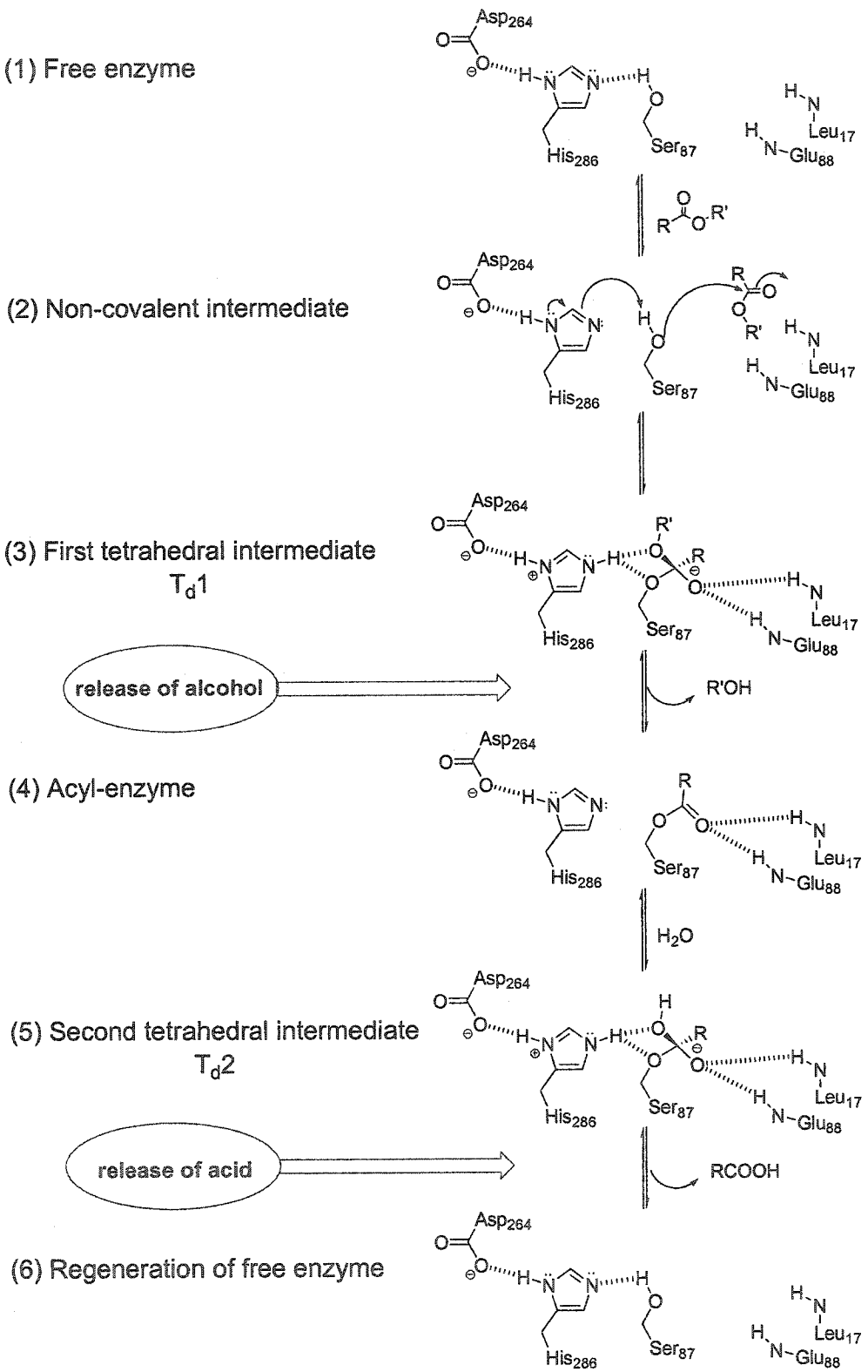

Figure 9 - Lipases catalytic mechanism (PCL is used as model enzyme).

Recently Rupert *et al.*[61] provided crystallographic evidence for the formation of the high-energy second tetrahedral intermediate in the hydrolysis of the heptapeptide human β-casomorphin-7 by porcine pancreatic elastase (PPE), a serine protease. The heptapeptide inhibits the enzyme at pH 5 by forming a stable acyl enzyme intermediate. However at higher pH the peptide is completely hydrolysed. They solved the cryogenically trapped structure of the second tetrahedral intermediate, formed after 1 minute at pH 9 upon nucleophilic attack of an activated water molecule on the acyl-enzyme. Their crystal structures confirm the double role of the oxyanion hole in stabilising both the acyl-enzyme and the tetrahedral intermediates by forming hydrogen bonds with the carbonyl oxygen of the substrate.

1.5.4 *Pseudomonas cepacia* lipase

Pseudomonas cepacia lipase (PCL), recently reclassified as *Burkholderia cepacia* lipase, is a bacterial lipase that belongs to the α/β hydrolases superfamily (Table 3). The structure of the open form of PCL[62,63] and a few other lipases have been solved. The central β sheet of PCL contains strands equivalent to strands β3 - β8 of the α/β hydrolase fold. Also all the expected helices are present. The acid moiety in the catalytic triad is aspartic acid, which forms a H-bond with catalytic histidine.

Table 3 – PCL classification

Enzyme Classification (E. C.)	3.1.1.3
Class	α and β proteins
Superfamily	α and β hydrolases
Family	bacterial lipases
Fold	α and β hydrolase fold

PCL is a 320 amino acid protein and has a molecular weight of 33128 Da. It is a globular protein with dimensions of about 30 Å x 40 Å x 50 Å, formed by three domains, a major one and two smaller ones, domains U1 and U2. The major domain, which spans amino acids 1 to 117, 167 to 214 and 262 to 320, consists of the six central β strands β3, β4, β5, β6, β7 and β8, of the two α helices α1 and α11 on one side and of the four α helices α2, α3, α7 and α10 on the other side (blue in Figure 10). Three α helices, α4, α5,

and α6, constitute one of the two smaller domains (domain U1, red in Figure 10), which spans amino acids 118 to 166. Two antiparallel β strands (β3 and β4) and two α helices (α8 and α9) constitute the second small domain (domain U2, green in Figure 10), which spans amino acids 213 to 261. Catalytic Ser87 is located at the C terminal end of strand β6, catalytic Asp264 belongs to a loop that follows strand β7 while catalytic His286 is in a loop that follows strand β8. The "lid" responsible for the interfacial activation phenomenon corresponds to the U1 domain (red in Figure 10), which opens to expose a large hydrophobic region that surrounds a deep cleft. At the centre of the cleft, which measures 10 Å x 25 Å x 15 Å (depth), resides Ser87. The bottom of the cleft, measuring 4 Å across, is formed by the C-terminal loops of the six-stranded β sheet of the major domain while U1 and U2 residues form the sides of the cleft. Leu17 projects into the cleft above Ser87, conferring the catalytic pocket a boomerang shape and dividing it into two branches.[62] The backbone nitrogens of Gln88 and Leu17 form the oxyanion hole.

PCL has a bonded six-coordinated Ca^{2+} ion. It makes contact with four oxygens of the protein and with two water molecules. The protein residues involved in this binding are Gln292, Val296 (backbone carbonyl oxygens), Asp242 and Asp 288 (side-chain Oδ2). The Ca^{2+} ion does not have any catalytic function but is believed to stabilise the structure of PCL.[62]

PCL has been used in the research detailed in Chapters 2, 3 and 4.

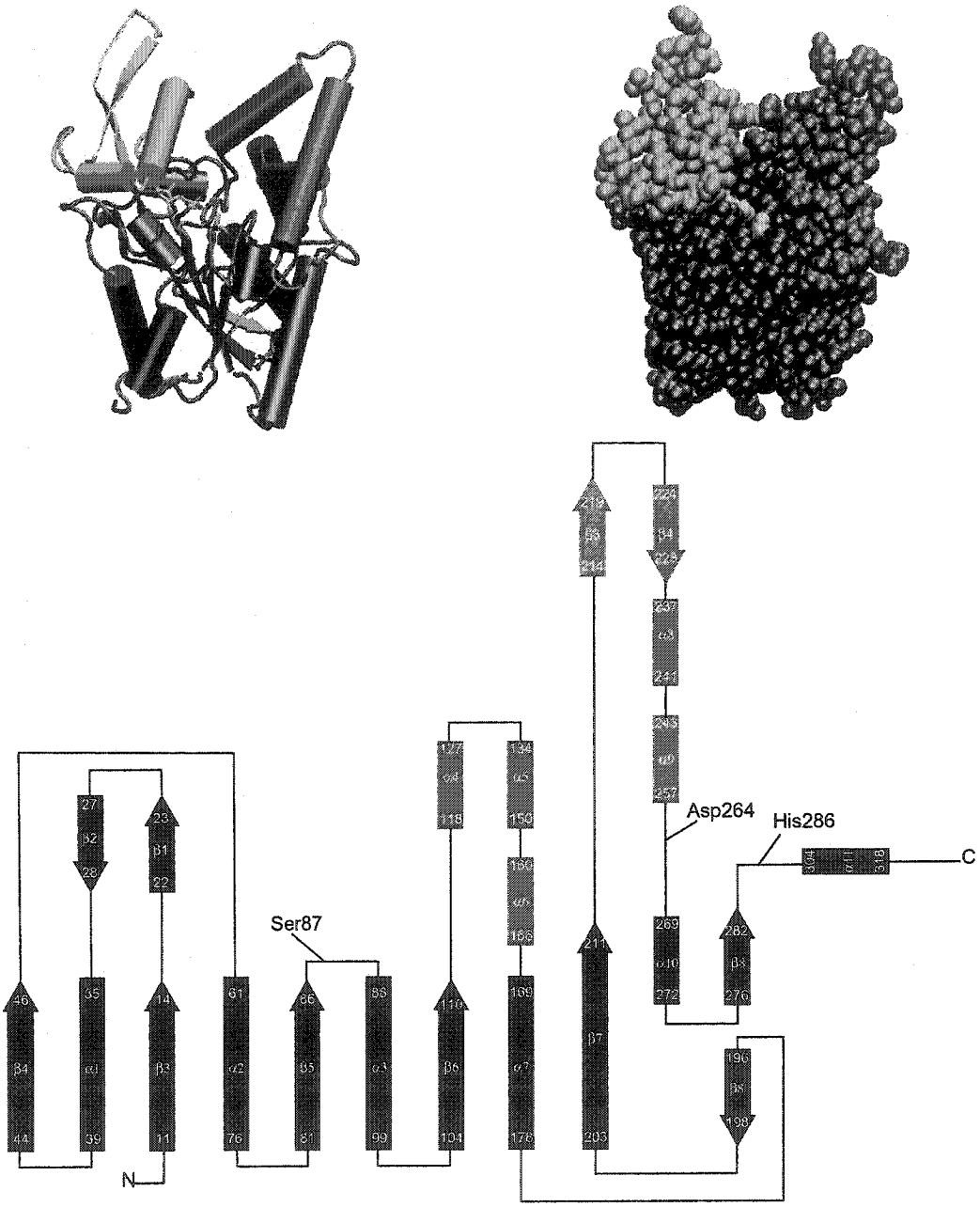

Figure 10 – Cartoon (upper left), spacefill (upper right) and diagram (bottom) of PCL (PDB ID 3LIP[62]). The major domain is in blue, the U1 domain is in red and the U2 in green. The catalytic triad is in yellow, and it is in "stick" representation in the cartoon. The cartoon and spacefill images were made with VMD 1.8.[64]

1.6 Transition state and transition state analogues for enzymatic reactions

Since the early days of biocatalysis scientists have tried to understand the exceptional rate acceleration in enzyme-catalysed reactions. Pauling in the 1940s applied

the reaction rate theory developed by Eyring and co-workers to enzyme-catalysed reactions.[65] Eyring's theory assumes that: (a) the reactants are in equilibrium with the "activated complex" and (b) the rate of the reaction depends on the decomposition of the "activated complex" into products. Pauling proposed that enzymatic catalysis could happen by the tight binding of the transition state to the enzyme, which would stabilise the transition state.

The thermodynamic cycle in Scheme 5 and Figure 11 relates K_S, K_{TS}, $K_{un}^{\ddagger}$ and $K_{cat}^{\ddagger}$ (equation 1.19), where K_S is the dissociation constant of the complex enzyme-substrate, K_{TS} is the hypothetical dissociation constant of the transition state $ES^{\ddagger}$, $K_{un}^{\ddagger}$ and $K_{cat}^{\ddagger}$ are the pseudo-equilibrium constants for the non-catalysed and the enzyme-catalysed reaction:

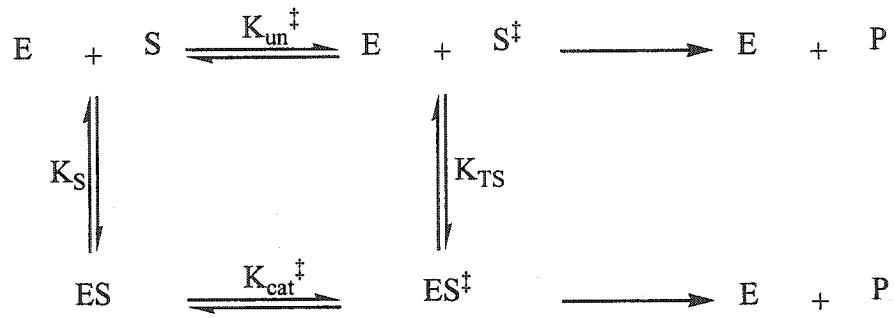

Scheme 5 - Thermodynamic cycle showing the relationship between ground state and transition state binding in an enzyme-catalysed and non-catalysed reaction with only one substrate.

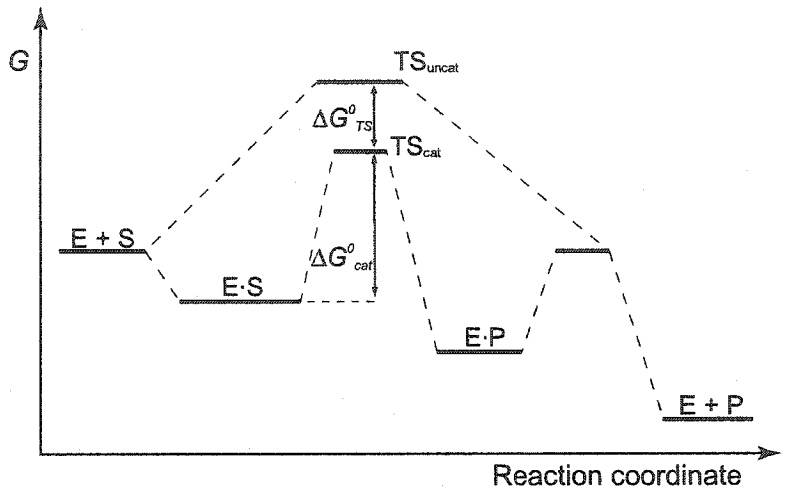

Figure 11 - Energy profile for enzyme-catalysed and non-catalysed reaction.

$$\frac{K_{TS}}{K_{un}^{\ddagger}} = \frac{K_S}{K_{cat}^{\ddagger}} \tag{1.19}$$

which can be rewritten as:

$$K_{TS} = K_{un}^{\ddagger} \frac{K_S}{K_{cat}^{\ddagger}} \tag{1.20}$$

A small K_{TS} indicates the tight binding of the transition state structure and is related to the catalytic power of the enzyme expressed by the ratio of $K_{cat}^{\ddagger}/K_{un}^{\ddagger}$.[66]

If enzymatic catalytic efficiency is directly related to transition state binding energy, then analogues of transition states may bind to enzymes with affinities 10^{10}-10^{15} higher than the substrate.[67] These analogues would be potent inhibitors of enzymes, however this binding affinity is never reached. Indeed, no stable molecules perfectly mimic all the geometric and electronic features of a labile transition state, where bond cleavage and bond formation are taking place. In a stable mimic of a transition state different elements replace one or more atoms. Therefore, bond lengths and bond angles do not perfectly coincide with the ones of transition states.

Hydrolases catalyse the hydrolysis of esters. The reaction involves the change from a carbon hybridised sp^2 to a tetrahedral carbon hybridised sp^3. Pentavalent phosphorous can replace the tetrahedral carbon, Figure 12.

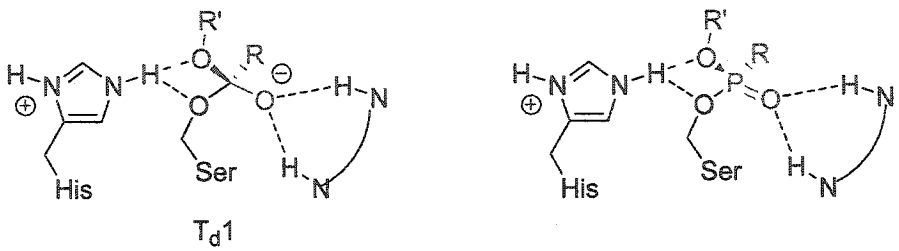

Figure 12 – Pentavalent phosphorus as sp^3 carbon substitute. On the left, the first tetrahedral intermediate T_d1 in the lipase-catalysed hydrolysis of esters, on the right a phosphonate analogue.

Phosphonate esters are not only transition state analogues but also potent inactivators of hydrolases.[68,69,70,71,72] Jackson *et al.*[68] synthesised thirty-six phosphonate esters that were evaluated as inhibitors of four proteases: lymphocyte granzymes A and K, pancreatic trypsin and human mast cell tryptase. They identified a few potent inhibitors, with potential use in the treatment of organ transplant rejection (granzymes A and K), reumathoid arthritis (granzymes A and K) and asthma (mast cell tryptase). Gillespie and co-workers[69] evaluated optically active phosphonate esters as inhibitors of pancreatic cholesterol esterase (CEase) for their potential in the treatment of atherosclerosis. Tramontano *et al.*[70] inhibited trypsin and chymotrypsin with phosphonate diesters. They also used biotinylated derivatives of these inhibitors to label the enzymes. They could thus detect chymotrypsin at a concentration of only 20 nM.

Transition state analogues are also valuable tools for gaining insight into the molecular basis for enzyme catalysis. While for simple gas-phase reactions it has been possible to spectroscopically measure signals from transition states, for enzymatic reactions these signals would be extremely weak due to the very low concentration of enzymatic transition states in solution and their short lifetime, about 10^{-13} s.[73] To gain insight into enzymatic transition states one possibility is to "freeze" the enzyme in a state that mimics them, using inhibitors like phosphonate esters in the case of hydrolases that once bound to the enzyme are transition state analogues.

Lipases can resolve esters of chiral alcohols. Figure 9 and Paragraph 1.5.3 illustrate the reaction mechanism of lipase catalysed ester hydrolysis. Since the alcohol moiety is released when T_d1 collapses forming the acyl enzyme, it is the interactions between enzyme and substrate in this particular intermediate, or in the transition state that leads to

its formation or collapse, that determine the enantioselectivity of lipases towards alcohols. As a result, the observation of these interactions would allow a better rationalisation of the enantiorecognition of chiral alcohols by lipases. To understand the molecular basis of CRL enantioselectivity towards secondary alcohols, Cygler *et al.*[57] inactivated the enzyme with phosphonate esters containing as alcohol moieties pure enantiomers of menthol (paragraph 1.9.2). To the same end, Luić *et al.*[74] inactivated PCL with a phosphonate ester containing a chiral secondary alcohol (paragraph 1.9.2). In Chapters 2 and 3 we will discuss the use of phosphonate esters containing chiral primary alcohols to explain the enantioselectivity of PCL towards these substrates.

1.7 Molecular modelling and biocatalysis

Recent advances in the knowledge of the three-dimensional structure of proteins have opened up the possibility of using computational techniques for understanding enzymatic mechanisms and selectivity and even for making the first steps towards quantifying enantioselectivity. Molecular modelling is the generic name of the ensemble of computational methods that describe molecules, study their structures, observe their reactions and derive their properties. In particular all molecular modelling methods describe the energy so that the most stable structure is characterised by the lowest energy.

1.7.1 Quantum mechanics

Quantum mechanics (QM) describes the behaviour of electrons and in theory can determine exactly every property of atoms and molecules.[75] In practice this is possible only for one-electron systems, while multiple electron systems require the use of approximations. QM describes systems in terms of nuclei, electrons and orbitals and it is based on the solution of the time independent Schrödinger equation $H\Psi = E\Psi$, where H is the Hamiltonian operator[viii], E is the energy and Ψ is a wave function that depends on the position of both electrons and nuclei and represents the probability of the electrons to be in a certain location. Solving the Schrödinger equation, thus determining the wave

[viii] The Hamiltonian operator gives the total energy of a system as eigenvalue of the time independent Schrödinger equation. Modelling uses the Born-Oppenheimer approximation, which allows decoupling the electronic and nuclear Hamiltonians.

function that describes the molecule, allows calculating every property of the molecule by applying the appropriate operator to the wave function. *Ab initio* and semi-empirical methods use different kinds of approximations to solve the time independent Schrödinger equation.

1.7.1.1 Ab initio methods

Ab initio methods do not rely on experimental data. The approximations used are only mathematical. One of the most common is the central field approximation[75], which is the basis of the Hartree-Fock calculations (HF). In the central field approximation the repulsion term of the Coulombic energy in the Hamiltonian operator is integrated, yielding an average repulsive effect. Because of this all the calculated energies are greater or equal to the exact energy of the system and tend to an asymptotic value called Hartree-Fock limit.

Other *ab initio* methods are MP2 (Møller-Plesset), CISD (Configuration Interaction[ix] Single and Double excitation), CCSD (Coupled Cluster Single and Double excitation), and FullCI. Describing this methods and the above HF method in detail is beyond the scope of this paragraph. More details can be found in Young D. C.[75] or other computational chemistry books. What is important to highlight is that the results of *ab initio* calculations are qualitatively good and can be also quantitatively very reliable if the approximations used are kept sufficiently small and the basis sets – sets of one electron wave functions used to build molecular orbital wave functions – are appropriately chosen.[75] However, because of the complexity of the calculations, they require huge computer power and cannot yet be applied to large biological systems such as proteins or DNA.

1.7.1.2 Semi-empirical methods

Semi-empirical methods are similar to *ab initio* methods, being based on the solution of the time independent Schrödinger equation as well. The difference with *ab*

[ix] Self Consistent Field (SCF) methods such as the HF method tend to underestimate the electron-electron repulsion. Configuration Interaction (CI) methods consider multiple electronic configurations and the resulting wave functions are linear combinations of those configurations.

initio methods is that they do not consider inner shell electrons, which are included together with the nucleus in the "core", they introduce other approximations to avoid calculating some two-electron orbitals and they are parameterised. While the approximations greatly reduce the computational time needed with respect to *ab initio* methods, the parameterisations are needed to correct for the missing values. The parameters may come either from experimental data or *ab initio* calculations.

Several different semi empirical methods have been designed. The most commonly used are based on the neglection of the differential overlap (NDO) and model valence orbitals using just a minimal basis set of Slater orbitals – algorithms that describe atomic orbitals. They are CNDO (Complete Neglect of Differential Overlap), MINDO (Modified Intermediate Neglect of Differential Overlap), MNDO (Modified Neglect of Diatomic Overlap), AM1 (Austin Model 1) and PM3 (Parameterisation Model 3).

1.7.2 Molecular mechanics

One of the most popular techniques for studying proteins is molecular mechanics (MM). A few examples, relevant to this thesis, are illustrated in section 1.9. In molecular mechanics, classical mechanics describes the structure and dynamics of molecular systems such as biological macromolecules. Atoms are treated as classical particles and bonds as springs, hence molecules are sets of vibrating spheres. The energy functions are the sum of steric interactions and non-bonded interactions and contain constants that are obtained from experimental or *ab initio* data. This approach is a great simplification over QM. However, because of its simplicity, it is possible to apply molecular mechanics to much larger systems than the ones that can be studied by QM methods.

Several force fields, sets of energy expressions and constants, have been developed. Among them AMBER (Assisted Model Building with Energy Refinement), parameterised for DNA and proteins, which uses five bonding and non bonding terms in the energy expression and an electrostatic term, but does not include cross terms.[x] Other popular forcefields are Allinger's MM2, MM3 and MM4 and Tripos.

---

[x]Cross terms represent couplings between deformations of internal coordinates, e.g. the coupling between the stretching of adjacent coordinates.

Despite the advantages offered by molecular mechanics, because it does not take into account electrons it cannot be used to study transient states such as transition states. Instead, researchers have to model transition state analogues such as phosphonate esters, which is only an approximation, or use a combination of molecular mechanics and quantum mechanics methods (*ab initio* or semi empirical). These methods are referred to as QM/MM.

1.7.3 Combined quantum mechanics/molecular mechanics methods

In combined quantum mechanics/molecular mechanics (QM/MM) methods the reactive part of a large chemical system, usually a biomolecule, is described using either *ab initio* or semi empirical methods, while the remainder of the molecule is treated with MM.[76] One of the difficulties encountered using these methodologies is the treatment of the interaction of the quantum part (treated with QM methods) with the classic part (treated with MM methods). Atoms at the frontier of the quantum part (W) are covalently bound to atoms (Y) that are at the frontier of the classic part and the electron of W involved in the bond with Y is not paired with any other electron because MM does not explicitly represents them. A solution is to add a "dummy" atom, like fluorine, along the W-Y bond to fill the valence of W. This and other methods are described in ref. 76.

1.7.4 Homology modelling

Deducing a protein three-dimensional structure from its primary amino acid sequence is difficult. Both X-rays diffraction studies and NMR analyses are labour intensive techniques. However there is no genetic mechanism that determines the folding of proteins[xi, 77] and this discovery has led to more than 20 years of efforts for determining three-dimensional protein structures solely from their sequences.

Among the methods available for protein structure prediction, comparative or homology modelling is based on the fact that evolutionarily related proteins, which have

---

[xi]There is experimental evidence that considerable changes to protein sequence may be made by mutagenesis without loss of protein function, therefore without loss of the proper fold.[77]

similar sequences, have similar structures. Levels of 25-30% sequence identity are enough to ensure that the proteins fold into similar structures.[78]

If a sequence of unknown structure has significant identity with a protein of known structure, it may be possible to build an appropriate model for the former by extrapolation from the structure of the latter.[79] Building a homology model involves first the alignment of the sequence of the protein of known structure (determined by experimental means such as crystallography or NMR studies) with the sequence of the protein of interest. The initial model (framework or template) is built by copying the coordinates of some main chains and side chains of the parent structure based on the equivalent residues in the sequence alignment. For every amino acid in the target that does not correspond to an identity in the alignment, side chains must be built. Also, the main chain must be built in the case of insertions, regions surrounding a deletion and regions of the main chain where there is a substantial difference between the two sequences.[80]

SWISS-MODEL is an automated comparative protein modelling server running at the GlaxoWellcome Experimental Research Centre in Geneva, Switzerland. The purpose of this server is to make protein modelling accessible to all scientists worldwide. The server is part of ExPASy[81] (Expert Protein Analysis System), the proteomics server of the Swiss Institute of Bioinformatics (SIB) dedicated to the analysis of protein sequences and structures. When the sequence identity of the protein of interest with known proteins is sufficiently high, a model can be received by e-mail within as little as 15 minutes from the submission of the primary amino acid sequence to "First Approach Mode". However, if the automated server cannot find any suitable protein for building a model, one can choose a homologous protein, manually align the one of interest on it, then submit the alignment and a modelling request in "Optimise-Model". Results obtained submitting to SWISS-MODEL through the "First Approach mode" 1200 target proteins whose 3D structure is known show that 79% of the sequences sharing 50 to 59% identity with their template yield a model deviating less than 3 Å from their control structure. The percentage decreases to 63% for the sequences sharing 40 to 49% identity with their template. Below 30% sequence identity, the accuracy of the models is very low.[82]

1.8 Early theories and models for enzymatic chiral and prochiral recognition

The building blocks of enzymes are *L*-amino acids. Their chirality and their position in the protein sequence determine the three-dimensional architecture of each enzyme, which confers their different chiral recognition abilities and properties. Enzymes can differentiate not only between enantiomers, but also between prochiral groups or faces. For example two enantiotopic hydrogens may be exposed to different environments within the enzyme catalytic pocket, only one of which is catalytically competent, or a carbonyl compound bound to an enzyme may expose only one face to nucleophilic attack.

The first theory for enzyme differentiation of enantiomers was proposed in 1933 by Easson and Stedman,[83] who introduced the concept of three-point attachment. Their study on drug-receptor interactions brought them to believe that a considerable part of a drug is involved in the interaction with a receptor. They also proposed that if the drug contained an asymmetric carbon, at least three of its substituents could be involved in the enantiorecognition process by the receptor (Figure 13). They believed that the nature of the interaction of the substrate with the three points in the enzyme could be covalent, "absorptive" or depend on "other forces". It could also "be of a loose type, somewhat analogous to the attachment of a glove to the hand, involving the contour of a large part of the molecule rather than points on its surface or finally a combination of these posibilities".[83]

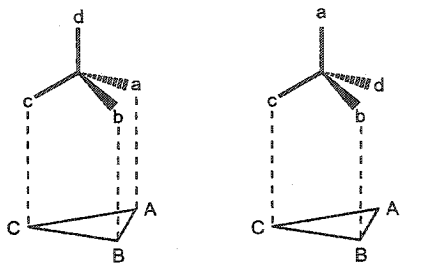

Figure 13 – Easson-Stedman model.[83] On the left: the drug groups a, b and c can bind to the receptor sites A, B and C. On the right: the enantiomer of the drug can match only groups b and c to the receptor sites B and C. It is assumed that the drug can approach the receptor only from "above".

Soon after Easson and Stedman, Bergmann *et al.*[84,85] developed a similar theory for the enantioselectivity of enzymatic reactions, referred to as the "polyaffinity theory": "If an enzyme catalyses only one of two antipodes, then it must contain at least three different atoms or atomic groups which are fixed in space with respect to one another, these groups entering during the catalysis into relation with a similar number of different atoms or atomic groups of the substrate. Through this polyaffinity relationship, the active groups of the enzyme force the active groups of the substrate into a definite spatial arrangement with respect to each other and to the enzyme. ...".[84]

The concept of the three-point attachment of a prochiral substrate to its receptor became more popular after Ogston's publication of a short note in *Nature*,[86] where he explains the enzymatic discrimination of prochiral substrates like aminomalonic acid to yield chiral molecules like *L*-serine. The theory, similar to Easson-Stedman model,[83] is illustrated in Figure 14.

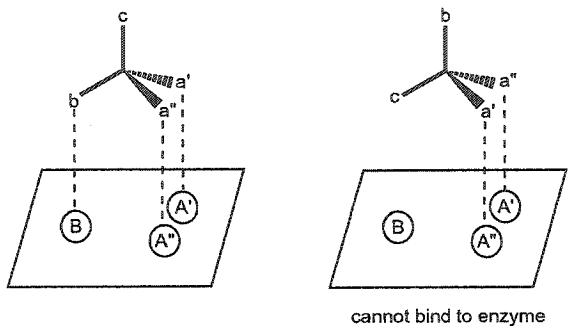

Figure 14 – Ogstron's three-point attachment rule for the enzymatic discrimination of a prochiral substrate.[86] Only one arrangement of the four substituents on the tetrahedral carbon can bind to the enzyme active site. a' and a" are identical groups, while the enzyme sites A' and A" have different catalytic abilities. Since a' and a" are identical, they can both bind to A' and A". Only one binding mode allows also b to bind to the third binding site in the enzyme, B. Although illustrated for prochiral molecules, this model can be extended to chiral ones (a' ≠ a").

Despite the fame achieved by the "three-point attachment rule", several stereochemists, in the late 1950s-early 1960s, started pointing out that the three-point attachment is not a prerequisite for the differentiation of chiral and prochiral groups by enzymes. Bentley points out in his review[87] that X-ray crystallographic analyses of enzyme-inhibitor complexes reveal a complexity of interactions enzyme-substrate greater than what is suggested by the three-point attachment rule. There are many ways to achieve a diastereoisomeric relationship enzyme-substrate and a concept more correct than the three-points attachment rule seems to be the one of Easson and Stedman: the interaction enzyme-substrate or receptor-drug is analogous to the one glove-hand, involving not just a few points on the surface of the molecule but a larger part of it.

In a recent, brief communication to the journal *Nature*, Mesecar and Koshland[88] report an umbrella-like inversion at the stereocentre as relative orientation of the two enantiomers of isocitrate in the catalytic pocket of isocitrate dehydrogenase (IDH). Three of the four substituents at the stereocentre occupy the same position and it is the fourth one that, pointing in different directions, interacts with different portions of the enzyme. They observe that the "three-point attachment rule" works only when the substrate approaches from the top a flat enzyme surface, while if the binding sites are, e.g., in an enzyme cleft, an additional interaction point is necessary for distinguishing enantiomers of the substrate. Therefore they propose a "four location" model to explain the

discrimination of *D* and *L* isomers (Figure 15). These four locations are not necessarily four anchor points in the catalytic pocket of the enzyme, they could be three points and a direction. What is important is that a minimum of four locations is needed.

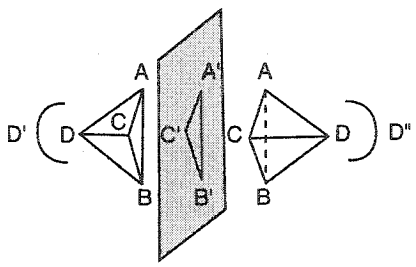

Figure 15 – The four-location model.[88] The inversion at the stereocentre places the groups A, B and C in the same position in both enantiomers such that they can both interact with the enzymes three sites A', B' and C'. The fourth substituent, D, points in different directions in the two enantiomers, thus they can interact only with one of the sites D' or D" in the enzyme.

Interactions enzyme-substrate are thus more complex than what the famous three-points attachment rule suggests. I would thus conclude this section with the same sentence used by Bentley in his debate on the above rule: "Honorary membership in the Society for the Abolition of Three-Point Attachment Theories (SATPAT) is available to all".[87]

1.9 Molecular basis of lipase enantioselectivity

As chiral catalysts, enzymes are increasingly being used in the synthesis of optically pure molecules. Despite their widespread use, the molecular basis of their enantioselectivity is poorly understood. Knowledge of the determinants of enzyme enantioselectivity would allow not only identifying the enzymes that are best suited for a particular application, but also help in developing new modelling protocols to predict the outcome of the reactions and, why not, the enantiomeric ratio E. What follows is a summary of the recent developments regarding the explanation of the molecular basis of lipase enantioselectivity towards chiral secondary and primary alcohols.

1.9.1 Elements necessary for a productive conformation of the substrate

For a lipase-catalysed hydrolysis reaction to take place, the substrate must be in a productive conformation in the first tetrahedral intermediate T_d1 (Figure 9 (3)). The carbonyl oxygen must reside in the oxyanion hole, where it is stabilised by the hydrogen bond with the backbone NH of usually two enzyme residues. The catalytic serine Oγ has to hydrogen bind to Nε2 hydrogen of catalytic histidine and the alcohol moiety of the substrate must accept a proton from Nε of catalytic histidine. Also, a hydrogen bond must be present between catalytic histidine and catalytic aspartate.

Some consider as important criteria for a productive conformation not only the presence of all the hydrogen bonds described above, but also the fulfilment of Deslongchamps' stereoelectronic theory.[89,90] According to this theory an efficient cleavage of the ester C-O bond can occur only when the two other oxygens in the tetrahedral intermediate have their lone-pair antiperiplanar to the breaking C-O bond. In this arrangement, achieved by the substrate when the R_{alc}-O bond is *gauche* to the C-O_γ bond, the oxygen lone pair *n* orbital overlaps with the breaking bond σ^* orbital, facilitating the cleavage of the bond. However no strong evidence has been found in the literature either in favour or against this theory for enzyme-catalysed reactions.

1.9.2 Esters of chiral secondary alcohols

Lipases and esterases exhibit different degrees of enantioselectivity but the same enantiopreference[xii] towards secondary alcohols.[91] Several researchers have proposed explanations for the enantioselectivity of lipases towards these substrates. The explanations originate from substrate mapping studies, kinetic experiments coupled with molecular modelling, molecular modelling experiments alone and X-ray crystal structures of transition state analogues.

Three relative orientations for the fast and slow enantiomer have arisen from these studies, Figure 16. In the LM-alignment there is an umbrella-like inversion at the stereocentre and the hydrogen points in opposite directions in the two enantiomers, Figure

---

[xii]The enantiopreference represents the *R* or *S* preference of one enzyme. The enantioselectivity quantifies this preference.

16 (a); in the H-alignment the large and medium group at the stereocentre exchange position, Figure 16 (b) while in the L-alignment it is the medium group and the hydrogen at the stereocentre that exchange position, Figure 16 (c).

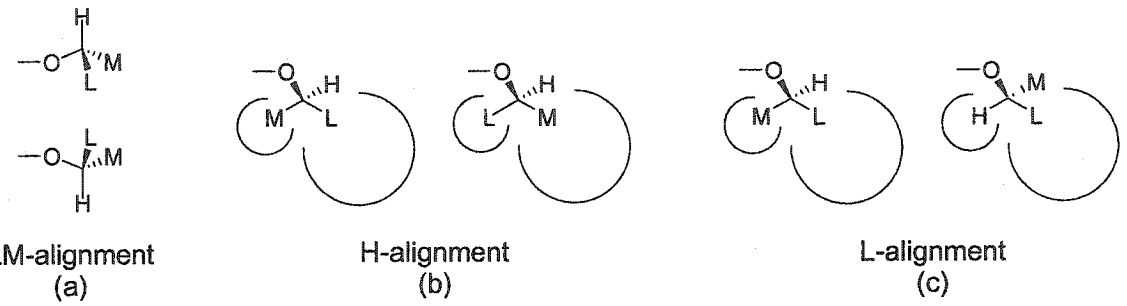

Figure 16 – Relative orientations of enantiomeric secondary alcohols. M is a medium group, e.g. CH_3, L is a large group, e.g. Ph. (a) in the LM-alignment there is an "umbrella-like" inversion at the stereocentre and the hydrogen points in opposite directions while L, M and the alcohol oxygen are oriented in a similar way; (b) in the H-alignment the large and medium group at the stereocentre exchange position, while the hydrogen points in the same direction; (c) in the L-alignment the medium group and the hydrogen at the stereocentre exchange position, while the large group L points in the same direction. The ovals represent enzyme pockets.

Despite the numerous studies on the molecular basis of lipases enantioselectivity towards secondary alcohols, a summary of which is given in Table 4, there is still no complete agreement on what are the mechanisms of enantiorecognition of these substrates by lipases or on the relative orientation of the two enantiomers within the enzyme catalytic pocket. Although most agree on the H-alignment of the two enantiomers, the large and medium group at the stereocentre are found in different pockets of the enzyme. The enantioselectivity seems to stem either from unfavourable steric interactions enzyme-substrate present in the slow enantiomer, from the impossibility of attaining a *gauche* conformation C-O-C-O_{Ser} or from the lack of a key hydrogen bond, Table 4.

Enzymes are large and complex molecules and the approaches used to understand their reactivity and specificity have been very diverse. Both the complex architecture of enzymes and the different methods used by scientist justify why there is still no complete agreement on the molecular basis of enzyme enantioselectivity towards chiral secondary alcohols.

Table 4 - Summary of the proposed molecular basis of lipase enantioselectivity towards secondary alcohols.

Authors	Method[a]	Alignment	Enzyme and enzyme pockets	Explanation
Cygler *et al.*[57]	X-ray	LM-alignment	CRL - L in large and M in medium hydrophobic pocket for both enantiomers	Lack of H-bond between alcohol O and His Nε2.
Uppenberg *et al.*[92] Orrenius *et al.*[93] Rotticci *et al.*[94]	X-ray + MM	H-alignment	CAL-B - Fast enantiomer binds M in stereoselectivity (small) pocket; slow enantiomer binds L in stereoselectivity (small) pocket.	Difference in size L-M important. Slow enantiomer sterically hindered because of L in stereoselectivity pocket. H-bond between alcohol O and His Nε2 present in both enantiomers.
Zuegg *et al.*[95]	SsMcm	H-alignment	CRL, PCL - Fast enantiomer binds L in large and M in medium hydrophobic pockets; slow enantiomer binds L in medium pocket and M in large pocket	Difference in size L-M important. Slow enantiomer sterically hindered because of L in medium pocket. H-bond between alcohol O and His Nε2 present in both enantiomers.
Luić *et al.*[74]	X-ray + MM	H-alignment	PCL - Fast enantiomer binds L in large and M in medium hydrophobic pockets; slow enantiomer binds L in medium pocket and M in large pocket	Higher conformational entropy and lower potential energy for fast enantiomer. H-bond between alcohol O and His Nε2 present in both enantiomers.
Ema *et al.*[96]	Kinetics + MO	H or L-alignment	RML - Fast enantiomer binds L in solvent exposed crevice; slow enantiomer binds L near triangular wall and M in solvent exposed crevice or L in solvent exposed crevice and M *syn* to C=O	*Gauche* conformation C-O-C-O_{Ser} difficult to attain for slow enantiomer, causes strain or repulsion with enzyme.
Tafi *et al.*[97]	MM + MD	H-alignment	PCL - Fast enantiomer binds L in alternate hydrophobic pocket and M in medium pocket; slow enantiomer binds L in medium pocket and M in solvent exposed crevice	Fast has *gauche* conformation, slow has *anti* (C-O-C-O_{Ser}) and steric repulsion caused by L in medium pocket. H-bond between alcohol O and His Nε2 present in both enantiomers.
Schulz *et al.*[98]	MM + MD	L-alignment	PCL - Fast enantiomer binds L in hydrophobic dent and M in hydrophobic trench; slow enantiomer binds L in hydrophobic dent and M towards oxyanion stop	Worse binding of slow enantiomer, M bumps into oxyanion stop. Distance $H_{N\varepsilon}$ – O_{alc} in slow enantiomer correlates to E.
Nishizawa *et al.*[59]	Kinetics	L-alignment	PCL - L binds in the same pocket in both enantiomers; M closer to catalytic His in slow enantiomer	M of slow enantiomer close to His causes loss of H-bond between alcohol O and His Nε2.

[a] SsMcm = Systematic search + Monte carlo minimisation; MM = Molecular Mechanics; MO = Molecular Orbitals; MD = Molecular Dynamics. [b] It is not clearly stated but it appears to be H-alignment from the diagrams and the text of ref. 97.

1.9.3 Esters of chiral primary alcohols

While several lipases resolve chiral secondary alcohols with high enantioselectivity, fewer, such as PCL[99,100], porcine pancreatic lipase (PPL)[99,100] and *Achromobacter* sp. lipase (AL),[101] effectively resolve chiral primary alcohols.[100] Also, lipases usually show opposite enantiopreference for secondary and primary alcohols.

As for secondary alcohols, several modelling experiments have been carried out in the last few years[95,102,103,104] to explain the molecular basis of lipase enantioselectivity towards primary alcohols. While substrate rules have been proposed also for primary alcohols, so far X-ray crystal structures of analogues of primary alcohol esters bound to enzymes active sites have been limited to triacylglycerol derivatives of the enzyme natural substrates.[58]

Unlike for secondary alcohols, two relative orientations for the fast and slow enantiomer have been proposed, L-alignment and H-alignment (Figure 17). While Zuegg *et al.*[95] propose a different relative orientation for the fast and slow enantiomer of primary alcohols, suggesting L-alignment when no oxygen is present at the stereocentre and H-alignment when it is, Tuomi and Kazlauskas[102] obtained *via* modelling experiments L-alignment for both kinds of alcohol. Tomić *et al.*[103] considered only primary alcohols without oxygen at the stereocentre, 2-methyl-3 (or 4)- arylalkanols, which showed L-alignment.

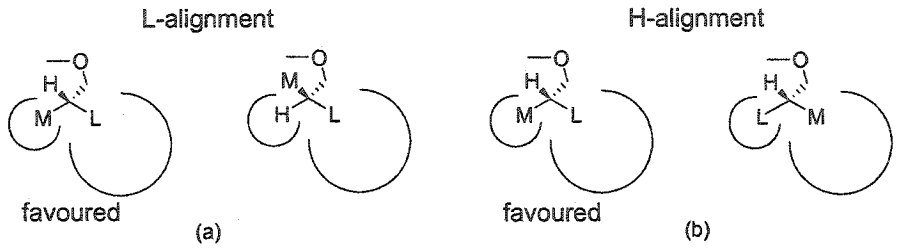

Figure 17 - Relative orientations for enantiomeric primary alcohols. M is a medium group, e.g. CH_3, L is a large group, e.g. Ph. (a) in the L-alignment the medium group and the hydrogen at the stereocentre exchange position; (b) in the H-alignment the large and medium group at the stereocentre exchange position.

1.9.3.1 Primary alcohols with no oxygen at the stereocentre

To understand the enantioselectivity of PCL towards primary alcohols Zuegg *et al.*[95] calculated the energy difference between diastereoisomeric transition states. They obtained the same (*S*)-enantiopreference experimentally observed in the hydrolysis of esters of chiral primary alcohols by PCL. They found two different binding modes for the fast enantiomer: the large substituent at the stereocentre was either bound in the large hydrophobic pocket of the enzyme like in the case of secondary alcohols, or it extended into the solvent. When the alcohols did not have polar groups at the stereocentre they showed L-alignment. They addressed the problem of opposite enantiopreference for primary and secondary alcohols and concluded that PCL shows opposite enantiopreference for primary alcohols because the extra methylene group between alcohol oxygen and stereocentre allows for a "kink" so that large and medium group at the stereocentre can bind in the same pockets as secondary alcohols. In the slow enantiomer the medium substituent at the stereocentre is pushed outside the pocket, which makes its binding less favourable. The authors propose the better binding of the fast enantiomer as molecular basis for enantioselectivity.

Tuomi and Kazlauskas[102] molecular mechanics calculations on phosphonate analogues of 2-methyl-3-phenyl-1-propyl butanoate covalently bound to PCL *via* catalytic Ser87 Oγ yielded the same L-alignment observed by Zuegg, however the large group at the stereocentre was bonded in a different pocket of PCL. They minimised nine possible conformations of the bound substrate. Ideally all of them should have converged to a global minimum. However they found several local minima that they "judged" for "catalytic competence" using two criteria: the presence of all the hydrogen bonds required

for catalysis and the good binding of the alcohol moiety in the catalytic pocket (qualitative parameter). They found the large substituent at the stereocentre bonded in a different hydrophobic region than secondary alcohols that they called "alternate hydrophobic pocket". The binding of primary alcohols in a different pocket than secondary alcohols explains the opposite enantioselectivity of the enzyme for these substrates. The authors agree with Zuegg *et al.*[95] that the molecular basis of PCL enantioselectivity towards primary alcohols without oxygen at the stereocentre is the better binding of the fast over the slow enantiomer.

Tomić *et al.*[103] studied the potential energy surfaces of the tetrahedral intermediates of the complexes enzyme-substrate (2-methyl-3 (or 4)- arylalkanols), their SASA (Solvent Accessible Surface Area) and their interactions with the amino acids in the PCL active site. They obtained several conformations that were judged for catalytic competency according to Tuomi and Kazlauskas.[102] The authors observed three different orientations for the large substituent at the stereocentre of the fast enantiomer: it was either bound in the alternate hydrophobic pocket, pointed outwards in the solvent or was only partly bound in the alternate hydrophobic pocket. The two enantiomers had L-alignment. Also, they noticed a *gauche* conformation of the dihedral angle O(Ser87)-C-O-R. Because of this conformation the medium substituent at the stereocentre of the preferred enantiomer pushes the catalytic His286 towards Ser87, increasing their hydrogen bonding and therefore speeding up the reaction of this particular enantiomer.

1.9.3.2 Primary alcohols with oxygen at the stereocentre

Zuegg *et al.*[95] found H-alignment, thus a different relative orientation of the two enantiomers of primary alcohols having polar groups like oxygen at the stereocentre. They propose that when a polar group is present at the stereocentre the enantio-differentiation arises from the large group at the stereocentre binding in the tight small pocket, thus being more constrained, instead than in the large binding pocket like in the fast enantiomer.

Tuomi and Kazlauskas[102] modelling studies on complexes PCL-transition state analogues containing single enantiomers of 2-phenoxy-1-propanol as alcohol moieties show L-alignment, in agreement with what they found for substrates without oxygen at the stereocentre. They explain PCL opposite enantiopreference for this substrate

compared to 2-methyl-3-phenyl-1-propanol with the presence of a hydrogen bond between the oxygen at the stereocentre of the slow enantiomer and Tyr29. The hydrogen bond to Tyr29 may cause this enantiomer to reside longer in the active site of the enzyme and undergo the reverse reaction (transesterification). This agrees with the much lower k_{cat} for the slow enantiomer, while the K_M for both enantiomers are similar. To prove their theory they chemically modified PCL. By acetylation they observed a decrease in enantioselectivity towards 2-phenoxy-1-propyl acetate that was considered consistent with an acetylated Tyr29 and the lack of the hydrogen bond with the alcohol. Upon ortho-nitration they found an increase in enantioselectivity towards the same substrate, which was justified by an increased strength of the hydrogen bond Tyr29-oxygen at the stereocentre because of the presence of the NO_2 group. These results, however, cannot be considered conclusive since other residues within the enzyme may have been chemically modified as well, which could have affected the enantioselectivity.

1.9.3.3 Primary alcohols in a ring structure

Gentner and co-workers[104] derived a model to predict the enantioselectivity of PCL towards primary alcohols having the stereocentre on a ring structure (e.g.. solketal). They placed the acyl chain in the large hydrophobic pocket of PCL and the large substituent at the stereocentre in the "alternate hydrophobic pocket" described by Tuomi and Kazlauskas.[102] They relaxed the complexes by energy minimisations and molecular dynamics simulations at 100 K. They observed that the substrate was bound in the "His gap",[105] a small pocket within PCL active site, defined by His286 and Leu287. In particular while the favoured enantiomer moved deeply inside the "His gap", the slow enantiomer did not enter it at all. They found a direct relationship between the level of entrance into the "His gap" and the increase in enantioselectivity. This movement into the "His gap" was accompanied with a motion of the imidazole ring of His286 and led to an increase in the size of the gap ($d_{His\ gap}$) proportional to E.

1.9.3.4 Substrate rules

A general rule to predict which enantiomer of a racemic pair of primary alcohols reacts faster with PCL has been developed.[99] This rule, however, applies only to PCL and

is reliable only when primary alcohols lacking oxygen at the stereocentre are involved (Figure 18).

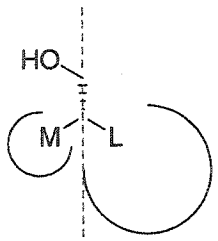

Figure 18 - Empirical rule that predicts which enantiomer of a primary alcohol reacts faster with PCL. The scheme shows the preferred enantiomer. M represents a medium sized substituent, e.g. CH_3, L is a large sized substituent, e.g. $CH_2C_6H_5$. The hydroxyl group points away from the viewer and the fast enantiomer is the one that has, once a line that passes through the bond defined by the chiral carbon atom and the methylene group alpha to it is drawn, the large substituent on the right hand side.

In developing this rule, Kazlauskas and Weissfloch proposed that the large and medium substituents at the stereocentre bind in the same hydrophobic pockets as secondary alcohols and the inversion of enantiopreference observed is due to the fact that the hydroxyl group points in opposite directions in the two cases.

1.9.3.5 X-ray crystal structures of transition state analogues

Lang *et al.*[58] solved the crystal structures of complexes PCL-phosphonate ester inhibitor covalently linked to Ser87 Oγ of PCL. The inhibitors used were R_C-(S_P)-1,2-dialkylcarbamoyl-glycero-3-*O*-*p*-nitrophenyl butyl phosphonate and R_C-(S_P)-1,2-dialkylcarbamoyl-glycero-3-*O*-*p*-nitrophenyl octyl phosphonate. The former underwent the so-called "aging" process in which part of the bound phosphonate was hydrolysed over time, and as a result only the R_C-trioctyl-complexed PCL structure was relevant for understanding the enzyme selectivity towards triglycerides. The structure highlighted well the binding pockets of the enzyme (Figure 19).

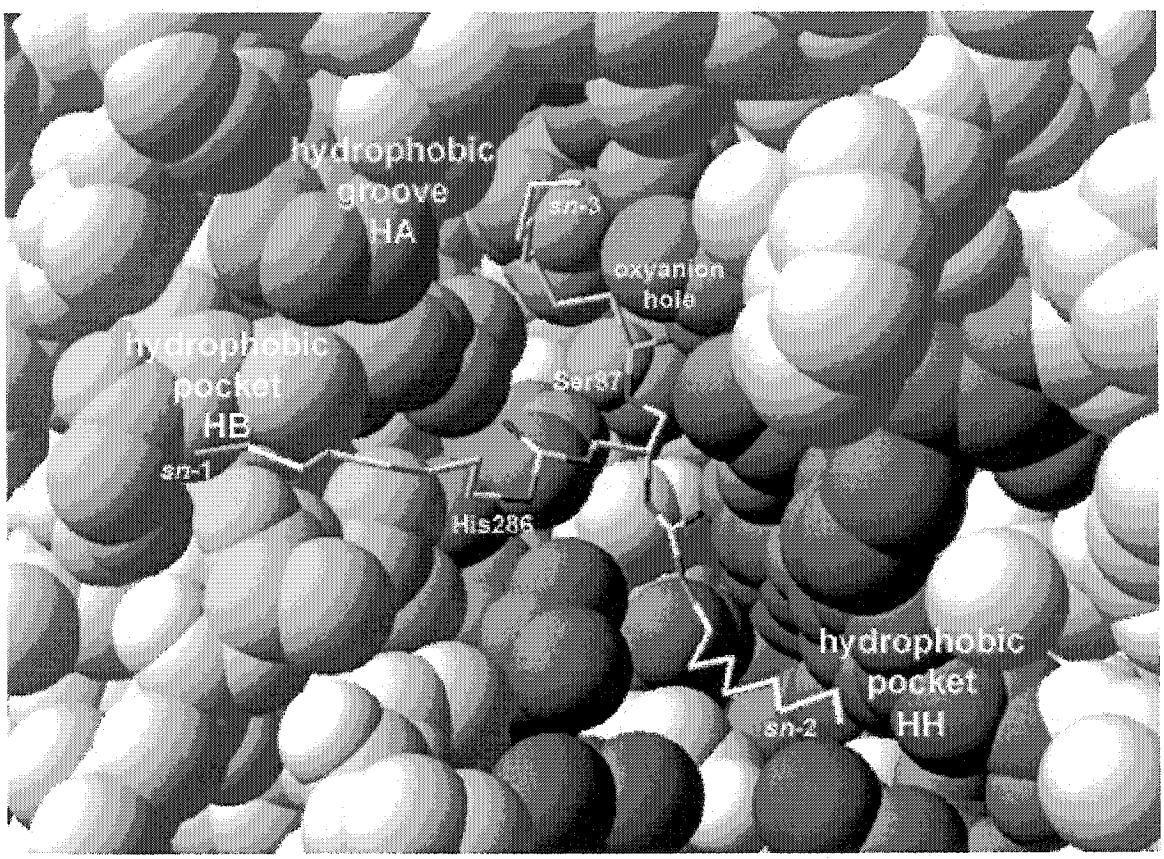

Figure 19 – PCL-trioctyl phosphonate complex (PDB ID 5LIP[58]). PCL is in spacefill representation while the phosphonate inhibitor is in stick representation. The hydrophobic groove HA is pink, the HH pocket is blue, the HB pocket yellow and the oxyanion hole in green. Catalytic Ser87 is orange and catalytic His286 pale ice-blue. Catalytic Asp264 is not visible. Figure prepared using Swiss PdbViewer v. 3.7.[51]

The *sn*-3 moiety of the triglyceride lays in the hydrophobic groove HA (8 x 10 Å, pink in Figure 19) formed by PCL hydrophobic residues 113, 119, 164, 167, 266 and 267 and forms van der Waals contacts with those residues. The HH pocket (blue in Figure 19), formed by residues 18, 23, 27, 29, 30, 146, 287 and 293, accommodates the *sn*-2 chain of the triglyceride while the HB hydrophobic pocket (residues 247, 248, 249, 250 and 251, yellow in Figure 19) binds the *sn*-1 moiety with a reduced number of hydrophobic interactions.

They did not solve the crystal structure of the complex between PCL and S_C-(S_P)-1,2-dialkylcarbamoyl-glycero-3-*O*-*p*-nitrophenyl octyl phosphonate but modelled it. They observed that the phosphonylalkyl chain of the S_C - trioctyl derivative was still bonded in the HA pocket although with the *sn*-1 chain (*sn*-3 in the R_C - trioctyl derivative), the *sn*-2

chain was in the HB pocket and the *sn*-3 moiety was in the HH pocket in spite of unfavourable interactions between its carbonyl group and the side chain of Leu287 and Ile290. They propose that these unfavourable interactions are responsible for the enantioselectivity of PCL towards the trioctyl derivative.

Unlike for secondary alcohols, fewer studies have been carried out for unravelling the molecular basis of lipase enantioselectivity towards chiral primary alcohols and, as for secondary alcohols, the origins of this enantioselectivity is still not clear, Table 5. Most propose L-alignment for fast and slow enantiomer, although the binding pockets where the large and medium group at the stereocentre are bonded differ. Different explanations for the enantiopreference of lipases towards primary alcohols are also reported.

Table 5 – Summary of the proposed molecular basis of lipase enantioselectivity towards primary alcohols.

Type of alcohol	Authors	Method[a]	Alignment	Enzyme and enzyme pockets	Explanation
No O at stereocentre	Zuegg *et al.*[95]	SsMcm	L-alignment	PCL - Fast enantiomer binds L in large and M in medium hydrophobic pockets; slow enantiomer binds L in large pocket and M is not well bonded	Better binding of fast enantiomer
	Tuomi & Kazlauskas[102]	MM	L-alignment	PCL - Fast enantiomer binds L in alternate hydrophobic pocket and M in medium hydrophobic pocket; slow enantiomer binds L in alternate hydrophobic pocket and M is not well bonded	Better binding of fast enantiomer
	Tomić *et al.*[103]	MM + MD	L-alignment	PCL - Fast enantiomer binds L in alternate hydrophobic pocket and M in medium hydrophobic pocket; slow enantiomer binds L in alternate hydrophobic pocket and M is not well bonded	Better H-bond Ser Oγ-His Nε2 for fast enantiomer + *Gauche* conformation
O at stereocentre	Zuegg *et al.*[95]	SsMcm	H-alignment	PCL - Fast enantiomer binds L in large and M in medium hydrophobic pockets; slow enantiomer binds L in medium pocket and M in large pocket	Steric strain for slow enantiomer because L is in medium pocket
	Tuomi & Kazlauskas[102]	MM	L-alignment	PCL - Fast enantiomer binds L in alternate hydrophobic pocket and M in medium hydrophobic pocket; slow enantiomer binds L in alternate hydrophobic pocket and M is not well bonded	Slow enantiomer resides longer in active site because of H-bond between O at stereocentre and Tyr29 OH.
In ring structure	Gentner *et al.*[104]	MM + MD	n.a.	PCL - Fast enantiomer deeper in "His-gap" than slow enantiomer	Fast enantiomer deeper in "His-gap"
Triacylglycerols	Lang *et al.*[58]	X-ray + MM	n.a.	PCL - Fast enantiomer in medium and alternate pocket	Sterics of slow enantiomer

[a] SsMcm = systematic search + Montecarlo minimisation; MM = Molecular Mechanics; MD = Molecular Dynamics.

1.10 Improving enzyme enantioselectivity

For synthetic purposes the enantioselectivity of an enzyme should be higher than 35.[34] One way of improving the enantioselectivity towards a particular compound is to screen rapidly as many biocatalysts as possible to find a better one. This may be a viable solution, however there are no guarantees that it will lead to a better catalyst with high enough enantioselectivity. An alternative is to optimise the reaction conditions, also known as "medium engineering". A third solution, "substrate engineering", involves slight modifications of the substrate. The next obvious strategy is "protein engineering" to alter the biocatalyst itself. Faber *et al.*[106] reviewed the enhancement of the selectivity of hydrolase reactions by medium, substrate and protein engineering.

1.10.1 Screening for finding a suitable biocatalyst

Testing commercially available enzymes by trial-and-error is one of the simplest approaches to find a suitable biocatalyst for kinetic resolutions. This lengthy process has been facilitated by the development, especially in the past few years, of high-throughput screening methods.[107] Screening has also been applied to the discovery of new biocatalysts prepared by protein engineering.

Janes *et al.*[108] screened commercially available hydrolases towards solketal butyrate. They monitored the reaction rate using a pH indicator, *p*-nitrophenol (PNP), in a solution buffered at pH 7.2. The decrease in absorbance at 404 nm is proportional to the protons released during the hydrolysis reaction (Figure 20). They measured the rate of hydrolase-catalysed hydrolysis of both (*R*) and (*S*)-solketal butyrate and obtained an estimate of the enzyme enantioselectivity from the ratio of these reaction rates. They were thus able to identify horse-liver esterase (HLE) as the enzyme with the highest E in the hydrolysis of solketal butyrate, albeit only 12. Because of the lack of competition between enantiomers for the enzyme active site the E values determined with this method are only an estimate of the real E.

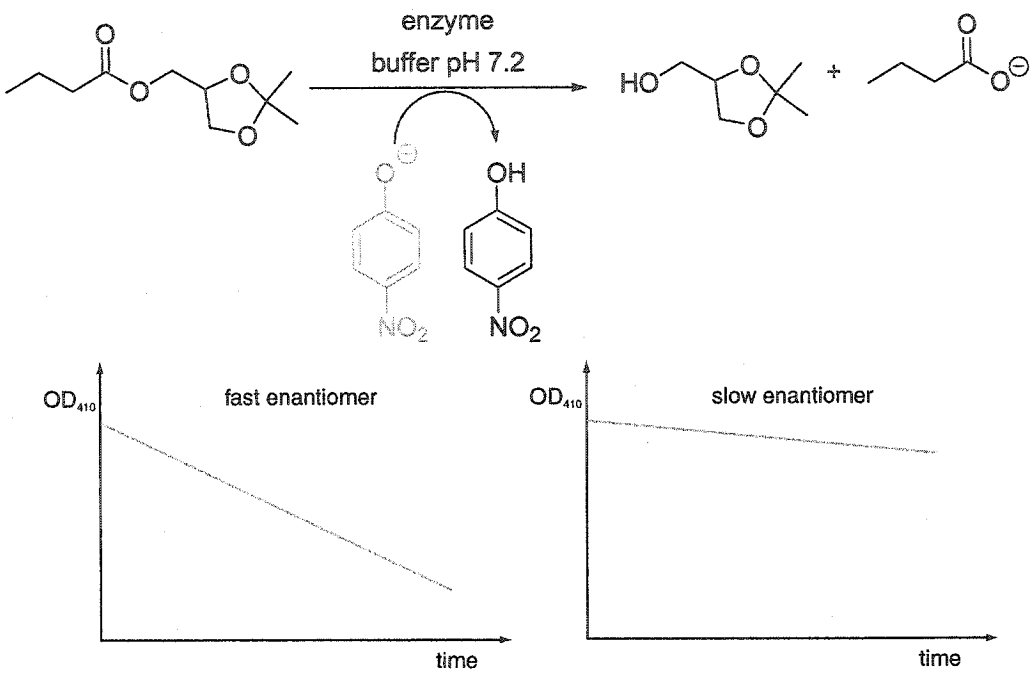

Figure 20 – "Estimated E" method used by Janes *et al.*[108] to identify a hydrolase enantioselective towards solketal butyrate.

Reetz *et al.*[109] used a similar spectrophotometry based system to screen libraries of mutants of *Pseudomonas aeruginosa* lipase (PAL) to find an improved catalyst for the resolution of 2-methyl decanoate. They synthesized pure enantiomers of the *p*-nitrophenyl ester of 2-methyl decanoate. They could thus detect the release of *p*-nitrophenyl ion in buffered solution at 410 nm and relate it to the speed of the reaction. By measuring the reaction rate of the lipase-catalysed hydrolysis of the two enantiomers separately, the ratio of the two rates yielded an estimated E value (Figure 21). As in the previous example, these E values are only an estimate of the real E because of the lack of substrate competition for the enzyme active site. Another limit of this method is the need of *p*-nitrophenyl esters of the substrate of interest to detect reaction rates because of the absence, in the reaction mixture, of a pH indicator.

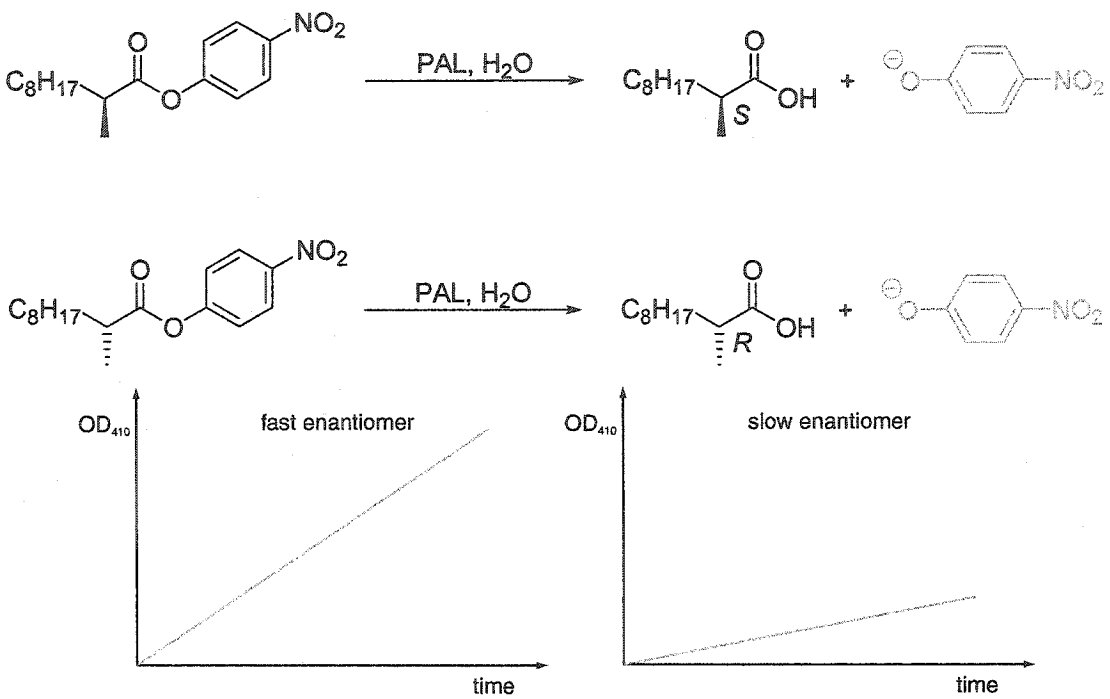

Figure 21 - High-throughput screening method used by the Reetz group for the discovery of improved mutants of PAL.[109] The release of the yellow *p*-nitrophenol ion allows for the measurement of the rate of hydrolysis of each enantiomer separately.

An improvement of this screening method came from Janes and Kazlauskas[110] with "Quick E". They reintroduced competition in the assay with the presence of a chromogenic reference compound, a resorufin ester (Figure 22). During a Quick E experiment the decrease in absorbance with time of a *p*-nitrophenol (PNP) pH indicator is monitored at 404 nm as it is protonated by the acid product of hydrolysis. This does not limit the possible substrates to *p*-nitrophenyl esters, thus the chirality can be either in the alcohol moiety, in the acyl chain or in both. The resorufin ester, which acts as reference compound, is hydrolysed by the lipase as well. Its rate of hydrolysis is monitored *via* its increase in absorbance at 574 nm (Figure 22).

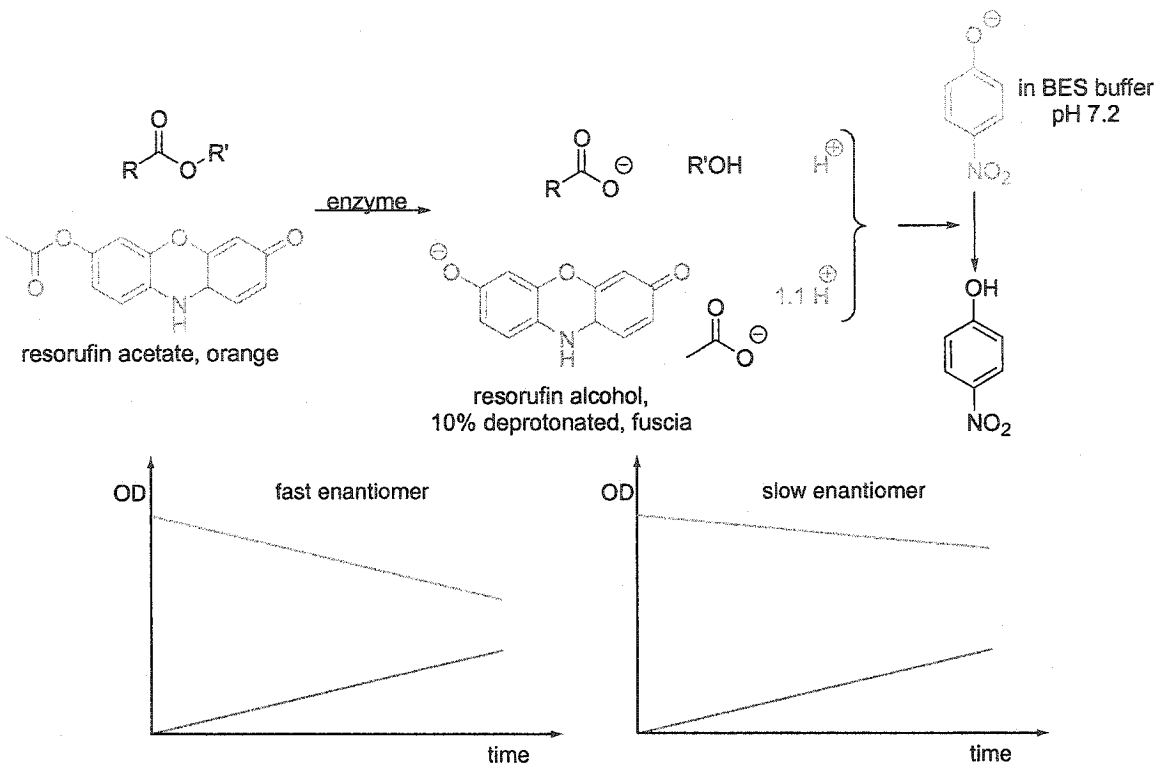

Figure 22 - Quick E scheme.[110] A resorufin ester (orange) acts as competitive substrate in the absence of the other enantiomer. The increase in absorbance (OD) of the resorufin alcohol (pink line) is monitored at 574 nm while at the same time the disappearance of the yellow color of the *p*-nitrophenyl ion is monitored at 404 nm.

After taking into account the contribution of the protons deriving from the hydrolysis of the reference compound (1 from the acid and 0.1 from the 10% deprotonated alcohol)[xiii] the rate of substrate hydrolysis can be determined. The rate of the reaction with the reference compound and with the substrate are expressed by equations 1.21 and 1.22:

$$\text{Rate}_{\text{reference compound}}\left(\frac{\mu\text{mol}}{\text{min}}\right)=\frac{dA_{574nm}}{dt}\times\frac{1}{\varepsilon_{574nm}\times l}\times V\times 10^{6} \qquad (1.21)$$

$$\text{Rate}_{\text{substrate}}\left(\frac{\mu\text{mol}}{\text{min}}\right)=\left(\frac{dA_{404nm}}{dt}\times\frac{1}{\Delta\varepsilon_{404nm}\times l}\times V\times 10^{6}\times \text{Q}\right)-1.1\left(\text{Rate}_{\text{reference compound}}\right) \qquad (1.22)$$

[xiii]Resorufin pKa being 8.15, 10% of the resorufin released from the hydrolysis of its acetate is deprotonated in the assay solution at pH 7.2.

Where

dA_{404nm}/dt and dA_{574nm}/dt = change in absorbance with time at 404 nm and 574 nm respectively,

ε_{574nm} = extinction coefficient of resorufin alcohol at 574 nm in $M^{-1}cm^{-1}$,

$\Delta\varepsilon_{404nm}$ = difference in extinction coefficient between protonated and deprotonated forms of *p*-nitrophenol at 404 nm in $M^{-1}cm^{-1}$,

l = pathlength in cm,

V = reaction volume in L,

$Q = \frac{[BES]}{[PNP]} + 1$ [xiv],

[PNP] = concentration of *p*-nitrophenol,

[BES] = concentration of BES buffer.

The enantioselectivity of the enzyme is then calculated as the ratio of the rate of the fast over the slow enantiomer, keeping into account the concentrations of reference compound and substrate for both reactions:

$$E = \frac{\left(\frac{Rate_{substrate1}}{Rate_{reference1}} \times \frac{[reference1]}{[substrate1]}\right)}{\left(\frac{Rate_{substrate2}}{Rate_{reference2}} \times \frac{[reference2]}{[substrate2]}\right)} \qquad (1.23)$$

The Quick E screening method was used to carry out the research described in Chapter 5.

1.10.2 Increasing E by medium engineering

Many factors related to the reaction medium can affect lipase enantioselectivity. Among these factors are solvent type, pH, temperature, water content, ionic strength of

---

[xiv] The buffer factor Q accounts for protons that are picked up by the BES buffer (BES and *p*-nitrophenol have the same pKa) and therefore are not detected with the decrease in absorbance at 404 nm. A previous publication[110] defines Q as [BES]/[PNP], which is true only when [BES]>>[PNP]. When this condition is not met the buffer factor is better described as [BES]/[PNP] + 1.

the medium and presence of additives. Being able to control and predict them would allow for an easy way to improve the performance of a biocatalyst.

1.10.2.1 Solvent effect

Kinetic resolutions in organic solvents are common and some researchers have tried to relate enzyme enantioselectivity and solvent characteristics. One of the most investigated solvent characteristics is the hydrophobicity, expressed in terms of partition coefficient P. If we consider the partition coefficient P of a solvent between 1-octanol and water, some researchers found that a logP > 2 indicates a good solvent for a kinetic resolution,[111] while others observed the opposite effect,[112] although in some cases there is no clear relationship between logP and enzyme E.[113,114] Sometimes not only the E of the enzyme is increased, but its enantiopreference is also reversed.[115] One explanation refers to the possibility of solvent molecules to bind in the enzyme active site thus causing different interactions of the enzyme with the two substrate enantiomers. Others propose that the substrate may be solvated differently in different solvents having different logP.[114] Finally, the solvent could affect the enzyme conformation and its interactions with the substrate, thus the enantioselectivity.

Other solvent characteristics that have been investigated include the dielectric constant and the dipole moment. In particular, the lower dielectric constant of organic solvents compared to water determines the formation of intramolecular electrostatic interactions, thus a decrease in flexibility of the enzyme.

Counter ions are also important when considering an enzymatic reaction. Halling emphasises that enzymes should not be considered as a single entity.[116] In fact, charged amino acids are usually associated with counter-ions, unless they are forming intramolecular ion-pairs. The characteristics of counter-ions are closely related to the acid-base properties of proteins because of their influence in the protonation state of the enzyme. Okamoto and Ueji[117] improved significantly (from 4 to 200) the enantioselectivity of CRL in the esterification of 2-(4-ethyl-phenoxy)-propanoic acid with butanol in di-isopropyl ether by the addition of water containing alkaline metal ions such as LiCl. Kinetic experiments demonstrated a significant enhancement of the reaction rate of the favourite enantiomer versus a slight inhibition of the reaction rate for the slow enantiomer upon the addition of LiCl containing water to di-isopropyl ether as compared

to the addition of only water. One possible explanation is the formation of tight ion-pairs in a low dielectric media like ether. Rariy and Klibanov[118] also reported an increase in protein refolding yields in organic solvents upon addition of LiCl, which may occur through "salting-in" of protein that otherwise would irreversibly form aggregates.

Enzyme catalysed reactions can also be performed in ionic liquids (ILs).[119] ILs are organic salts that remain liquid at room temperature because of the bad packing of their ions. Schöfer *et al.*[120] tested 9 lipases and 2 esterases in the enantioselective esterification of (±)-1-phenylethanol with vinyl acetate in several commercially available ionic liquids. While CAL-B performed equally well in the reference organic solvent *tert*-butyl methyl ether (*t*-BME) and in several different ILs, the enantioselectivity of a *Pseudomonas* sp. lipase and an *Alcaligenes* sp. lipase was significantly increased in ILs. In particular *Pseudomonas* sp. lipase passed from about E = 30 in *t*-BME to E > 200 in 1-butyl-3-methylimidazolium (BMIM) based ILs such as [BMIM]CF_3SO_3 and [BMIM]$(CF_3SO_2)_2N$ while *Alcaligenes* sp. lipase performed better in 1-methyl-3-octylimidazolium trifluoroborate [OMIM]BF_4 (E > 200).

Ottosson *et al.*[38], after a thermodynamic analysis of CAL-B enantioselectivity towards 3-methyl-2-butanol in 9 different solvents suggested a correlation between enantioselectivity and solvent size. They plotted CAL-B enantioselectivity at 298 K as a function of the van der Waals volume of the solvent and noticed a direct correlation between them. The larger the solvent, the larger the E.

1.10.2.2 Temperature effect

One of the oldest known means to control a reaction is through temperature manipulation. That temperature changes affect enantioselectivity is not surprising if one thinks of the correlation between E and $\Delta\Delta G^{\ddagger}$ (equation 1.16). Secundo *et al.*[121] doubled the enantioselectivity of PCL (from 17 to 32) in the esterification of racemic (3-bromo-4,5-dihydro-isoxazol-5-yl)-methanol with trifluoroethyl butyrate by lowering the temperature from 65°C to 22°C.

Since $\Delta\Delta G^{\ddagger} = \Delta\Delta H^{\ddagger} - T\Delta\Delta S^{\ddagger}$, by knowing $\Delta\Delta H^{\ddagger}$ and $\Delta\Delta S^{\ddagger}$ it is possible to determine the temperature at which there is no enantioselectivity, which corresponds to $\Delta\Delta G^{\ddagger} = 0$. This temperature is known as "racemic temperature"[122] and is given by:

$$T_{rac} = \frac{\Delta\Delta H^{\ddagger}}{\Delta\Delta S^{\ddagger}} \qquad (1.24)$$

The activation enthalpy difference $\Delta\Delta H^{\ddagger}$ determines the stereochemical outcome of reactions performed at temperatures below T_{rac}. A further decrease in temperature yields increased enantioselectivity. On the other hand at temperatures above T_{rac} it is the difference in activation entropy $\Delta\Delta S^{\ddagger}$ that determines the enzyme enantioselectivity. In this case, an increase in temperature is accompanied by an increase in enantioselectivity. Phillips[123] reported that the enantioselectivity of SADH (secondary alcohol dehydrogenase) from *Thermoanaerobacter ethanolicus* in the oxidation of secondary alcohols is temperature dependent. At temperature below T_{rac} one enantiomer was favoured while at temperatures higher than the T_{rac} the other was preferentially oxydised.

Although temperature modulation may not be sufficient for increasing dramatically the enantioselectivity of an enzyme catalysed reaction,[123] it is certainly a means to fine-tune it.

1.10.3 Increasing E by substrate engineering

Modification of the substrate structure has also been used as a strategy to improve enantioselectivity. Different approaches involve the modification of the substrate near the stereocentre, far from it, or at the acyl chain.

To improve lipase enantioselectivity towards secondary alcohols some researchers have increased the size of one substituent at the stereocentre compared to the other, according to the empirical rule proposed by Kazlauskas *et al.*[91] Acetates of the allylic secondary alcohols 2-cyclopentenol, 2-cyclohexenol and 2-cycloheptenol are poorly resolved by PCL (E ~ 1). Gupta and Kazlauskas[124] showed that increasing the size of one of the substituents at the stereocentre by introducing bromine in position 2 significantly increased the enantioselectivity of PCL. Thus 2-bromocyclopentyl acetate was hydrolysed by PCL with E = 80. The same enzyme hydrolysed 2-bromocyclohexenyl acetate and 2-bromocycloheptenyl acetate with E > 100.

Ueji *et al.*[125] recently showed that both steric and electronic effects control the enantioselectivity of lipase-catalysed esterifications. They investigated the lipase

catalysed esterification of 2-(4-substituted phenoxy)propionic acids with *n*-butyl alcohol where the substituents in para position of the benzyl ring were H, F, Cl, CF_3 and CH_3. They obtained the lowest enantioselectivity (E = 1.5) with F and the highest with CH_3 (E = 27). They proposed that an increase in the size of the substituent may determine a better binding of the substrate in the large binding pocket of the enzyme, while electron-withdrawing groups, which lower the π electron-density of the substrate, may decrease the stabilisation due to CH-π interactions between the enzyme active site and π electrons of the substituent. Rotticci *et al.*[126] have also observed electronic effects in enzymatic resolutions: while CAL-B can efficiently resolve 3-nonanol by esterification with vinyl butyrate (E = 200), it shows poor enantioselectivity towards 1-bromo and 1-chloro-2-octanol (E = 6.5 and 14 respectively).

A method called *active-site-directed transient chemical modification*[127,128] allows transforming the enzyme into an acyl-enzyme that can exert some stereocontrol in the transesterification reaction. By changing acylating agent researchers have improved the enantioselectivity of lipases. Miyazawa *et al.*[129] increased the E of lipase AL towards 2-phenoxy-1-propanol from 1.4 to 36 by passing from vinyl trifluoroacetate to vinyl pentanoate as acylating agent. Chiral acyl donors have also been used.[130]

1.10.4 Protein engineering

Natural enzymes are not well suited for industrial applications. Over millennia they have evolved to become extremely specialised for carrying out highly particular functions in living organisms. To improve their performance in non-natural reactions they can be genetically altered. This implies the use of recombinant DNA technologies, which allow modifying the protein genetic code either site-specifically or randomly. The gene coding for the protein of interest has to be available and has to be cloned and inserted in a suitable vector before carrying out the necessary transformations. Vectors or plasmids are circular pieces of DNA extensively used in molecular biology manipulations such as site directed mutagenesis, directed evolution and protein over-expression. Vectors generally contain the following elements (Figure 23):

Promoter: a DNA sequence necessary for the binding of the RNA polymerase in order to initiate transcription of the gene.

Inducible elements: DNA sequences of extreme importance that act together with the promoters by binding either repressors or inducers to induce or repress the transcription at will.

Transcriptional termination sequences: in prokaryotes, these sequences signal the RNA polymerase when to release the DNA template and stop the synthesis of mRNA.

Origin of replication: a DNA sequence that binds the DNA polymerase in order to generate an exact copy of the original plasmid.

Affinity purification tag: a useful DNA sequence which codes for six to eight consecutive histidines that, once fused with the protein of interest, can facilitate protein purification by binding to a nickel column.

Multiple cloning sites (MCS or Polylinker): MCS are synthetic DNA sequences that code for restriction endonucleases recognition sites. These sites are very useful for cutting the DNA template at a specific position within the vector.

Selectable markers: provide a very useful means of selecting, by growth, only the cells that contain the vector. While drug resistance markers enable cells to detoxify an exogenously added drug that would otherwise kill them, auxotrophic markers allow cells to synthesize an essential component (usually an amino acid) in media that do not contain it.

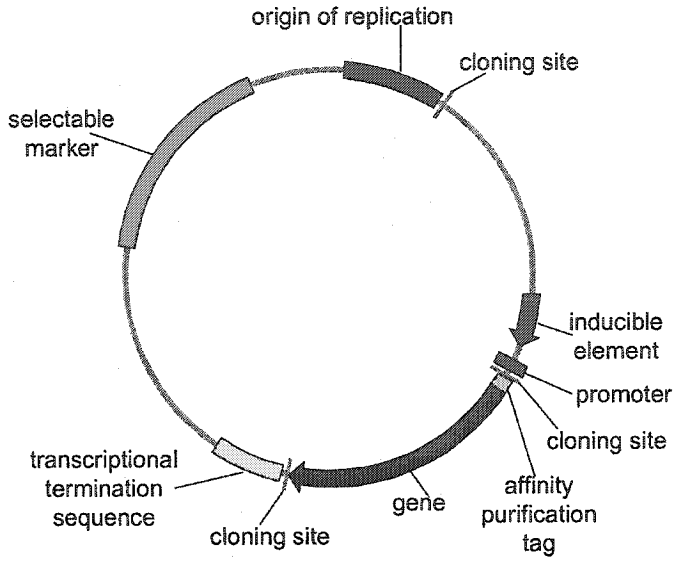

Figure 23 – Scheme of typical vector/plasmid used in protein engineering.

1.10.4.1 Rational protein design

This approach requires not only the availability of the protein gene, but also a detailed knowledge of the protein structure (X-ray, NMR or homology model), function and mechanism. Mutations are then introduced by site-directed mutagenesis.[131]

A very common and simple method used to introduce point mutations in a protein by site-directed mutagenesis is shown in Figure 24. Both forward and reverse primers containing the desired mutation are used to amplify plasmid DNA carrying the gene of interest by polymerase chain reaction (PCR). Methylated parental plasmid has to be used so that, after the PCR reaction has been carried out, the restriction enzyme *Dpn* methylase can be used to destroy the template plasmid leaving the mutated plasmids unaffected. The latter can thus be transformed into *Escherichia coli* (*E. coli*) or other hosts.

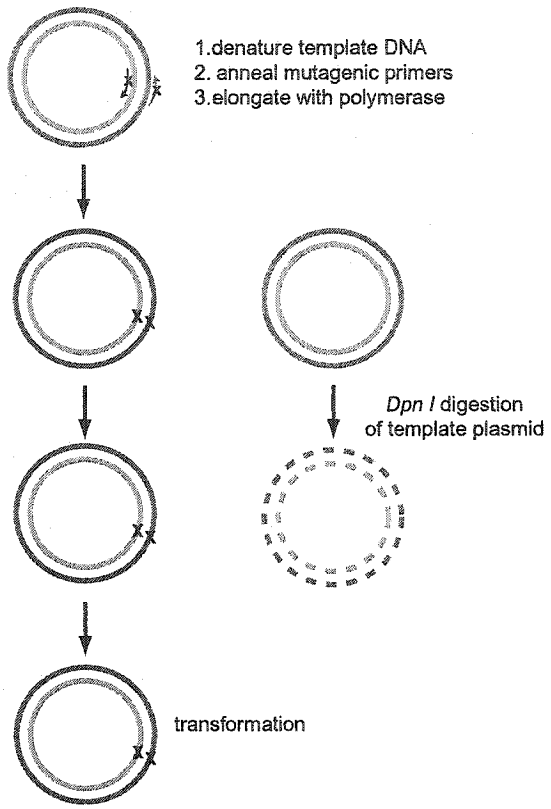

Figure 24 – Site directed mutagenesis experiment scheme. Adapted from Braman *et al.*[132]

Because we do not yet possess the means for unravelling exactly how every amino acid in a protein sequence affects enzymatic functionality, it is extremely difficult to use rational design for performance improvement. To increase the enantioselectivity of CAL-B towards halohydrins, Rotticci *et al.*[126] used molecular modelling and identified important residues in the enzyme stereoselectivity pocket. Using this information they mutated Ser47 to Ala and doubled the enantioselectivity of CAL-B for 1-bromo-2-octanol and 1-chloro-2-octanol.

An extension of site-directed mutagenesis is site-saturation mutagenesis, where all the possible amino acids are introduced at one position. It is performed exactly like site-directed mutagenesis, but the primers contain degenerate sequences. This generates all possible mutants at one position and permits the identification of the best amino acid replacement for that position. This method has been used to generate mutant libraries of *Bacillus thermocatenulatus* lipase 2 (BTL2) as described in Chapter 5.

1.10.4.2 Directed evolution

Evolution, a process by which proteins that now catalyse very different reactions have evolved from the same ancestor by random mutations, recombination and selection, can be carried out in the laboratory within a short time frame. The difference between evolution as it occurs in Nature and directed evolution is that the former is directed towards survival, while the latter is driven by a specific need.

The width of protein sequence space is very large: from 20 different naturally occurring amino acids, there are 20^{400} ways to form a 400 amino acid long protein. Since most of this space is devoid of function and beneficial mutations are very rare, the strategy used must be well thought. It is believed that protein evolution for practical applications is best done according to Nature, by random mutations, to a protein with an activity close to the desired one.[133]

For a successful directed evolution experiment a few elements are needed:

1. expression of the enzyme in a suitable microbial host
2. availability of a screening method
3. workable evolutionary strategy[134]

A typical directed evolution experiment is exemplified in Figure 25 and consists in the following steps:

1. gene selection
2. creation of a library of mutants (usually by error-prone PCR)
3. insertion of the gene library in a suitable expression vector
4. transformation of the vector into the bacteria
5. screening/selection of colonies for the property of interest
6. isolation of the genes and their use for other rounds of mutagenesis (back to step 2.)

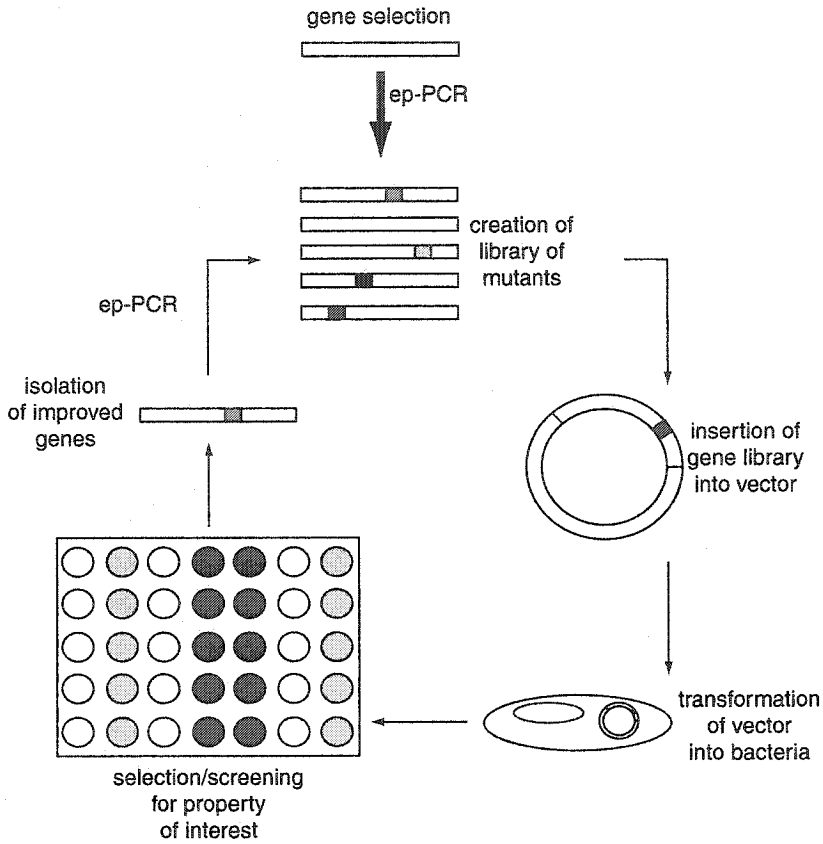

Figure 25 – Scheme of directed evolution experiment.

Methods to generate mutant libraries by directed evolution are divided in two categories: asexual and sexual methods. While asexual methods involve the introduction of random mutations in one gene of choice, sexual methods entail the combination of several different genes *in-vitro*.

Asexual methods for generating libraries of mutant enzymes

There are two general methods for inducing random mutations in a gene. One is solely based on the intrinsic error frequency of the polymerase. *Taq* DNA polymerase lacks the proofreading capability of other polymerases and has a mutation rate, under the standard conditions used for PCR, of 5.5×10^{-4} mutations per base pair (bp).[135, 136] This corresponds, in a PCR of 25 cycles, to a total error rate of approximately 0.1%, which in a 1200 DNA bases long gene, coding for 400 amino acids, represents 1 DNA base. For a mutation rate of one amino acid substitution per gene, about 2 to 5 DNA bases

substitutions are needed due to the degeneracy of the genetic code. Thus the mutation rate of *Taq* DNA polymerase in the standard PCR may not be sufficiently high for directed evolution experiments.

A second method, error prone PCR[137,138,139,140,141] (ep-PCR), is based on the increase of the mutation rate of *Taq* DNA polymerase by the use of high nucleotide concentrations, by high bivalent magnesium concentration and by the presence of bivalent manganese.[142] While magnesium bivalent ions stabilise non-complementary pairs, the effect of manganese bivalent ions is more complex. Goodman *et al.*[143] after kinetic studies and K_M measurements, suggested that the action of Mn^{2+} is primarily to cause a large decrease in the K_M of the mismatched nucleotide for the polymerase-template complex. This engenders an increase of the time that a mismatched nucleotide resides on the complex relative to a matched one, which in turn allows for an increased frequency of misinsertion. There is also evidence for the loss of proofreading specificity. Both effects are due to the ability of the nucleotides to assume distorted configurations at the polymerase insertion and excision active sites in the presence of Mn^{2+}, which results in increased non-specific enzyme-substrate binding forces. Error rates range from 0.11 to 2%.[137,140,141,143] Three different ep-PCR sets of conditions, yielding three different mutation rates of 1 to 2, 2 to 5 and 5 to 7 base substitutions per 1000 bp have been published.[142]

It must be emphasised that, despite the name, random mutagenesis is not really random. Because of the degeneracy of the genetic code, with single base mutations only an average of 5.7 amino acids can be accessed from any given residue.[144] To access all the amino acids it is necessary to change two nucleotides in the same codon. At the mutation rates used this is practically impossible. Thus there is not an equal probability of substituting any one of the twenty amino acids for another using random mutagenesis. Hence while ep-PCR may identify important residues in the protein of interest, it may not replace them with the best amino acid for the given goal. A solution consists in using saturation mutagenesis, a method for generating all the 20 possible amino acids at a precise position in the protein gene, to mutate the position identified by ep-PCR.

Liebeton *et al.*[145] evolved a lipase from *Pseudomonas aeruginosa* (PAL) to catalyse the hydrolysis of 2-methyldecanoic acid *p*-nitrophenyl ester with high enantioselectivity.

After screening about 30,000 mutants, they achieved E = 25.8 from an initially non-selective enzyme by successive rounds of random mutagenesis and saturation mutagenesis. The best mutant contained five amino acid substitutions and all of them were located outside the active site. Four out of the five new amino acids were glycines. Moreover, all the substitutions were near loops involved in the transition between the open and the closed conformation of PAL, which led the authors to hypothesise an increased flexibility of the enzyme directly related to its enantioselectivity.

Sexual methods for generating libraries of mutant enzymes

Sexual methods require the availability of several genes of high identity that can be mixed together to generate diversity. DNA-shuffling was the first method described for this kind of *in-vitro* recombination.[146, 147] Several homologous DNA sequences are first amplified to yield a large amount of genetic material. These genes are then fragmented by digestion with a restriction endonuclease such as *Dnase I* to give a number of small random DNA fragments (10-50 bp). Recombination occurs because one fragment that originates from one gene may anneal to a fragment coming from a different gene. PCR is then used to reconnect these new genes (Figure 26).

Numerous other methods have arisen form this original technique, such as staggered extension[148], random-priming recombination[149] and heteroduplex recombination.[150]

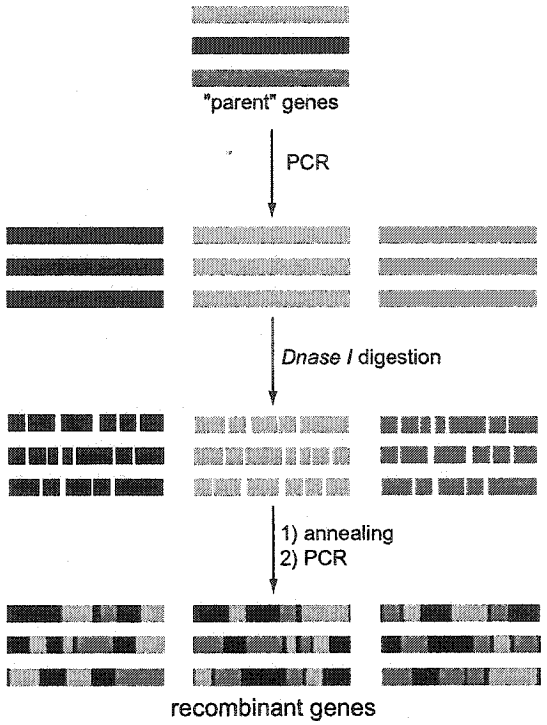

Figure 26 - Scheme of DNA shuffling to generate recombinant genes. Initially, "parent" genes, of high sequence identity, are chosen. They are amplified by PCR, then digested with Dnase I to produce small DNA fragments. They are then re-connected based on the complementary cohesive ends and re-sealed by PCR in the absence of primers.

1.11 Origins of *Pseudomonas cepacia* lipase enantioselectivity towards chiral primary alcohols – thesis outline

Currently there is still controversy on the molecular basis of lipases enantioselectivity towards chiral primary alcohols. Scientists have tackled the problem by kinetic methods and modelling.

In this thesis, the enantioselectivity of PCL towards chiral primary alcohols is explained *via* structural studies of transition state analogues, kinetic measurements and combined QM/MM modelling experiments.

Chapter 2 considers chiral primary alcohols without oxygen at the stereocentre while Chapter 3 studies two different primary alcohols, both having an oxygen atom at the stereocentre: 2-phenoxy-1-propanol, which does not follow a simple empirical rule (section 1.9.3.4),[99] and solketal, which follows it. Using a combination of the three methods above we explain the opposite enantiopreference of the enzyme for primary and secondary alcohols and show that the enantioselectivity of PCL towards these substrates

rests on both the better hydrogen bond between catalytic His286 Nε2 and the alcohol oxygen of the fast enantiomer and on a sum of small interactions enzyme-substrate.

In Chapter 4 we exploit PCL interfacial activation and we achieve for the first time a highly enantioselective kinetic resolution of esters of 2-methyl-3-benzyl-1-propanol and 2-phenoxy-1-propanol by medium and substrate engineering.

In Chapter 5 we try to exploit our findings on the molecular basis of lipase enantioselectivity towards chiral primary alcohols to engineer a lipase structurally related to PCL with the goal of improving its enantioselectivity towards chiral primary alcohols.

References

[1]Gardner, M. *The new ambidextrous universe*, W.H. Freeman & Co: New York, NY, **1992**; Chapter 10.

[2]Guiffre, P. *Pour La Science* **1994**, 84-88.

[3]Gros, C.; Boni, G. *L' Actualité Chimique* **1995**, *3*, 9-15.

[4]Shakespeare, W. *A midsummer-night's dream*, Act 4, Scene 1.

[5]Weyer, J. *Angew Chem. Int. Ed.* **1974**, *13*, 591-598.

[6]Pasteur, L. *Compt. Rend. Acad. Sci.* **1849**, *29*, 297-300.

[7]Pasteur, L. *Ann. Chim. Phys.* **1850**, *28*, 56-99.

[8]Suh, I.-H.; Park, K. H.; Jensen, W. P.; Lewis, D. E. *J. Chem. Edu.* **1997**, *74*, 800-805.

[9]Roberts, R.M. *Serendipity. Accidental discoveries in science*, J. Wiley & Sons: New York, NY, **1989**; pp 59-65.

[10]Le Bel, J. A. *Bull. Soc. Chim. Paris* **1874**, *22*, 337-347.

[11]Drayer, D. E. *Clin. Pharmacol.* **1993**, *18*, 1-24.

[12]Enders, D. *Chemtech* **1981**, *11(8)*, 504-513.

[13]Winter, W.; Frankus, E. *Lancet* **1992**, *339*, 365.

[14]Crosby, J. *Tetrahedron* **1991**, *47*, 4789-4846.

[15]Elliott, M.; Farnham, A. W.; Janes, N.F.; Needham, P. H.; Pulman, D. A. *Nature* **1974**, *248*, 710-711.

[16]Elliott, M.; Farnham, A. W.; Janes, N. F.; Soderlund, D. M. *Pestic. Sci.* **1978**, *9*, 112-116.

[17]Drayer, D. E. *Clin. Pharmacol. Ther.* **1986**, *40*, 125-133.

[18]Cotzias, G.C.; Papavasiliou, P. S.; Gellene, R. *N. Engl. J. Med.* **1969**, *280*, 337-345.

[19]Ariëns, E. J. In *Chiral separations by HPLC*; Krstulovic, A. M., Ed.; Ellis Horwood Series in Medicinal Chemistry; Ellis Horwood: Chichester, West Sussex, UK; **1989**, Chapter 2, p. 31.

[20]Hauck, R.- S.; Wegner, C.; Blumtritt, P.; Fuhrhop, J. - H.; Nau, H. *Life Sci.* **1990**, *46*, 513-518.

[21]White, P. F.; Ham, J.; Way, W. L.; Trevor, A. J. *Anesthesiology* **1980**, *52*, 231-239.

[22]Sugavanam, B. *Pestic. Sci.* **1984**, *15*, 296-302.

[23]Glatt, H.; Oesch, F. *Biochem. Pharmacol.* **1985**, *34*, 3725-3728.

[24] http://www.fda.gov/cder/guidance/stereo.htm

[25]Rouhi, A. M. *C. & E.N.* **2002**, *80*, 43-50.

[26]Rudolph, J.; Hannig, F.; Theis, H.; Wischnat, R. *Org. Lett.* **2001**, *3*, 3153-3155.

[27]Vicario, J.L.; Badia, D.; Carrillo, L. *Tetrahedron: Asymmetry* **2003**, *14*, 489-495.

[28]Pasteur, L. *Compt. Rend. Acad. Sci.* **1858**, *46*, 615-618.

[29]Pasteur, L. *Compt. Rend. Acad. Sci.* **1860**, *48*, 298-299.

[30]Patel, R.N.; Howell, J. M.; McNamee, C. G.; Fortney, K. F.; Szarka, K. F. *Biotechnol. Appl. Biochem.* **1992**, 34-47.

[31]Larsson, A. L. E.; Persson, B. A.; Bäckvall, J.-E. *Angew. Chem. Int. Ed.* **1997**, *36*, 1211-1212.

[32]Persson, B. A.; Larsson, A. L. E.; Le Ray, M.; Bäckvall, J.-E. *J. Am. Chem. Soc.* **1999**, *121*, 1645-1650.

[33]Choi, J. H.; Kim, Y. H.; Nam, S. H.; Shin, S. T.; Kim, M.- J.; Park, J. *Angew. Chem. Int. Ed.* **2002**, *41*, 2373-2376.

[34]Faber, K. *Biotransformations in organic chemistry*, 2nd ed., Springer-Verlag: Berlin, Heidelberg, New York; **1995**, pp. 32-38.

[35]Michaelis L., Menten M.L. *Biochem. Z.* **1913**, *49*, 333-369.

[36]Hein, G.E.; Neimann, C. *J. Am. Chem. Soc.* **1962**, *84*, 4487-4494.

[37]Chen, C. - S.; Fujimoto, Y.; Girdaukas, G.; Sih, C. J. *J. Am. Chem. Soc.* **1982**, *104*, 7294-7299.

[38]Ottosson, J.; Fransson, L.; King, J. W.; Hult, K. *Biochim. Biophys. Acta* **2002**, *1594*, 325-334.

[39]Pandley, A.; Benjamin, S.; Soccol, C. R.; Nigam, P.; Krieger, N.; Soccol, V. T. *Biotechnol. Appl. Biochem.* **1999**, *29*, 119-131.

[40]Undurraga, D.; Markovits, A.; Erazo, S. *Process Biochem.* **2001**, *36*, 933-939.

[41]http://www.novozymes.com

[42]Murzin, A.G.; Brenner, S. E.; Hubbard, T.; Chothia, C. *J. Mol. Biol.* **1995**, *247*, 536-540.

[43]http://scop.berkeley.edu

[44]Schrag, J. D.; Cygler, M. *Methods in Enzymology* **1997**, *284*, 85-107.

[45]Ollis, D.L.; Cheah, E.; Cygler, M.; Dijkstra, B.; Frolow, F.; Franken, S. M.; Harel, M.; Remington, S. J.; Silman, I.; Schrag, J.D. *Prot. Eng.* **1992**, *5*, 197-211.

[46]Faber, K. *Biotransformations in organic chemistry*, 2nd ed., Springer-Verlag: Berlin, Heidelberg, New York; **1995**, pp. 94-95.

[47]Brzozowski, A. M.; Derewenda, U.; Derewenda, Z. S.; Dodson, G. G.; Lawson, D. M.; Turkenburg, J. P.; Bjorkling, F.; Huge-Jensen, B.; Patkar, S. A.; Thim, L. *Nature* **1991**, *351*,491-4941.

[48]Derewenda, U.; Brzozowski, A. M.; Lawson, D. M.; Derewenda, Z. S. *Biochemistry* **1992**, *31*, 1532-1541.

[49]Brady, L.; Brzozowski, A. M.; Derewenda, Z. S.; Dodson, E.; Dodson, G.; Tolley, S; Turkenburg, J. P.; Christiansen, L.; Huge-Jensen, B.; Norskov, L.; Menge, U. *Nature*, **1990**, *343*, 767-770.

[50]Brzozowski, A. M.; Derewenda, Z. S.; Dodson, E. J.; Dodson, G. G.; Turkenburg, J. P. *Acta Crystallogr.* **1992**, *B48*, 307-319.

[51]Guex, N.; Peitsch, M. C. *Electrophoresis* **1997**, *18*, 2714-2723.

[52]Peters, G. H.; Bywater, R. P. *Biophys. J.* **2001**, *81*, 3052–3065.

[53] Uppenberg, J.; Hansen, M. T.; Patkar, S.; Jones, T.A. *Structure*, **1994**, *2*, 293-308.

[54]Martinelle, M.; Holmquist, M.; Hult, K. *Biochim. Biophys. Acta* **1995**, *1258*, 272 - 276.

[55]Fersht, A. *Enzyme, structureand mechanism*; Freeman: San Francisco, **1977**.

[56]Kraut, J. *Science* **1988**, *242*, 533-540.

[57]Cygler, M.; Grochulski, P.; Kazlauskas, R. J.; Schrag, J. D.; Bouthillier, F.; Rubin, B.; Serreqi, A. N.; Gupta, A. K. *J. Am. Chem. Soc.* **1994**, *116*, 3180-3186.

[58]Lang, D. A.; Mannesse, M. L. M.; de Haas, G. H.; Verheij, H. M.; Dijkstra, B. W. *Eur. J. Biochem.* **1998**, *254*, 333-340.

[59]Nishizawa, K.; Ohgami, Y.; Matsuo, N.; Kisida, H., Hirohara, H. *J. Chem. Soc. Perkin Trans. 2* **1997**, 1293-1298.

[60]Hu, C.-H.; Brinck, T.; Hult, K. *Int. J. Quantum Chem.* **1998**, *69*, 89-103.

[61]Rupert C. Wilmouth, R. C.; Edman, K.; Neutze, R.; Wright, P. A.; Clifton, I.J.; Schneider, T. R.; Schofield, C. J.; Hajdu, J. *Nature Structural Biol.* **2001**, *8*, 689-694.

[62]Schrag, J. D.; Li, Y.; Cygler, M.; Lang, D.; Burgdorf, T.; Hecht, H.-J.; Schmid, R.; Schomburg, D.; Rydel, T. J.; Oliver, J. D.; Strickland, L. C.; Dunaway, C. M.; Larson, S. B.; Day, J.; McPherson, A. *Structure* **1997**, *5*, 187-202.

[63]Kim, K. K.; Song, H. K.; Shin, D. H.; Hwang, K. Y.; Suh, S. W. *Structure* **1997**, 5, 173-185.

[64]Humphrey, W.; Dalke, A.; Schulten, K. *J. Mol. Graphics* **1996**, *14.1*, 33-38.

[65]Pauling, L. *Am. Sci.* **1948**, *36*, 50-58.

[66]Mader, M. M.; Bartlett, P. A. *Chem. Rev.* **1997**, *97*, 1281-1301.

[67]Wolfenden, R. *Acc. Chem. Res.* **1972**, *5*, 10-18.

[68]Jackson, D.S.; Fraser, S. A.; Ni, L.-M.; Kam, C.-M.; Winkler, U.; Johnson, D. A.; Froelich, C. J.; Hudig, D.; Powers, J.C. *J. Med. Chem.* **1998**, *41*, 2289-2301.

[69]Gillespie, S. G.; Lau, S. L.; Paulson, S. C. *Phosphorus, sulfur, and silicon* **1997**, *122*, 205-208.

[70]Tramontano, A.; Ivanov, B.; Gololobov, G.; Paul, S. *Appl. Biochem. Biotechnol.* **2000**, *83*, 233-243.

[71]Stadler, P.; Zandonella, G.; Haalck, L.; Spener, F.; Hermetter, A.; Paltauf, F. *Biochim. Biophys. Acta* **1996**, *1304*, 229-244.

[72]Mannesse, M. L. M.; Boots, J. - W. P.; Dijkman, R.; Slotboom, A. J.; van der Hijden H. T. W .M.; Egmond, M. R.; Verheij, H. *Biochim. Biophys. Acta* **1995**, *1259*, 56-64.

[73]Schramm, V. L.; Horenstein, B. A.; Kline, P. C. *J. Biol. Chem.* **1994**, *28*, 18259-18262.

[74]Luić, M.; Tomić, S.; Leščić, I.; Ljubović, E.; Šepac, D.; Šunjić, V.; Vitale, L.; Saenger, W.; Kojić-Prodić, B. *Eur. J. Biochem.* **2001**, *268*, 3964-3973.

[75]Young D. C. *Computational Chemistry. A Practical Guide for Applying Techniques to Real-World Problems.* Wiley-Interscience: New York, NY, **2001**.

[76]Monard, G.; Prat-Resina, X.; Gonzáles-Lafont A.; Lluch J. M. *Int. J. Quantum Chem.* **2003**, *93*, 229-244.

[77]Anfinsen, C. B. *Science* **1973**, *181*, 223-230.

[78]Sander, C.; Schneider, R. *Proteins* **1991**, *9*, 56-68.

[79]Rost, B. *Folding & Design* **1997**, *2*, S19-S24.

[80]Mosimann, S.; Meleshko, R.; James, M. *Proteins* **1995**, *23*, 301-317.

[81]http://www.expasy.org/

[82]http://www.expasy.org/swissmod/SWISS-MODEL.html

[83]Easson, L. E.; Stedman, E. *Biochem. J.* **1933**, *27*, 1257-1266.

[84]Bergmann, M.; Zervas, L.; Fruton, J. S. *J. Biol. Chem.* **1936**, *115*, 593-611.

[85]Bergmann, M.; Fruton, J. S. *J. Biol. Chem.* **1937**, *117*, 189-202.

[86]Ogston, A. G. *Nature* **1948**, *162*, 963.

[87]Bentley, R. *Trans. N. Y. Acad. Sci.* **1983**, *41*, 1- 25.

[88]Mescar, A. D.; Koshland, D. E. Jr. *Nature* **2000**, *403*, 614-615.

[89]Deslongchamps, P.; Atlani, P.; Fréhel, D.; Maval, A. *Can. J. Chem.* **1972**, *50*, 3405-3408.

[90]Deslongchamps, P.; Lebreux, C.; Taillefer, R. *Can. J. Chem.* **1973**, *51*, 1655-1669.

[91]Kazlauskas, R. J.; Weissfloch, A. N. E.; Rappaport, A. T.; Cuccia, L. A. *J. Org. Chem.* **1990**, *56*, 2656-2665.

[92]Uppenberg, J.; Oehrner, N.; Norin, M.; Hult, K.; Kleywegt, G. J.; Patkar, S.; Waagen, V.; Anthonsen, T.; Jones, T. A. *Biochemistry* **1995**, *34*, 16838-16851.

[93]Orrenius, C.; Hæffner, F; Rotticci, D.; Ohrner, N.; Norin, T.; Hult, K. *Biocatal. Biotransform.* **1998**, *16*, 1-15.

[94]Rotticci, D; Hæffner, F; Orrenius, C.; Norin, T.; Hult, K. *J. Mol. Cat. B: Enzymatic* **1998**, *5*, 267-272.

[95]Zuegg, J.; Hönig, H.; Schrag, J. D.; Cygler, M. *J. Mol. Cat. B: Enzymatic* **1997**, *3*, 83-98.

[96]Ema, T.; Kobayashi, J.; Maeno, S.; Sakai, T.; Utaka, M. *Bull. Chem. Soc. Jpn.* **1998**, *71*, 443-453.

[97]Tafi, A.; van Almsick, A.; Corelli, F.; Crusco, M.; Laumen, K. E.; Schnider, M. P.; Botta, M. *J. Org. Chem.* **2000**, *65*, 3659-3665.

[98]Schulz, T.; Pleiss, J.; Schmid, R. D. *Prot. Sci.* **2000**, *9*, 1053-1062.

[99]Weissfloch, A. N. E.; Kazlauskas, R. J. *J. Org. Chem.* **1995**, 60, 6959-6969.

[100]Bornscheuer, U. T.; Kazlauskas, R. J. *Hydrolases in Organic Synthesis*, Whiley-VCH: Weinheim, Germany, **1999**, pp. 88-95.

[101]Miyazawa, T.; Yukawa, T.; Koshiba, T.; Ueji, S; Yanagihara, R.; Yamada, T. *Biotechnol. Lett.* **2001**, *23*, 1547-1550.

[102]Tuomi, W.V.; Kazlauskas, R.J. *J. Org. Chem.* **1999**, *64*, 2638-2647.

[103]Tomić, S.; Dobovičnik, V.; Šunjić, Ć.; Kojić-Prodić, B. *Croat. Chem. Acta* **2001**, *74*, 343-357.

[104]Gentner, C.; Schmid, R. D.; Pleiss, J. *Colloids and surfaces B: Biointerfaces* **2002**, *26*, 57-66.

[105]Pleiss, J.; Scheib, H.; Schmid, R. D *Biochimie* **2000**, *82*, 1043-1052.

[106]Faber, K.; Ottolina, G.; Riva, S. *Biocatalysis* **1993**, *8*, 91-132.

[107]Reetz, M. T. *Angew. Chem. Int. Ed.* **2001**, *40*, 284-310.

[108] Janes, L. E.; Löwendahl, A. C.; Kazlauskas, R. J. *Chem. Eur. J.* **1998**, *4*, 2317-2324.

[109]Reetz, M. T.; Zonta, A.; Schimossek, K.; Liebeton, K; Jaeger, K.-E. *Angew. Chem. Int. Ed.* **1997**, *36*, 2830 - 2832.

[110]Janes, L. E.; Kazlauskas, R. J. *J. Org. Chem.* **1997**, *62*, 4560-4561.

[111]Fitzpatrick, P. A.; Klibanov A. M. *J. Am. Chem. Soc.* **1991**, *113*, 3166-3171.

[112]Ducret, A.; Trani, M.; Lortie, R. *Enzyme Microb. Technol.* **1998**, *22*, 212-216.

[113]Carrea, G.; Ottolina, G.; Riva, S. *Trends Biotechnol.* **1995**, *13*, 63-70 (erratum 122).

[114]Wescott, C. R.; Klibanov, A. M. *Biochim. Biophys. Acta* **1994**, *1206*, 1-9.

[115]Hirose, Y.; Kariya, K.; Sasaki, I.; Kurono, Y.; Ebiike, H.; Achiwa, K. *Tetrahedron Lett.* **1992**, *33*, 7157-7160.

[116]Halling, P.J. *Curr. Opin. Chem. Biol.* **2000**, *4*, 74-80.

[117]Okamoto, T.; Ueji, S. *Chem. Commun.* **1999**, 939-940.

[118]Rariy, R.V.; Klibanov, A.M. *Biotechnol. Bioeng.* **1999**, *62,* 704-710.

[119]Lau, R. M.; Rantwijk, F. V.; Seddon, K. R.; Sheldon, R. A. *Org. Lett.* **2000**, *2*, 4189-4192.

[120]Schöfer, S. H.; Kaftzik, N.; Wasserscheid, P.; Kragl, U. *Chem. Commun.* **2001**, 425–426.

[121]Secundo, F.; Riva, S.; Ottolina, C. *Tetrahedron: Asymmetry* **1992**, *3*, 267-280.

[122]Phillips, R. S. *Enzyme Microb. Technol.* **1992**, *14*, 417-419.

[123]Phillips, R. S. *Trends. Biotech.* **1996**, *14*, 13-16.

[124]Gupta, A. K.; Kazlauskas, R. J.*Tetrahedron: Asymmetry* **1993**, *4*, 879-888.

[125]Ueji, S.-I.; Watanabe, K.; Koshiba, T.; Nakamura, M.; Oh-ishi, K.; Yasufuku, Y.; Miyazawa, T. *Biotechnol. Lett.* **1999**, *21*, 865-868.

[126]Rotticci, D.; Rotticci-Mulder, J. C.; Stuart, D.; Norin, T.; Hult, K. *Chembiochem* **2001**, *2*, 766-770.

[127]Ema, T.; Maeno, S.; Takaya, Y.; Sakai, T.; Utaka, M. *Tetrahedron: Asymmetry* **1996**, *7*, 625-628

[128]Ema, T.; Maeno, S.; Takaya, Y.; Sakai, T.; Utaka, M. *J. Org. Chem.* **1996**, *61*, 8610-8616.

[129]Miyazawa, T.; Yukawa, T.; Koshiba, T.; Sakamoto, H.; Ueji, S; Yanagihara, R.; Yamada, T. *Tetrahedron: Asymmetry* **2001**, *12*, 1595-1602.

[130]Hirose, K; Naka, H.; Yano, M.; Ohashi, S.; Naemura, K.; Tobe, Y. *Tetrahedron: Asymmetry* **2000**, *11*, 1199-1210.

[131]Hedstrom, L.; Graf, L.; Stewart, C. B.; Rutter, W. J.; Phillips, M.A. *Methods Enzymol.* **1991**, *202*, 671-687.

[132]Braman, J.; Papworth, C.; Greener, A. *Methods Mol. Biol.* **1996**, *57*, 31-44.

[133]Arnold, F.H. *Acc. Chem. Res.* **1998**, *31*, 125-131.

[134]Kuchner, O.; Arnold, F. H. *Trends Biotechnol.* **1997**, *15*, 523-530.

[135]Eckert, K. A.; Kunkel, T. A. *Nucleic Acids Res.* **1990**, *18*, 3739-3744.

[136]Eckert, K. A.; Kunkel, T. A. *PCR Methods Applic.* **1991**, *1*, 17-24.

[137]Fromant, M.; Blanquet, S.; Plateau, P. *Anal. Biochem.* **1995**, *224*, 347-353.

[138]Lin-Goerke, J. L.; Robbins, D. J.; Burczak, J. D. *BioTechniques* **1997**, *23*, 409-412.

[139]Spee, J. H.; de Vos, W. M.; Kuipers, O. P. *Nucl. Acids Res.* **1993**, *21*, 777-778.

[140]Leung, D. W.; Chen, E.; Goeddel, D. V. *Technique* **1989**, *1*, 11-15.

[141]Cadwell, R. C.; Joyce, G. F. *PCR Methods Appl.* **1992**, *2*, 28-33.

[142]Jaeger, K.- E.; Eggert, T.; Eipper, A.; Reetz, M. T. *Appl. Microbiol. Biotehnol.* **2001**, *55*, 519-530.

[143]Goodman, M. F.; Keener, S.; Guidotti, S.; Branscomb, E. W. *J. Biol. Chem.* **1982**, *258*, 3469-3475.

[144]Miyazaki, K.; Arnold, F. H. *J. Mol. Evol.* **1999**, *49*, 716-720.

[145]Liebeton, K.; Zonta, A.; Schimossek, K.; Nardini, M.; Lang, D.; Dijkstra, B. W.; Reetz, M.; Jaeger, K.- E. *Chem. & Biol.* **2000**, 7, 709-718.

[146]Stemmer, W. P. C. *Nature* **1994**, *370*, 389-391.

[147]Stemmer, W. P. C. *Proc. Natl. Acad. Sci. USA* **1994**, *91*, 10747-10751.

[148]Zhao, H.; Giver, L.; Shao, Z.; Affholter, J. A.; Arnold, F. H. *Nat. Biotechnol.* **1998**, *16*, 258-261.

[149]Shao, Z.; Zhao, H.; Giver, L.; Arnold, F. H. *Nucl. Acids Res.* **1998**, *26*, 681-683.

[150]Volkov, A. A.; Shao, Z.; Arnold, F. H. *Methods Enzymol.* **2000**, *328*, 456-463.

Chapter 2

Explaining the molecular basis of enzymes enantioselectivity is a problem that has been tackled by several research groups. In this chapter we explain the enantioselectivity of PCL towards chiral primary alcohols without oxygen at the stereocentre by the combined use of X-ray crystallography of transition state analogues, molecular modelling and kinetic experiments. This is the first time that crystal structures of a lipase complexed with transition state analogues containing both enantiomers of a primary alcohol are reported.

Contributors

This work was done under the supervision of Professor Romas J. Kazlauskas and in collaboration with the Macromolecular Structure Group of the Biotechnology Research Institute (BRI), National Research Council of Canada and with Professor Michael A. Whitehead of the Chemistry Department, McGill University. Dr. Chan Seong Cheong, postdoctoral fellow in our laboratory in 1997, first synthesised the inhibitors and prepared pure enantiomers of 2-methyl-3-phenyl-1-propanol, which I used for the synthesis of the phosphonate inhibitors. Dr. Joseph D. Schrag of the BRI crystallised the PCL-inhibitor complexes, collected X-ray diffraction data and solved the structures. Mrs Cécile Malardier-Jugroot, Ph.D. candidate in the Chemistry Department, McGill University, helped finding a strategy for the semi-empirical calculations and guided me during the modelling experiments. Professor Michael A. Whitehead of the Chemistry Department, McGill University, assisted in interpreting the modelling results. Dr. Mirek Cygler of the BRI helped interpret the electron density maps. I synthesised the inhibitors that were used for this publication, inactivated PCL, participated in the first steps of the refinement of the structures (fitting the protein model in the density map), analysed the resulting structures, determined the kinetic constants, performed end-point E measurements and combined QM/MM calculations.

X-ray crystal structures of transition state analogues explain the enantioselectivity of *Pseudomonas cepacia* lipase towards 2-methyl-3-phenyl-1-propanol.

Abstract

Pseudomonas cepacia lipase (PCL) shows high enantioselectivity towards a wide range of primary alcohols. Synthetic chemists often exploit this enantioselectivity to prepare key starting materials for synthesis, but the molecular basis of this enantioselectivity remains unknown. To address this question the X-ray crystal structures of two phosphonate transition state analogues bound to PCL were solved with resolution of 1.10 Å and 1.50 Å. The analogues contained as alcohol moieties the slow- and the fast-reacting enantiomer of a simple primary alcohol: 2-methyl-3-phenyl-1-propanol. Although PCL shows high enantioselectivity towards esters of this alcohol (E ≥190 for the hydrolysis of the heptanoate), the transition state analogues exhibit only subtle differences in their orientation. The alcohol oxygen, the methyl and the benzyl substituent at the stereocentre lie in similar positions for both enantiomers, while the hydrogen at the stereocentre points in opposite directions due to the enantiomeric configuration of the stereocentre. Combined QM/MM calculations on the first tetrahedral intermediates T_d1 suggest a better key hydrogen bond between catalytic His286 Nε2 and alcohol oxygen in the fast enantiomer, which is supported by the 100-fold higher turnover number determined for such enantiomer.

Introduction

One of the major uses of lipases in organic chemistry is in enantioselective hydrolyses involving primary and secondary alcohols. The molecular basis for this enantioselectivity towards primary alcohols is still an open question. Understanding it would allow for a more rational design of substrates (substrate engineering), reaction conditions (medium engineering) and catalyst (protein engineering) to improve the overall enantioselectivity of the enzyme towards chiral primary alcohols.

Only a few lipases, i.e. PCL, porcine pancreatic lipase and *Achromobacter sp.* lipase,[1,2] resolve esters of chiral primary alcohols with high enantioselectivity. Optically

active primary alcohols are important building blocks for the synthesis of chiral drugs. (*R*) and (*S*)-2-methyl-3-phenyl propanol (MPP) have been used for the preparation of fungicidal compounds,[3] for the synthesis of adenosine receptor agonists and antagonists[4] and for the synthesis of the side chain of zaragozic acid A.[5]

PCL, a 320 amino acids long α/β-hydrolase with molecular weight of about 33 kDa and dimensions of about 30 Å x 40 Å x 50 Å, is one of the most used enzymes for biocatalytic applications.[1] Like other lipases, it has a lid or flap that is responsible for the phenomenon of interfacial activation. Also, the crystal structure of the open form of PCL is available.[6,7]

The reaction mechanism of lipase-catalysed ester hydrolysis is analogous to the one of serine proteases and involves the formation of two successive tetrahedral intermediates: T_d1, the first tetrahedral intermediate, leads to the formation of the acyl enzyme (Scheme 1), while T_d2 is the second tetrahedral intermediate, which leads to the free acid. Since the alcohol moiety is released when T_d1 collapses forming the acyl enzyme, it is the interactions enzyme-substrate present in this particular intermediate and in the transition state that leads to its formation or collapse that control the enantioselectivity (E)[i] of the enzyme towards the chiral alcohol.

[i] $\Delta\Delta G^{\ddagger}$=-RTlnE where $\Delta\Delta G^{\ddagger}$ is the difference in activation energy for the reaction of the enzyme with the two enantiomers of the substrate.

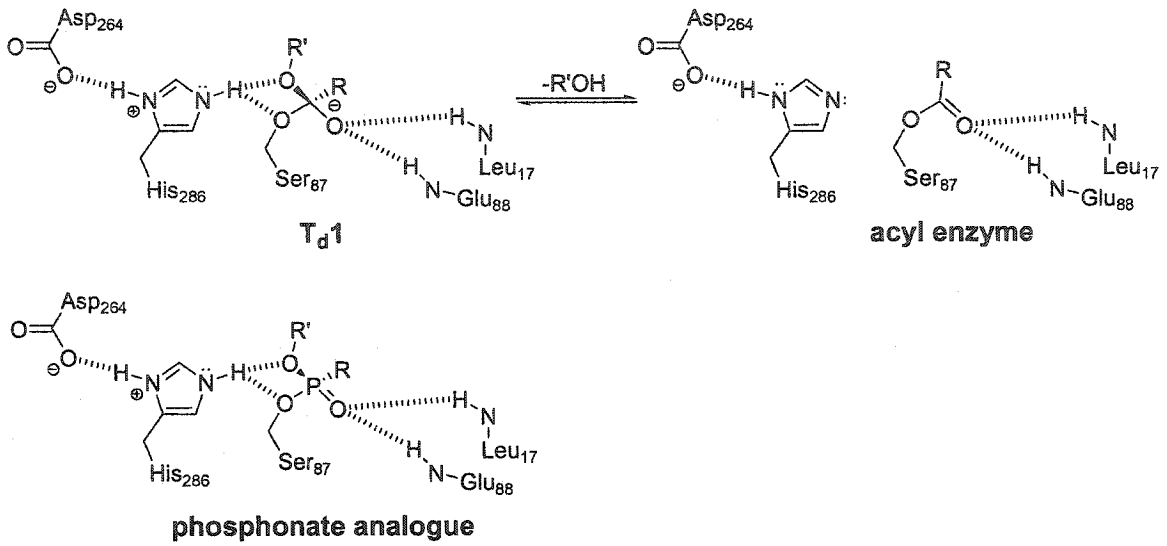

Scheme 1 - First tetrahedral intermediate T_d1 (left), acyl enzyme (right) in the PCL-catalysed hydrolysis of esters. The phosphonate analogue is shown below T_d1.

It is unfortunately still not possible, with the current spectroscopic techniques, to directly observe the transition state that leads to T_d1. "Freezing" the lipase in a state that mimics it may allow understanding the modes of enantiorecognition of chiral primary alcohols by lipases. We used phosphonate analogues[8] covalently linked to catalytic Ser87 for the purpose of mimicking the transition state that leads to the T_d1 involved in the hydrolysis of esters of MPP. Phosphonate esters are potent inhibitors of hydrolases.[9,10,11,12,13,14] These esters, once irreversibly bound to the enzyme by a covalent bond to the Oγ of catalytic serine, mimic the transition state that leads to T_d1.[ii]

Lipases exhibit opposite enantiopreference for primary and secondary alcohols. They also usually display lower enantioselectivity for primary alcohols. To understand how PCL catalyses the hydrolysis of esters of chiral primary alcohols and why its enantiopreference for primary alcohols is opposite to the one for secondary alcohols, several modelling experiments have been carried out in the past few years,[15,16,17] however the conclusions drawn from these studies do not agree on the productive conformation of T_d1.

[ii] In the literature there is some ambiguity on whether phosphonate esters mimic T_d1 or the transition state that leads to its formation.[15,16] Most refer to phosphonate-enzyme complexes as transition states because of the slightly distorted geometry of such esters in comparison to T_d1 (slightly longer bond length P=O and P-O versus C-O$^-$ and C-O and slightly bigger angles O-P-O versus O-C-O).[34]

To determine the enantioselectivity of PCL, Zuegg *et al.*[15] calculated the energy difference between diastereoisomeric tetrahedral intermediates, which they assumed to be close in conformation to the transition states structure. Using systematic search and Monte-Carlo minimization (SsMcm) they obtained the same (*S*)-enantiopreference experimentally observed in the hydrolysis of esters of chiral primary alcohols by PCL. Furthermore they found that primary alcohols without oxygen at the stereocentre have the large substituent at the stereocentre either binding in the large hydrophobic pocket of the enzyme (hydrophobic groove HA,[18] pink in Figure 1) like secondary alcohols, or extending into the solvent. Also, they show "L-alignment", i.e. the large substituent at the stereocentre points in the same direction in both enantiomers while the medium substituent and the hydrogen exchange places (Figure 2(a)).

Tuomi and Kazlauskas[16] performed molecular mechanics calculations on phosphonate analogues of 2-methyl-3-phenyl-1-propyl butanoate (Figure 2(b)) covalently bound to PCL *via* catalytic Ser87 Oγ. By systematically minimising nine possible conformations along bonds b and c they found several local minima that they "judged" for "catalytic competence". They found that the large substituent at the stereocentre in primary alcohols binds in a different hydrophobic region than secondary alcohols, the hydrophobic pocket HH (alternate hydrophobic pocket[16], blue in Figure 1; Figure 2(c)).

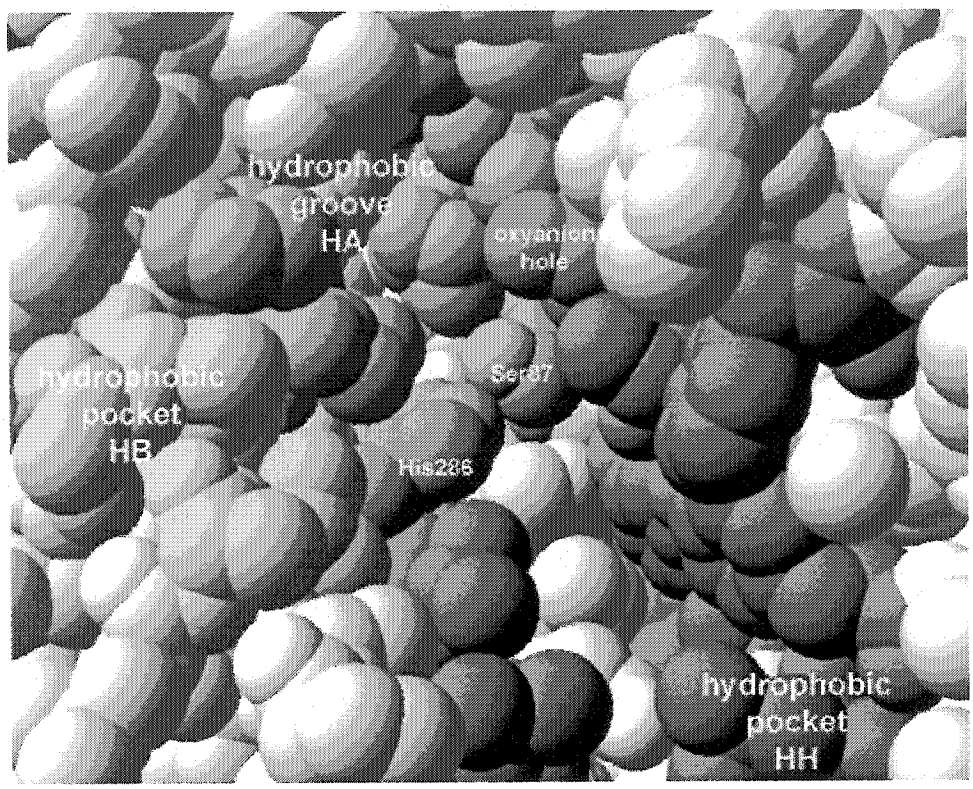

Figure 1 - PCL active site pockets (PDB ID: 3LIP[6]). The hydrophobic groove HA is in pink, the hydrophobic pocket HH is in blue, the hydrophobic pocket HB is in yellow, the oxyanion hole in green, catalytic Ser 87 is in orange and catalytic His 286 is in ice-blue, catalytic Asp 264 is not visible.

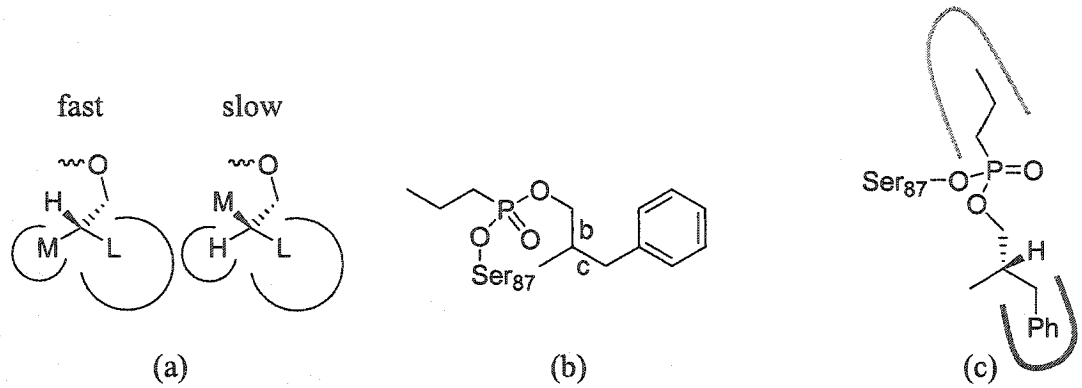

Figure 2 - Modelling results. (a) Zuegg *et al.*[15] obtained "L-alignment" (the large substituent at the stereocentre points in the same direction in both enantiomers) for primary alcohols without polar groups at the stereocentre. (b) Tuomi and Kazlauskas[16] performed conformational searches by systematically minimising nine possible conformations along bonds b and c. They found that the large substituent at the stereocentre in primary alcohols does not bind in the hydrophobic groove HA, pink in Figure 1 and in (c), but in the hydrophobic pocket HH (alternate hydrophobic pocket, blue in Figure 1 and in (c)).

Last, Tomić *et al.*[17] studied the potential energy surfaces of the tetrahedral intermediates of the complexes enzyme-substrate, their Solvent Accessible Surface Area (SASA) and their interactions with the amino acids in the PCL active site. They observed three different orientations for the large substituent at the stereocentre: it was either in the hydrophobic pocket HH (blue in Figure 1), pointed outwards in the solvent or was only partly bonded in the hydrophobic pocket HH. In the latter case the medium substituent at the stereocentre of the preferred enantiomer pushed the catalytic His286 towards Ser87, increasing their hydrogen bonding and therefore speeding up the reaction of this particular enantiomer.

Because none of the above agrees on the productive conformation[iii] for the PCL catalysed hydrolysis of esters of chiral primary alcohols, we tackled the problem differently and solved X-ray crystal structures of complexes PCL-inhibitors that are transition state analogues. The analogues contained as alcohol moieties the slow- and the fast-reacting enantiomer of MPP. PCL catalyses the hydrolysis of MPP heptanoate (MPP-

[iii]For a productive conformation of T_d1 the carbonyl oxygen must reside in the oxyanion hole and hydrogen bind to the backbone N-H of the oxyanion hole residues. Catalytic histidine must have a bifurcated H-bond between Nε2-H and the oxygen of the alcohol moiety and of the catalytic serine. Catalytic histidine must also hydrogen bind through Nδ2-H to catalytic aspartate COO^-.

C_7) with E ≥190). The crystal structures of these complexes, together with combined QM/MM modelling of the corresponding tetrahedral intermediates and the kinetic constants for the PCL-catalysed hydrolysis of MPP-C_7, provide additional insight into the modes of chiral recognition of primary alcohols without oxygen at the stereocentre by PCL. The crystal structures show that the benzyl group of both MPP enantiomers lie in a solvent exposed crevice and that there are only subtle interactions enzyme-alcohol moiety. These subtle interactions are both difficult to interpret and not sufficient to explain E ≥190. Energy minimisations of the tetrahedral intermediates were performed using a combined QM/MM approach on a 15 Å enzyme shell centred on the tetrahedral carbon. These minimisations show that the hydrogen bond between His286 Nε2 and alcohol oxygen is stronger in the T_d1 of the fast (*S*)-enantiomer (for (*S*)-MPP 2.77 Å, 150.8°; for (*R*)-MPP 3.30 Å, 142.9°). Thus the transition state for the release of the alcohol, mimicked by the crystal structures of complexes PCL-phosphonate esters, should be attained faster and with lower activation energy in such enantiomer, in agreement with the determined 100-times lower k_{cat}.

The enantioselectivity of PCL towards MPP seems to arise from the better hydrogen bond between His286 Nε2 and alcohol oxygen of the fast enantiomer. The subtlety of the interactions enzyme-substrate observed in the crystal structures and in the modelling output structures explains the difficulty to rationally increase the enantioselectivity of PCL towards primary alcohols by substrate engineering.[19]

Materials and methods

All chemicals were purchased from Sigma-Aldrich Co. (Oakville, ON) unless otherwise specified. Lipase from *Pseudomonas cepacia* was purchased from Genzyme Diagnostics (Cambridge, MA). Diffraction data were collected at beamline X8C at the National Synchrotron Light Source, Brookhaven National Laboratory (Upton, NY) using an ADSC (San Diego, CA) Quantum-4 CCD detector. Refinements were done with Refmac 5.1.24[20] ^{1}H NMR spectra were collected at 270 MHz, ^{13}C NMR at 68 MHz and ^{31}P NMR at 109 MHz. Kinetic data were collected on a SpectraMAX 340 microplate reader using SoftMaxPro 2.2.1 software (Molecular Devices Corp., Sunnyvale, CA). Molecular

modelling was performed with HyperChem™ 7 (Hypercube Inc, Gainesville, FL). All the protein three-dimensional images were generated with Swiss PdbViewer v. 3.7.[21]

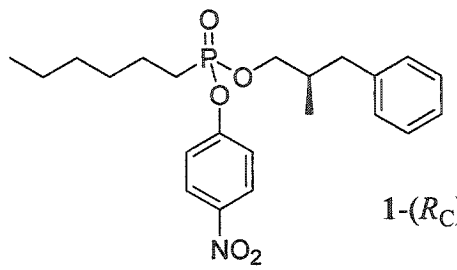

1-(R_C)

(R_C, R_PS_P) Hexylphosphonic acid 2-methyl-3-phenylpropyl ester 4-nitrophenyl ester, 1-(R_C).

A solution of (*R*)-2-methyl-3-phenyl-propan-1-ol (0.17 g, 1.11 mmol) in dichloromethane (2 mL) was added to a solution of hexylphosphonic dichloride (0.21 mL, 1.11 mmol) and diisopropyl ethyl amine (0.55 mL, 3.16 mmol) in dichloromethane (9 mL) previously cooled to 5 °C with an ice bath. After one hour stirring, 1*H*-tetrazole (0.07 mg, 0.10 mmol) was added. When the (*R*)-2-methyl-3-phenyl-propan-1-ol was consumed (TLC observation, 1.5 hours), the ice bath was removed and an excess of 4-nitrophenol (0.30 g, 2.12 mmol) was added to the reaction mixture. After 3 h an excess of diisopropyl ethyl amine (0.40 mL, 2.30 mmol) was added. The solution was stirred overnight at room temperature, then the solvent was evaporated under vacuum. The product was purified by column chromatography over silica gel using hexane/ethyl acetate as eluent, and concentrated by rotary evaporation to a yellow oil. Yield 22%. R_f = 0.55 (silica gel, 6:4 hexane-ethyl acetate); ^{1}H NMR ($CDCl_3$) δ 8.20 (d, 2H, CH, J = 7.2 Hz), 7.2-7.35 (m, 5H), 7.10 (d, 2H, CH, J = 6.4 Hz), 3.92-3.96 (m, 2H), 2.65-2.75 (m, 1H), 2.39-2.48 (m, 1H), 1.85-2.20 (m, 3H), 1.24-1.80 (m, 8H), 0.8-0.93 (m, 6H); ^{13}C NMR ($CDCl_3$) δ 155.5, 139.3, 139.2, 128.6, 128.2, 125.5, 120.8, 70.5, 39.0, 35.9, 31.0, 29.9, 26.2, 25.1, 22.0, 16.2, 13.8; ^{31}P NMR ($CDCl_3$) δ 31.39, 31.37; MS (CI, NH_3) *m/z* (rel. intensity) 420.0 (5, M + H^+), 132 (100, M^+ - $P(O)(C_6H_{13})(OC_6H_4NO_2)OH$), 117 (67, M^+ - $P(O)(C_6H_{13})(OC_6H_4NO_2)OH$ - CH_3), 91 (25, tropylium).

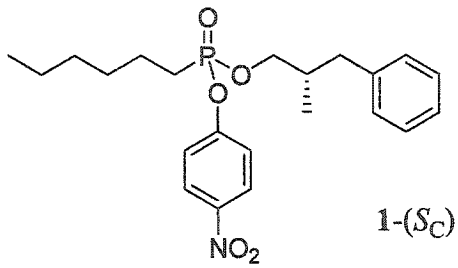

1-(S_C)

(S_C, R_PS_P) Hexylphosphonic acid 2-methyl-3-phenylpropyl ester 4-nitrophenyl ester, 1-(S_C).

The reaction was performed as for 1-(R). Yield 20% (yellow oil). R_f = 0.55 (silica gel, 6:4 hexane-ethyl acetate); NMR and MS are the same as those for 1-(R_C).

Inactivation of PCL by 1-(R_C) and 1-(S_C).

PCL was dissolved in potassium phosphate buffer (50 mM, pH 7.5), to a final concentration of 22.5 nM. 1-(R_C) and 1-(S_C) were dissolved in *n*-propanol to a final concentration of 32 mM. The PCL solution (0.25 mL) was mixed with the inhibitor solution (0.25 mL) and incubated at room temperature overnight. The hydrolytic activity against *p*-nitrophenol acetate had dropped to <2%. The solutions were dialysed against water for 24 hours. After dialysis, a white precipitate (PCL-inhibitor complex) formed. The suspensions were centrifuged at 4300 rpm and 4 °C, the supernatant was eliminated and the protein was re-dissolved in a solution of 50% *n*-propanol and 50% imidazole buffer (50 mM pH 6.5). The complexes were concentrated using Microcon YM-30® ultrafiltration membranes (Millipore Corp., Nepean, Ontario) and the concentrated protein diluted in the same buffer to a concentration of 10 mg/mL.

Crystallisation, diffraction data collection and structure determination for the complexes PCL-1-(R_C) and PCL-1-(S_C).

Crystals of the complexes were grown by vapour diffusion. The drop contained about 10 mg protein/mL in imidazole buffer (50 mM, pH 6.5 containing 50 vol% *n*-propanol), while the reservoir contained imidazole buffer (50 mM, pH 6.5) and 25 vol% *n*-propanol. The crystals were isomorphous to the unligated open form of PCL and the coordinates for this form yielded the initial phases for the structural refinements by molecular replacement. Diffraction data for complex PCL-1-(R_C) were collected at a wavelength of 0.9794 Å in two 180° steps. The first sweep was collected in 180 frames with 1°

oscillations, 30 sec exposures and a crystal to detector distance of 90 mm. The low-resolution reflections that were overloaded in the first sweep were re-collected in a second 180 frames sweep collected at 140 mm using 4 sec exposures. The PCL-1-(S_C) data were collected at a wavelength of 0.9795 Å in 180 frames using 1° oscillations, 60 sec exposures, and a distance of 140 mm. Data reduction was performed with the DENZO/SCALEPACK suite of programs.[22] The phosphonate molecules were located in the F_o-F_c difference maps. All refinements were done using Refmac 5.1.24.[20]

Determination of k_{cat} and K_M for the PCL catalysed hydrolysis of (*R*) and (*S*)-2-methyl-3-phenyl-1-propyl heptanoate.

Spectrophotometric determination of k_{cat} and K_M was performed using a 96-well microliter plate and a microplate reader using a pH indicator to monitor ester hydrolysis. Assay solutions were prepared by mixing appropriate amounts of substrate solutions in *n*-propanol [150 mM (*R*)-2-methyl-3-phenyl-1-propyl heptanoate, 130 mM (*S*)-2-methyl-3-phenyl-1-propyl heptanoate] with *N*,*N*-bis-(2-hydroxymethyl)-2-aminoethanesulfonic acid (BES) solutions (12 mM, pH 7.2, containing 2 mM *p*-nitrophenol (PNP)). Assay solutions (90 μL) and PCL solution (10 μL of 285 μg protein/mL for the (*R*) enantiomer and 10 μL of 28.5 μg protein/mL for the (*S*) enantiomer) were added in the microplate and the decrease in absorbance at 404 nm was monitored. Concentrations in wells were as follows: [BES] = 7.44 mM, [PNP] = 1.24 mM, [PCL] = 2.85 μg/mL, [(*R*) and (*S*)-2-methyl-3-phenyl-1-propyl heptanoate] = 0.6 to 4.5 mM, [*n*-propanol] = 28.8%. Data were analysed using Eadie-Hofstee plots.[23,24]

Combined QM/MM calculations

The enzyme-inhibitor crystal structures were pruned to a 15 Å sphere centred on the phosphorus atom. Truncated residues were capped by adding H atoms. Residues Ser87, Asp264, His286, Gly16, Leu17 (oxyanion hole), Thr18, Tyr29, His86, Gln88 (oxyanion hole) Leu287 and the bound phosphonate ester formed the "enzyme reaction zone" which was minimised using the semi-empirical PM3 method.[25,26] The remainder of the sphere was treated as a fixed potential using the AMBER forcefield for the atoms definitions. His286 Nδ1 was positively charged and Asp264 Oδ2 was negatively charged. The inhibitors were modified to tetrahedral intermediates by replacing P=O with C-O$^-$ and

treated as above. The structures were minimised in vacuum using the Polak-Ribière conjugate gradient[27] until an r.m.s. of 0.02 kcal/mol/Å was reached.

Results

A straightforward modification of literature procedures[8,28] yielded two phosphonate *p*-nitrophenyl esters that contain as alcohol moieties pure enantiomers of (*R*)-MPP and (*S*)-MPP (Scheme 2). While phosphonyl chlorides incorporating secondary alcohol moieties are relatively stable and can be easily handled,[8,28] this was not the case when they contain primary alcohols. Hence we added a second step to the literature synthesis to replace the chlorine with *p*-nitrophenol. Nucleophilic displacement of one chlorine of hexylphosphonic dichloride by one equivalent of chiral alcohol yielded a mono-substituted phosphonyl chloride, which was converted *in situ* to the desired *p*-nitrophenyl derivative by treatment with two equivalents of *p*-nitrophenol in the presence of di-isopropyl ethyl amine. Each reaction formed an equimolar mixture of (S_P) and (R_P) epimers due to the phosphorous stereocentre (^{31}P NMR showed two resonances for the phosphorous atom (see Materials and Methods, ^{31}P NMR)). We employed these esters without separation of the epimers.

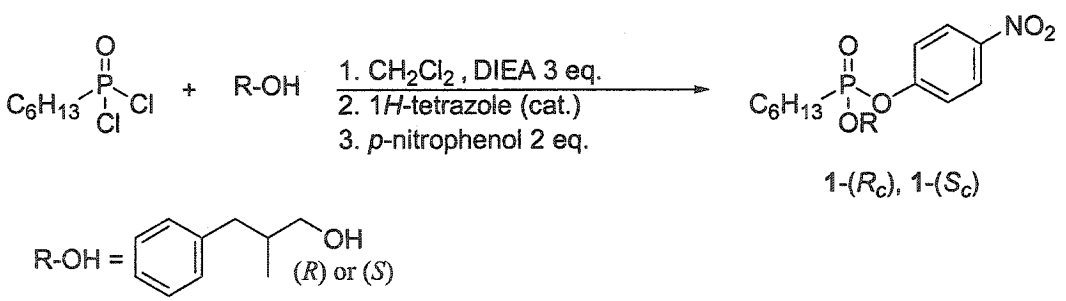

Scheme 2 - Phosphonate esters synthesis (DIEA = diisopropyl ethyl amine).

Inactivation of PCL with 1000-fold excess of either 1-(*R*) or 1-(*S*) irreversibly inhibited more than 98% of the hydrolytic activity of the enzyme towards *p*-nitrophenol acetate. The solvent for the inactivation of PCL was 50 vol% *n*-propanol in aqueous buffer since the PCL-inhibitor complexes precipitated from buffer containing less than 50 vol% *n*-propanol (see Materials and Methods).

PCL-inhibitor complexes were crystallised by the hanging drop method. The reservoir contained 25 vol% *n*-propanol in imidazole buffer (50 mM, pH 6.5). These conditions use excess water instead of excess *n*-propanol in the reservoir. The crystallisation conditions used by Schrag *et al.*[6] for the open form of PCL were thus modified (their reservoir contained 50% *n*-propanol in 50 mM Tris buffer pH 8.5). This change was needed because the PCL-inhibitor complexes are less water-soluble. The crystals formed at a concentration of *n*-propanol of ~30 vol% and were isomorphous with the open form of PCL for both complexes.

Diffraction data were collected and the X-ray crystal structures were solved using initial phases calculated from the open form of PCL (PDB ID: 3LIP[6]), by the molecular replacement method (Table 1). No significant differences with the unligated open conformation of PCL were observed in the polypeptide backbone or in the side-chain conformation (for the complex PCL-**1**-(*R*) r.m.s. = 0.41 Å; for the complex PCL-**1**-(*S*) r.m.s. = 0.39 Å). Like the open form of PCL,[6,7] both PCL-inhibitor complexes belong to the C2 space group (Table 1). Both structures were solved with very good resolution: 1.10 Å for PCL-**1**-(*R*) and 1.50 Å for PCL-**1**-(*S*) (Table 1).

Table 1 – Data collection statistics and refinement parameters.

	PCL-**1**-(R_C)	PCL-**1**-(S_C)
Data statistics		
resolution range (Å)	44.4 – 1.10	37.8 – 1.50
highest resolution shell (Å)	1.14 – 1.10	1.55 – 1.50
space group	C2	C2
unit cell dimensions		
a (Å)	88.8	88.9
b (Å)	46.2	46.2
c (Å)	84.6	84.7
α (°)	90	90
β (°)	121.3	121.3
γ (°)	90	90
mosaicity (°)	0.22	0.27
R merge (%)	4.1 (10.6)	4.3 (12.7)
completeness of the data (%)	89.2 (40.8)	90.3 (53.5)
no. of observations	495813	152333
no. of unique reflections	105990	42707
mean I/σI	21.0 (4.6)	19.0 (5.4)

Refinement statistics		
refinement program	Refmac 5.1.24	Refmac 5.1.24
no. of atoms used in the refinement (not hydrogens)	2498	2498
no. of waters	147	147
no. of calcium ions	1	1
final R factor (%)[a]	16.0	16.7
final R free (%)[b]	17.2	18.1
r.m.s. deviations from ideality for		
bond lengths (Å)	0.008	0.014
bond angles (°)	1.38	1.47
mean B-factors (Å2)		
protein	8.47	9.01
solvent	13.15	13.89
calcium ion	6.39	6.66
inhibitor	12.17	10.42

[a] R factor = $\Sigma \| F_c | - | F_o \| / \Sigma | F_o | \times 100$ where F_c and F_o are the calculated and observed structure factor amplitudes; [b]a small percentage of the total reflections were randomly selected and used to calculate the final R free.

Both phosphonate esters containing as alcohol moiety (*R*)-MPP and (*S*)-MPP bind similarly to PCL (Figure 3). Both covalently link the phosphorous to Oγ of catalytic Ser87 and have an R_P configuration. Because the configuration of the bound phosphonates is R_P, the favourite epimer presumably had S_P configuration prior to the reaction, since nucleophilic attack at phosphorus by Oγ of catalytic serine proceeds by an in-line mechanism.[29]

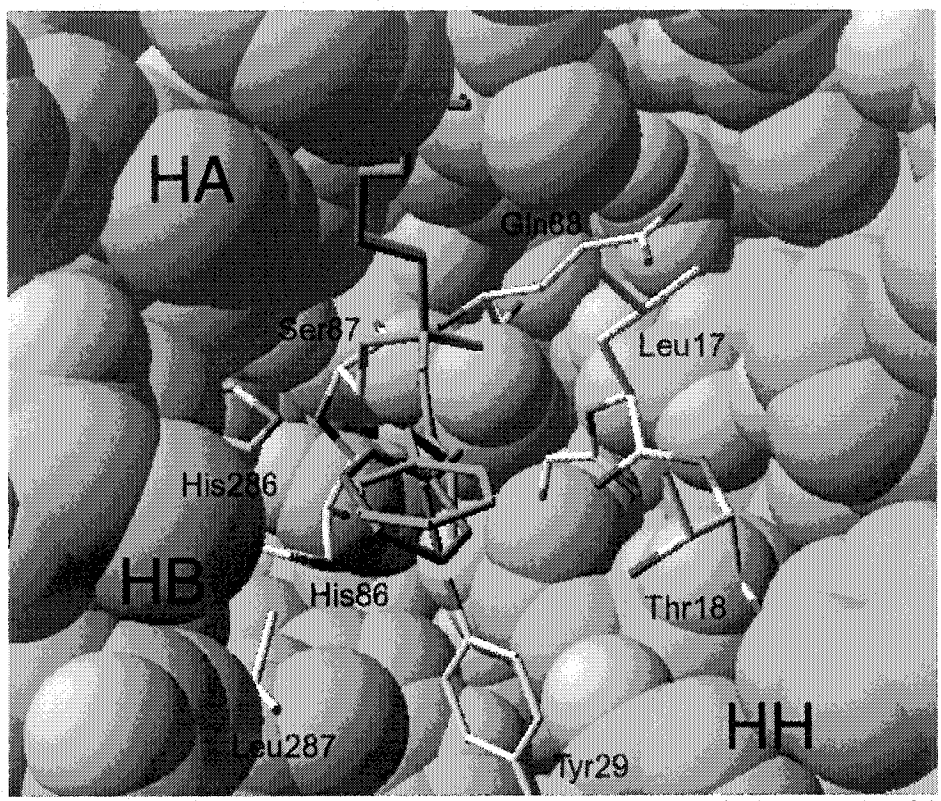

Figure 3 – Overlay of PCL-**1**-(R_C) (the phosphonate inhibitor is in green) with PCL-**1**-(S_C) (the phosphonate inhibitor is in purple). Catalytic triad residues His286 and Ser87, oxyanion hole residues Glu88 and Leu17 and "enzyme reaction zone" residues Thr18, Tyr29 and Leu287 are in stick representation and CPK colours.

The hexyl chain of the phosphonate esters extends in both cases in the hydrophobic groove HA (Figure 3). Lang *et al.* reported a similar binding of the acyl chain for their triacylglycerol analogue and trybutyl inhibitor bound to PCL.[18] The inhibitor folds to hairpin in both complex PCL-**1**-(R_C) and complex PCL-**1**-(S_C), with similar distance of the hexyl chain from the benzylic CH_2 (4.9 Å in PCL-**1**-(R_C) and 5.3 Å in PCL-**1**-(S_C)). The alcohol oxygen O_I is in a similar position in both PCL-**1**-(R_C) and PCL-**1**-(S_C). The medium and large substituent at the stereocentre are directed roughly towards the same regions of the catalytic pocket while the hydrogen is different. This is due to an "umbrella-like" inversion at the stereocentre ("LM-alignment"; Figure 4 (a) and (b)). The large substituent in both complexes is not well bonded to the hydrophobic regions of the catalytic pocket of PCL but lie in a solvent exposed crevice (Figure 4).

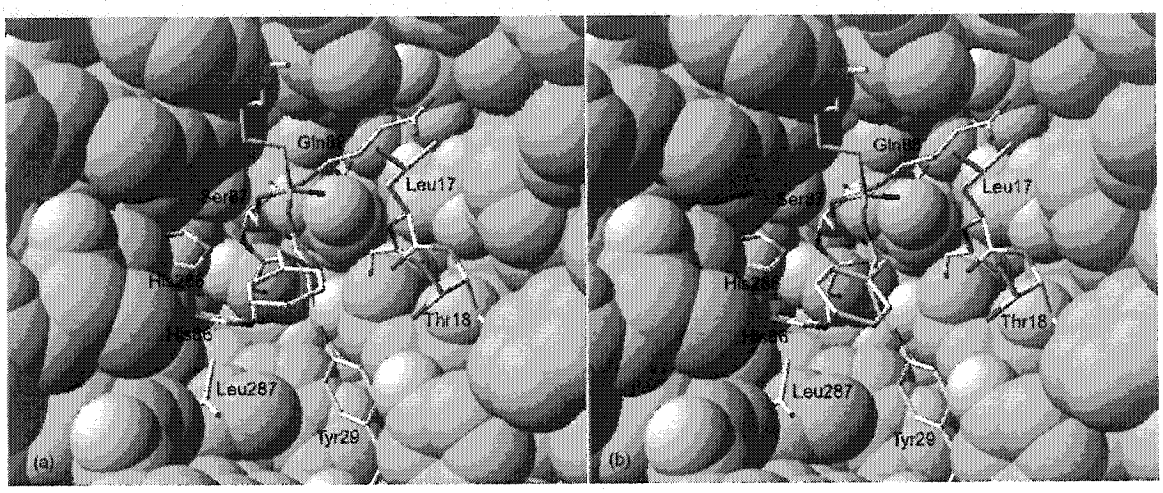

Figure 4 - PCL-inhibitor complexes. (a) PCL-**1**-(R_C), (b) PCL-**1**-(S_C). Catalytic triad residues His286 and Ser87, oxyanion hole residues Glu88 and Leu17 and "enzyme reaction zone" residues Thr18, Tyr29 and Leu287 are in stick representation and CPK colours.

In the PCL-**1**-(R_C) complex, the phenyl ring of the alcohol moiety shows approximately equal amounts of two different orientations, which differ only in the torsion angle along the CH_2-Ph bond (44° vs. 95°). In the PCL-**1**-(S_C) complex only one conformer fits in the electron density map. The presence of two different conformers for the slow enantiomer suggests a worse binding in the catalytic pocket.

Both inhibitors appear to be in a catalytically productive orientation. All the hydrogen bonds necessary for catalysis are present in both complexes and are very similar (Table 2). The phosphonyl oxygens reside in the oxyanion hole, at hydrogen bonding distance from NH of Leu17 and Glu88 (2.73 Å and 2.81 Å in PCL-**1**-(R_C); 2.73 Å and 2.82 Å in PCL-**1**-(S_C)). Catalytic Ser87 is hydrogen bonded to catalytic His286 Nε2 through Oγ (3.05 Å, 116.4° in PCL-**1**-(R_C); 3.02 Å, 115.3° in PCL-**1**-(S_C)). The alcohol oxygen O_I is also hydrogen bonded to catalytic His286 Nε2 in both enantiomers (3.30 Å, 126.5° in PCL-**1**-(R); 3.17 Å, 132.3° in PCL-**1**-(S_C)), but the bond is weaker in PCL-**1**-(R_C).[iv] Furthermore, both inhibitors have a *gauche* conformation between the Ser87 Oγ-P bond and the O_I-CH_2 bond of the alcohol moiety (dihedral angle Ser87Oγ-P-O_I-CH_2 of 72.3° in PCL-**1**-(R_C) and of 76.8° in PCL-**1**-(S_C)), which allows for an overlap between the

[iv] Usually $d < 3.2$ Å and $120° < \theta < 180°$.

lone pair *n* orbital of the alcohol oxygen and the σ^* orbital of the Oγ-P bond, in agreement with the stereoelectronic theory.[30]

Table 2 – Key hydrogen bond distances (heavy atom to heavy atom) and key angles in the two PCL-inhibitor complexes.

	PCL-1-(R_C)	PCL-1-(S_C)
Leu17 N(H) – O=P (Å)[a]	2.73	2.73
Gln88 N(H) – O=P (Å)[a]	2.81	2.82
Nδ1 His286 – Oδ2 Asp264 (Å)	2.81	2.82
Nε2 His286 – Oγ Ser87 (Å)	3.05	3.02
Nε2 His286 – Oγ Ser87 (Nε2-H-Oγ θ, °)	116.4	115.3
Nε2 His286 – O_I (Å)[b]	3.30	3.17
Nε2 His286 – O_I (Nε2-H-O_I θ, °)[b]	126.5	132.3
Ser87Oγ-P-O_I-CH_2 θ (°)	72.3	76.8

[a] the angles N-H-O are typical of hydrogen bonds. [b] O_I is the MPP alcohol oxygen

To interpret these structures, PCL enantioselectivity towards the substrate MPP-C_7 was measured in a solvent similar to the one used for the crystallisation of the PCL-inhibitor complexes.[v] In 30 vol% *n*-propanol in potassium phosphate buffer, PCL hydrolysed MPP-C_7 with high enantioselectivity (E ≥190) favouring the (*S*)-enantiomer (Scheme 3). PCL-catalysed hydrolysis of racemic MPP-C_7 was stopped at 40% conversion. Gas chromatographic analysis of both remaining starting material and hydrolysed product was used to calculate their respective optical purities, which in turn served to determine PCL enantioselectivity according to Chen *et al.*[31]

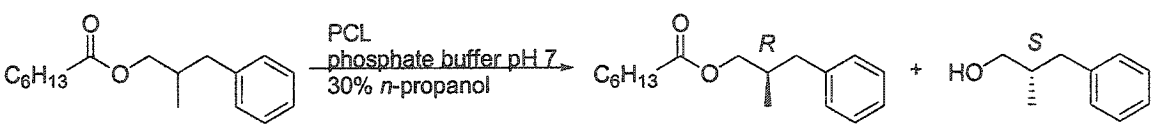

Scheme 3 – PCL catalysed kinetic resolution of MPP-C_7

[v] The complexes used mimic the transition state for the PCL catalysed hydrolysis of (*R*)- and (*S*)-MPP-C_7.

Additionally, the kinetic constants relative to the PCL-catalysed hydrolysis of both (*R*) and (*S*)-MPP-C_7 were spectrophotometrically determined in a solvent similar to the one used for the crystallisation of the PCL-inhibitor complexes (potassium phosphate instead of imidazole buffer; Table 3). Because of the poor solubility of heptanoic esters in this solvent the maximum substrate concentration was approximately equal to K_M (see Materials and Methods). Thus the measured k_{cat} and K_M values have large errors. Nevertheless, since E is defined as the ratio of the specificity constant k_{cat}/K_M of the fast enantiomer over the specificity constant of the slow enantiomer,[32] PCL enantioselectivity using these parameters was calculated to be 80 ± 50 (Table 3). Considering the large errors involved in this determination, we find agreement between this value and the more accurately determined end-point E value.

The two calculated K_M values (3 mM for (*R*)-MPP-C_7 and 4 mM for (*S*)-MPP-C_7) indicate similar binding affinities of the two alcohol moieties within PCL catalytic pocket while the different turnover numbers (k_{cat}) of 0.4 min^{-1} for (*S*)-MPP-C_7 and 0.004 min^{-1} for (*R*)-MPP-C_7 suggest that PCL enantioselectivity is due to its faster reaction with (*S*)-MPP-C_7.

Table 3 - Kinetic constants for (*R*) and (*S*)-MPP-C_7[a].

	(R)-MPP-C_7	(S)-MPP-C_7
k_{cat} (min^{-1})	$(0.4 \pm 0.1)10^{-2}$	0.4 ± 0.1
K_M (mM)	3 ± 1	4 ± 1
(k_{cat}/K_M) ($min^{-1}mM^{-1}$)	$(1.3 \pm 0.6)10^{-3}$	0.10 ± 0.04
E[b] $[(k_{cat}/K_M(S))/(k_{cat}/K_M(R))]$	80 ± 50	
End point E[c]	$> 190 \pm 30$	

[a] Reaction conditions:[BES] = 7.44 mM, [PNP] = 1.24 mM, [PCL] = 2.85 μg/mL, [(*R*) and (*S*)-MPP-C_7] = 0.6 to 4.5 mM, [*n*-propanol] = 28.8%. Data were analysed by Eadie-Hofstee plots.[23,24] [b] Calculated from the k_{cat} and K_M values. [c] Determined by GC analysis of reaction products and starting materials at 40% conversion according to Chen *et al.*[31], ee_s = 63%, ee_p > 98% , c = 39%.

The subtlety of the enzyme-substrate interactions renders it difficult to assess which ones are responsible for PCL enantioselectivity towards MPP-C_7. Also, the similar hydrogen bond His286 Nε2H - MPP O_I (difference 0.13 Å), although weaker for the slow enantiomer, does not agree with the calculated k_{cat} values (Table 3), that indicate a 100 times faster reaction for the (*S*)-enantiomer. Thus a portion of the complex enzyme-

inhibitor was modelled: a sphere of 15 Å centred on the phosphorus atom. A combined QM/MM approach was used to treat semi-empirically only the catalytic triad residues Ser87, Asp263 and His286, the oxyanion hole residues Leu17 and Gln88, residues Gly16, Thr18, Tyr29, His86, Leu287 and the inhibitor, while the remainder of the sphere was considered as potential field. Energy minimisations help both in conferring to the protein the mobility that may have been lost in the crystal structures[33] and hopefully in estimating the contribution to the enantioselectivity of the residues that subtly interact with the bound substrate. The first tetrahedral intermediate T_d1, rather than an analogue of the transition state, was minimised. It as been shown that, although phosphonate analogues appear to be isosteric to transition states, the distances P-O are overestimated with respect to the mimicked C-O distances and they also show a different electrostatic recognition pattern.[34]

Because the X-ray crystal structures contain a bound phosphonate ester that mimics the transition state for the reaction studied, conformational searches to determine the corresponding tetrahedral intermediate conformation within the catalytic pocket of PCL were not performed. Instead, the conformation found in the crystal structures was used directly in the optimisation. The resulting structures show significant differences in the hydrogen bond between His286 Nε2 and alcohol O_I (Table 4). While in the slow (*R*)-enantiomer only the angle Nε2-H-O_I improves to 142.9°, the (*S*)-enantiomer has a much stronger hydrogen bond between His286 Nε2 and alcohol O_I (2.77 Å, 150.8°) compared to both PCL-1-(*S*), PCL-1-(*R*) and the minimised T_d1 of PCL-1-(*R*). This agrees with the higher k_{cat} calculated for the hydrolysis of (*S*)-MPP-C_7.

The carbonyl oxygens reside in the oxyanion hole, at hydrogen bonding distance from NH of Leu17 and Glu88 (2.74 Å and 2.76 Å in (*R*) T_d1; 2.81 Å and 2.77 Å in (S) T_d1). Noticeably, the hydrogen bond angle Nε2-H-Oγ between Ser87 and His286 changes from 116.4° to 150.7° in the slow enantiomer and from 115.3° to 136.9° in the fast (S) enantiomer.

Table 4 - Key hydrogen bond distances (heavy atom to heavy atom) and key angles in the two tetrahedral intermediates T_d1 after PM3 minimisation.

	(*R*) T_d1	(*S*) T_d1
Leu17 N(H) – O=P[a] (Å)	2.74	2.81
Gln88 N(H) – O=P[a] (Å)	2.76	2.77
Nδ1 His286 – Oδ2 Asp264 (Å)	2.66	2.65
Nε2 His286 – Oγ Ser87 (Å)	2.70	2.68
Nε2 His286 – Oγ Ser87 (Nε2-H-Oγ θ, °)	150.7	136.9
Nε2 His286 – O_I (Å)	3.30	2.77
Nε2 His286 – O_I (Nε2-H-O_I θ, °)	142.9	150.8
Ser87Oγ-C-O_I-CH_2 θ (°)	76.8	105.6

[a] the angles N-H-O are typical of hydrogen bonds.

Although the T_d1 relative to the (*R*) enantiomer maintained a dihedral angle Ser87Oγ-P-O_I-CH_2 conform to the stereoelectronic theory (76.8°),[30] the one relative to the fast enantiomer lost it (105.6°). The same situation, however, has been observed in the crystal structures of *Candida rugosa* lipase (CRL)-inhibitor complexes containing chiral secondary alcohols.[8] A recent review[35] criticises several assumptions of the stereoelectronic theory and affirms that this theory cannot always explain reactions involving tetrahedral intermediates. Also, the stabilisation gained by having antiperiplanar lone pairs is, in the best case, less than 2 kcal/mol.[35] Since for enzyme-catalysed ester hydrolyses no strong experimental evidence has been provided either in favour or against this theory, especially concerning its influence on enzyme enantioselectivity, the loss of the *gauche* conformation in the fast enantiomer (Ser87Oγ-P-O_I-CH_2 ~ 60°) is not a concern to us.

Despite the modelling of the tetrahedral intermediates, the differences in the orientation of the two MPP alcohol moieties within PCL catalytic pocket remained – excluding the hydrogen bond between alcohol oxygen and His286 Nε2 – subtle (Figure 5).

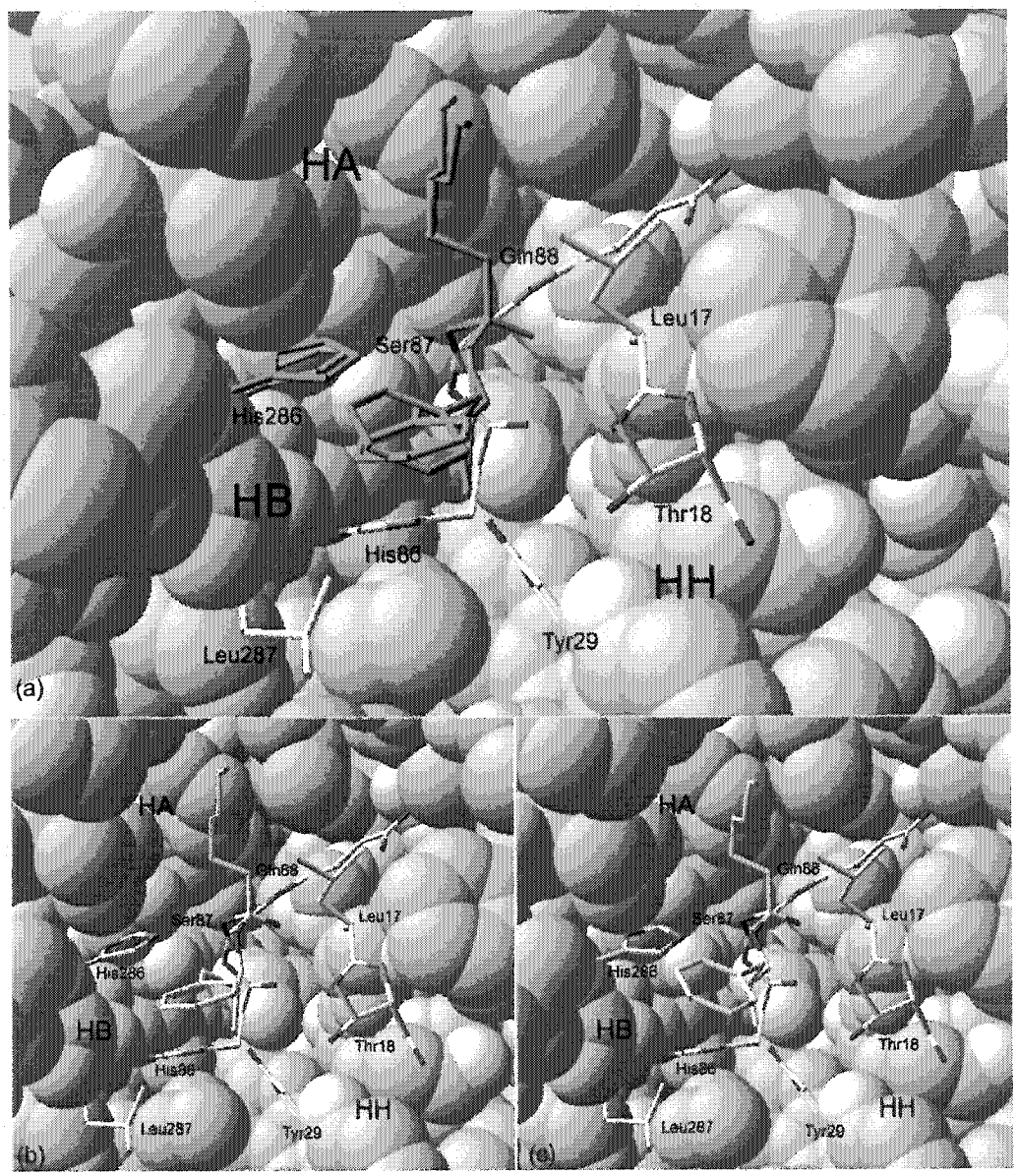

Figure 5 – Combined QM/MM modelling output structures. (a): overlay of the tetrahedral intermediates of the fast (*S*)-enantiomer (T_d1 and His286 in purple) and of the slow (*R*)-enantiomer (T_d1 and His286 in green); (b): tetrahedral intermediate of the slow (*R*)-enantiomer; (c): tetrahedral intermediate of the fast (*S*)-enantiomer. Catalytic triad residues His286 and Ser87, oxyanion hole residues Glu88 and Leu17 and "enzyme reaction zone" residues Thr18, Tyr29 and Leu287 are in stick representation and CPK colours.

Like in the crystal structures, the alcohol moieties lie in a solvent exposed crevice. A clash between the benzylic CH_2 of the alcohol moiety and His286 Cδ2 (3.60 Å) and between the phenyl ring and Thr18 side-chain CH_3 was however observed in the T_d1 of the slow reacting enantiomer. In the fast enantiomer the benzylic CH_2 lie close to the

carbonyl oxygen of Leu17 (3.38 Å). Schultz *et al.*[36] observed that atoms other than hydrogen cause repulsion when directed towards this residue, while interaction with hydrogens is preferred. Also, as pointed out above, the orientation of the hydrogen at the stereocentre is different in the two enantiomers. There seems to be a propensity of the alcohol oxygen to orient itself with the lone pairs directed roughly in the same direction of the hydrogen at the stereocentre. In the fast (*S*)-enantiomer this brings the oxygen close to His286 Nε2, thus favouring the hydrogen bond formation. In the slow (*R*)-enantiomer this tends to distance the oxygen from catalytic His286, which results in the loss of the hydrogen bond.

Discussion

The different enantiopreference of PCL for primary and secondary alcohols has puzzled several scientists.[15,16,17,19] Luic *et al.*[37] published the X-ray crystal structure of PCL complexed with inhibitor (R_P)-O-(2*R*)-(1-phenoxy-2-butyl)-methylphosphonic acid chloride (PDB ID: 1HQD[37]), which mimics the transition state for the PCL-catalysed hydrolysis of (*R*)-1-phenoxy-2-butyl acetate (this is also the favourite enantiomer in the PCL-catalysed hydrolysis of the corresponding racemate). By comparison of this crystal structure with the one of PCL-1-(S_C) it is clear that the primary alcohol moiety of MPP-C_7 does not bind to the same regions of PCL as the secondary alcohol moiety of the fast reacting enantiomer of 1-phenoxy-2-butyl acetate (Figure 6). The large substituent at the stereocentre of (*R*)-1-phenoxy-2-butanol binds in the HA pocket, where lie the acyl chain of both our inhibitors. This is possible because of the very short acyl chain of the phosphonate ester they used (methyl group) that leaves room for the benzyl ring of the alcohol to bind to HA (Figure 6). Because Luić *et al.*[37] did not publish the structure of the complex PCL-inhibitor with the slow reacting enantiomer of 1-phenoxy-2-butanol as alcohol moiety, one can only speculate about the difference between the binding of the slow reacting enantiomers of secondary and primary alcohols in PCL. From their modelling experiments the slow and fast enantiomer show H-alignment and the large substituent at the stereocentre of the slow enantiomer binds in the HH pocket of PCL. However the large substituent at the stereocentre of both MPP enantiomers points towards the solvent. Thus primary and secondary alcohols bind differently to PCL. This binding

difference explains why PCL shows opposite enantiopreference for primary and secondary alcohols.

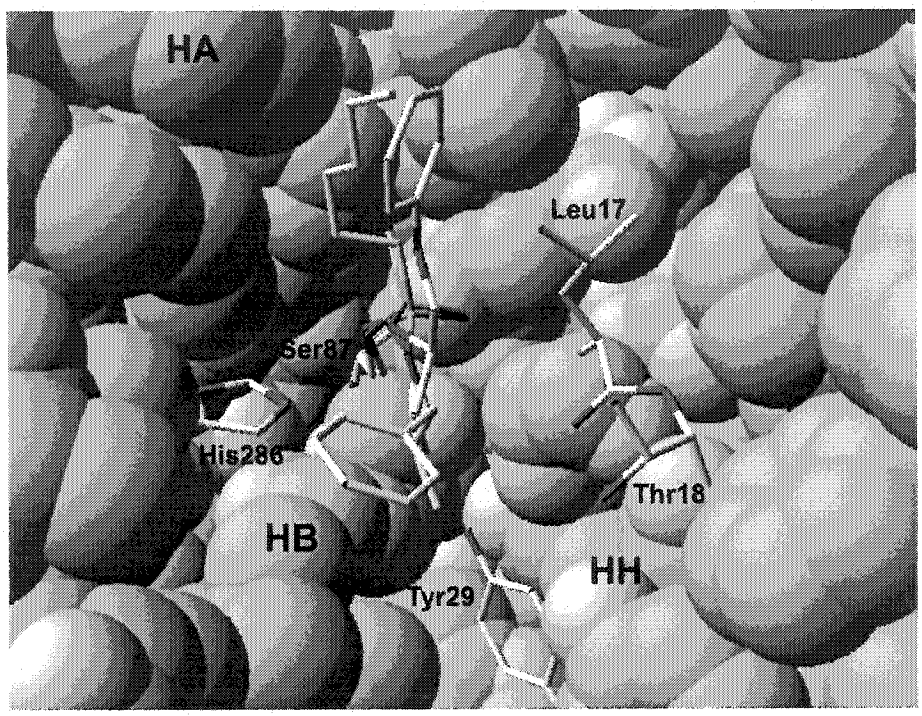

Figure 6 – Different binding of primary and secondary alcohols in PCL. Overlap (stick representation and CPK colours) of the PCL complex with inhibitor (R_PS_P)-O-(2*R*)-(1-phenoxy-2-butyl)-methylphosphonic acid chloride[37] with the complex PCL-**1**-(S_C). The large substituents at the stereocentre do not bind in the same regions of PCL. Catalytic triad residues His286 and Ser87, oxyanion hole residue Leu17, residues Thr18 and Tyr29 are in stick representation and CPK colours.

Cygler *et al.*[8] solved the crystal structures of CRL complexed with a phosphonate inhibitor containing menthol as chiral secondary alcohol moiety. They observed that in the complex containing the fast enantiomer of menthol both the catalytic serine and the fast enantiomer where hydrogen bonded to Nε2 of catalytic histidine (3.15 Å, 125.8°). On the other hand in the complex containing the slow enantiomer of menthol only serine Oγ was hydrogen bonded to Nε2 of catalytic histidine (distance His449 Nε2 – O alcohol 4.16 Å). They deduced that the lack of that bond is one of the key factors that determine the enantioselectivity of CRL towards secondary alcohols. From the crystal structures described here one cannot likewise affirm that the enantioselectivity towards primary alcohols depends on the lack of a key H-bond in the slow reacting enantiomer, since both

MPP enantiomers have the alcohol oxygen at hydrogen bonding distance to His286 Nε2, although borderline in (*R*)-MPP (3.30 Å, 126.5°). The two MPP enantiomers show LM-alignment. This has been observed also in the menthol moiety of Cygler *et al.*[8] complexes. However, the extra methylene between the alcohol oxygen and the stereocentre, absent in secondary alcohols, not only allows the alcohol oxygen to maintain its hydrogen bond with His286, but also explains the very similar orientation of the two MPP enantiomers within the active site of PCL (Figure 4). This particular orientation of the large and medium group at the stereocentre (LM-alignment) had not been observed in any of the modelling experiments, where the authors suggest an exchange of the medium group and the hydrogen at the stereocentre.[15,16,17]

Geometry optimisations of the "enzyme reaction zone" of the tetrahedral intermediates show a better hydrogen bond between alcohol oxygen and His286 Nε2 in the fast enantiomer, which is confirmed by the 100-fold higher k_{cat} determined for such enantiomer. However the modelled structures displayed again only subtle differences between the (*R*) and (*S*) enantiomer of MPP. Both crystal structures and minimised structures suggest a propensity of the alcohol oxygen (O_I) to orient its lone pairs towards the same direction of the hydrogen at the stereocentre. This allows the fast enantiomer to achieve this key hydrogen bond with His286, but brings the oxygen of the slow enantiomer too far for binding the same way. Also, the bumping of the slow enantiomer into His286 Cδ2 and the presence of two different conformers for the alcohol moiety in complexes PCL-**1**-(R_C) suggest a worse binding of this enantiomer within the catalytic pocket of PCL. Although the experimentally determined K_M values for the PCL-catalysed hydrolysis of MPP-C_7 (Table 3) indicate a similar binding of the two alcohol moieties within PCL catalytic pocket (K_M is 3 mM for (*R*)-MPP-C_7 and 4 mM for (*S*)-MPP-C_7), in certain circumstances a substrate can bind to an enzyme in a non-productive way, which is in competition with its productive binding.[38] The presence of both productive and non-productive binding leads to an apparent overall tighter binding of the substrate, hence a decrease in K_M. This is probably what happens in our case with the slow (*R*)-enantiomer.

In conclusion the difference in enantiopreference of PCL between secondary and primary alcohols has been explained by showing that MPP binds differently than 1-phenoxy-2-butanol. More importantly, the combination of different techniques, i.e.

crystallography, modelling and kinetic studies, has demonstrated that PCL discriminates between enantiomers of MPP on the basis of hydrogen bond differences and of the better binding of the fast enantiomer. The very similar orientation of (*R*)- and (*S*)-MPP in PCL catalytic pocket, due to the relative "umbrella-like" inversion at the stereocentre of the two enantiomers, has been shown. The subtle differences in the binding of the two enantiomers justify the fact that rational methods to increase the enantioselectivity of PCL towards primary alcohols have often failed.[19] An ensemble of small differences between the binding of the fast and the slow enantiomer renders it extremely hard to design substrates or engineer the enzyme for increasing its E.

Acknowledgements

I whish to thank Les Fonds Québécois de la Recherche sur la Nature et les Technologies for two post-graduate fellowships and Mr. Tobie Généreux-Vincent for insightful discussions and precious help. We also thank Dr. Alexandra Weissfloch for initial synthesis of racemic inhibitors and National Sciences and Engineering Research Council of Canada (NSERC) for financial support.

References

[1]Bornscheuer, U. T.; Kazlauskas, R. J. *Hydrolases in Organic Synthesis*; Wiley-VCH: Weinheim, Germany, **1999**, pp. 65-106.

[2]Miyazawa, T.; Yukawa, T.; Koshiba, T.; Ueji, S.; Yanagihara, R.; Yamada, T. *Biotechnol. Lett.* **2001**, *23*, 1547-1550.

[3]Martin, C.; Himmele, W.; Siegel, H. *US Pat. No. 4410734* **1983**.

[4]Delinck, D. L.; Margolin, A. L. *Tetrahedron Lett.* **1990**, *31*, 6797-6798.

[5]Stoermer, D.; Caron, S.; Heathcock, C. H. *J. Org. Chem.* **1996**, *61*, 9115-9125.

[6]Schrag, J. D.; Li, Y.; Cygler, M.; Lang, D.; Burgdorf, T.; Hecht, H.-J.; Schmid, R.; Schomburg, D.; Rydel, T.J.; Oliver, J. D.; Strickland, L. C.; Dunaway, C. M.; Larson, S.B.; Day, J.; McPherson, A. *Structure* **1997**, *5*, 187-202.

[7]Kim, K. K.; Song, H.K.; Shin, D. H.; Hwang, K. Y.; Suh, S. W. *Structure* **1997**, *5*, 173-185.

[8]Cygler, M.; Grochulski, P.; Kazlauskas, R. J.; Schrag, J. D.; Bouthillier, F.; Rubin, B.; Serreqi, A. N.; Gupta, A. K. *J. Am. Chem. Soc.* **1994**, *116*, 3180-3186.

[9]Jackson, D. S.; Fraser, S. A.; Ni, L.-M.; Kam, C.-M.; Winkler, U.; Johnson, D. A.; Froelich, C. J.; Hudig, D.; Powers, J. C. *J. Med. Chem.* **1998**, *41*, 2289-2301.

[10]Gillespie, S. G.; Lau, S. L.; Paulson, S. C. *Phosphorus, sulfur, and silicon* **1997**, *122*, 205-208.

[11]Tramontano, A.; Ivanov, B.; Gololobov, G.; Paul, S. *Appl. Biochem. Biotechnol.* **2000**, *83*, 233-243.

[12]Rahil, J.; Pratt, R. F *Biochemistry* **1994**, *33*, 116-125.

[13]Stadler, P.; Zandonella, G.; Haalck, L.; Spener, F.; Hermetter, A.; Paltauf, F. *Biochim. Biophys. Acta* **1996**, *1304*, 229-244.

[14]Mannesse, M. L. M.; Boots, J. - W. P.; Dijkman, R.; Slotboom, A. J.; van der Hijden, H. T. W. M.; Egmond, M. R.; Verheij, H. *Biochim. Biophys. Acta* **1995**, *1259*, 56-64.

[15]Zuegg, J.; Hönig, H.; Schrag, J. D.; Cygler, M. *J. Mol. Cat. B: Enzymatic* **1997**, *3*, 83-98.

[16]Tuomi, W. V.; Kazlauskas, R .J. *J. Org. Chem.* **1999**, *64*, 2638-2647.

[17]Tomić, S.; Dobovičnik, V.; Šunjić, Ć.; Kojić-Prodić, B. *Croat. Chem. Acta* **2001**, *74*, 343-357.

[18] Lang, D.A.; Mannesse, M. L. M.; de Haas, G. H.; Verheij, H. M.; Dijkstra, B. W. *Eur. J. Biochem.* **1998**, *254*, 333-340.

[19]Weissfloch, A. N. E.; Kazlauskas, R. J. *J. Org. Chem.***1995**, *60*, 6959-6969.

[20]Murshudov, G. N.; Lebedev, A.; Vagin, A. A.; Wilson, K. S.; Dodson, E. J. *Acta Cryst.* **1999**, *D55*, 247-255.

[21]Guex, N.; Peitsch, M. C. *Electrophoresis* **1997**, *18*, 2714-2723.

[22]Otwinowski, Z.; Minor, W. *Methods in Enzymology*, **1997**, *276*, 307-326.

[23]Eadie, G. S. *J. Biol. Chem.* **1942**, *146*, 85-93.

[24]Hofstee, B. H. J. *Nature* **1959**, *184*, 1296-1298.

[25]Stewart, J. J. P. *J. Comput. Chem.* **1989**, *10*, 209-220.

[26]Stewart, J. J. P. *J. Comput. Chem.* **1989**, *10*, 221-264.

[27]Polak, E.; Ribière, G *Rev. Fr. d'Informatique et de Recherche Operationnelle* **1969**, *16*, 35-43.

[28]Zhao, K.; Landry, D.W. *Tetrahedron* **1993**, *49*, 353-368.

[29]Kovach, I. M.; Huhta, D.; Baptist, S. *J. Mol. Struct.* **1991**, *72*, 99-110.

[30]Deslongchamps, P.; Atlani, P.; Fréhel, D.; Malaval, A. *Can. J. Chem.* **1972**, *50*, 3405-3408.

[31]Chen, C. - S.; Fujimoto, Y.; Girdaukas, G.; Sih, C. J. *J. Am. Chem. Soc.* **1982**, *104*, 7294–7299.

[32]Hein, G. E.; Niemann, C. *J. Am. Chem. Soc.* **1962**, *84*, 4487-4494.

[33]Pedersen, T. G.; Sigurskjold, B. W.; Andersen, K. V.; Kjaer, M.; Poulsen, F. M.; Dobson, C. M.; Redfield, C. *J. Mol. Biol.* **1991**, *218*, 413-426.

[34]Tantillo, D. J.; Houk, K. N. *J. Org. Chem.* **1999**, *64*, 3066-3076.

[35]Perrin, C. L. *Acc. Chem. Res.* **2002**, *35*, 28-34.

[36]Schulz, T.; Pleiss, J.; Schmid, R.D. *Prot. Sci.* **2000**, *9*, 1053-1062.

[37]Luić, M.; Tomić, S.; Leščić, I.; Ljubović, E.; Šepac, D.; Šunjić, V.; Vitale, L.; Saenger, W.; Kojić-Prodić, B. *Eur. J. Biochem.* **2001**, *268*, 3964-3973.

[38]Fersht, A. *Enzyme structure and mechanism*, 2nd edition; W. H. Freeman and Co.: New York, NY, **1985**, pp. 109-111.

CHAPTER 2 - APPENDIX 1

Interactions PCL-alcohol moiety in complexes PCL-1-(R_C) and PCL-1-(S_C) and in the modelled tetrahedral intermediates

The alcohol moieties in complexes PCL-1-(R_C) and PCL-1-(S_C) differ in an "umbrella-like" inversion at the alcohol stereocentre (LM-alignment) that places the hydrogen substituent in a different location in the two complexes. The other three substituents at the alcohol stereocentre lie in the same position in both enantiomers, but show subtle differences. The substituents at the stereocentre were broken up as shown in Scheme 1. Their differences in the two complexes are highlighted in Table 1, while their differences in the modelled tetrahedral intermediates are shown in Table 2.

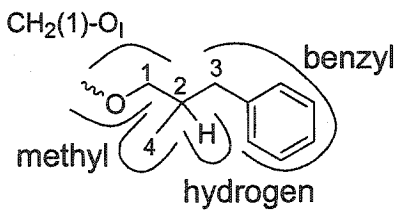

Scheme 1 – Schematic representation of the four different substituents at the stereocentre of MPP.

Complexes PCL-1-(R_C) and PCL-1-(S_C)

In complexes PCL-1-(R_C) and PCL-1-(S_C), three differences were identified in the benzyl substituent orientations of (*S*)-MPP and (*R*)-MPP (Table 1). The phenyl ring of (*S*)-MPP is slightly closer to the side chain methyl groups of Leu287 (mean distance of 4.43 Å in (*S*)-MPP versus 4.72 in (*R*)-MPP), which may suggest better hydrophobic interactions for this substituent. On the other hand the phenyl ring of (*R*)-MPP is closer to Cγ1 of Thr18 (mean distance of 5.17 Å versus 5.42 Å). A significant difference in the benzyl group orientation is the position of the benzylic CH_2(3) relative to the side-chain of catalytic His286. The inversion at the stereocentre orients this group differently in the two enantiomers, so that it interacts with the enzyme catalytic pocket, in particular with

His286, only in the slow (*R*)-enantiomer (4.07 Å to Nε2, 3.77 Å to Cδ2 and 3.87 Å to Cγ of His286).

Table 1 - Summary of subtle interactions alcohol moiety-enzyme residues that may contribute to the enantioselectivity in the complexes PCL-inhibitor.

Interaction	(*R*)-MPP	(*S*)-MPP
Benzyl substituent		
Leu287 s.c.[a] – Ph	mean 4.72 Å	mean 4.43 Å
Thr18 Cγ1 - Ph	mean 5.17 Å	mean 5.42 Å
His286 s.c. – CH_2(3)	4.07 Å to Nε2	-
	3.77 Å to Cδ2	-
	3.87 Å to Cγ	-
CH_2(1)-O_I substituent		
Leu17 C=O - CH_2(1)	3.60 Å	3.50 Å
His286 Nε2 - O_I	3.30 Å, 126.5°	3.17 Å, 132.3°
His86 s.c. - CH_2(1)	4.41 Å to Cε1	4.24 Å to Cε1
	5.36 Å to Nε2	5.23 Å to Nε2
	4.64 Å to Nδ1	4.41 Å to Nδ1
Hydrogen substituent		
Leu17 C=O - CH(2)	3.25 Å	-
Methyl substituent		
Thr 18 Cγ1 - CH_3(4)	4.81 Å	5.37 Å
Thr 18 Oγ1 - CH_3(4)	3.79 Å	4.06 Å
Leu17 C=O - CH_3(4)	3.37 Å	3.62 Å
Tyr29OH -CH_3(4)	4.11 Å	3.62 Å
His86 s.c.- CH_3(4)	4.85 Å to Cε1	4.32 Å to Cε1
	6.03 Å to Nε2	5.54 Å to Nε2
	5.19 Å to Nδ1	4.61 Å to Nδ1

In the $CH_2(1)O_I$ substituent, CH_2(1) is slightly closer to Leu17 carbonyl in (*S*)-MPP than in (*R*)-MPP (3.50 Å versus 3.60 Å). A slightly better hydrogen bond between alcohol O_I and His286 Nε2 favours the fast reacting (*S*)-enantiomer (3.17 Å and 132.3° versus 3.30 Å and 126.5°). Another difference between the two enantiomers comes from the interaction of CH_2(1) with His86. (*S*)-MPP is at 4.24 Å from Cε1, 5.23 Å from Nε2 and 4.41 Å from Nδ1, while (*R*)-MPP is at 4.41 Å from Cε1, 5.36 Å from Nε2 and 4.64 Å from Nδ1, hence slightly farther.

A bumping between CH_2(1) and the carbonyl oxygen of Leu17 (3.25 Å), present only in the slow enantiomer, may favour the fast enantiomer.

Last, there are four differences in the orientation of the methyl substituent. $CH_3(4)$ is at 4.81 Å from Thr18 Cγ1 in (*R*)-MPP and at 5.37 Å from Cγ1 in (*S*)-MPP. $CH_3(4)$ also interacts with Oγ1 of Thr18: in (*R*)-MPP it is at 3.79 Å while in (*S*)-MPP it is at 4.06 Å. The methyl group makes van der Waals contacts with Leu17 carbonyl oxygen in both enantiomers, being at 3.62 Å from the oxygen in (*S*)-MPP and at 3.37 Å in (*R*)-MPP. There is also a difference in the distance of $CH_3(4)$ to Tyr29 side-chain: the methyl group of the fast (*S*)-enantiomer is at 3.62 Å from Tyr29 OH while it is at 4.11 Å from Tyr29 OH in the slow (*R*)-enantiomer. Last, $CH_3(4)$ is closer to His86 side-chain in (*S*)-MPP. The methyl group of (*S*)-MPP is at 4.32 Å, 5.54 Å and 4.61 Å from Cε1, Nε2 and Nδ1. In (*R*)-MPP it is at 4.85 Å, 6.03 Å and 5.19 Å from Cε1, Nε2 and Nδ1 respectively.

Modelled tetrahedral intermediates (*R*)-1 T_d1 and (*S*)-1 T_d1

Like in the crystal structures, the differences in binding between the two enantiomers appear to be very subtle (Table 2). There are three differences in the orientation of the benzyl substituent of (*S*)-MPP and (*R*)-MPP after modelling of the tetrahedral intermediates. The phenyl ring of (*S*)-MPP is slightly closer to the side chain methyl groups of Leu287 (mean distance of 4.60 Å in (*S*)-MPP versus 4.86 in (*R*)-MPP), however both enantiomers are slightly farther from this residue than in the crystal structure. The phenyl ring of the (*R*)-enantiomer is closer to Cγ1 of Thr18 (4.65 Å versus 5.31 Å). Compared to the crystal structures, the difference in distance to this residue increases from 0.25 Å to 0.66 Å. The benzylic $CH_2(3)$ of the slow (*R*)-enantiomer remains close to the side-chain of catalytic His286, although slightly farther than in the crystal structures (4.14 Å to Nε2, 3.60 Å to Cδ2 and 4.84 Å to Cγ of His286).

In the $CH_2(1)O_I$ substituent, the difference between the two enantiomers increases. The $CH_2(1)$ is now 0.29 Å closer to Leu17 carbonyl in (*S*)-MPP than in (*R*)-MPP (3.42 Å vs 3.71 Å), while in the crystal structures the difference in this distance was only 0.10 Å. A better hydrogen bond between alcohol O_I and His286 Nε2 favours the fast reacting (*S*)-enantiomer (2.77 Å, 150.8° versus 3.30 Å and 142.9°).

Table 2 - Summary of subtle interactions that may contribute to the enantioselectivity in the minimised tetrahedral intermediates.

Interaction	(*R*)-1 T_d1	(*S*)-1 T_d1
Benzyl substituent		
Leu287 s.c.[a] – Ph	mean 4.86 Å	mean 4.60 Å
Thr18 Cγ1 - Ph	mean 4.65 Å	mean 5.31 Å
His286 s.c. – CH_2(3)	4.14 Å to Nε2	-
	3.60 Å to Cδ2	-
	4.84 Å to Cγ	-
CH_2(1)-O_I substituent		
Leu17 C=O - CH_2(1)	3.71 Å	3.42 Å
His286 Nε2 - O_I	3.30 Å, 142.9°	2.77 Å, 150.8°
Hydrogen substituent		
Leu17 C=O - CH(2)	3.38 Å	-
Methyl substituent		
Tyr29OH -CH_3(4)	3.50 Å	3.91 Å

The CH_2(1) substituent of (*R*)-MPP is farther from the carbonyl oxygen of Leu17 in the modelled structure than in the crystal structure (3.38 Å versus 3.25 Å). The propensity of the modelled tetrahedral intermediate to distance itself from this residue suggests an unfavourable interaction of the hydrogen at the stereocentre of the slow enantiomer with Leu17.

Last, there is only one significant difference in the orientation of the methyl substituent. CH_3(4) of the slow (*R*)-enantiomer is closer to Tyr29 side-chain hydroxyl group than the fast (*S*)-enantiomer (3.50 Å versus 3.91 Å).

Chapter 3

As we have seen in the previous chapters, understanding the mechanism of enzymes enantiorecognition has been the subject of extensive research by several scientists. To date there is still no agreement on how enzymes differentiate enantiomers of primary alcohols. In this chapter we describe the results of our research aimed at explaining the enantioselectivity of PCL towards chiral primary alcohols carrying an oxygen atom at the stereocentre.

Contributors

This work was done under the supervision of Professor Romas J. Kazlauskas and in collaboration with the Macromolecular Structure Group of the Biotechnology Research Institute (BRI), National Research Council of Canada and with Professor Michael A. Whitehead of the Chemistry Department, McGill University. Dr. Chan Seong Cheong, postdoctoral fellow in our laboratory in 1997, prepared pure enantiomers of 2-phenoxy-1-propanol, which I used for the synthesis of the phosphonate inhibitors **1**-(*R*) and **1**-(*S*). Dr. Joseph D. Schrag of the BRI crystallised the PCL-inhibitor complexes, collected X-ray diffraction data and solved the structures. Mrs Cécile Malardier-Jugroot, Ph.D. candidate in the Chemistry Department, McGill University, helped finding a strategy for the semi-empirical calculations and guided me during the modelling experiments. Professor Michael A. Whitehead of the Chemistry Department, McGill University, assisted in interpreting the modelling results. Dr. Mirek Cygler of the BRI helped in interpreting the electron density maps. I synthesised the inhibitors that were used for this publication, inactivated PCL, participated in the very first steps of the refinement of the structures of complexes PCL-**1**-(*R*) and PCL-**1**-(*S*) (fitting the protein model in the density map), analysed the resulting structures, determined the kinetic constants, performed end-point E measurements and combined QM/MM calculations.

X-ray crystal structures of transition state analogues explain the enantioselectivity of *Pseudomonas cepacia* lipase towards primary alcohols with oxygen at the stereocentre.

Abstract

Pseudomonas cepacia lipase (PCL) catalyses the hydrolysis of esters of primary alcohols having oxygen atoms at the stereocentre in an unpredictable manner, in contrast to primary alcohols without oxygen at the chiral carbon. To understand the origins of PCL enantioselectivity towards this class of compounds, four phosphonate inhibitors were synthesised. Two contained enantiomeric configurations of 2-phenoxy-1-propanol (POP), the other two incorporated pure enantiomers of 2,2-dimethyl-[1,3]dioxolan-4-methanol (solketal) as alcohol moieties. The crystal structures of the PCL-inhibitor complexes, solved at resolutions ranging from 1.65 Å to 1.80 Å, reveal that both POP and solketal moieties bind to PCL with the large substituent at the stereocentre laying in a solvent exposed crevice. However, the POP enantiomers display an "umbrella-like" inversion at the stereocentre and show "LM-alignment" (the hydrogen at the stereocentre points in opposite directions in the two enantiomers), while solketal exhibits the so-called "H-alignment" (exchange of the large and medium substituents at the stereocentre). This may explain why it is not possible to predict PCL enantiopreference with a simple empirical rule.[1,2] The difference between the two POP enantiomers consists mainly in the orientation of the hydrogen and oxygen at the stereocentre. In the slow enantiomer, (*R*)-POP, the oxygen is subject to electrostatic repulsion due to its proximity to the carbonyl oxygen of Leu17 (3.29 Å). We believe that this is the major determinant of PCL enantioselectivity (E = 70) for (*S*)-POP. In (*S*)-solketal, the repulsion due to the proximity of the oxygen at the stereocentre to the carbonyl of Leu17 (2.76 Å) is counterbalanced by a hydrogen bond with Thr18 side-chain Oγ (3.17 Å). This may determine the enantiopreference of the enzyme, although very small (E = 5.2), for this enantiomer.

Introduction

In order to speed-up the choice of the proper enzyme to use as catalyst in the kinetic resolution of esters of chiral primary alcohols a very general rule, based on the difference

in size of the substituents at the stereocentre, has been developed[1,2] (Figure 1(a)). Interestingly, this rule applies only to PCL and is reliable only when primary alcohols lacking oxygen at the stereocentre are involved.[1]

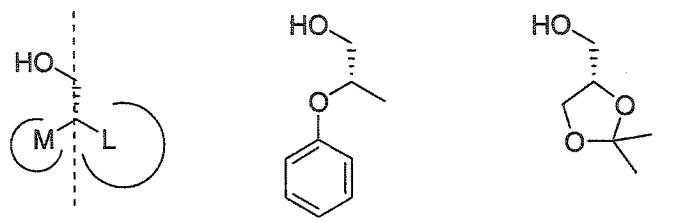

(*S*)-POP (*S*)-solketal

(a) (b) (c)

Figure 1 - (a) An empirical rule predicts which enantiomer of a primary alcohol reacts faster with PCL.[1] The preferred enantiomer is shown. M represents a medium sized substituent, e.g. CH_3, L is a large sized substituent, e.g. $CH_2C_6H_5$. The fast enantiomer is the one that has, as shown here, the large substituent on the right hand side once a line that passes through the bond defined by the chiral carbon atom and the methylene group alpha to it is drawn. (b) 2-phenoxy-1-propanol (POP) does not follow the rule. (c) 2,2-dimethyl-[1,3]dioxolan-4-methanol (solketal) follows the rule. The figure shows the fast enantiomers (*S*)-POP and (*S*)-solketal.

To explain PCL enantioselectivity towards esters of chiral primary alcohols with oxygen at the stereocentre and understand why the above empirical rule is not reliable when applied to these substrates, the binding of the enantiomers of two chiral primary alcohols possessing oxygen at the stereocentre within PCL catalytic pocket was investigated. These alcohols (Figure 1) present very interesting features. POP possesses an oxygen atom at the stereocentre, is structurally related to MPP (Chapter 2) and does not behave according to the empirical rule.[1,2] Solketal, on the other hand, does have oxygen at the stereocentre and it is also possible to predict which is the fast reacting enantiomer by means of the empirical rule. Pure enantiomers of POP have been used for the synthesis of juvenoids, analogues of the insect juvenile hormone,[3] while pure enantiomers of solketal have been used as building blocks in the synthesis of several bioactive compounds such as the β-adrenergic blocker timolol[4] and the macrolide antibiotic brefeldin A, a specific inhibitor of exocytosis.[5] Because of the changes in priority of the groups at the stereocentre, the favourite enantiomers of both POP and solketal have *S* configuration.

Lipases catalyse the hydrolysis of esters by forming two successive tetrahedral intermediates. The alcohol moiety being released upon breakdown of the first tetrahedral intermediate T_d1 (Scheme 1), it is this intermediate that determines the enantioselectivity of lipases towards chiral alcohols. Phosphonate analogues,[6] covalently linked to catalytic Ser87, were used to "freeze" the enzyme in a state that mimics T_d1.[i]

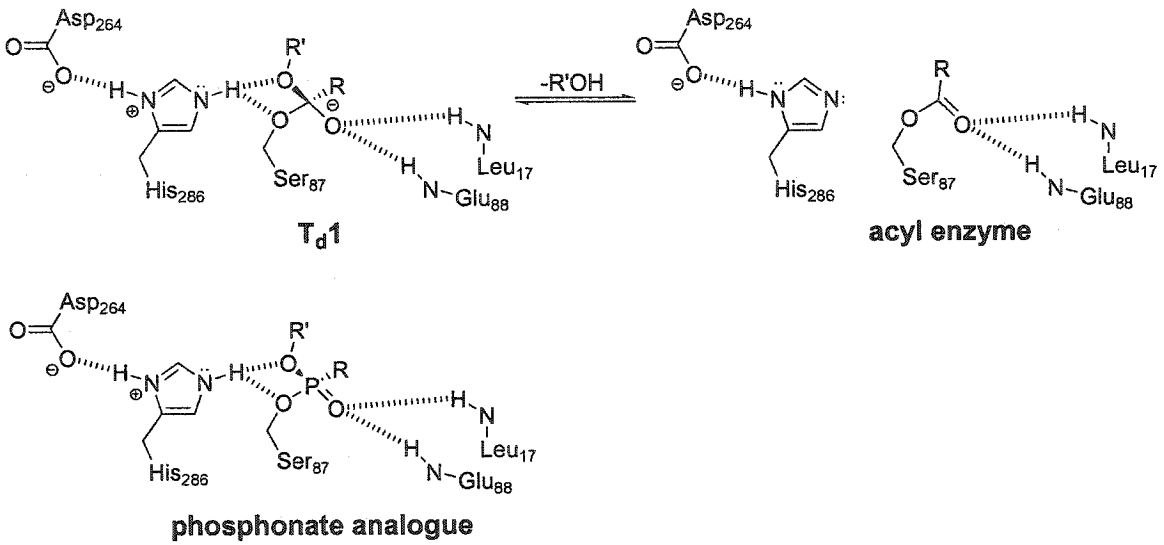

Scheme 1 - First tetrahedral intermediate T_d1 (left) and acyl enzyme (right) in the PCL-catalysed hydrolysis of esters.

Four X-ray crystal structures of PCL-phosphonate inhibitors were solved. They contained, as alcohol moieties, pure enantiomers of POP and solketal. PCL catalyses the hydrolysis of POP heptanoate (POP-C_7) with E = 70 and of solketal heptanoate (solketal-C_7) with E = 5.2, favouring in both cases the (*S*)-enantiomer (Chapter 4). The crystal structures of these complexes, together with combined QM/MM modelling of the corresponding tetrahedral intermediates and the kinetic constants for the PCL-catalysed hydrolysis of POP-C_7 and solketal-C_7, shed some light into the modes of chiral recognition of primary alcohols with oxygen at the stereocentre by PCL.

[i] Phosphonate-enzyme complexes are usually referred to as transition state analogues because of the slightly distorted geometry of such esters in comparison to T_d1 (slightly longer bond length P=O and P-O versus C-O^- and C-O and slightly bigger angles O-P-O versus O-C-O) (Tantillo, D. J.; Houk, K. N. *J. Org. Chem.* **1999**, *64*, 3066-3076).

Materials and methods

All chemicals were purchased from Sigma-Aldrich Co. (Oakville, ON) unless otherwise specified. Lipase from *Pseudomonas cepacia* was purchased from Genzyme Diagnostics (Cambridge, MA). (±) 2-Phenoxy-1-propanol was purchased from TCI America (Portland, OR). Diffraction data were collected on a RAXIS-IIC image plate area detector mounted on a Rigaku RU-300 rotating-anode X-ray generator operated at 50 kV and 250 mA. Refinements were done with Refmac 5.1.24.[7] ^{1}H NMR spectra were collected at 270 MHz, ^{13}C NMR at 68 MHz and ^{31}P NMR at 109 MHz. Kinetic data were collected on a SpectraMAX 340 microplate reader using SoftMaxPro 2.2.1 software (Molecular Devices Corp., Sunnyvale, CA). Molecular modelling was performed with HyperChem™ 7 (Hypercube Inc, Gainesville, FL). All the protein three-dimensional images were generated with Swiss PdbViewer v. 3.7.[8]

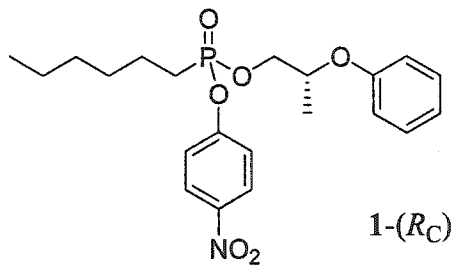

1-(R_C)

(R_C, R_PS_P) Hexylphosphonic acid 2-phenoxypropyl ester 4-nitrophenyl ester, 1-(R_C). A solution of (*R*)-2-phenoxy-1-propanol (0.13 g, 0.84 mmol) in benzene (2.2 mL) was added to a solution of hexyl phosphonic dichloride (0.14 mL, 0.84 mmol) and diisopropyl ethyl amine (0.35 mL, 2.01 mmol) in benzene (7 mL) cooled to 5 °C with an ice bath. After one hour stirring 1*H*-tetrazole (0.05 mg, 0.07 mmol) was added. When the (*R*)-2-phenoxy-1-propanol was consumed (TLC observation, 1.5 hours), the ice bath was removed and an excess of 4-nitrophenol (0.21 g, 1.52 mmol) in 7 mL dichloromethane was added to the reaction mixture. After 3 hours an excess of diisopropyl ethyl amine (0.23 mL, 1.32 mmol) was added. The reaction was stirred overnight at room temperature, then the solvent was evaporated under vacuum. The reaction mixture was extracted with diethyl ether, dried over sodium sulphate anhydrous and concentrated under vacuum. The product was purified by column chromatography over silica gel using hexane/ethyl acetate as eluent, and concentrated by rotary evaporation to a yellow oil.

Yield 17%. *Rf* = 0.36 (silica gel, 6:4 hexane-ethyl acetate); ^{1}H NMR ($CDCl_3$) δ8.08-8.13 (m, 2H), 7.2-7.4 (m, 4H), 6.83-7.0 (m, 3H), 4.45-4.65 (m, 1H), 4.1-4.35 (m, 2H), 1.85-2.05 (m, 2H), 1.55-1.75 (m, 2H), 1.15-1.45 (m, 9H), 0.8-0.95 (t, 3H, CH_3, *J* = 7.2 Hz); ^{13}C NMR ($CDCl_3$) δ 144.6, 139.5, 129.1, 128.4, 126.3, 125.7, 121.0, 120.9, 72.3, 70.7, 31.2, 30.3, 30.0, 22.4, 22.3, 16.4, 14.0; ^{31}P NMR ($CDCl_3$) δ 32.2, 31.6; MS(EI) *m/z* (rel. intensity) 421 (3, M^+), 328 (15, M^+- PhO), 134 (47, M^+- $OC_6H_4NO_2$ – $PhOCH(CH_3)CH_2OH$), 93(19, PhO).

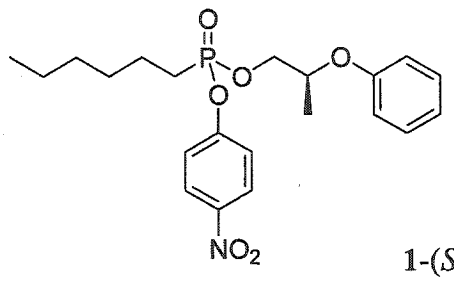

1-(S_C)

(S_C, R_PS_P) Hexylphosphonic acid 2-phenoxypropyl ester 4-nitrophenyl ester, 1-(S_C). The reaction was performed as for 1-(R_C). Yield 15 % (yellow oil). *Rf* = 0.36 (silica gel, 6:4 hexane-ethyl acetate); NMR and MS are the same as those for 1-(R_C).

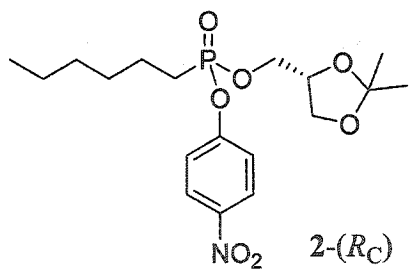

2-(R_C)

(R_C, R_PS_P) Hexylphosphonic acid 2,2-dimethyl-[1,3]dioxolan-4-methyl ester 4-nitrophenyl ester, 2-(R_C).

The reaction was performed as for 1-(R_C) by replacing (*R*)-2-phenoxy-1-propanol with (*S*)-2,2-dimethyl-[1,3]dioxolan-4-methanol. Yield 44% (yellow oil). *Rf* = 0.50 (silica gel, 6:4 hexane-ethyl acetate); ^{1}H NMR ($CDCl_3$) δ 8.19 (d, 2H, CH, *J* = 9.1 Hz), 7.35 (d, 2H, CH, *J* = 9.2 Hz), 4.30-4.20 (m, 2H), 4.20-3.90 (m, 5H), 3.74-3.70 (m, 2H), 2.05-1.90 (m, 2H), 1.76-1.58 (m, 2H), 1.44-1.18 (m, 14H), 0.83 (t, 3H, CH_3, *J* = 6.7 Hz); ^{13}C NMR ($CDCl_3$)

δ 155.0, 144.7, 125.7, 121.1, 115.6, 110.1 74.3, 66.7, 65.8, 31.2, 30.2, 30.0, 26.9, 25.2, 22 .4, 14.2; ^{31}P NMR ($CDCl_3$) δ 32.0, 31.7; MS (CI, NH_3) *m/z* (rel. intensity) 402 (36.0, M + H^+), 344 (100, M^+ - O-$C(CH_3)_2$), 288 (17.8, M^+ - 2,2,4-Trimethyl-[1,3]dioxolane).

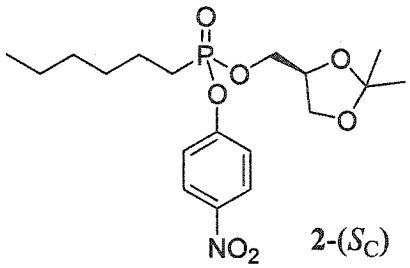

2-(S_C)

(S_C, R_PS_P) Hexylphosphonic acid 2,2-dimethyl-[1,3]dioxolan-4-methyl ester 4-nitrophenyl ester, 2-(S_C).

The reaction was performed as for 2-(R_C) using (*R*)-2,2-dimethyl-[1,3]dioxolan-4-methanol. Yield 44% (yellow oil). *Rf* = 0.50 (silica gel, 6:4 hexane-ethyl acetate); NMR and MS are the same as those for 2-(R_C).

Inactivation of PCL by 1-(R_C), 1-(S_C), 2-(R_C), 2-(S_C).

PCL was dissolved in potassium phosphate buffer (50 mM, pH 7.5) to a final concentration of 22.5 nM. 1-(R_C), 1-(S_C), 2-(R_C) and 2-(S_C) were dissolved in *n*-propanol to a final concentration of 32 mM. The PCL solution (0.25 mL) was mixed with the inhibitor solution (0.25 mL) and incubated at room temperature overnight. The hydrolytic activity against *p*-nitrophenol acetate had dropped to <2%. The solutions were dialysed against water for 24 hours. After dialysis, a white precipitate (PCL-inhibitor complex) formed, due to the increase in the ratio water: *n*-propanol. The suspensions were centrifuged at 4300 rpm and 4 °C, the supernatant was eliminated and the protein was redissolved in a solution of 50 vol% *n*-propanol and 50 vol% imidazole buffer 50 mM pH 6.5. The solutions were passed through Microcon YM-30® ultrafiltration membranes (Millipore Corp., Nepean, Ontario) and the concentrated protein dissolved in the same buffer to a concentration of 10 mg/mL.

Crystallisation, diffraction data collection and structure determination for the complexes PCL-1-(R_C) and PCL-1-(S_C).

Crystals of the complexes were grown by vapour diffusion. The drop contained about 10 mg protein/mL in imidazole buffer (50 mM, pH 6.5 containing 50 vol% *n*-propanol), while the reservoir contained imidazole buffer (50 mM, pH 6.5) and 25 vol% *n*-propanol. The crystals were isomorphous to the unligated open form of PCL and the coordinates for this form yielded the initial phases for the structural refinements by molecular replacement. Copper Kα radiation was monochromated by a graphite crystal. Oscillation images were collected using an oscillation angle of 1.0°. The crystal to detector distances for the **1**-(R_C) and **1**-(S_C) datasets were 80 mm and 90 mm respectively. The **2**-(R_C) and **2**-(S_C) datasets were collected with a crystal to detector distance of 85 mm. Data were reduced and merged using the DENZO/SCALEPACK suite of programs or the HKL2000 suite of programs.[9] All refinements were done using Refmac 5.1.24.[7]

Determination of k_{cat} and K_M for the PCL catalysed kinetic resolution of (*R*) and (*S*)-2-phenoxy-1-propyl heptanoate and (*R*) and (*S*) solketal heptanoate.

Spectrophotometric determination of k_{cat} and K_M was performed using a 96-well microliter plate and a microplate reader using a pH indicator to monitor ester hydrolysis. Assay solutions were prepared by mixing appropriate amounts of substrate solutions in *n*-propanol (180 mM (*R*)-2-phenoxy-1-propyl heptanoate, 166 mM (*S*)-2-phenoxy-1-propyl heptanoate, 204 mM (*R*)-solketal heptanoate, 204 mM (*S*)-solketal heptanoate) with N,N-bis-(2-hydroxymethyl)-2-aminoethanesulfonic acid (BES) solutions (12 mM, pH 7.2, containing 2 mM *p*-nitrophenol (*p*NP)). 90 μL of this solution and 10 μL of PCL solution were added in the microplate and the decrease in absorbance at 404 nm was monitored. Concentrations in wells were as follows: [BES] = 7.44 mM, [*p*NP] = 1.24 mM, [PCL] = 14 μg/mL (for (*R*)-2-phenoxy-1-propyl heptanoate, (*R*) and (S)-solketal heptanoate) or 1.4 μg/mL, (for (*S*)-2-phenoxy-1-propyl heptanoate), [(*R*) and (*S*)-2-phenoxy-1-propyl heptanoate]= 0.8 to 5.5 mM, [(*R*) and (*S*)-solketal heptanoate] = 1 to 10 mM [*n*-propanol] = 28.8 vol%. Data were analysed by the Eadie-Hofstee method.[10,11]

Combined QM/MM calculations

The enzyme-inhibitor crystal structures were pruned to a 15 Å sphere centred on the phosphorus atom. Truncated residues were capped by adding H atoms. Residues Ser87, Asp264, His286, Gly16, Leu17 (oxyanion hole), Gln88 (oxyanion hole) and the bound

phosphonate ester, either as such or modified to T_d1, formed the "enzyme reaction zone" for complexes PCL-**1**-(*R*) and PCL-**1**-(*S*), while we added residues Thr18, His86 and Leu287 for PCL-**2**-(*R*) and PCL-**2**-(*S*). The enzyme reaction zone was minimised using the semi-empirical PM3 method.[12,13] The remainder of the sphere was treated as fixed potential. His286 Nδ1 was positively charged and Asp264 Oδ2 was negatively charged. The inhibitor was modified to tetrahedral intermediate by replacing P=O with C-O$^-$. The structures were minimised in vacuum using the Polak-Ribière conjugate gradient[14] until a r.m.s. of 0.02 kcal/mol/Å was reached.

Results

Four phosphonate *p*-nitrophenyl esters that contain as alcohol moieties pure enantiomers of (*R*)-POP, (*S*)-POP, (*R*)-solketal and (*S*)-solketal were synthesised (Scheme 2). Contrary to phosphonyl chlorides having secondary alcohol moieties, which are fairly stable,[6,15] phosphonyl chlorides containing primary alcohols are rapidly hydrolysed in water. For this reason the chlorine was replaced with *p*-nitrophenol. Nucleophilic displacement of one chlorine of hexylphosphonic dichloride by one equivalent of chiral alcohol yielded a mono-substituted phosphonyl chloride, which was converted *in situ* to the desired *p*-nitrophenyl derivative by treatment with two equivalents of *p*-nitrophenol in the presence of di-isopropyl ethyl amine.

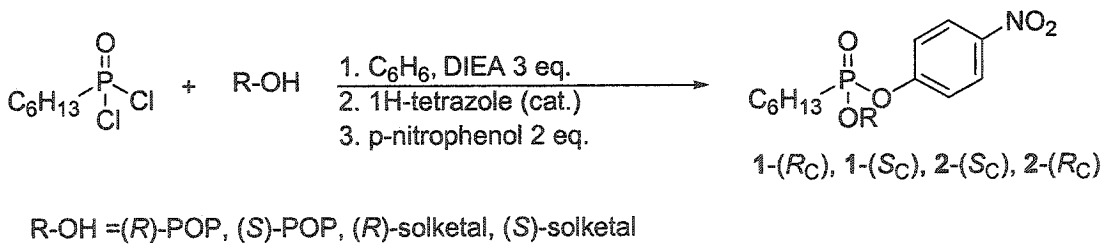

Scheme 2 - Phosphonate esters synthesis.

The two resonances for the phosphorous atom in the ^{31}P NMR (see Materials and Methods, ^{31}P NMR) show that each reaction formed an equimolar mixture of (S_P) and (R_P) epimers due to the presence of a phosphorous stereocentre. The phosphonates were used without separation of the epimers.

By reacting PCL with 1000-fold excess of either 1-(R_C), 1-(S_C), 2-(R_C) and 2-(S_C) more than 98% of the hydrolytic activity of the enzyme towards *p*-nitrophenol acetate was irreversibly inhibited. The inhibited PCL was then crystallised by the hanging drop method using a reservoir containing 25 vol% *n*-propanol in imidazole buffer (50 mM, pH 6.5). The crystals formed at a concentration of *n*-propanol of about 30 vol% and were isomorphous with the open form of PCL for all four complexes.

Diffraction data were collected and the four crystal structures were solved with resolution ranging from 1.65 to 1.80 Å by molecular replacement, using initial phases calculated from the open form of PCL (PDB ID: 3LIP[16]) (Table 1). The four PCL-inhibitor complexes belong to the C2 space group like the open form of PCL.[16,17] There was no significant difference between the PCL-inhibitor complexes and the unligated open conformation of PCL (rms 0.37 to 0.40 Å).

Table 1 - Data collection statistics and refinement parameters.

	PCL-1-(R_C)	**PCL-1-(S_C)**	**PCL-2-(S_C)**	**PCL-2-(R_C)**
Data statistics				
resolution range (Å)	72.3 – 1.70	72.1 – 1.80	19.7 – 1.65	19.7 – 1.65
highest resolution shell (Å)	1.76 – 1.70	1.86 – 1.80	1.71 – 1.65	1.71 – 1.65
space group	C2	C2	C2	C2
unit cell dimensions				
a (Å)	88.7	88.6	88.7	88.6
b (Å)	46.2	46.2	46.1	46.2
c (Å)	84.5	84.4	84.5	84.6
α (°)	90	90	90	90
β (°)	121.3	121.3	121.3	121.3
γ (°)	90	90	90	90
mosaicity (°)	0.94	0.85	0.44	0.47
R merge (%)	5.7 (35.6)	5.2 (18.5)	4.6 (26.7)	4.1 (18.4)
completeness of the data (%)	86.1 (61.1)	87.3 (53.5)	88.6 (37.2)	87.0 (36.3)
no. of observations	89658	81742	98586	98467
no. of unique reflections	27968	23820	31380	30823
mean I/σI	13.42 (2.3)	18.0 (4.6)	19.8 (3.1)	21.3 (3.9)
Refinement statistics				
refinement program	Refmac 5.1.24	Refmac 5.1.24	Refmac 5.1.24	Refmac 5.1.24
no. of atoms used in the refinement (not H)	2492	2495	2483	2485
no. of waters	141	147	139	141
no. of calcium ions	1	1	1	1
final R factor (%)[a]	18.4	17.7	16.2	16.9
final R free (%)[b]	19.4	20.7	18.9	19.7

rms deviations from ideality for				
bond lengths (Å)	0.014	0.023	0.015	0.015
bond angles (°)	1.48	1.87	1.49	1.49
mean B-factors (Å2)				
protein	11.85	12.75	13.10	11.08
solvent	17.50	18.16	16.96	15.16
calcium ion	9.46	10.11	10.77	8.89
inhibitor	15.20	11.98	15.84	16.50

[a] R factor = $\Sigma \| F_c | - | F_o \| / \Sigma | F_o | \times 100$ where F_c and F_o are the calculated and observed structure factor amplitudes; [b] a small percentage of the total reflections were randomly selected and used to calculate the final R free.

Complexes PCL-1-(R_C) and PCL-1-(S_C)

The two phosphonate esters containing as alcohol moieties (*R*)-POP and (*S*)-POP bind to PCL by a covalent bond between the phosphorous atom and catalytic Ser87 Oγ. Both phosphonates have R_P configuration. Since nucleophilic attack at phosphorus by Oγ of catalytic serine proceeds by an in-line mechanism,[18] the favourite epimer presumably had S_P configuration prior to the reaction. In both PCL-**1**-(R_C) and PCL-**1**-(S_C) the hexyl chain of the phosphonate esters extends in the large hydrophobic pocket (hydrophobic groove HA, Figure 3) as the acyl chain of both Lang's triacylglycerol analogues[19] and the previously reported primary alcohol ester analogues (Chapter 2). As observed in Chapter 2, the inhibitor folds to hairpin, with similar distance hexyl chain-benzyl ring (4.36 Å in PCL-**1**-(R_C) and 4.23 Å in PCL-**1**-(S_C)). The alcohol oxygen O_1 binds in a similar position in both alcohol moieties and it is weekly hydrogen bonded[ii] to catalytic His286 (3.17 Å, 129.8° for PCL-**1**-(R_C) and 3.24 Å, 132.4° for PCL-**1**-(S_C)) The stereocentre of the two enantiomers shows an "umbrella-like" inversion analogous to the one exhibited by similar phosphonate esters containing the structurally related MPP as alcohol moiety (CH_2 versus O at the stereocentre, Chapter 2). Because of this inversion and because of the presence of the stereocentre in β to the alcohol oxygen, which confers flexibility to the alcohol moiety, the medium and large substituent at the stereocentre are directed roughly towards the same regions of the catalytic pocket, with the phenyl ring and the methyl substituent of the two enantiomers bonded in a very similar fashion to PCL catalytic pocket (Figure

[ii] A hydrogen bond is considered present when the distance heavy atom to heavy atom (here N and O) is < 3.2 Å and the angle heavy atom-hydrogen-heavy atom (here N-H-O) is $120° < \theta < 180°$.

3). As for our previous complexes, the large substituent is not well bonded to the hydrophobic regions of the catalytic pocket of PCL but lays in a solvent exposed crevice (Figure 3).

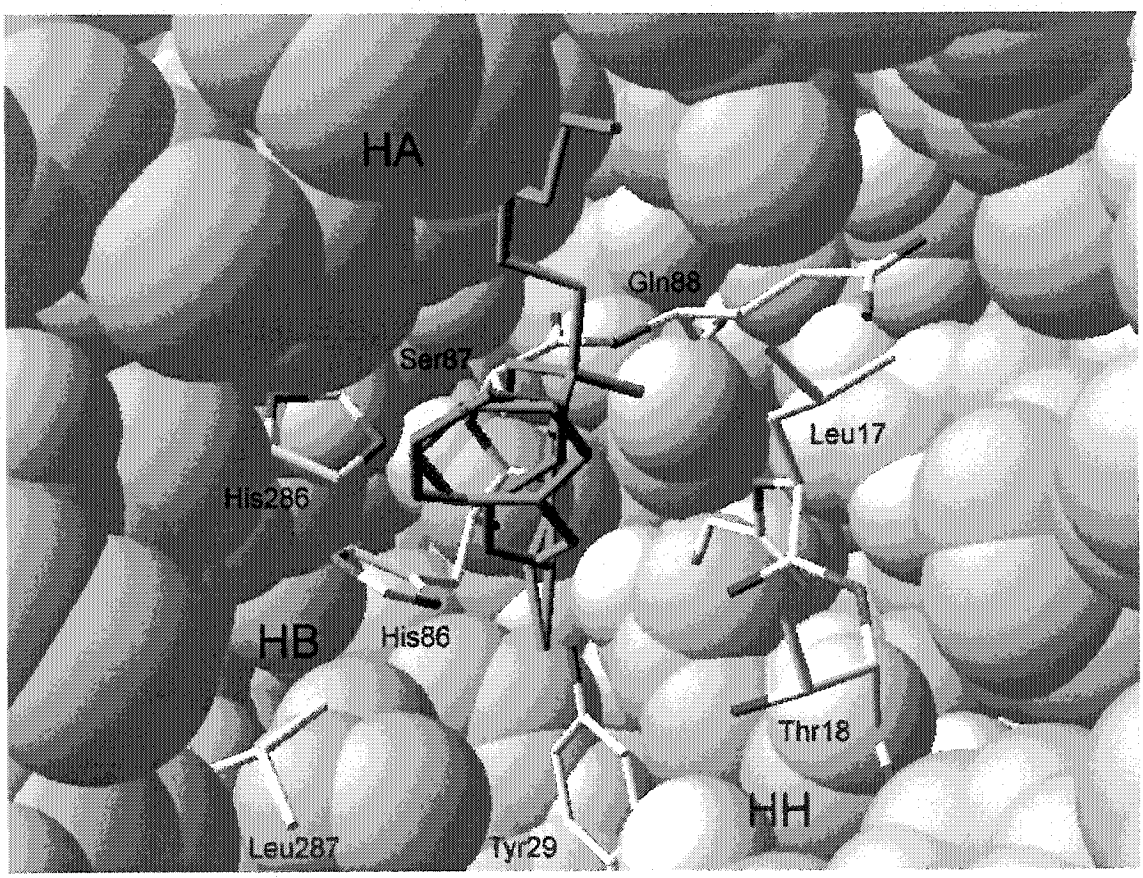

Figure 2 - Overlay of PCL-1-(R_C) (the phosphonate inhibitor is in green) with PCL-1-(S_C) (the phosphonate inhibitor is in purple). Catalytic triad residues His286 and Ser87, oxyanion hole residues Glu88 and Leu17 and "enzyme reaction zone" residues Thr18, Tyr29 and Leu287 are in stick representation and CPK colours.

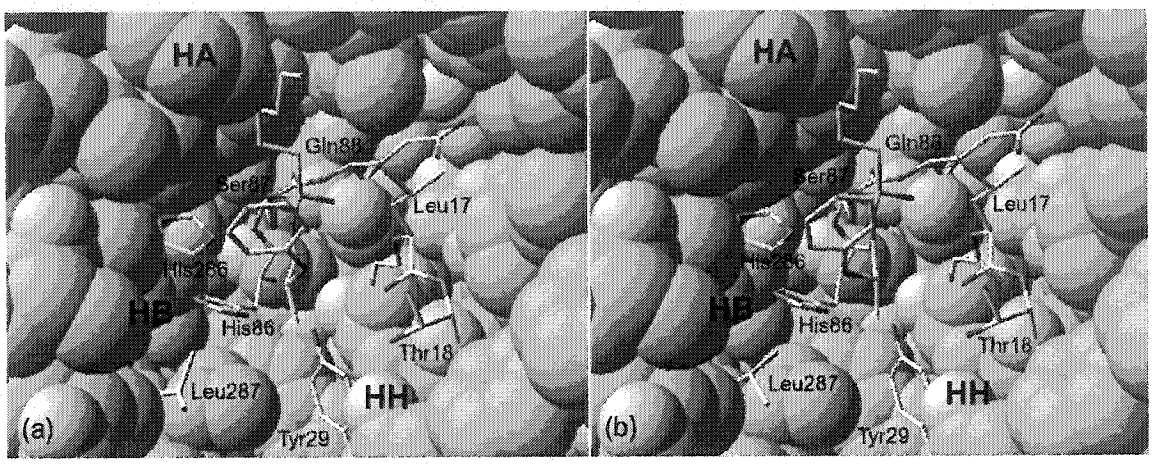

Figure 3 - PCL-inhibitor complexes. (a) PCL-1-(R_C), (b) PCL-1-(S_C). Catalytic triad residues His286 and Ser87, oxyanion hole residues Glu88 and Leu17, phosphonate inhibitor and "enzyme reaction zone" residues Thr18, Tyr29 and Leu287 are in stick representation and CPK colours.

Both inhibitors mimic a catalytically productive orientation[iii] since the key hydrogen bonds for catalysis are present (Table 2). Catalytic Ser87 Oγ accepts hydrogen bonds from the catalytic His286 Nε2 (3.00 Å, 115.2° for PCL-1-(R_C) and 3.02 Å, 119.8° for PCL-1-(S_C)). The phosphonyl oxygens accept two hydrogen bonds from the NH of oxyanion hole residues Leu17 and Glu88 (2.75 Å and 2.86 Å in PCL-1-(R_C); 2.68 Å and 2.78 Å in PCL-1-(S_C)). Also, both inhibitors have a *gauche* conformation between the Ser87 Oγ-P bond and the O-CH_2 bond of the alcohol moiety. This permits an overlap between the lone pair *n* orbital of the alcohol oxygen and the σ^* orbital of the Oγ-P bond (dihedral angle Ser87 Oγ-P-O_l-CH_2 of 70.4° in PCL-1-(R_C) and of 68.0° in PCL-1-(S_C)), in agreement with Deslongchamps' stereoelectronic theory.[20] However, this conformation does not seem a necessary element for the enzymatic hydrolysis of esters since previous transition state analogues do not have it while here both fast and slow enantiomers present it.[6]

[iii] For a productive conformation of T_d1 the carbonyl oxygen must reside in the oxyanion hole and hydrogen bind to the backbone N-H of the oxyanion hole residues. Catalytic histidine must have a bifurcated H-bond between Nε2-H and the oxygen of the alcohol moiety (O_l) and of the catalytic serine (Oγ). Catalytic histidine must also hydrogen bind through Nδ2-H to catalytic aspartate COO^-.

Table 2 - Key hydrogen bond distances (heavy atom to heavy atom) and key angles in the complexes PCL-1-(R_C) and PCL-1-(S_C).

	PCL-1-(R_C)	PCL-1-(S_C)
Leu17 N(H) – O=P (Å)[a]	2.75	2.68
Gln88 N(H) – O=P (Å)[a]	2.86	2.78
Nδ1 His286 – Oδ2 Asp264 (Å)[a]	2.78	2.74
Nε2 His286 – Oγ Ser87 (Å)	3.00	3.02
Nε2 His286 – Oγ Ser87 (Nε2-H-Oγ θ, °)	115.2	119.8
Nε2 His286 – O_I (Å)	3.17	3.24
Nε2 His286 – O_I (Nε2-H-O_I θ, °)	129.8	132.4
Ser87Oγ -P-O_I-CH_2 θ (°)	70.4	68.0

[a]the angles N-H-O are typical of hydrogen bonds.

PCL-1-(R_C) and PCL-1-(S_C) differ due to the "umbrella-like" inversion at the stereocentre that places the hydrogen and the oxygen at the stereocentre in different positions in the two enantiomers (Figure 2 and Figure 3). The oxygen at the stereocentre of (*R*)-POP is close to the carbonyl oxygen of Leu17 (3.29 Å), which likely causes repulsion. In (*S*)-POP, it is close to both His286 Nε–H (3.79 Å to the heavy atom) and His286 Cδ2-H (3.37 Å to the heavy atom). In the fast (*S*)-enantiomer the hydrogen at the stereocentre bumps into Leu17 carbonyl (3.16 Å), while in the slow (*R*)-enantiomer is close to His286 Nε2 (3.74 Å to the heavy atom). According to Shultz *et al.*[21] the vicinity of the hydrogen at the stereocentre to Leu17 carbonyl does not cause stability problems.

Complexes PCL-2-(R_C) and PCL-2-(S_C)

As for PCL-1-(R_C) and PCL-1-(S_C), the two phosphonate esters containing as alcohol moiety (*R*) and (*S*)-solketal bind similarly to PCL by covalently linking the phosphorous to Oγ of Ser87. They both have R_P configuration (see above). Again the hexyl chain of the phosphonate esters extends in the hydrophobic groove HA (Figure 4 and Figure 5).

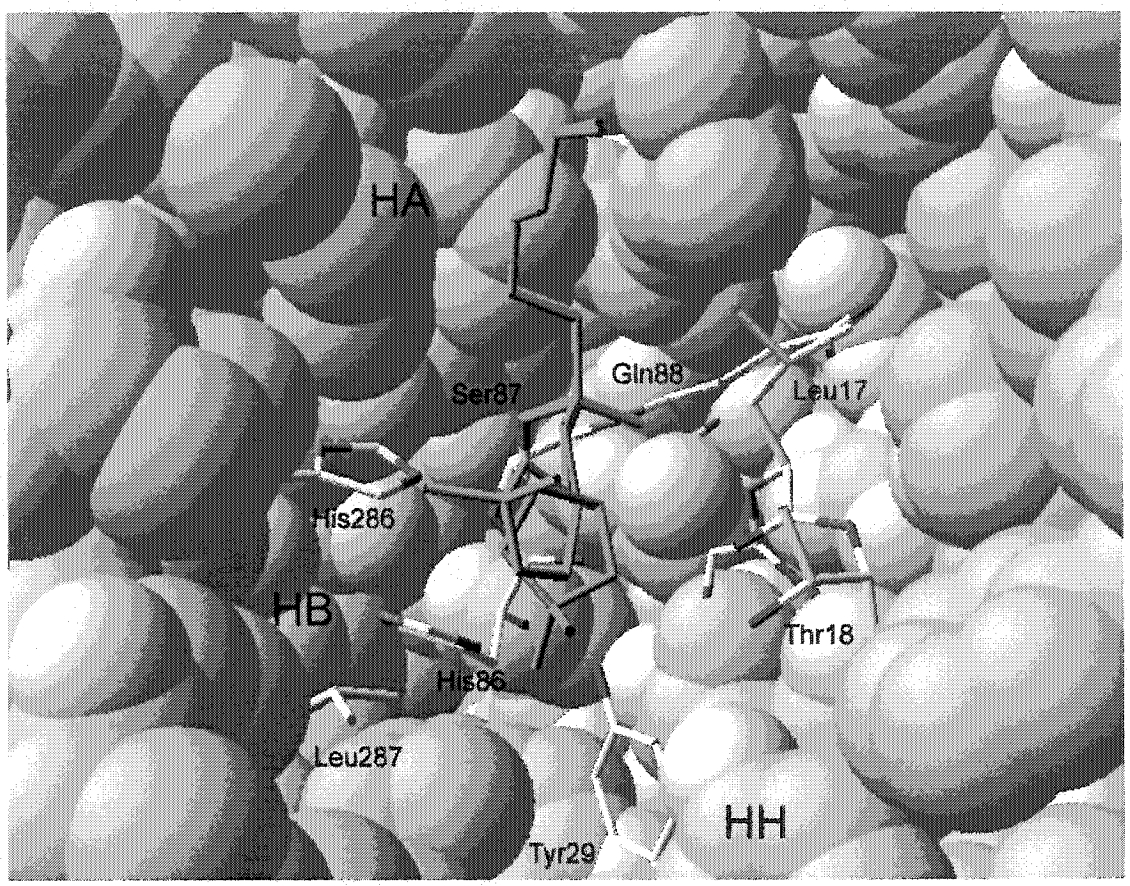

Figure 4 – Overlay of PCL-**2**-(R_C) (purple), containing the fast (*S*)-solketal, and PCL-**2**-(S_C) (green) containing the slow (*R*)-solketal . Active site residues His286 and Ser87 as well as the "enzyme reaction zone" are in stick representation and CPK colours.

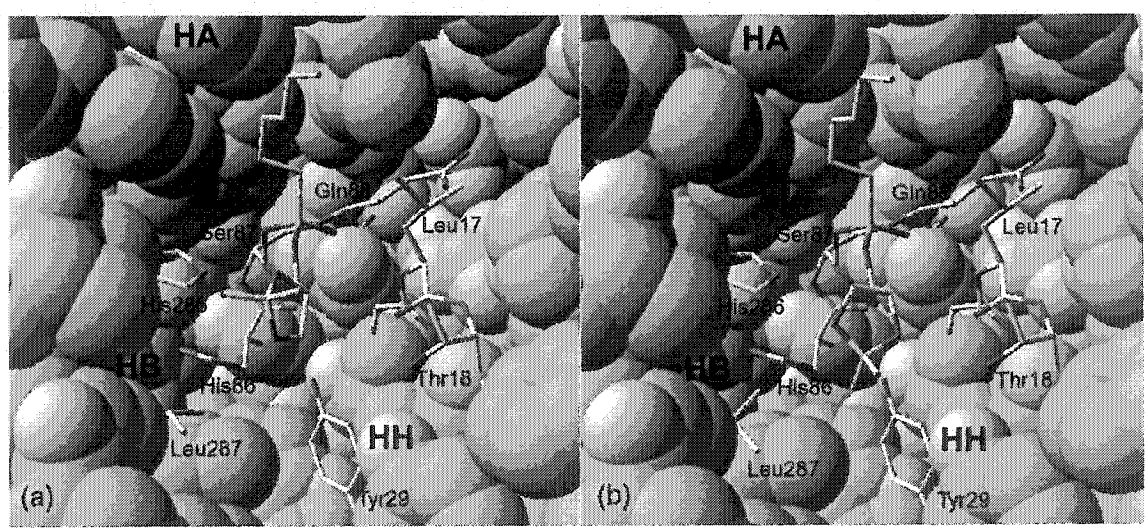

Figure 5 - PCL-inhibitor complexes. (a) PCL-**2**-(S_C), containing the slow (*R*)-solketal. (b) PCL-**2**-(R_C), containing the fast (*S*)-solketal. Active site residues His286 and Ser87 as well as the "enzyme reaction zone" and the bound phosphonates are in stick representation and CPK colours.

Both inhibitors appear to be in a catalytically productive orientation, presenting all the hydrogen bonds necessary for catalysis (Table 2). Both enantiomers weekly hydrogen bind to catalytic His286 Nε2 through the alcohol oxygen (3.30 Å, 126.9° in PCL-**2**-(S_C) and 3.26 Å, 128.2° in PCL-**2**-(R_C)).[iv] Also, both inhibitors have a *gauche* conformation between the Ser87 Oγ-P bond and the O-CH_2 bond of the alcohol moiety (dihedral angle Ser87 Oγ-P-O_I-CH_2 of 68.9° in PCL-**2**-(S_C) and of 77.0° in PCL-**2**-(R_C)).

Table 3 - Key hydrogen bond distances and key angles in the complexes PCL-**2**-(S_C) and PCL-**2**-(R_C).

	PCL-2-(S_C)[b]	PCL-2-(R_C)[b]
Leu17 N(H) – O=P (Å)[a]	2.77	2.74
Gln88 N(H) – O=P (Å)[a]	2.86	2.87
Nδ1 His286 – Oδ2 Asp264 (Å)	2.77	2.84
Nε2 His286 – Oγ Ser87 (Å)	2.96	2.97
Nε2 His286 – Oγ Ser87 (Nε-H-Oγ θ, °)	118.6	117.1
Nε2 His286 – O_I (Å)	3.30	3.26
Nε2 His286 – O_I (Nε-H-O_I θ, °)	126.9	128.2
Oγ Ser87-P-O_I-CH_2 θ (°)	68.9	77.0

[a]The angles N-H-O are typical of hydrogen bonds. [b] Due to priority changes complex PCL-**2**-(*S*) incorporates the slow (*R*)-solketal and complex PCL-**2**-(*R*) incorporates the fast (*S*)-solketal.

In complexes PCL-**2**-(R_C) and PCL-**2**-(S_C), contrary to what is observed in complexes PCL-**1**-(R_C) and PCL-**1**-(S_C), the difference between the two alcohol moieties within the catalytic pocket of PCL is due to the exchange of the medium and large group at the stereocentre (Figure 5). This places the oxygen at the stereocentre of (*S*)-solketal (PCL-**2**-(R_C)) close to both Leu17 carbonyl (2.76 Å) and Thr18 OH (3.17 Å). While the first interaction supposedly is repulsive, the second may give rise to a hydrogen bond, thus favouring the fast (*S*)-enantiomer.

End-point E and kinetic constants determination

[iv] Usually d < 3.2 Å and 120° < θ < 180°.

To interpret these structures, PCL enantioselectivity towards the substrates POP-C_7 and solketal-C_7 was measured in a solvent analogous to the one used for the crystallisation of PCL-inhibitor complexes.[v]

In 30 vol% *n*-propanol in potassium phosphate buffer, PCL hydrolyses POP-C_7 with high enantioselectivity, E = 70 favouring the (*S*)-enantiomer, while its enantioselectivity towards solketal-C_7 is low, E = 5.2, again favouring (*S*)-solketal (Scheme 3). Both PCL catalysed hydrolysis of (±)-POP-C_7 and of (±)-solketal-C_7 in 30 vol% *n*-propanol were stopped at 30 to 50% conversion. Gas chromatographic analysis of remaining starting materials and hydrolysed products yielded their respective optical purities that were used to determine PCL enantioselectivity according to Chen *et al.*[22]

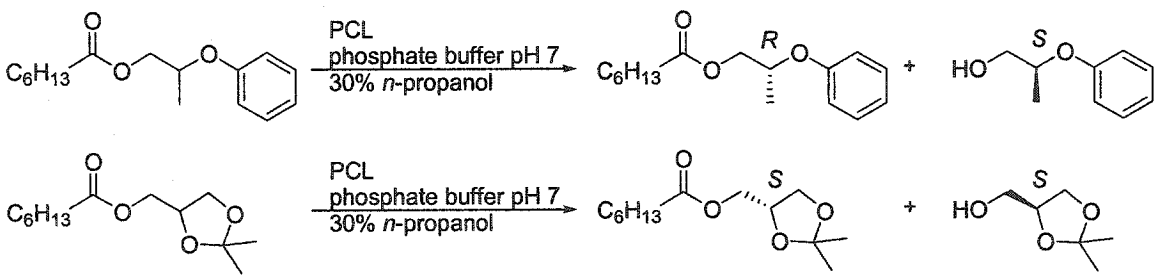

Scheme 3 – PCL catalysed kinetic resolution of POP-C_7 and solketal-C_7.

To gain additional insight into the enantioselectivity of PCL towards POP-C_7 and solketal-C_7, the kinetic constants relative to the PCL-catalysed hydrolysis of each enantiomer of POP-C_7 and solketal-C_7 were determined in a solvent similar to the one used for the crystallisation of the PCL-inhibitor complexes (Table 4). Heptanoic esters are poorly soluble in this solvent, thus the maximum substrate concentration attained was lower than K_M in almost all cases (see Materials and Methods). This explains the large errors in the measured k_{cat} and K_M values. Since E is defined as the ratio of the specificity constant k_{cat}/K_M of the fast enantiomer over the specificity constant of the slow enantiomer,[23] using these parameters PCL enantioselectivity was found to be 25 ± 14 for POP-C_7 and 1.7 ± 0.9 for solketal-C_7 (Table 4). Considering the large errors involved in

[v] Complexes PCL-**1**-(R_C) and PCL-1-(S_C) mimic the transition state leading to T_d1 in the PCL-catalysed hydrolysis of (*R*) and (*S*)-POP-C_7. Complexes PCL-**2**-(R_C) and PCL-**2**-(S_C) mimic the transition state leading to T_d1 in the PCL-catalysed hydrolysis of (*S*) and (*R*)-solketal-C_7.

this determination, these values are in reasonable agreement with the more accurately determined end-point E values. From these data it seems that PCL binds similarly both enantiomers of POP-C_7 (comparable K_M) and that the enantioselectivity towards this substrate is mainly due to the 17-fold larger k_{cat} value of the fast (*S*)-enantiomer. On the other hand the solketal-C_7 enantiomers have identical k_{cat} while the fast (*R*)-solketal-C_7 is slightly better bonded (lower K_M) to the enzyme, which may explain PCL enantioselectivity towards this substrate.

Table 4 - Kinetic constants for (*R*) and (*S*)-POP-C_7 and (*R*) and (*S*)-solketal-C_7[a].

	(*R*)-POP-C_7	(*S*)-POP-C_7	(*R*)-solketal-C_7[d]	(*S*)-solketal-C_7
k_{cat} (min^{-1})	$(7 \pm 2)10^{-2}$	1.2 ± 0.3	$(7 \pm 2)10^{-2}$	$(7 \pm 2)10^{-2}$
K_M (mM)	8 ± 2	5 ± 1	14 ± 3	21 ± 5
k_{cat}/K_M ($min^{-1}mM^{-1}$)	$(8 \pm 3)10^{-3}$	0.24 ± 0.07	$(5 \pm 2)10^{-3}$	$(3 \pm 1)10^{-3}$
E[b]	25 ± 14		1.7 ± 0.9	
End point E[c]	70 ± 15		5.2 ± 0.1	

[a] Reaction conditions:[BES] = 7.44 mM, [*p*NP] = 1.24 mM, [PCL] = 2.85 μg/mL, [(*R*) and (*S*)-2-phenoxy-1-propyl heptanoate] = 0.8 to 5.5 mM, [(*R*) and (*S*)-solketal heptanoate] 1 to 10 mm, [*n*-propanol] = 28.8%. Data were analysed by the Eadie-Hofstee method.[10,11] [b] $E = [(k_{cat}/K_M(S))/(k_{cat}/K_M(R))]$ [c] Determined by GC analysis of reaction products and starting materials at 40% conversion according to Chen *et al.*[22] For POP-C_7 ee_s = 95%, ee_p = 90%, c = 51%; for solketal-C_7 ee_s = 23%, ee_p = 62%, c = 27%.[d] (*R*)-solketal-C_7 yields (*S*)-solketal after hydrolysis.

Modelling of the T_d1s [vi]

As previously observed in Chapter 2, the subtlety of the interactions enzyme-substrate makes it difficult to determine which ones are responsible for PCL enantioselectivity towards POP-C_7. Also, the similar hydrogen bond His286 Nε2H - POP O_I (difference 0.07 Å), disagrees with the 17-fold larger k_{cat} value of the fast enantiomer. Thus, a portion of complexes PCL-**1**-(R_C) and PCL-**1**-(S_C) was modelled as T_d1 as described in Chapter 2. The resulting structures reveal a productive conformation for both enantiomers (Table 5). The carbonyl oxygen is in the oxyanion hole and hydrogen binds both Leu17 and Gln88 (2.74 Å and 2.79 Å in (*R*)-**1** T_d1; 2.76 Å and 2.82 Å in (*S*)-**1** T_d1).

[vi] Attempts to model tetrahedral intermediates relative to complexes PCL-**2**-(R_C) and PCL-**2**-(S_C) so far have not yielded results consistent with experimental evidence, in particular with PCL enantiopreference for (*S*)-solketal, probably because of the low enantioselectivity of PCL towards the corresponding solketal-C_7.

Catalytic Ser87 is hydrogen bonded to catalytic His286 Nε2 (2.68 Å, 137.6° in (*R*)-1 T_d1; 2.73 Å, 141.1° in (*S*)-1 T_d1). The alcohol oxygen O_I forms a hydrogen bond with catalytic His286 Nε2 in both enantiomers (2.76 Å, 150.9° in (*R*)-1 T_d1; 2.80 Å, 147.4° in (*S*)-1 T_d1). Last, neither T_d1 has a *gauche* conformation between the Ser87 Oγ-C bond and the O-CH_2 bond (dihedral angle Oγ Ser87-C-O_I-CH_2 132.9° in (*R*)-1 T_d1 and 94.5 in (*S*)-1 T_d1). However, no strong experimental proof has been offered either in favour or against this theory, especially relating to its influence on enzyme enantioselectivity.

Table 5 - Key hydrogen bond distances (heavy atom to heavy atom) in the tetrahedral intermediates after PM3 minimisation.

	(*R*)-1 T_d1	(S)-1 T_d1
Leu17 N(H) – O=P (Å)[a]	2.74	2.76
Gln88 N(H) – O=P (Å)[a]	2.79	2.82
Nδ1 His286 – Oδ2 Asp264 (Å)	2.66	2.64
Nε2 His286 – Oγ Ser87 (Å)	2.68	2.73
Nε2 His286 – Oγ Ser87 (Nε-H-Oγ θ, °)	137.6	141.1
Nε2 His286 – O_I (Å)	2.76	2.80
Nε2 His286 – O_I (Nε-H-O_I θ, °)	150.9	147.4
Oγ Ser87-C-O_I-CH_2 θ (°)	132.9	94.5

[a] The angles N-H-O are typical of hydrogen bonds.

After geometry optimisation, the differences in the orientation of the two POP alcohol moieties within PCL catalytic pocket remained subtle. Still present, however, a repulsive interaction between oxygen at the stereocentre and Leu17 carbonyl oxygen in the slow (*R*)-enantiomer (3.83 Å). In the fast (*S*)-enantiomer, it is the hydrogen at the stereocentre to be close to Leu17 carbonyl oxygen (3.48 Å).

Discussion

A comparison of the crystal structures of complexes PCL-1-(R_C), PCL-1-(S_C), PCL-2-(R_C) and PCL-2-(S_C) with the ones of complexes PCL-inhibitor having as alcohol moiety pure enantiomers of MPP (Chapter 2) and with the complex between PCL and inhibitor (R_P)-O-(2*R*)-(1-phenoxy-2-butyl)-methylphosphonic acid chloride[24] (PBD ID:

1HQD), incorporating the secondary alcohol moiety 1-phenoxy-2-butanol, shows that primary alcohols bind in different regions of PCL than secondary alcohols. While the fast enantiomer of secondary alcohols binds the large group at the stereocentre in the hydrophobic pocket HA and the medium substituent in the hydrophobic pocket HH,[24] primary alcohols all have the large group at the stereocentre in a solvent exposed crevice and the acyl chain in the HA pocket (Chapter 2; this Chapter Figure 2 and Figure 4).

The enantioselectivity of PCL towards primary alcohols with oxygen at the stereocentre does not depend on the lack of a key H-bond in the slow reacting enantiomer since both enantiomers of POP and solketal have the alcohol oxygen at hydrogen bonding distance to His286 Nε2. PCL can fit reasonably well both enantiomers of POP and of solketal within its active site. However differences in their binding were observed.

The POP enantiomers exhibit an "umbrella-like" inversion at the stereocentre. This has already been found in the menthol moiety of Cygler *et al.* complexes[6] and in the complexes PCL-inhibitor containing MPP as alcohol moiety (Chapter 2). Like in MPP, this allows the alcohol oxygen O_1 of POP to maintain its hydrogen bond with His286 and justifies the very similar orientation of the two enantiomers within the active site of PCL (Figure 2 and Figure 3). Only the hydrogen and the oxygen at the stereocentre point in opposite directions in the two enantiomers of POP. Solketal, on the other hand, does not show an inversion at the stereocentre but the medium and large substituent at the chiral carbons switch positions in the two enantiomers (Figure 4 and Figure 5). This results in almost the same position for the hydrogen at the stereocentre, the so-called "H-alignment", while the other substituents bind differently.

The different ways of fitting the slow enantiomer of the two primary alcohols with oxygen at the stereocentre, i.e. the "LM-alignment" of POP versus the "H-alignment" of solketal, explain the limits of the very simple empirical rule,[1,2] which may consider only one possible binding mode for the slow enantiomer (Figure 1).

Despite the same enantiopreference of the enzyme for the (*S*)-enantiomer of both POP and solketal, they have a different spatial arrangement of the substituents and only because of priority changes they both have (*S*) configuration (Figure 1(b) and (c)). (*S*)-solketal, which would spatially correspond to (*R*)-POP (position of hydrogen, medium and large group at the stereocentre) and (*R*)-POP are subject to the same repulsion, caused

by the vicinity of the oxygen at the stereocentre to Leu17 carbonyl. Nevertheless (*S*)-solketal is the fast enantiomer because this repulsion is counterbalanced by a hydrogen bond between the same oxygen and Thr18 side-chain hydroxyl group, not present in (*R*)-POP. Thus peculiar features of the substrates with oxygen at the stereocentre determine which enantiomer is better bonded within the enzyme catalytic pocket. This may be an additional explanation for the failure of the empirical rule, which cannot take each substrate characteristic, such as presence of rings, etc., into account.

From these results one would also conclude that the enantioselectivity of PCL towards POP stems from the better binding of (*S*)-POP over (*R*)-POP. However the k_{cat} and K_M values experimentally determined (Table 4) suggest that the enzyme enantioselectivity does not depend on the better binding of one enantiomer over the other (K_M is 8 mM for (*R*)-POP-C_7 and 5 mM for (*S*)-POP-C_7), but on the higher turnover number associated with the fast enantiomer (1.2 min^{-1} for (*S*)-POP-C_7 versus 0.07 min^{-1} for (*R*)-POP-C_7, Table 4). Nevertheless, in certain circumstances a substrate can bind to an enzyme in a non-productive way, which is in competition with its productive binding.[25] This has the effect of lowering both k_{cat} and K_M. k_{cat} decreases because a smaller number of substrates are bonded productively and can react with the enzyme. K_M decreases because the presence of both productive and non-productive bindings leads to an apparent overall tighter binding of the substrate. It is the ratio k_{cat}/K_M that remains unaffected by these happenings and that should be taken into account.[25] This is probably what happens in the case of POP with the slow (*R*) enantiomer. The difference in hydrogen bonding distance and angle in the complexes PCL-inhibitor (Table 2) and in the modelled T_d1s (Table 5) does not account for a 17-fold difference in k_{cat} between (*S*)-POP and (*R*)-POP. At the same time the repulsion between the oxygen at the stereocentre of (*R*)-POP and Leu17 carbonyl, not present in (*S*)-POP, is not reflected in the almost equal K_M values of the two substrates. The K_M value for the slow enantiomer may thus be underestimated because of non-productive tight binding to the enzyme and for the same reason the k_{cat} value is likely underestimated as well.

In the case of solketal-C_7, the identical k_{cat} values for both enantiomers and the differences in K_M (14 mM for the slow enantiomer and 21 mM for the fast enantiomer)

are in reasonable agreement with the evidence of a slight better binding of the fast (*S*)-solketal (corresponding to (*R*)-solketal-C_7).

In conclusion, the difference in enantiopreference of PCL for secondary and primary alcohols has been shown once more to arise form their binding to different pockets within the enzyme active site. This could be a general characteristic of primary alcohols. Also, the different relative binding of the two enantiomers of different primary alcohols with oxygen at the stereocentre ("LM-alignment" versus "H-alignment") has been proposed as explanation for the non-reliability of the empirical rule in such cases. More importantly, the molecular basis of PCL enantioselectivity towards esters of primary alcohols with oxygen at the stereocentre has been shown to depend on the binding differences between the alcohol moiety of the fast and slow enantiomers with residues Leu17 and Thr18 of PCL.

Acknowledgements

I wish to thank NATEQ (Les Fonds Québécois de la Recherche sur la Nature et les Technologies) for two post-graduate fellowships.

References

[1]Weissfloch, A. N. E.; Kazlauskas, R. J. *J. Org. Chem.*, **1995**, *60*, 6959-6969.

[2]Weissfloch, A. N. E.; Kazlauskas, R. J. *Methods Biotech.* **2001**, *15*, 243-259.

[3]Wimmer, Z.; Saman, D.; Francke, W. *Helv. Chim. Acta* **1994**, *77*, 502-508.

[4]Weinstock, L. M.; Mulvey, D. M.; Tull, R. *J. Org. Chem.* **1976**, *41*, 3121-3124.

[5]Kitahara, T.; Mori, K.; Matsui, M. *Tetrahedron Lett.* **1979**, *32*, 3021-3024.

[6]Cygler, M.; Grochulski, P.; Kazlauskas, R. J.; Schrag, J. D.; Bouthillier, F.; Rubin, B.; Serreqi, A. N.; Gupta, A. K. *J. Am. Chem. Soc.* **1994**, *116*, 3180-3186.

[7]Murshudov, G. N.; Lebedev, A.; Vagin, A. A.; Wilson, K. S.; Dodson, E. J. *Acta Cryst.* **1999**, *D55*, 247-255.

[8]Guex, N.; Peitsch, M. C. *Electrophoresis* **1997**, *18*, 2714-2723.

[9]Otwinowski, Z.; Minor, W. *Methods in Enzymology*, **1997**, *276*, 307-326.

[10]Eadie G.S. *J. Biol. Chem.* **1942**, *146*, 85-93.

[11]Hofstee B. H. J. *Nature* **1959**, *184*, 1296-1298.

[12]Stewart, J. J. P. *J. Comput. Chem.* **1989**, *10*, 209-220.

[13]Stewart, J. J. P. *J. Comput. Chem.* **1989**, *10*, 221-264.

[14]Polak, E.; Ribière, G. *Rev. Fr. d'Informatique et de Recherche Operationnelle* **1969**, *16*, 35-43.

[15]Zhao, K.; Landry, D.W. *Tetrahedron* **1993**, *49*, 353-368.

[16]Schrag, J. D.; Li, Y.; Cygler, M.; Lang, D.; Burgdorf, T.; Hecht, H.-J.; Schmid, R.; Schomburg, D.; Rydel, T.J.; Oliver, J. D.; Strickland, L. C.; Dunaway, C. M.; Larson, S.B.; Day, J.; McPherson, A. *Structure* **1997**, *5*, 187-202.

[17]Kim, K. K.; Song, H. K.; Shin, D. H.; Hwang, K. Y.; Suh, S. W. *Structure* **1997**, *5*, 173-185.

[18]Kovach, I. M.; Huhta, D.; Baptist, S. *J. Mol. Struct.***1991**, *226*, 99-110.

[19]Lang, D.A.; Mannesse, M. L. M.; de Haas, G. H.; Verheij, H. M.; Dijkstra, B. W. *Eur. J. Biochem.* **1998**, *254*, 333-340.

[20]Deslongchamps, P.; Atlani, P.; Fréhel, D.; Malaval, A. *Can. J. Chem.* **1972**, *50*, 3405-3408.

[21]Schulz, T.; Pleiss, J.; Schmid, R.D. *Prot. Sci.* **2000**, *9*, 1053-1062.

[22]Chen, C.-S.; Fujimoto, Y.; Girdaukas, G.; Sih, C. J. *J. Am. Chem. Soc.* **1982**, *104*, 7294-7299.

[23]Hein, G. E.; Niemann, C. *J. Am. Chem. Soc.* **1962**, *84*, 4487-4494.

[24]Luić, M.; Tomić, S.; Leščić, I.; Ljubović, E.; Šepac, D.; Šunjić, V.; Vitale, L.; Saenger, W.; Kojić-Prodić, B. *Eur. J. Biochem.* **2001**, *268*, 3964-3973.

[25]Fersht, A. *Enzyme structure and mechanism*, 2nd edition; W. H. Freeman and Co.: New York, NY, **1985**, pp. 109-111.

CHAPTER 3 - APPENDIX 1

Interactions PCL-alcohol moiety in complexes PCL-1-(R_C), PCL-1-(S_C), PCL-2-(R_C) and PCL-2-(S_C)

Complexes PCL-1-(R_C) and PCL-1-(S_C)

The alcohol moieties in complexes PCL-1-(R_C) and PCL-1-(S_C) differ in an "umbrella-like" inversion at the alcohol stereocentre (LM-alignment) that places the hydrogen substituent in a different location. The other three substituents lie in the same position in both enantiomers, but show subtle differences. The substituents at the stereocentre were broken up as shown in Scheme 1 and their differences are highlighted in Table 1.

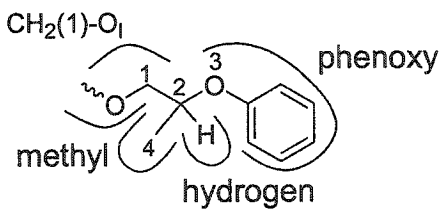

Scheme 1 – Schematic representation of the four different substituents at the stereocentre of POP.

Table 1 - Summary of subtle interactions present in the complexes PCL – inhibitor that may contribute to the enantioselectivity of PCL towards POP.

Interaction	(*R*)-POP	(*S*)-POP
$CH_2(1)$-O_I substituent		
His286 Nε - O_I	3.17 Å, 129.8°	3.24 Å, 132.4°
Phenoxy substituent		
Leu17 C=O - O(3)	3.29 Å	-
His286 Nε - O(3)	-	3.79 Å
His286 Cδ2 - O(3)	-	3.37 Å
Hydrogen substituent		
Leu17 C=O - CH(2)	-	3.16 Å
His286Nε - CH(2)	3.78 Å	-
His286 Cδ2 - CH(2)	3.76 Å	-
Methyl substituent		
	same position in both enantiomers	

In complexes PCL-**1**-(R_C) and PCL-**1**-(S_C) both enantiomers have similar hydrogen bonding distances and angles between the alcohol oxygen O_I and His286 Nε2 (3.17 Å, 129.8° in (*R*)-POP and 3.24 Å, 132.4° in (*S*)-POP)(Table 1). A striking difference between (*R*) and (*S*)-POP in complexes PCL-**1**-(*R*) and PCL-**1**-(*S*) is the position of O(3). The "umbrella-like" inversion at the stereocentre places O(3) of (*R*)-POP close to the carbonyl oxygen of Leu17 (3.29 Å). In (*S*)-POP, the major interaction is the vicinity of O(3) to both His286 Nε (3.79 Å) and His286 Cδ2 (3.37 Å). Last, the hydrogen substituent points in different orientations in the two enantiomers. In the fast (*S*)-enantiomer it bumps into Leu17 carbonyl (3.16 Å), while in the slow (*R*)-enantiomer is close to His286 Nε2 (3.74 Å).

Complexes PCL-2-(R_C) and PCL-2-(S_C)

In complexes PCL-**2**-(R_C) and PCL-**2**-(S_C), contrary to what we have seen with PCL-**1**-(R_C) and PCL-**1**-(S_C), the difference between the two alcohols moieties within the catalytic pocket of PCL is due to the exchange of the medium and large group at the stereocentre (H-alignment). These differences are evaluated in Table 2, breaking up the substituents as in Scheme 2.

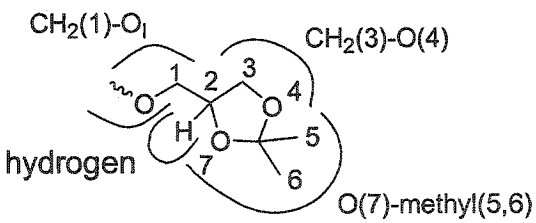

Scheme 2– Schematic representation of the four different substituents at the stereocentre of solketal.

In the CH_2(1)-O_I substituent, apart from the subtly different hydrogen bond alcohol O_I-His286 Nε2 (3.30 Å, 126.9° in PCL-**2**-(*S*) and 3.26 Å, 128.2° in PCL-**2**-(*R*)), CH_2(1) is slightly closer to His286 Nε2 in (*R*)-solketal than in (*S*)-solketal (3.30 Å vs. 3.43 Å) (Table 2).

In the CH_2(3)-O(4) substituent the methylene group interacts with Leu17 carbonyl only in the slow (*R*)-enantiomer (3.49 Å). A small difference is also present in the

distance between Leu287 side-chain methyl group and O(4) of the two enantiomers (in (*R*)-solketal it is at 3.41 Å while in (*S*)-solketal it is at 3.26 Å).

Table 2 - Summary of interactions that may contribute to the enantioselectivity of PCL towards solketal in the complexes PCL – inhibitor. PCL-**2**-(S_C) contains (*R*)-solketal and PCL-**2**-(R_C) contains (*S*)-solketal as alcohol moiety.

Interaction	(*R*)-solketal	(*S*)-solketal
CH_2(1)-O_I substituent		
His286 Nε2 - O_I	3.30 Å, 126.9°	3.26 Å, 128.2°
His286 Nε2 - CH_2(1)	3.30 Å	3.43 Å
CH_2(3)-O(4) substituent		
Leu17 C=O - CH_2(3)	3.49 Å	-
Leu287 CH_3 - O(4)	3.41 Å	3.26 Å
O(7)-methyl(5,6) substituent		
Leu17 C=O - O(7)	-	2.76 Å
Thr18 OH - O(7)	-	3.17 Å
Tyr29 OH - CH_3(5)	7.67 Å	3.64 Å
Leu287 CH_3 - CH_3(5)	4.21 Å	3.48 Å
Hydrogen substituent		
Leu17 C=O - CH(2)	3.25 Å	3.04 Å

The major difference between the two solketal enantiomers is the interaction of the O(7)-methyl (5,6) substituent. In (*S*)-solketal the oxygen at the stereocentre O(7) is close to both Leu17 carbonyl (2.76 Å) and Thr18 OH (3.17 Å). While the first interaction supposedly is repulsive, the second may give rise to a hydrogen bond, thus favour the fast (*S*)-enantiomer. The methyl CH_3(5) is closer to Tyr29 hydroxyl group in (*S*)-solketal (3.64 Å vs 7.67 Å). Also, the CH_3(5) has better hydrophobic interactions with Leu287 side-chain in (*S*)-solketal (3.48 Å vs 4.21 Å).

Last, because of the "H-alignment" present in these complexes, the hydrogen at the stereocentre is not very different in the two enantiomers, being at 3.25 Å from Leu17 carbonyl in (*R*)-solketal and at 3.04 Å from the same residue in (*S*)-solketal.

Chapter 4

Only a few lipases resolve esters of chiral primary alcohols with high enantioselectivity, albeit often lower than for secondary alcohols. One possibility to enhance enzyme enantioselectivity is to modify the substrate to a more efficiently resolved one. Another option is medium engineering.

In Chapter 2 and 3 we have identified the molecular basis of PCL enantioselectivity towards primary alcohols. In this chapter we study PCL interfacial activation and we increase its enantioselectivity towards primary alcohols of the type Ph-X-$CH(CH_3)$-CH_2-OH (X = O, CH_2) by optimising the acyl chain length (substrate engineering) and the reaction conditions (medium engineering).

Contributors

This work was done under the supervision of Prof. Romas J. Kazlauskas. Curtis Keith, a summer student in 1992, studied PCL interfacial activation towards achiral esters. I carried out the syntheses of the chiral substrates, the kinetic resolutions, the characterisation of the products and the E determinations.

Highly enantioselective kinetic resolution of primary alcohols of the type Ph-X-CH(CH_3)-CH_2OH by *Pseudomonas cepacia* lipase-catalysed hydrolysis of their esters. Effect of solvent and acyl chain length.

Abstract

The *Pseudomonas cepacia* lipase (PCL)-catalysed kinetic resolution of esters of chiral primary alcohols 2-methyl-3-phenyl-1-propanol (**1**), 2-phenoxy-1-propanol (**2**) and solketal (**3**) was investigated in conditions of interfacial activation, which are typical of lipases. Both the effect of different solvents and different acyl chain lengths was examined. Solvent **A**, 30 vol% *n*-propanol in potassium phosphate buffer, gave the best results for both **1** and **2** (E $\geq$190 and E = 70 respectively), while a long acyl chain (C_7) yielded better enantioselectivity only for **1**. PCL interfacial activation towards a series of achiral substrates was also evaluated. The activation energy for the PCL-catalysed hydrolysis of ethyl acetate was found to be at least 2.6 kcal/mol lower in the presence of a water-lipid interface, demonstrating a rate acceleration in conditions of interfacial activation.

Introduction

Lipases (triacylglycerol hydrolases, EC 3.1.1.3) have been extensively used in the last two decades for the resolution of chiral alcohols. Although several lipases successfully resolve chiral secondary alcohols, fewer resolve with high enantioselectivity chiral primary alcohols[1] either *via* enantioselective acylation or hydrolysis of their esters. In particular, only *Pseudomonas cepacia* lipase (PCL),[1,2] porcine pancreatic lipase (PPL)[1,2] and *Achromobacter* sp. lipase (AL)[3] resolve some primary alcohols, although with lower enantioselectivities (E) than for secondary alcohols.[1] A useful approach to increase lipase enantioselectivity is the optimisation of the reaction conditions, especially important when they show only moderate to low E towards the substrate of interest.

Transesterification in organic solvents has been more successful for resolving chiral primary alcohols than the hydrolysis of the corresponding esters.[4,5,6] By changing the acylating agent in the enzymatic transesterification, scientists have improved the enantioselectivity of lipases towards primary alcohols. Different acylating agents

transform the enzyme into different acyl enzyme intermediates. This changes the structure of the transition state obtained by nucleophilic attack of the chiral alcohol on the acyl enzyme. Thus Miyazawa *et al.*[3] improved the enantioselectivity of lipase AL towards 2-phenoxy-1-propanol (**2**) from 1.1 to 19 by replacing vinyl trifluoroacetate with vinyl butanoate as acylating agent. With PCL, vinyl acetate gave higher E (E = 42) than the butanoate (E = 35) or the trifluoroacetate (E = 1.5).[4,6]

Scientists have also increased the enantioselectivity of enzymes by changing only the solvent, especially for transesterification reactions. Miyazawa *et al.*[6] showed that the lipase AK-catalysed transesterification of **2** with vinyl butanoate is highly solvent dependent. Indeed, lipase AK gave the highest enantioselectivity (E = 35) in diisopropyl ether while benzene was the worse solvent (E = 4.5). Despite the numerous attempts of relating the change in enzyme enantioselectivity to either the logP (P being the partition coefficient between 1-octanol and water), the dielectric constant, the hydrophobicity, the dipole moment of the solvent, etc., scientists have not yet been able to relate the enzyme enantioselectivity to the physico-chemical properties of the solvent.[7,8,9,10]

Unlike for transesterification reactions, fewer examples exist for lipase-catalysed hydrolysis of esters of primary alcohols. Goj *et al.*[11] achieved E = 97 in the PCL-catalysed hydrolysis of (±)-1-acetoxy-2-fluoro-2-phenylbutane in phosphate buffer. Cipriani and Bellezza[12] reported E = 100 for the *Candida rugosa* lipase (CRL)-catalysed hydrolysis of 2,2-dimethyl-hexa-3,4-dienyl acetate in water/hexane at 4°C.

In this paper, we study the PCL-catalysed hydrolysis of three chiral primary alcohols: 2-methyl-3-phenyl-1-propanol (**1**), 2-phenoxy-1-propanol (**2**) and solketal (**3**). Pure enantiomers of **1** have been used for the preparation of fungicidal compounds,[13] for the synthesis of adenosine receptor agonists and antagonists[14] and for the synthesis of the side chain of zaragozic acid A.[15] Pure enantiomers of **2**, structurally related to **1**, have proven useful for the synthesis of juvenoids, analogues of the insect juvenile hormone[16] and pure enantiomers of **3** have been used as building blocks in the synthesis of several bioactive compounds such as the β-adrenergic blocker timolol.[17] (*R*)-**1** has been prepared in ee >98% by baker's yeast catalysed reduction of (2-dimethoxymethyl-allyl)-benzene[18] while both the PCL-catalysed hydrolysis of **1**-acetate and the transesterification of **1** with vinyl acetate in *t*-butyl methyl ether proceeded with moderate enantioselectivity (E = 16[2]

and E = 12[19] respectively). More successful resolutions have been reported for alcohol **2**. Lipase PS catalyses the highly enantioselective transesterification of **2** with vinyl acetate in chloroform (E = 116[20] and E = 120[21]), although the PCL-catalysed hydrolysis of **2**-acetate proceeds with moderate enantioselectivity (E = 17).[22] The resolution of alcohol **3** has been the subject of extensive research in the past 15 years. The best results have been achieved in the enantioselective oxidation (E >100) of solketal to solketalic acid by two alcohol dehydrogenases[23] and in the lipase AK-catalysed acylation of **3** with vinyl butanoate at –40°C (E = 55).[24] The PCL catalysed hydrolysis of **3**-benzoate, however, gave low enantioselectivities, ranging from E = 3.7 to E = 9.[25]

To increase the enantioselectivity of PCL towards esters of chiral primary alcohols **1**, **2** and **3**, we optimised both the reaction conditions and the acyl chain length of the substrate. Furthermore, we carried out kinetic resolutions in conditions of interfacial activation by maintaining the substrate concentration above its solubility limit in the reaction media. We also verified the rate enhancement of PCL-catalysed hydrolysis in condition of interfacial activation using a number of achiral esters.

Materials and Methods

All chemicals were purchased from Sigma-Aldrich Co. (Oakville, ON) unless otherwise specified. Lipases from *Pseudomonas cepacia* were purchased from Genzyme Diagnostics (Cambridge, MA) (2190 U/mg powder) and Amano Enzyme U.S.A. Co., Ltd. (Lombard, IL) (LPL200S 2260 U/mg powder or Lipase PS ≥30 U/mg powder). (±) 2-phenoxy-1-propanol was purchased from TCI America (Portland, OR). Rates of hydrolysis of achiral substrates were measured by a Radiometer Copenhagen pH-stat (Copenhagen, Denmark). The chiral column used for the GC analyses was a Chirasil-DEX CB, 25 m x 0.25 mm x 0.25 μm (Life Sciences, Peterborough, ON). The chiral column used for the HPLC analysis was a Chiracel OD, 25cm x 4.6 mm (Daicel Chemical Industries, Ltd., Exton, PA). NMR spectra were collected at 270 Mz for ^{1}H and 68 MHz for ^{13}C.

Interfacial activation

Rates of ester hydrolysis were measured by pH-stat in potassium phosphate buffer (10 mM, pH 7.0), with an endpoint set at pH 7.15. PCL (Amano LPL200S) in buffer (10 mL,

0.5 mg lipase/mL) in a polypropylene cup was stirred vigorously with the mechanical stirrer until a constant pH was attained (5 min). Upon addition of substrate, the recorder was started and the initial rate measured. The activity of the enzyme was calculated from these slopes and a [substrate]-rate profile plotted for each ester assayed. In some cases with soluble substrates, a magnetic stirrer replaced the mechanical stirrer.

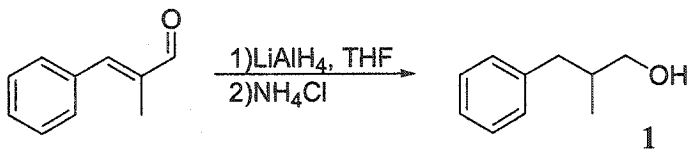

1

(±)-2-Methyl-3-phenyl-1-propanol, 1.

Lithium aluminium hydride (4.30 g, 110 mmol) was placed in a flame-dried reaction flask under argon atmosphere. The flask was cooled to 0°C and anhydrous tetrahydrofuran (100 mL) was added. 2-Methyl-3-phenyl propenal (3.70 g, 25 mmol) dissolved in anhydrous tetrahydrofuran (25 mL) was added dropwise. The reaction was stirred overnight under argon atmosphere, quenched with a saturated solution of ammonium chloride, filtered, extracted with ethyl acetate, dried over anhydrous $MgSO_4$ and the solvent was evaporated under vacuum. The product was purified by flash chromatography on a silica gel column (eluent: 7:3 hexane:ethyl acetate). Yield 89%. R_f = 0.55 (silica gel, 7:3 hexane:ethyl acetate); ^{1}H NMR ($CDCl_3$) δ 7.15-7.30 (m, 5H, Ph), 3.42.-3.55 (m, 2H, CH_2), 2.75 (dd, 1H, CH_2, J_1 = 6.2 Hz, J_2 = 13.4 Hz), 2.41 (dd, 1H, CH_2, J_1 = 8.2 Hz, J_2 = 13.4 Hz), 1.87-2.00 (m, 1H, CH), 0.91 (d, 3H, CH_3, J = 6.7 Hz); ^{13}C NMR ($CDCl_3$) δ 16.5, 37.9, 39.8, 67.5, 125.9, 128.3, 129.3, 140.9; MS (EI) *m/z* (rel. intensity) 150 (26, M^+), 132 (16, M - H_2O), 117 (39, M^+ - H_2O - CH_3), 91 (100, M^+ - $CH(CH_3)CH_2OH$), 77 (8, Ph).

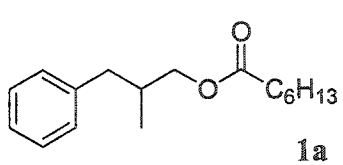

1a

(±)-2-Methyl-3-phenyl-1-propyl heptanoate, 1a.

A solution of (±)-2-methyl-3-phenyl-1-propanol (0.50 g, 3.3 mmol) and pyridine (0.42 mL, 5 mmol) in dry ether (50 mL) was stirred at 4°C. Heptanoyl chloride (0.97 mL, 6.7 mmol) was added dropwise to the solution at 4°C. After 2 h the reaction mixture was washed with a saturated solution of $NaHCO_3$, water and brine, dried over anhydrous $MgSO_4$ and the solvent was evaporated under vacuum. The product was purified by flash chromatography on a silica gel column (eluent: 8:2 hexane:ethyl acetate) and isolated as a yellow oil. Yield 90%. R_f=0.78 (silica gel, 8:2 hexane:ethyl acetate); ^{1}H NMR ($CDCl_3$) δ 7.07-7.30 (m, 5H, Ph), 3.87-4.00 (m, 2H, CH_2), 2.40-2.76 (m, 2H, CH_2), 2.31 (t, 2H, CH_2, J = 7.4 Hz), 2.04-2.17 (m, 1H, CH), 1.57-1.68 (m, 2H, CH_2), 1.23-1.35 (m, 6H, $3CH_2$), 0.86-0.93 (m, 6H, $2CH_3$); ^{13}C NMR ($CDCl_3$) δ 14.1, 16.7, 22.6, 25.1, 28.9, 31.6, 34.4, 34.7, 39.9, 68.5, 126.1, 128.3, 129.2, 140.1, 174.0; MS (CI/NH_3) *m/z* (rel. intensity) 263 (4, M + H^+) 132 (100, M^+ - $C_6H_{13}COOH$), 91 (44, tropylium), 77 (2, Ph).

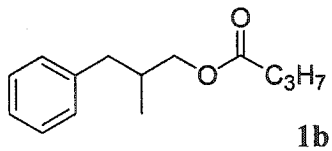

1b

(±)-2-Methyl-3-phenyl-1-propyl butanoate, 1b.

A solution of (±)-2-methyl-3-phenyl-1-propanol (0.50 g, 3.3 mmol), butyric anhydride (0.55 g, 3.5 mmol), triethylamine (0.48 mL, 6.7 mmol) and 4-(dimethylamino)pyridine (10 mg, 0.08 mmol) in methylene chloride (25 mL) was stirred at room temperature for 3 hours. The reaction mixture was washed with a saturated solution of $NaHCO_3$, water and brine, dried over anhydrous $MgSO_4$ and the solvent was evaporated under vacuum. The product was purified by flash chromatography on a silica gel column (eluent: 8:2 hexane:ethyl acetate) and isolated as a yellow oil. Yield 89%. R_f =0.72 (silica gel, 8:2 hexane:ethyl acetate); ^{1}H NMR ($CDCl_3$) δ 7.06-7.30 (m, 5H, Ph), 3.87-4.00 (m, 2H, CH_2), 2.40-2.76 (m, 2H, CH_2), 2.29 (t, 2H, CH_2, J = 7.4 Hz), 2.04-2.17 (m, 1H, CH), 1.59-1.73 (m, 2H, CH_2), 0.90-0.98 (m, 6H, $2CH_3$); ^{13}C NMR ($CDCl_3$) δ 13.8, 16.8, 18.6, 34.7, 36.3, 39.9, 68.5, 126.1, 128.4, 129.2, 140.1, 173.8; MS (CI/NH_3) *m/z* (rel. intensity) 221 (9, M + H^+) 132 (>81, M^+ - C_3H_7COOH), 117 (>100, M^+ -), 91 (>84, $PhCH_2$), 77 (3, Ph), 71 (27, C_4H_7O).

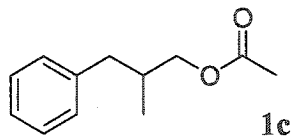

1c

(±)-2-Methyl-3-phenyl-1-propyl acetate, 1c.

A solution of (±)-2-methyl-3-phenyl-1-propanol (2.50 g, 16.7 mmol), acetic anhydride (1.85 mL, 16.7 mmol), triethylamine (2.37 mL, 33.4 mmol) and 4-(dimethylamino) pyridine (10 mg, 0.08 mmol) in methylene chloride (30 mL) was stirred at room temperature for 3 hours. The reaction mixture was washed with a saturated solution of $NaHCO_3$, water and brine, dried over anhydrous $MgSO_4$ and the solvent was evaporated under vacuum. The product was purified by flash chromatography on a silica gel column (eluent: 7:3 hexane:ethyl acetate) and isolated as a yellow oil. Yield 94%. R_f = 0.76 (silica gel, 7:3 hexane:ethyl acetate); ^{1}H NMR ($CDCl_3$) δ 7.06-7.30 (m, 5H, Ph), 3.85-3.98 (m, 2H, CH_2), 2.40-2.76 (m, 2H, CH_2), 2.02-2.11 (m, 1H, CH), 2.01 (s, 3H, CH_3), 0.91 (d, 3H, CH_3, J = 6.7 Hz); ^{13}C NMR ($CDCl_3$) δ 14.3, 16.7, 34.6, 40.1, 68.7, 126.1, 128.4, 129.2, 141.6, 171.1; MS (CI/NH_3) *m/z* (rel. intensity) 193 (15, M + H^+) 133 (48, M^+ - CH_3COOH), 117 (100, M^+ - H_2O - CH_3), 91 (84, tropylium), 77 (4, Ph).

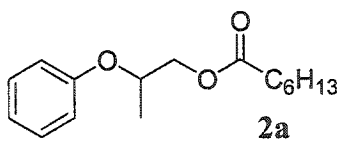

2a

(±)-2-Phenoxy-1-propyl heptanoate, 2a.

The reaction was performed as for **1a**. Yield 89% (yellow oil). R_f =0.77 (silica gel, 8:2 hexane:ethyl acetate); ^{1}H NMR ($CDCl_3$) δ 6.90-7.30 (m, 5H, Ph), 4.54-4.65 (m, 1H, CH), 4.12-4.29 (m, 2H, CH_2), 2.29 (t, 2H, CH_2, J = 7.4 Hz), 1.53-1.68 (m, 2H, CH_2), 1.22-1.36 (m, 9H, $3CH_2$ + CH_3), 0.86 (t, 3H, CH_3, J = 5.2 Hz); ^{13}C NMR ($CDCl_3$) δ 14.1, 16.9, 22.5, 24.9, 28.8, 31.5, 34.3, 66.8, 71.8, 116.2, 121.2, 129.6, 157.8, 173.8; MS (EI) *m/z* (rel. intensity) 264 (4, M^+), 171 (100, M^+ - PhO), 113 (27, $C_6H_{13}CO$), 94(20.6, PhOH), 77 (9, Ph).

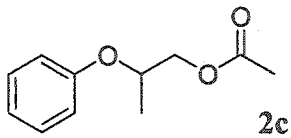

2c

(±)-2-Phenoxy-1-propyl acetate, 2c.

The reaction was performed as for **1c**. Yield 91 % (yellow oil). R_f = 0.59 (silica gel, 7:3 hexane:ethyl acetate); ^{1}H NMR ($CDCl_3$) δ 7.23-7.30 (m, 2H, Ph), 6.88-6.95 (m, 3H, Ph), 4.55-4.66 (m, 1H, CH), 4.25 (dd, 1H, CH_2, J_1 = 6.4 Hz, J_2 = 11.6 Hz), 4.15 (dd, 1H, CH_2, J_1 = 4.3 Hz, J_2 = 11.6 Hz), 2.06 (s, 3H, CH_3), 1.32 (d, 3H, CH_3, J = 6.2 Hz); ^{13}C NMR ($CDCl_3$) δ 16.7, 20.9, 67.0, 71.8, 116.2, 121.3, 129.6, 157.8, 171.0; MS (EI) *m/z* (rel. intensity) 194 (8, M^+), 101 (89, M^+ - PhO), 94 (83, PhOH), 77 (19, Ph), 43 (>100, CH_3CO).

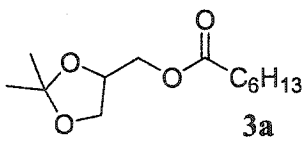

3a

(±)-2,2-dimethyl-[1,3]dioxolan-4-methyl heptanoate, 3a.

The reaction was performed as for **1a**. Yield 92% (yellow oil). R_f =0.71 (silica gel, 7:3 hexane:ethyl acetate); ^{1}H NMR ($CDCl_3$) δ 4.23-4.31 (m, 1H, CH), 3.99-4.15 (m, 2H, CH_2), 3.67-3.71 (m, 2H, CH_2), 2.30 (t, 2H, CH_2, J = 7.7 Hz), 1.52-1.63 (m, 2H, CH_2), 1.39 (s, 3H, CH_3), 1.32 (s, 3H, CH_3), 1.21-1.30 (m, 6H, $3CH_2$), 0.84 (t, 3H, CH_3, J = 6.9 Hz); ^{13}C NMR ($CDCl_3$) δ 14.0, 22.5, 24.9, 25.4, 26.7, 28.8, 31.5, 34.2, 64.5, 66.4, 73.7, 109.8, 173.6; MS (CI/NH_3) *m/z* (rel. intensity) 245 (12, M + 1), 229 (61, M^+ - CH_3), 113 (33, M^+ - (2,2-dimethyl-[1,3]dioxolan-4-methanol).

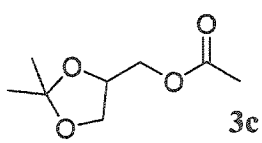

3c

(±)-2,2-dimethyl-[1,3]dioxolan-4-methyl acetate, 3c.

The reaction was performed as for **1c**. Yield 93% (yellow oil). R_f =0.71 (silica gel, 7:3 hexane:ethyl acetate); ^{1}H NMR ($CDCl_3$) δ 4.22-4.31 (m, 1H, CH), 3.99-4.15 (m, 2H,

CH_2), 3.65-3.70 (m, 2H, CH_2), 2.10 (s, 3H, CH_3), 1.37 (s, 3H, CH_3);), 1.29 (s, 3H, CH_3); ^{13}C NMR ($CDCl_3$) δ 20.8, 25.4, 26.7, 64.9, 66.3, 73.6, 109.9, 170.8; MS (CI/NH_3) *m/z* (rel. intensity) 175 (27, M + 1), 159 (83, M – CH_3).

PCL-catalysed kinetic resolution of esters (±)-1a-c.

Substrates (±)-**1a-c** (0.08 mmols) were suspended or dissolved in the appropriate solvent (3.28 mL) (Table 1). PCL solutions (0.05 mL) in 0.4 M potassium phosphate buffer at pH 7.0 (GPCL and LPL200S 0.0084 mg/mL, PS 0.2050 mg/mL) were added to the reaction vials. The mixtures were stirred at room temperature and monitored by thin layer chromatography (TLC) (hexane:ethyl acetate 8:2) until about 50% conversion (visual estimate). The reactions were quenched with 2% HCl until pH 2, extracted with ethyl ether and the solvent evaporated under vacuum. Starting material ester and product alcohol were separated by preparative TLC (hexane:ethyl acetate 8:2). The recovered esters **1a** and **1b** were converted to the corresponding alcohol **1** by NaOH promoted hydrolysis in aqueous ethanol (15 w/v% NaOH in 50 vol% aqueous ethanol) at room temperature. The alcohols were converted to **1c** by pyridine-catalysed esterification using acetic anhydride. The enantiomeric excesses (ee) of the non-reacted starting materials (**1a**, **1b** and **1c**) and of the product (**1**) of the reactions were derived from the ee of **1c** measured by gas chromatograpy: 120 °C isothermal for 35 min and raised to 180°C at a rate of 10°C/min, 8.5 psi. Retention times were 31.2 min for (*S*)-3-methyl-2-phenyl-1-propyl acetate ((*S*)-**1c**) and 31.9 min for (*R*)-3-methyl-2-phenyl-1-propyl acetate ((*R*)-**1c**); α = 1.02. (*S*)-**1** $[\alpha]^{20}_D$ – 11.3 (c = 0.124, C_6H_6), lit.[26] $[\alpha]^{20}_D$ – 11.08 (c = 4.6, C_6H_6);

PCL- catalysed kinetic resolution of esters (±)-2a,c.

Kinetic resolutions were carried out as for (±)-**1a-c**. Starting ester and product alcohol were separated by preparative TLC (hexane:ethyl acetate 8:2). The recovered esters **2a,c** were converted to the corresponding alcohol **2** by NaOH promoted hydrolysis in aqueous ethanol (15% NaOH in 50 vol% aqueous ethanol) at room temperature. The alcohols thus obtained were derivatised to the corresponding trifluoroacetates by pyridine-catalysed esterification using trifluoroacetic anhydride. The enantiomeric excesses (ee) of the non-reacted starting materials **2a** and **2c** and of the product (**2**) of the reactions were derived

from the ee of the trifluoroacetates measured by gas chromatograpy: 120 °C isothermal for 10 min and raised to 180°C at a rate of 10°C/min, 10 psi. Retention times were 10.3 min for (*S*)-2-phenoxy-1-propyl trifluoroacetate and 10.5 min for (*R*)- 2-phenoxy-1-propyl trifluoroacetate; $\alpha = 1.03$. The absolute configuration of the resolved alcohol was determined by oxidising the alcohol product of a kinetic resolution to the corresponding carboxylic acid by means of the Jones' reagent and analysing it by HPLC using hexane:isopropanol:formic acid (90:10:1) as mobile phase. Retention times were 10 min for (*S*)-2-phenoxy-propionic acid and 16.1 min for (*R*)-2-phenoxy-propionic acid; $\alpha = 1.61$.[27]

PCL catalysed kinetic resolution of esters (±)-3a,c.

The reactions were performed as for (±)-**1a,c** and were submitted to gas chromatographic analysis to determine the enantiomeric excesses of non-reacted starting materials and products using 100 °C for 10 min, then raised to 180°C at a rate of 5 °C/min, 8 psi. Retention times were 15.2 min for (*S*)-**3**, 15.0 min for (*R*)-**3** ($\alpha = 1.02$), 28.3 min for (*S*)-**3a** and 28.5 min for (*R*)-**3a** ($\alpha = 1.01$). The retention time of the enantiomers was confirmed by comparison with commercially available samples of pure enantiomers of (*R*)-**3** and (*S*)-**3**.

Results

We screened PCL from different commercial sources for the hydrolysis of (±)-2-methyl-3-phenyl-1-propyl heptanoate, **1**-heptanoate (Scheme 1). The reactions were carried out in potassium phosphate buffer 0.4 M, pH 7.0, containing 30 vol% of *n*-propanol as cosolvent (solvent A). The concentration of 1-heptanoate and of all the substrates used in the reactions described in this work was above their solubility limit in the solvent used to benefit of PCL interfacial activation. We had previously used solvent A for crystallising PCL-transition state analogue complexes[28] but here the concentration of PCL in solvent A is kept below 10 mg/mL to avoid its crystallisation while stabilising the open form of the enzyme.

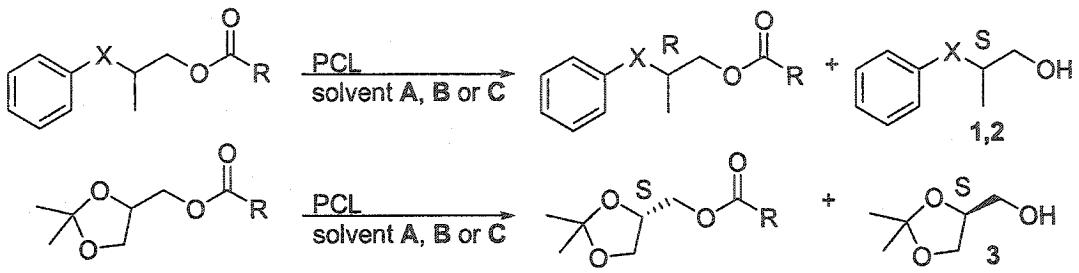

1 X= CH_2 , **2** X= O
a R = C_6H_{13} , **b** R = C_3H_7 , **c** R = CH_3
A 30 vol% *n*-propanol in potassium phosphate 0.4 M, pH 7.0; **B** 30 vol% *t*-butyl methyl ether in potassium phosphate 0.4 M, pH 7.0; **C** potassium phosphate 0.4 M pH 7.0

Scheme 1 - PCL catalysed hydrolysis of esters.

No substantial differences were observed between PCL from Genzyme Diagnostics (GPCL), Amano LPL200S and Amano lipase PS. Indeed, the differences between the calculated E values were within experimental error (Table 1, entries 1-3). GPCL gave E ≥ 190 ± 30, Amano LPL 200S yielded E ≥180 ± 30 and lipase PS gave E ≥170 ± 30, all favouring the (*S*) enantiomer. Thus only GPCL was used for all the subsequent kinetic resolutions.

We then explored the solvent dependence of the enantioselectivity in the hydrolysis reaction by conducting kinetic resolutions of (±)-**1**-heptanoate in two other solvents: 30 vol% *t*-butyl methyl ether (*t*-BME) in potassium phosphate buffer 0.4 M, pH 7.0 (solvent **B**) and potassium phosphate buffer 0.4 M, pH 7.0 (solvent **C**) (Table 1, entries 4 and 5). The highest E (E ≥190 ± 30) remained the one obtained with solvent **A**, while we recorded the lowest E (E = 61 ± 4) in solvent **C**.

Because of the high enantioselectivity obtained for the hydrolysis of (±)-**1**-heptanoate in solvent **A**, we investigated the influence of the acyl chain length on the enzyme enantioselectivity in this solvent. We carried out kinetic resolutions of the heptanoate, butanoate and acetate of alcohol **1** and of the heptanoate and acetate of alcohols **2** and **3** in solvent **A** (Table 1, entries 6, 7, 9, 10, 12 and 13). In the case of alcohol **1**, PCL favoured a longer acyl chain length, displaying the highest E with the heptanoate (E ≥190, Table 1, entry 1) and the lowest with the acetate (E = 38, Table 1, entry 7). In the case of alcohol **2** however, the E values were within experimental error (E = 70 ± 20 and E = 52 ± 6, Table 1, entries 9 and 10) and PCL seemed not to have a clear-

cut preference for long versus short acyl chain. We did not detect any reaction for (±)-3-acetate, while the enantioselectivity of PCL towards (±)-3-heptanoate (E = 5.2 ± 0.1) was significantly lower than for substrates **1** and **2** and similar to what previously reported for the hydrolysis of solketal benzoate by PCL (E = 3.7 to 9).[25] For all the alcohols we observed faster reactions with long acyl chain esters.

To determine the interfacial activation of PCL, i.e. the rate enhancement upon changing from a soluble to an insoluble substrate form, we measured its reaction rate of hydrolysis in potassium phosphate buffer with increasing concentration of the substrate for ethyl acetate, isopropenyl acetate, *n*-pentyl acetate and ethyl butanoate, as well as for methyl acetate (Scheme 2, Figure 1 A). While methyl acetate, a soluble ester, displayed a steady increase in reaction rate with increasing concentration, the other four substrates showed a sharp rate enhancement at a particular substrate concentration. This concentration matched the solubility limit of the substrate as seen by an increase in cloudiness of the solution. The rate increase ranged from about 10-fold for ethyl butanoate to about 40-fold for *n*-pentyl acetate. Isopropenyl acetate showed almost a 15-fold amplification upon reaching the solubility limit and ethyl acetate exhibited a 25-fold enhancement.

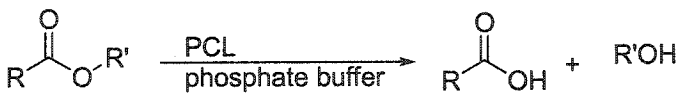

Scheme 2 – PCL-catalysed hydrolysis of esters. Reaction rates are measured by titrating the released carboxylic acid with NaOH and plotting the amount of base added as a function of time.

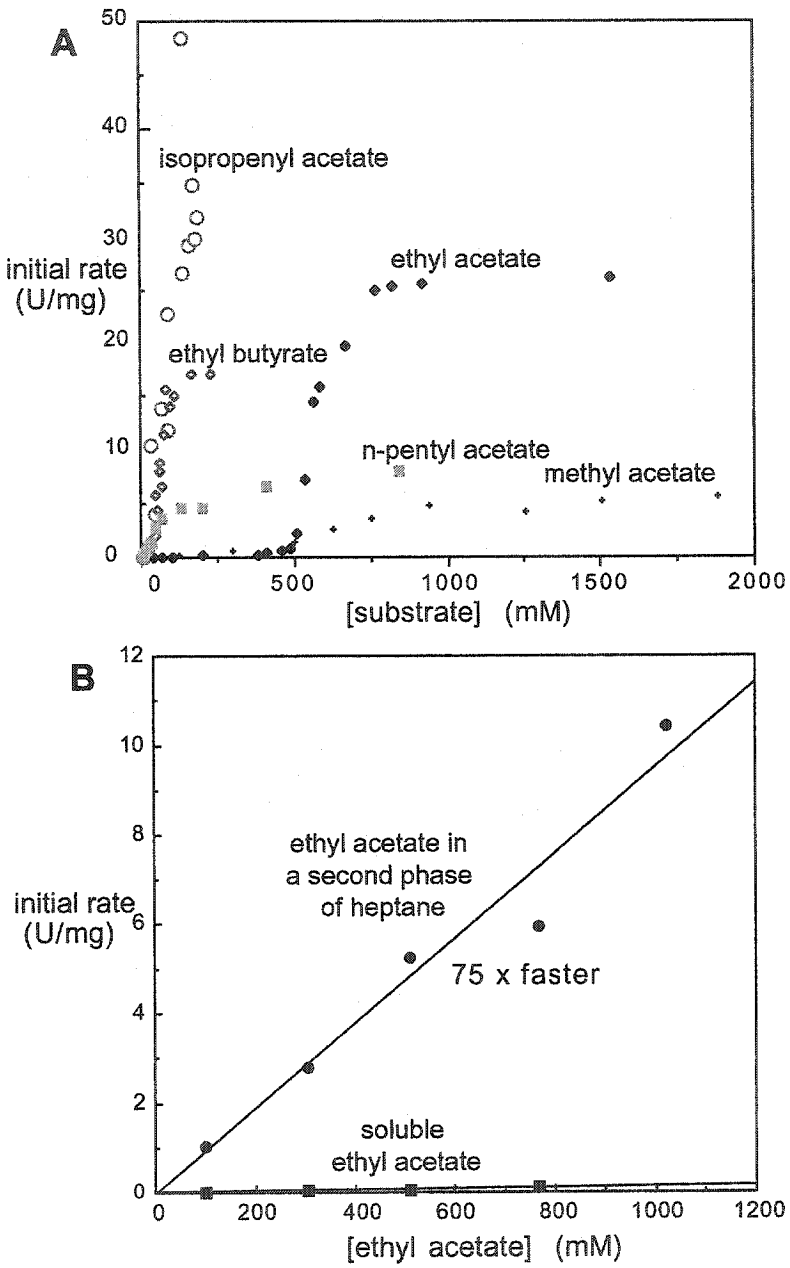

Figure 1 - Initial rate versus substrate concentration for PCL-catalysed hydrolysis of several esters. (A) The observed rates of hydrolysis increase 10 to 40-fold at a particular concentration (~50 mM for ethyl butanoate, isopropenyl acetate and pentyl acetate; ~600 mM for ethyl acetate). These concentrations match the solubility limit of the ester as seen by the increased cloudiness of the solution. The maximum rate for isopropenyl acetate was ~300 U/mg, but this is beyond the y-axis limit of this chart. (B) Initial rate of hydrolysis of ethyl acetate, either dissolved or present in a separate heptane phase, as a function of ethyl acetate concentration. At the same substrate concentration, the initial rate was 75-fold faster in heptane. This increase is due to interfacial activation. All experiments used Amano LPL-200S, a purified lipase preparation.

These experiments demonstrate the classical interfacial activation phenomenon that is characteristic of lipases,[29,30] but likely underestimate the degree of interfacial activation because the experiments contained an interface even at concentrations where the ester was still soluble. The ester may absorb to the polyethylene surface of the reaction vessel or to the surface of bubbles formed by stirring. These effects render the rate of hydrolysis of the soluble substrate faster that the true soluble rate.

To measure the degree of interfacial activation, we compared the rates of hydrolysis of ethyl acetate by PCL at identical substrate concentrations with and without an interface present. The ethyl acetate was either dissolved in water or in a second phase of heptane. The rates with interface were seventy-five times higher than those without interface (Figure 1 B). In other words, in the presence of an interface the activation energy is lower by 2.6 kcal/mol (RTln75). This value is a lower limit since the without-interface experiments still contained the unavoidable air-water interface and the water-reaction vessel interface. Solubility limits prevented the measurement of the kinetic parameters k_{cat} and K_m. Other esters were not soluble enough in water to measure the without-interface rate.

Table 1 - PCL catalysed hydrolysis of esters of **1**,**2** and **3** in different solvents.

Entry	Substrate[a]	Enzyme source	Solvent[b]	% Conv.	ee_p%	ee_s%	E[c]
1	(±)-**1a**	GPCL	**A**	39.2 ± 0.1	≥98.0 ± 0.2	63.0 ± 0.2	≥190 ± 30 (*S*)
2	(±)-**1a**	LPL 200S	**A**	36.4 ± 0.1	≥98.0 ± 0.2	56 ± 5	≥180 ± 30 (*S*)
3	(±)-**1a**	lipase PS	**A**	35.1 ± 0.1	≥98.0 ± 0.2	52.5 ± 0.7	≥170 ± 30 (*S*)
4	(±)-**1a**	GPCL	**B**	15.5 ± 0.5	98.0 ± 0.2	19.0 ± 0.2	120 ± 20 (*S*)
5	(±)-**1a**	GPCL	**C**	32.0 ± 0.1	95.0 ± 0.2	45.0 ± 0.2	61 ± 4 (*S*)
6	(±)-**1b**	GPCL	**A**	17 ± 2	98.0 ± 0.2	21 ± 3	130 ± 30 (*S*)
7	(±)-**1c**	GPCL	**A**	28.0 ± 0.5	93± 1	35.0 ± 0.3	38 ± 6 (*S*)
8	(±)-**1c**[2]	LPL 200S or PS30	**n.r.**[d]	44	79	62	16 (*S*)
9	(±)-**2a**	GPCL	**A**	51.0 ± 0.1	90 ± 1	94 ± 1	70 ± 20 (*S*)
10	(±)-**2c**	GPCL	**A**	18 ± 3	95.5 ± 0.4	21 ± 4	52 ± 6 (*S*)
11	(±)-**2c**[31]	LPL 200S	**B**	n.a.	n.a.	n.a.	17 (*S*)
12	(±)-**3a**	GPCL	**A**	27 ± 4	62 ± 2	23 ± 4	5.2 ± 0.1 (*S*)
13	(±)-**3c**	GPCL	**A**	n.r.[e]	-	-	-

[a] **a** = heptanoate, **b** = butyrate, **c** = acetate; [b] **A** = 30 vol% *n*-propanol in potassium phosphate 0.4 M, pH 7.0; **B** = 30 vol% *t*-butyl methyl ether in potassium phosphate 0.4 M, pH 7.0; **C** = potassium phosphate 0.4 M, pH 7.0; [c] determined from ee_p% and ee_s% according to Chen *et al.*[32], alcohol enantiopreference in parentheses; [d] "a rapidly stirred suspension of substrate dissolved in a small amount of ether and phosphate buffer (10 mM, pH 7) containing lipase from *P. cepacia* ..."[2]; [e] No enzymatic hydrolysis was observed after 48 hours.

Discussion

In this work we explored the enantioselectivity of PCL towards different esters of two structurally related primary alcohols **1** and **2**, and the important chiral synthon solketal, **3**. PCL from different commercial sources, different solvents and substrate acyl chain lengths were evaluated.

The largest change in enantioselectivity, observed during the resolution of esters of alcohol **1** (from 38 to ≥190, corresponding to a free energy change of ~ 1.0 kcal/mol in the transition state), occurred upon extending the ester acetyl group to a heptanoyl group. This may cause a reduced flexibility of the alcohol moiety. X-ray crystal structures show that the acyl chain binds to the large hydrophobic pocket (hydrophobic groove HA) of PCL.[33] This pocket comprises PCL hydrophobic residues Pro113, Phe119, Leu164, Leu167, Val266 and Val267, which form van der Waals contacts with the acyl chain. Luić *et al.*[34] found that, when a shorter acyl chain like an acetyl group is present, both the large substituent at the stereocentre and the acyl chain can bind in this pocket. Binding of the longer heptanoyl chain restricts the flexibility of the alcohol moiety as compared to the smaller acetyl group.

Upon changing from solvent **B** (a two phase mixture of *t*-BME and phosphate buffer) to solvent **A** (a single phase of phosphate buffer containing 30 vol% *n*-propanol) a smaller change in enantioselectivity towards **1** (from 120 to ≥190, corresponding to a free energy change of ~ 0.3 kcal/mol in the transition state) was observed. This change from a two-phase solvent system to a single-phase solvent may alter the lipase lid conformation. The enantioselectivity was much lower (E = 61) in the absence of an interface other than the substrate (solvent **C**).

Like most lipases, PCL exists in two different forms. In the closed form, a lid covers the active site of the enzyme. In the open form, the lid is displaced to expose the active site to the reaction medium. The enzyme is considered to be in equilibrium between these two forms and in an aqueous environment, devoid of interfaces, there is a prevalence of the closed form.[35] The X-ray crystal structure of the closed form of *Pseudomonas glumae* lipase (PGL),[36] sharing 83% identity with PCL, strongly suggests

that PCL is catalytically inactive in this conformation.[i] The active site of PGL in the closed form is blocked and Leu17, needed to stabilize the oxyanion of the tetrahedral intermediate, is incorrectly oriented. The open form of PCL[37,38] is catalytically active since the active site is accessible and all amino acid residues necessary for catalysis, including the conserved Leu17, are correctly oriented. The opening of the lid represents a dramatic change in the enzyme conformation and the position of the equilibrium between the closed and the open form of the lipase may affect the catalytic properties of the enzyme. Van Tol *et al.*[39] reported an increase in E from 8 to 16 for the PPL-catalysed hydrolysis of glycidyl butanoate when passing from water to a biphasic water/substrate system, i.e. in conditions of interfacial activation. Overbeeke *et al.*[40] studied the influence of the conformation of the lid on lipase enantioselectivity. They showed that the activation barrier leading to the Michaelis-Menten complex (enzyme-substrate complex) can be affected by the opening of the lid. In the absence of an interface this barrier is equally increased for both enantiomers and may dominate the enantioselectivity, decreasing it.[ii] The closed and open forms of PCL likely equilibrate in solution. The

---

[i] We assume that the closed form of PCL is the same as that of PGL

[ii] According to Overbeeke *et al.*[40] the enantiomeric ratio E can be written as: $E = [(e^{\beta\Delta G_{A,S}} + e^{\beta\Delta G_{B,S}})/(e^{\beta\Delta G_{A,R}} + e^{\beta\Delta G_{B,R}})]$, where $\Delta G_{A,S}$ and $\Delta G_{A,R}$ are the activation energies of the *S* and *R* enantiomer to form the Michaelis-Menten complex and $\Delta G_{B,S}$ and $\Delta G_{B,R}$ are the activation energies of the *S* and *R* enantiomer for product formation. When no interface is present, $\Delta G_{B,S}$ and $\Delta G_{B,R}$ are dominated by the energy necessary to open the lid of the enzyme ΔG_A ($\Delta G_{A,S} = \Delta G_{A,R}$). This would lead to decreased enantioselectivity. This concept is illustrated in the free energy diagrams below, adapted from Overbeeke *et al.*[40]

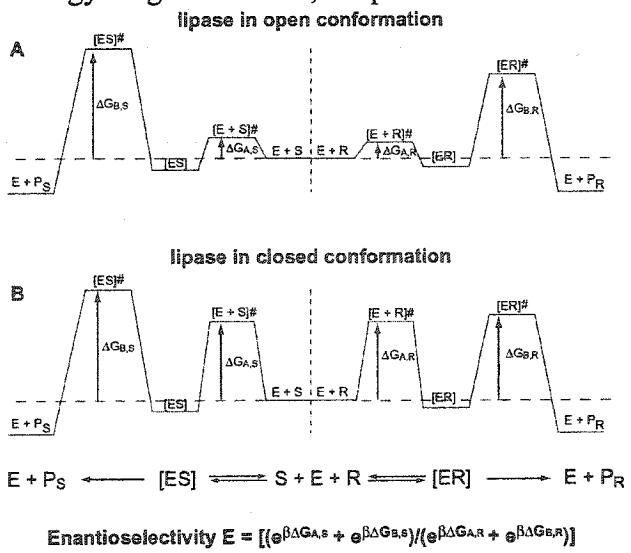

reaction observed without an interface presumably comes from the small equilibrium amount of open form in solution.[35] The presence of an interface has been observed to shift this equilibrium towards the open form and our experiment suggests that this shift amounts at least to a factor of seventy-five or ~ 2.6 kcal/mol. The crystallization conditions for the open form of PCL (30 vol% *n*-propanol) presumably stabilize this form of the enzyme, thus maximising the difference in activation energy for product formation and increasing the enzyme enantioselectivity.

A treatment with 2-propanol was previously found to dramatically increase the enantioselectivity of *Candida rugosa* lipase (CRL).[41] The increased enantioselectivity was attributed to a stabilization of the open form of the lipase as observed for PCL. The case of CRL is slightly different however, since the X-ray crystal structure of the closed form shows that all amino acid residues are already correctly oriented for catalysis. Another possible explanation is that the decrease in enzyme flexibility due to the crystallisation solvent contributes to increasing the enzyme E. This is similar to the increase in enzyme enantioselectivity observed in organic solvents, which is attributed to decreased enzyme flexibility caused by the prevalence of intramolecular electrostatic interactions in the low dielectric constant medium as compared to an aqueous environment.[42,43]

Another important contribution to the enantioselectivity of PCL may arise from the binding of the acyl chain. Weissfloch and Kazlauskas[2] reported E = 16 for the resolution of (±)-**1**-acetate in an ether/water mixture. The fact that PCL exhibited, in all the solvents used, higher enantioselectivity for (±)-**1**-heptanoate (E = 120 in the very similar solvent **B**, E ≥190 in solvent **A** and E = 61 in solvent **C**), shows not only the important role of the solvent, but also of the acyl chain length in determining PCL enantioselectivity.

This is the first time that esters of chiral primary alcohols **1** and **2** have been resolved with high E *via* PCL-catalysed hydrolysis. By maintaining the substrate concentration above its solubility limit to ensure conditions of interfacial activation, and by the accurate choice of solvent and acyl chain length, we increased the enantioselectivity of PCL from 16[2] to ≥190 for the hydrolysis of (±)-**1**-heptanoate and from 17[22] to 70 for the hydrolysis of (±)-**2**-heptanoate. Unfortunately this strategy did not improve the enantioselectivity of PCL towards alcohol **3**. It is clear to us that the

resolution of esters of chiral primary alcohols remains more difficult than the resolution of secondary alcohols, probably due to their greater flexibility. These results show that the enantioselectivity of PCL is highly substrate dependent and each primary alcohol must be evaluated individually to determine the best set of conditions for its resolution.

Acknowledgements

I wish to thank Le Fonds Québécois de la Recherche sur la Nature et les Technologies for two post-graduate fellowships. We also thank the National Sciences and Engineering Research Council of Canada (NSERC) for financial support and Dr. Enikö Forro for her work on the PCL catalysed transesterifications of alcohols **1** and **2** (unpublished results).

References

[1]Bornscheuer, U. T.; Kazlauskas, R. J. *Hydrolases in Organic Synthesis*; Wiley-VCH: Weinheim, Germany, **1999**, pp. 65-106.

[2]Weissfloch, A. N. E.; Kazlauskas, R. J. *J. Org. Chem.* **1995**, *60*, 6959-6969.

[3]Miyazawa, T.; Yukawa, T.; Koshiba, T.; Ueji, S; Yanagihara, R.; Yamada, T. *Biotechnol. Lett.* **2001**, *23*, 1547-1550.

[4]Miyazawa, T.; Yukawa, T.; Ueji, S.; Yanagihare, R. Yamada, T. *Biotechnol. Lett.* **1998**, *20*, 235 - 238.

[5]Nordin, O.; Nguyen, B.-V.; Vörde, C.; Hedenstrom, E.; Högberg, H.-E. *J. Chem. Soc. Perkin Trans. 1* **2000**, 367-376.

[6]Miyazawa, T.; Yukawa, T.; Koshiba, T.; Sakamoto, H.; Ueji, S.; Yanagihara, R.; Yamada, T. *Tetrahedron: Asymmetry* **2001**, *12*, 1595-1602.

[7]Fitzpatrick, P. A.; Klibanov A. M. *J. Am. Chem. Soc.* **1991**, *113*, 3166-3171.

[8]Ducret, A.; Trani, M.; Lortie, R. *Enzyme Microb. Technol.* **1998**, *22*, 212-216.

[9]Carrea, G.; Ottolina, G.; Riva, S. *Trends Biotechnol.* **1995**, *13*, 63-70 (erratum 122).

[10]Wescott, C. R.; Klibanov, A. M. *Biochim. Biophys. Acta* **1994**, *1206*, 1-9.

[11]Goj, O.; Burchardt, A.; Haufe, G. *Tetrahedron: Asymmetry* **1997**, *8*, 399-409.

[12]Cipriani, A.; Bellezza, F. *J. Mol. Cat. B: Enzymatic* **2002**, *17*, 261-266.

[13]Martin, C.; Himmele, W.; Siegel, H. *US Pat. No. 4410734* **1983**.

[14]Delinck, D. L.; Margolin, A. L. *Tetrahedron Lett.* **1990**, *31*, 6797-6798.

[15]Stoermer, D.; Caron, S.; Heathcock, C. H. *J. Org. Chem.* **1996**, *61*, 9115-9125.

[16] Wimmer, Z.; Saman, D.; Francke, W. *Helv. Chim. Acta* **1994**, *77*, 502-508.

[17] Weinstock, L. M.; Mulvey, D. M.; Tull, R. *J. Org. Chem.* **1976**, *41*, 3121-3124.

[18] Ferraboschi, P; Reza-Elahi, S; Verza, E; Santaniello, E.*Tetrahedron: Asymmetry* **1999**, *10*, 2639-2642.

[19] Delinck, D. L.; Margolin, A. L. *Tetrahedron: Lett.* **1990**, *31*, 6797-6798.

[20] Nordin, O.; Nguyen, B.-V.; Vörde, C.; Hedenström, E.; Högberg, H.-E. *J. Chem. Soc., Perkin Trans. 1*, **2000**, 367–376.

[21] Högberg, H.-E.; Berglund, P.; Edlund, H.; Fggerhag, J.; Hedenstrijm, E; Lundh, M; Nordin, O.; Servi, S; Vörde, C. *Catalysis Today*, **1994**, *22*, 591-606.

[22] Tuomi, W. V.; Kazlauskas, R. J. *J. Org. Chem.* **1999**, *64*, 2638-2647.

[23] Geerlof, A.; van Tol, B. A.; Jongejan, J. A.; Duine, J. A. *Biosci. Biotech. Biochem.* **1994**, *58*, 1028-1036.

[24] Sakai T., Kishimoto T., Tanaka Y., Ema T., Utaka M. *Tetrahedron Lett.* **1998**, 39, 7881-7884.

[25] Bosetti A., Bianchi D., Cesti P., Golini P. *Biocatalysis* **1994**, 9, 71-77.

[26]Evans, D. A.; Ennis, M. D.; Mathre, D. J. *J. Am. Chem. Soc.* **1982**, *104*, 1737-1739.

[27]Wu, S.-H.; Lay, S.-Y.; Lin, S.-L.; Chu, F.-Y.; Wang, K.-T. *Chirality* **1991**, *3*, 67-70.

[28]Mezzetti, A; Cheong, C. S.; Malardier-Jugroot, C.; Whitehead, M.A.; Schrag, J. D.; Cygler, M; Kazlauskas, R. J. in preparation.

[29]Brzozowski, A. M.; Derewenda, U.; Derewenda, Z. S.; Dodson, G. G.; Lawson, D. M.; Turkenburg, J. P.; Bjorkling, F.; Huge-Jensen, B.; Patkar, S. A.; Thim, L. *Nature* **1991**, *351*, 491-494.

[30]Derewenda, U.; Brzozowski, A. M.; Lawson, D. M.; Derewenda, Z. S. *Biochemistry* **1992**, *31*, 1532-1541.

[31]Tuomi, W. V.; Kazlauskas, R. J. *J. Org. Chem.* **1999**, *64*, 2638-2647.

[32]Chen, C.-S.; Fujimoto, Y.; Girdaukas, G.; Sih, C. J. *J. Am. Chem. Soc.* **1982**, *104*, 7294-7299.

[33]Lang, D.A.; Mannesse, M. L. M.; de Haas, G. H.; Verheij, H. M.; Dijkstra, B. W. *Eur. J. Biochem.* **1998**, *254*, 333-340.

[34]Luić, M.; Tomić, S.; Leščić, I.; Ljubović, E.; Šepac, D.; Šunjić, V.; Vitale, L.; Saenger, W.; Kojić-Prodić, B. *Eur. J. Biochem.* **2001**, *268*, 3964-3973.

[35]Nigel A. Turner, Eric C. Needs, Jeffrey A. Khan, Evgeny N. Vulfson, *Biotechnol. Bioeng.* **2001**, *72*, 108-118.

[36]Lang, D.; Hofmann, B; Haalck, L; Hecht, H. J.; Spener, F.; Schmid, R. D.; Schomburg, D. *J. Mol. Biol.* **1996**, *259*, 704- 717.

[37]Schrag, J. D.; Li, Y.; Cygler, M.; Lang, D.; Burgdorf, T.; Hecht, H.-J.; Schmid, R.; Schomburg, D.; Rydel, T. J.; Oliver, J. D.; Strickland, L. C.; Dunaway, C. M.; Larson, S. B.; Day, J.; McPherson, A. *Structure* **1997**, *5*, 187-202.

[38]Kim, K. K.; Song, H. K.; Shin, D. H.; Hwang, K. Y.; Suh, S. W. *Structure* **1997**, 5, 173-185

[39]Van Tol, J. B. A.; Jongejan, J. A.; Duine, J. A. *Biocatal. Biotransform.* **1995**, *12*, 99-118.

[40]Overbeeke, P. L. A.; Govardhan, C.; Khalaf, N.; Jongejan, J. A.; Heijnen, J. J. *J. Mol. Cat. B: Enzymatic* **2000**, *10*, 385-393.

[41]Colton, I. J.; Ahmed, S. N.; Kazlauskas, R. J. *J. Org. Chem.* **1995**, *60*, 212-217.

[42]Affleck, R.; Haynes, C. A.; Clark, D. S. *Proc. Natl. Acad. Sci. U.S.A.* **1985**, *82*, 5167-5170.

[43]Klibanov, A. *Trends Biotechnol.* **1997**, *15*, 97-101.

Chapter 5

In the previous chapters we identified the molecular basis of PCL enantioselectivity towards primary alcohols. In this chapter we attempt to increase the enantioselectivity of a lipase structurally related to PCL, *Bacillus thermocatenulatus* lipase 2 (BTL2), towards primary alcohols. BTL2 is moderately enantioselective towards solketal-*n*-octanoate; solketal-*n*-heptanoate was used in Chapter 3 for our X-ray crystallography studies.

Contributors

This work was done under the supervision of Prof. Romas J. Kazlauskas and Prof. Karl Hult and in collaboration with Dr. Johanna C. Rotticci-Mulder and Miss Agneta Eriksson. Dr. Rotticci-Mulder helped design the histidine tag of the BTL2 gene and helped optimise the production of BTL2. Miss Eriksson was a Swedish diploma student (analogous to Masters student) that, under my supervision, screened BTL2 mutants towards three substrates. Prof. Romas J. Kazlauskas performed the PCL-BTL2 alignment that I used for generating the first homology modelled structure of BTL2. I carried out all the experiments for his-tagging the BTL2 gene and for the optimisation of the lipase production. I chose the positions to be mutated and I performed the saturation mutagenesis, screened the mutants libraries towards solketal-*n*-octanoate and the double mutants towards solketal-*n*-octanoate and two other substrates that I synthesised.

Attempt to increase the enantioselectivity of *Bacillus thermocatenulatus* lipase 2 (BTL2) towards primary alcohols by structure-guided saturation mutagenesis.

Abstract

To generalise our findings on the molecular basis of enantioselectivity towards primary alcohols to lipases other than *Pseudomonas cepacia* lipase (PCL), *Bacillus thermocatenulatus* lipase 2 (BTL2) was chosen to attempt to increase its enantioselectivity towards solketal-*n*-octanoate by structure-guided saturation mutagenesis. BTL2 shows moderate enantioselectivity towards solketal-*n*-octanoate (E = 4.5). The conditions for protein extraction from the periplasmic space of *E. coli* were first optimised and the BTL2 gene was engineered introducing a His_8-tag to purify the protein by metal affinity chromatography. Then, from an alignment between BTL2 and PCL, a homology-modelled structure of BTL2 was obtained. Last, by comparing this structure with the one of the complex PCL-solketal inhibitor (Chapter 3) five residues within the catalytic pocket of BTL2 were chosen and saturation mutagenesis experiments were performed. Four libraries of mutants, at positions G15, Y29, H112 and the double mutants at position F16-T17 were obtained. The screen of the mutant libraries towards solketal-*n*-octanoate and a few other chiral primary alcohols for increased enantioselectivity did not identify any improved variant. Instead, several inactive enzymes were generated by mutating residues probably too close to the catalytic machinery of BTL2. The mutants that retained a certain activity towards the primary alcohols screened were often found to be wild type enzyme.

Introduction

Most enzymes for biotransformations come from mesophiles and are limited to the "usual" temperatures, pressures, pHs and solvents. On the other hand extremozymes, enzymes from extremophilic organisms, possess higher stability to "unusual" reaction conditions, making their use as biocatalysts very appealing. Extremophiles inhabit the harshest conditions on earth, with temperatures ranging from – 50 °C to + 113 °C, pressures that can reach 120 MPa and pH values as low as 0.5 and as high as 12.0.

Although the majority of extremophiles belongs to the Archaea kingdom (previously Archeabacteria)[1], bacteria, especially some *Bacillus* species, also produce a few.

Bacillus thermocatenulatus lipase

Bacillus thermocatenulatus is a thermoalkalophilic organism that produces a 16 kDa (BTL1) and a 43 kDa lipase (BTL2). R.D. Schmid and his collaborators[2,3] screened an expression library for the smaller lipase. Subsequent analyses showed that the isolated lipase, found at the DNA level, was not BTL1 but a new lipase, with a molecular weight of 43 kDa, BTL2, which had not been detected in the culture broth of *Bacillus thermocatenulatus*.

BTL2 differs from BTL1 by its larger size and higher stability to organic solvents, high pH and temperature (T)[4,5] (Table 1). BTL2 also showed higher specific activity than BTL1. BTL2 was stable at temperatures up to 75 °C and to pH up to 11, therefore being a thermoalkalophilic enzyme. Stability to organic solvents was also observed. The characteristics of BTL2 are different from the ones of the most common lipases from *Bacillus* strains. Those lipases are smaller in size, having a molecular weight similar to BTL1, they have a lower specific activity towards tributyrin and show a maximum activity at a lower pH than BTL2, usually in the range of 6 to 8.

Table 1 – Comparison of BTL1 and BTL2[4,5]

Properties	BTL1	BTL2
molecular weight (Da)	16000	43000
T_{opt} (°C)[a]	60 - 70	60 - 70
T_{stab} (°C)[b]	40	50
pH_{opt}[c]	7 - 8	8 - 9
pH_{stab}[d]	7 - 8	9 - 11
organic solvent stability	moderate	high
specific activity[e]	29	1300

[a]Temperature corresponding to optimal enzyme performance; [b]temperature stability after 30 min incubation the lipase; [c]pH range at which the lipase shows the best activity; [d]pH stability; [e]specific activity towards *p*-nitrophenyl palmitate (PNPP) in U/min*mg protein (U = µmol of PNPP hydrolysed).

The initial BTL2 expression system used a natural promoter, which gave low expression levels of the BTL2 lipase. To increase expression, Schmid and co-workers placed the gene into plasmid pCYTEXP1,[6] which contains the temperature inducible bacteriophage λ promoters P_R and P_L and the thermo-labile λ repressor *cIts*857, which regulates the promoters P_R and P_L by preventing transcription at temperatures below 42°C. The vector also contains the OmpA signal sequence for secretion of the lipase in the periplasmic space of *E. coli*, the *aptE* translational initiation region (TIR) and the bacteriophage fd transcriptional terminator. Also, an f1-ORI origin of replication sequence, derived from vector pUC-f1 (Pharmacia LKB Biotechnology, Sweden) is present (Scheme 1). With this expression system lipase production by *E. coli* was enhanced, especially when expressed in *E. coli* strain JM105 (from 600 to 600,000 U/g of cells).[3,7]

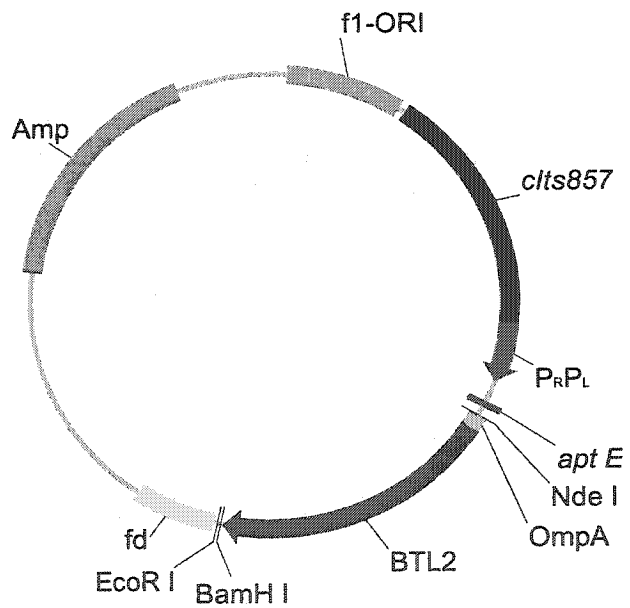

Scheme 1 - pCYTEXP1-OmpABTL2 (pCOB) map.

BTL2 stability to organic solvents, high pH and temperatures make it a potentially good and robust biocatalyst for organic synthesis. BTL2 shows high enantioselectivity (E > 100), although low reaction rates, towards the secondary alcohol 1-phenylethanol both in the hydrolysis of its acetate and in the transesterification with vinyl acetate and butyrate.[8] In previous screenings by the Quick E method BTL2 showed low to moderate

enantioselectivity towards five chiral primary alcohols[8] (Figure 1). The enantioselectivity towards solketal butyrate was determined by Quick E to be 7.9 favouring the (*R*) enantiomer, the one towards solketal octanoate 4.9 again favouring the (*R*) enantiomer. The latter was confirmed by scale up measurements to be 4.4 ± 0.4.[8] BTL2 shows very low enantioselectivity towards 2-methylglycidyl-4-nitrobenzoate (estimated E = 1.2[8]) and is moderately enantioselective towards glycidyl 4-nitrobenzoate (estimated E = 5.2[8]), while later Quick E measurements showed that BTL2 has E = 3.9 towards glycidyl butyrate.[9]

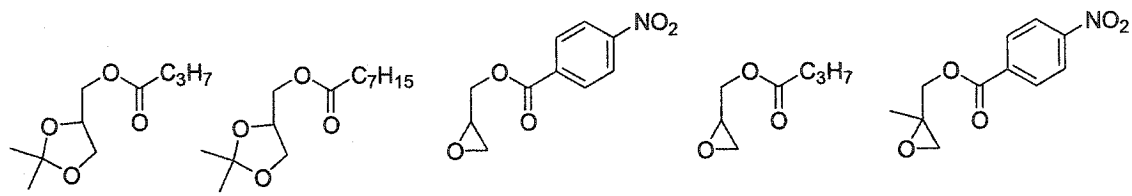

Figure 1 – Primary alcohols screened by Liu *et al.*[8]

Only a few lipases show high enantioselectivity towards chiral primary alcohols.[10] The thermoalkalophilicity of BTL2 and its ability to hydrolyse chiral primary alcohols with moderate E make it a good candidate for protein engineering to increase its enantioselectivity towards esters of chiral primary alcohols.

Solketal

2,2-dimethyl-[1,3]-dioxolane-4-methanol or solketal, was synthesised as a racemate for the first time by Emil Fisher in the late 1800s *via* coupling of glycerol with acetone in the presence of zinc chloride.[11] Its pure enantiomers are important chiral synthons. For example, they have been used as building blocks in the synthesis of the β-adrenergic blocker timolol[12] and the macrolide antibiotic brefeldin A, a specific inhibitor of exocytosis[13].

Several methods yield pure enantiomers of solketal. (*S*)-solketal was prepared by cleavage of *D*-mannitol[14] or ascorbic acid[15]. (*R*)-solketal was first made from unnatural *L*-mannitol.[16] (*R*)-solketal was also synthesised in six steps and 7% yield from its enantiomer[17] and in four steps with higher yield from *L*-serine.[18] Other methods are

described in Jurczak *et al.*[19] The disadvantages of these methods are the several steps involved in the synthesis and the low yield. Also, if both enantiomers of solketal are needed, two separate syntheses need to be carried out.

Noteworthy is the effort, in the past 15 years, to resolve racemic solketal using enzymes (Table 2), which yields both enantiomers. The best results were the highly enantioselective oxidation (E >100) of solketal to solketalic acid by two alcohol dehydrogenases.[20] The dehydrogenases favoured opposite enantiomers, thus being able to produce enantiomerically pure (*R*) or (*S*)-solketal without the need of reducing solketalic acid. Good enantioselectivities were also obtained by lipase-catalysed acylation of solketal (E = 23 - 55, Table 2, ref. 21,22,23,24). However, very poor enantioselectivity has been obtained in hydrolysis reactions of different esters of solketal catalysed by both lipases and proteinases (E = 3 - 9, Table 2, ref. 25,26,27).

Table 2 – Reported enzymatic resolution of solketal. Results from selected publications.

Biocatalyst[a]	**Reaction**	**E**[b]
QH-EDH (type I)[20]	oxidation of solketal to solketalic acid	> 100 (*R*)
PEG-DH [20]	oxidation of solketal to solketalic acid	> 100 (*S*)
Lipase AK[21]	acylation of solketal with butyric anhydride at 4 °C	24 to 29 (*S*)
Lipase AK[22]	acylation of solketal with vinyl butyrate at -40 °C	55 (*S*)
RDL[23]	acylation with vinyl butanoate	23 (*S*)
PPL[24]	acylation with vinyl valerate	42 (*S*)
PPL[25]	hydrolysis of solketal decanoate	3.0 (*R*)
PCL[26]	hydrolysis of solketal benzoate	3.7 to 9 (*R*)
AOP[27]	hydrolysis of solketal butanoate	7.2 to 9.0 (*R*)

[a] QH-EDH = Quinohaemoprotein alcohol dehydrogenase from *Comamonas testosteroni*; PEG-DH = Polyethylene alcohol dehydrogenase from *Flavobacterium* sp. Strain 203; RDL = *Rhizopus delmar* lipase; PPL = Porcine pancreatic lipase; AOP = Proteinase from *Aspergillus oryzae*. [b] Either retrieved from the publication or calculated from the reported ee_p%, ee_s% and c% according to Chen *et al.*[28]

Despite the exceptionally high enantioselectivity shown by alcohol dehydrogenases in the resolution of solketal[20] and the high enantioselectivity of lipase AK in the acylation of solketal at -40 °C, to date there is no available biocatalyst capable of hydrolysing esters

of solketal with high enantioselectivity. Such biocatalyst would expand the range of methods available for the enzymatic resolution of solketal.

One strategy to improve enzymes for biocatalysis is protein engineering. As shown in Chapter 1, rational protein design by site-directed mutagenesis requires detailed information of the structure and mechanism of the enzyme property to be improved so as to choose both the sites from mutations and the kind of amino acids to use to replace the natural ones. One of the advantages of this method is the very limited screening involved. However the major disadvantages are the sometimes unpredictable structural changes brought about by the point mutations introduced.

Directed evolution, the cyclical generation of large libraries of random mutants and their screening for an improved variant, is an alternative to site-directed mutagenesis that does not require structural or mechanistic information. Its greatest disadvantage is the extremely large number of mutants that needs to be screened.[i,29] Reetz *et al.*[30] screened 40,000 *Pseudomonas aeruginosa* lipase (PAL) mutants to find a mutant with E = 55 towards nitrophenyl 2-methyldecanoate (wild-type E = 1.1).

Hybrid approaches consist in the selection of residues to be mutated by site-directed mutagenesis and in the use of directed evolution to fix problems caused by the mutations or to further improve the new properties.[31]

Here a different approach was chosen. The substrate-binding region of BTL2 was identified and libraries of mutants were generated by structure-guided saturation mutagenesis of residues that may be involved in enantiorecognition. BTL2, whose X-ray or NMR structure are not yet available, shares low sequence identity with PCL (17%). A homology model[32] of BTL2 was built and overlapped to the X-ray crystal structure of the complex PCL-inhibitor containing solketal as alcohol moiety.[33] A few residues were selected within the catalytic pocket of BTL2 and, *via* saturation mutagenesis, libraries of mutants at positions G15, Y29, H112 and F16-T17 were prepared. It has been shown in Chapter 3 and in the related Appendix 1 that PCL distinguishes between the two enantiomers of solketal by a number of small interactions between the alcohol and a few

---

[i] The number of possible mutants P is given by: P = (19M*n!)/((n-M)!*M! where M is the number of amino acid substitutions and n is the number of amino acids in the protein.

residues within the catalytic pocket. Among those residues there are L17 and T18, corresponding to F16 and T17 of BTL2, Y29 and H86, corresponding to BTL2 Y29 and H112. Residue G15 of BTL2, corresponding to G15 of PCL, is situated just before the oxyanion hole residue F16. Changing it to a different amino acid could change the shape of the oxyanion hole, possibly in the desired direction. Screening these mutants towards solketal-*n*-octanoate and a few other chiral primary alcohols did not uncover improved variants. Several of the residues that seem to be involved in the enantiorecognition of primary alcohols are conserved among lipases and are often very close to the catalytic machinery. Their mutation generated several inactive variants and the few enzymes still capable of hydrolysing the substrates chosen were either wild-type or less enantioselective variants (i.e. Y29S, E = 1.8 and F16G-T17V, E = 3.4 towards solketal-*n*-octanoate). Even the screen of the double mutants library, which showed the highest number of active mutants towards the primary alcohols screened, did not identify any improved enzyme.

Materials and Methods

All chemicals were purchased from Sigma-Aldrich Co. (Oakville, ON) unless otherwise specified. ^{1}H NMR spectra were collected at 270 MHz and ^{13}C NMR at 68 MHz. LB (Luria Bertani) media and agarose were obtained from Difco Laboratories (Detroit, MI). The primers for his-tagging the BTL2 gene were purchased from Interactiva (Thermo Hybaid, Thermo BioSciences GmbH, Germany). Degenerate primers and sequencing primers were from the Sheldon Biotechnology Centre (McGill University, Montreal, QC). Restriction endonucleases were from New England Biolabs Ltd (Pickering, ON). Plasmid isolation and gel extraction kits were from Qiagen Inc. (Mississauga, ON). Sequencing of wild type and his-tagged BTL2 gene was done at KTH Department of Biotechnology (Stockholm, Sweden). Sequencing of mutants was done either at the Sheldon Biotechnology Centre (McGill University, Montreal, Canada) or at DNA Landmarks (St-Jean-sur-Richelieu, QC, Canada) by the dideoxy termination method. Saturation mutagenesis kits were purchased from Stratagene (La Jolla, CA). 2,3-Epoxypropyl 4-nitrobenzoate and glycidyl butyrate were from Sigma-Aldrich Co. (Oakville, ON). Figures containing protein structures were made either with VMD 1.8[34] or with Swiss PdbViewer v. 3.7.[35]

Homology modelling.

The PCL-BTL2 alignment of Scheme 3 was submitted to "Swiss Model-Optimise Model"[36] to obtain the first homology modelled structure. This structure was imperfect due to the presence of several gaps and to the incorrect position of catalytic Asp317. A better model, based on 95% identity of BTL2 with *Bacillus stearothermophylus* lipase (Tlip), was obtained at a later date by submitting to Swiss-Model[37] only the amino acid sequence of BTL2.

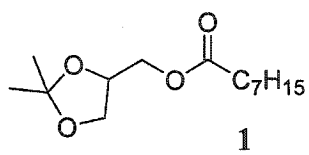

1

(R) and (S) solketal octanoate, 1.

Were synthesized according to Liu *et al.*[8] Yield 70% (clear oil). R_f, ^{1}H NMR and MS agreed with Liu *et al.*[8]

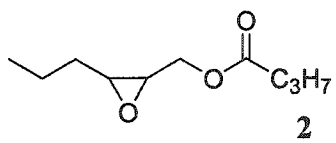

2

(2*R*, 3*R*) and (2*S*, 3*S*) 3-propyloxiranylmethyl butanoate, 2.

Butyric anhydride (1 equiv.), 4-dimethylaminopyridine (0.05 equiv.) and triethylamine (1.5 equiv.) were added to a solution of either (2*R*,3*R*)-(+)-3-propyloxiranemethanol or (2*S*,3*S*)-(-)-3-propyloxiranemethanol (1 equiv.) in methylene chloride and stirred at room temperature until all the alcohol was consumed. The solvent was evaporated under vacuum and the residue was dissolved in diethyl ether. The solution was washed with water, saturated sodium bicarbonate and brine, then dried over magnesium sulfate. The solvent was evaporated under vacuum and the residue purified by silica gel chromatography. After evaporation of the solvent (2*R*,3*R*)-**2** and (2*S*,3*S*)-**2** were obtained as yellow oil. Yield: 62-71%. R_f = 0.81 (silica gel, 7:3 hexane:ethyl acetate); ^{1}H NMR ($CDCl_3$) δ 4.30 (dd, 1H, CH_2, J_1 = 3.2 Hz, J_2 = 12.1 Hz), 3.90 (dd, 1H, CH_2, J_1 = 6.2 Hz, J_2 = 12.1 Hz), 2.93-2.88 (m, 1H, CH), 2.81-2.77 (m, 1H, CH), 2.27 (t, 2H, CH_2, J = 7.4

Hz), 1.66-1.35 (m, 6H, $3CH_2$), 0.90 (t, 6H, $2CH_3$, $J = 7.3$ Hz); ^{13}C NMR ($CDCl_3$) δ 173.4, 64.5, 56.5, 55.3, 36.0, 33.6, 19.2, 18.4, 13.8, 13.7; MS (CI, NH_3) *m/z* (rel. intensity) 187 (38.0, M + H^+), 169 (12.5, M^+ - CH_3), 144 (3.0, M^+ - C_3H_7), 71 (>100, M^+ -(3-propyl-oxiranyl)-methanol), 43 (57.0, M^+ - C_3H_7 - $C_3H_7CO_2$).

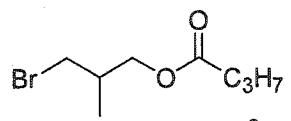

3

(R) and (S)-3-bromo-2-methyl-1-propyl butanoate, 3.

The reaction was performed as for **2**, using 3-bromo-2-methyl-1-propanol as alcohol. Yield (yellow oil): 60-61%. R_f = 0.63 (silica gel, 7:3 hexane-ethyl acetate); ^1H NMR ($CDCl_3$) δ 4.09-3.95 (m, 2H, CH_2), 3.40 (m, 2H, CH_2), 2.28 (t, 2H, CH_2, $J = 7.4$ Hz), 2.21- 2.09 (m, 1H, CH), 1.70-1.57 (m, 2H, CH_2), 1.04 (d, 3H, CH_3, $J = 6.9$ Hz), 0.93 (t, 3H, CH_3, $J = 7.4$ Hz); ^{13}C NMR ($CDCl_3$) δ 173.5, 66.3, 36.8, 36.2, 34.7, 18.5, 15.8, 13.7; MS (CI, NH_3) *m/z* (rel. intensity) 242 and 244 (7.3, M + NH_3), 223 and 225 (6.5, M + H^+), 143 (16.7, M^+ – Br), 71 (100, M^+- (3-bromo-2-methyl-1-propanol).

BTL2 his-tagging.

1. Amplification of OmpA-BTL2 gene with His_8 containing primer.

Plasmid pCOB (pCYTEXP1-OmpA-BTL2[3])(2 ng) was mixed with 30 pM dNTPs, 20 pmol of each primer (Table 3), DNA polymerase reaction buffer and sterile water to a 50 μL final volume. *Taq* DNA polymerase (1 U) was added to the mixture. The tube was placed into a thermal cycler programmed with the parameters listed in Table 4.

Table 3 – Primers for his-tagging the BTL2 gene.

Primer	Sequence	T_m (°C)
fBTL2pcrAM	5'-GGCGAATTCCATATGAAAAAGACA GCTATCGCG-3'	67
rBTL2His8pcrAM	5'-CGAATTCTCAATGATGATGATGATG ATGATGATGAGGCCGCAAACTCGCC-3'	83

Table 4 – Program used for the amplification of BTL2 gene.

Temperature (°C)	Time (min)	Cycles
95	5	1
95	0.5	
50	0.5	7
72	1.5	
95	0.5	
60	0.3	15
72	1.5	
72	7	1
4	infinity	1

2. Restriction of pCOB to pC and OmpA-BTL2-His_8 gene to OBH.

To pCOB (2 μg) or OmpA-BTL2-His_8 (OBH, his-tagged BTL2 gene from the amplification above) (2 μg) 2 units of each *Nde I* and *EcoR I* were added. Appropriate volumes of water and buffer 4 (sold with the endonucleases) were also added, to a final volume of 50 μL. The reaction mixture was placed at 37 °C for 3 hours, then alkaline phosphatase (1 unit) was added to the pCOB mixture. The samples were kept another hour at 37 °C, and then the temperature was raised to 85 °C for 30 min. Desired DNA fragments (linear pC vector and OBH) were isolated and purified by gel electrophoresis using Quiagen Inc. kit QIAEX II.

3. Ligation of pC and OBH fragments and reconstruction of the plasmid (pCOBH).

To every 20 ng of linear pC vector, 60 ng of OBH fragment and 2 units of T4 along with T4 DNA ligase reaction buffer and water were added (total volume 20 μL). The vial was incubated at 15 °C for 15 hours, then brought to 65 °C for 10 min.

The ligated pCOBH was purified by phenol-chloroform extraction and transformed in competent *E. coli* cells by electroporation according to BioRad Laboratories (Mississauga, ON) standard protocol.

General procedure to prepare cell lysate using lysozyme.[38]

A bacterial culture containing the plasmid (1 mL) was incubated in the shaker overnight at 37 °C and 200 rpm until an $OD_{600nm} = 1$ was reached. The temperature was increased to 42 °C to induce BTL2 expression. After 3 hours the bacterial culture was centrifuged

(3829 g, 4 °C, 20 minutes) and the exhausted LB broth was decanted. The cell pellet was washed with BES buffer (5 mM, pH 7.20). It was re-suspended to a final volume of 110 μL of 5 mM BES. Lysozyme solution (20 μL, 10 mg/mL in 5 mM BES, 3 mM EDTA, pH 7.20) was added to lyse the cell membrane. Incubation at 37 °C for three hours ensured complete lysis of the cell membrane. The tube was then frozen at –20 °C and thawed to aid the release of the protein. The cell debris was removed by centrifugation (3829 g, 4°C, 30 min) and the supernatant was kept as the enzyme solution.

General procedure to prepare cell lysate using osmotic shock (adapted from ref. 39). A bacterial culture (1 mL) was incubated in the shaker overnight at 37 °C and 200 rpm until an OD_{600nm} = 1 was reached. The temperature was increased to 42 °C to induce BTL2 expression. After 3 hours the flask was removed from the incubator and placed on ice. The bacterial culture was centrifuged (10 min, 3829 g, 4 °C), the supernatant removed and the cell pellets suspended in ice-cold osmotic shock solution (0.25 mL of 200 g/L saccharose and 1 mM EDTA in 0.3 M Tris-HCl pH 8). The suspension was incubated at room temperature for 10 minutes, centrifuged (10 min, 3829 g, 4 °C), the supernatant was discarded and the pellets suspended in ice-cold doubly distilled water (0.1 mL) and incubated at 4 °C for 10 min. The suspension was centrifuged (15 min, 3829 g, 4 °C) and the supernatant containing the protein transferred to a clean test tube.

His_8-BTL2 purification.

His_8-BTL2 protein was produced from a 200 mL bacterial culture and extracted according to the osmotic shock procedure. The protein extract was concentrated 20-fold using a Microcon YM-30® ultrafiltration membrane (Millipore Corp., Nepean, ON). The concentrated protein was recovered from the ultrafiltration membrane with 1 mL of extraction buffer (50 mM sodium phosphate buffer pH 7 containing 300 mM NaCl). A Ni-NTA column was prepared by applying Ni-NTA agarose slurry (Qiagen Inc., Mississauga, ON) to a Poly-Prep column (BioRad Laboratories, Mississauga, ON). The column was washed repeatedly with wash buffer (50 mM sodium phosphate pH 7 containing 300 mM NaCl and 5 mM imidazole), and then equilibrated with extraction buffer. The protein sample was applied to the column. The column was washed with 15 volumes of "wash buffer". The His-tagged protein was eluted by adding 1 mL of "elution

buffer" (45 mM sodium phosphate pH 7 containing 300 mM NaCl and 150 mM imidazole) to the column, incubation for 2 minutes before elution and repeating this last two steps for 5 times. The collected fractions were analysed by UV/Vis at 280 nm for identifying the samples containing the purified protein. Some fractions were also analysed by SDS-PAGE and compared to the crude extract (see Results).

Saturation mutagenesis.

pCOBH served as a template for the polymerase present in the QuickChange® Site-Directed Mutagenesis Kit,[40] which was used according to manufacturer's instructions with complementary degenerate primers[ii] listed in Table 5.

Table 5 – List of complementary primers used for the saturation mutagenesis experiments.

Position	Primer	Sequence	Length
G15	dirG15X	5'-CCCATCGTGCTTCTCCATNN NTTTACAGGATGGGGGCGAG-3'	40
	revG15X	5'-CTCGCCCCCATCCTGTAAANN NATGGAGAAGCACGATGGG-3'	40
Y29	dirY29X	5'-GGATTCAAANNNTGGGGCGGC-3'	21
	revY29X	5'-GCCGCCCCANNNTTTGAATCC-3'	21
H112	dirH112X	5'-CGCGTCCATATCATCGCT NNNAGCCAAGGACAGACG-3'	39
	revH112X	5'-CGTCTGTCCTCCTTGGCTNN NAGCGATGATATGGACGCG-3'	39
F16T17	dirF16XT17X	5'-CGTGCTTCTCCATGGGNNK NNKGGATGGGGGCGAGAGG-3'	38
	revF16XT17X	5'-CCTCTCGCCCCCATCCMNN MNNCCCATGGAGAAGCACG-3'	38

BTL2 expression in 96-wells assay blocks.

[ii] A degenerate primer is a mixture of 32 or 64 primers, each being a permutation of the degenerate codon NNK (complementary: MNN) or NNN respectively, where N stands for a mixture of all four nucleotides, K is a mixture of G (guanosine) and T (thymidine) based nucleotides, M is a mixture of C (cytidine) and A (adenosine) based nucleotides.

Overnight culture or stock cultures (10 μL) were added to each well in 96-wells assay blocks (2 mL, Costar #3960), followed by the addition of 1.2 mL of LB broth containing 100μg/mL of ampicillin. The assay block, sealed with Thermowell sealer (Costar #6570), were incubated at 37 °C and 325 rpm for about 3 h, until an approximate OD_{600} of 1 was reached. Protein expression was induced by increasing the temperature to 42°C. After 3 hours the assay blocks were removed from the incubator and placed on ice. The cells were then centrifuged (10 min, 3829 g, 4 °C), the supernatant removed and the cell pellets suspended in ice-cold osmotic shock solution (0.3 mL of 200 g/L saccharose and 1 mM EDTA in 0.3 M Tris-HCl pH 8). The plates were incubated at room temperature for 10 minutes, centrifuged (10 min, 3829 g, 4 °C), the supernatant was discarded, the pellets suspended in 0.12 mL ice-cold doubly distilled water and incubated at 4 °C for 10 min. The plates were centrifuged (15 min, 3829 g, 4 °C) and the supernatant containing the protein transferred to another 96-wells assay block and stored at 4°C.

Screening towards p-nitrophenyl acetate (PNPA).

Assay solutions were prepared by mixing PNPA (50 μL of a 200 mM solution in acetonitrile), BES buffer (1850 μL of 5.0 mM, pH 7.2) and acetonitrile (ACN, 100 μL) for a total volume of 2 mL. Enzyme solutions (5 μL/well) were transferred from the 96-wells assay block to a 96-wells microplate using an eight-channel automatic pipette. Assay solution (95 μL/well) was added to each well using a eight-channel automatic pipette. The total volume in each well was 100μL and the concentrations were: [BES] = 4.4 mM, [PNPA] = 4.8 mM; [ACN] = 7 vol%. The plate was placed in the microplate reader and the increase in absorbance at 404 nm was monitored at 25°C.

Quick E screening.

The screening of enzyme libraries prepared by osmotic shock was carried out according to Janes *et al.*[41] using resorufin acetate as reference compound. The wells contained the following concentrations: [BES] = 4.4 mM, [PNP] = 0.4 mM; [ACN] = 7 vol%, [resorufin acetate] = 0.04 mM, [substrate] = 1.0 mM, Triton X-100 0.3 mM.

Scale-up reactions.

Were performed as in Liu *et al.*[8] using purified enzymes.

Results

Optimisation of lipase extraction from E. coli

Initial experiments, described below, show that the osmotic shock method to extract the proteins is simpler and faster than the lysozyme method. Furthermore, it can be applied to the production of large libraries of proteins and the protein extracts are purer thus better suited for screening.

To produce the BTL2 lipase, *E. coli* strain JM105 transformed with pCOB was grown as previously described.[2,4,5,7] At the same time a control experiment was run by growing *E. coli* JM105 not containing any plasmid. Samples of both cultures were collected at different time intervals and the protein was extracted from the bacteria using two different methods: osmotic shock and lysozyme cell breakage.

The BTL2 lipase is transported in the periplasmic space of the bacteria due to the OmpA signal sequence, hence the osmotic shock method represents an alternate cell lysis protocol. The method is based on the treatment of the bacterial cells with hypertonic solutions containing EDTA salts. This changes the permeability of the bacteria outer membrane. Subsequent incubation with a hypotonic solution, even just cold water, causes the lysis of the outer cell wall and the release of components from the periplasmic space,[42] leaving the cytoplasmic membrane intact. This prevents contamination by proteins from the cytoplasm.

The lysozyme method[43] is based on the ability of this small enzyme to break the carbohydrate chains that constitute the bacterium cell membrane. This destroys the structural integrity of the cell wall and the bacterium bursts because of its own internal pressure. Protein samples obtained using this method contain every protein present in both cytoplasm and periplasm of the bacteria.

The activity of each protein fraction towards *p*-nitrophenyl acetate (PNPA) was determined and the test revealed that the protein produced with the osmotic shock method was as active as the one produced by the lysozyme method (Figure 2). The protein before 260 min, which is before the heat shock induction of BTL2 protein expression, shows no activity towards PNPA. This indicates that the repressor gene *cIts*857 functions properly and the promoters P_R and P_L are activated only when a heat-shock at 42°C is produced (Figure 2). The bacteria pellets discarded after protein extraction either by osmotic shock

or lysozyme and the controls, represented by *E. coli* JM105 not containing the plasmid coding for BTL2, do not contain any protein that shows significant activity towards PNPA (Figure 2).

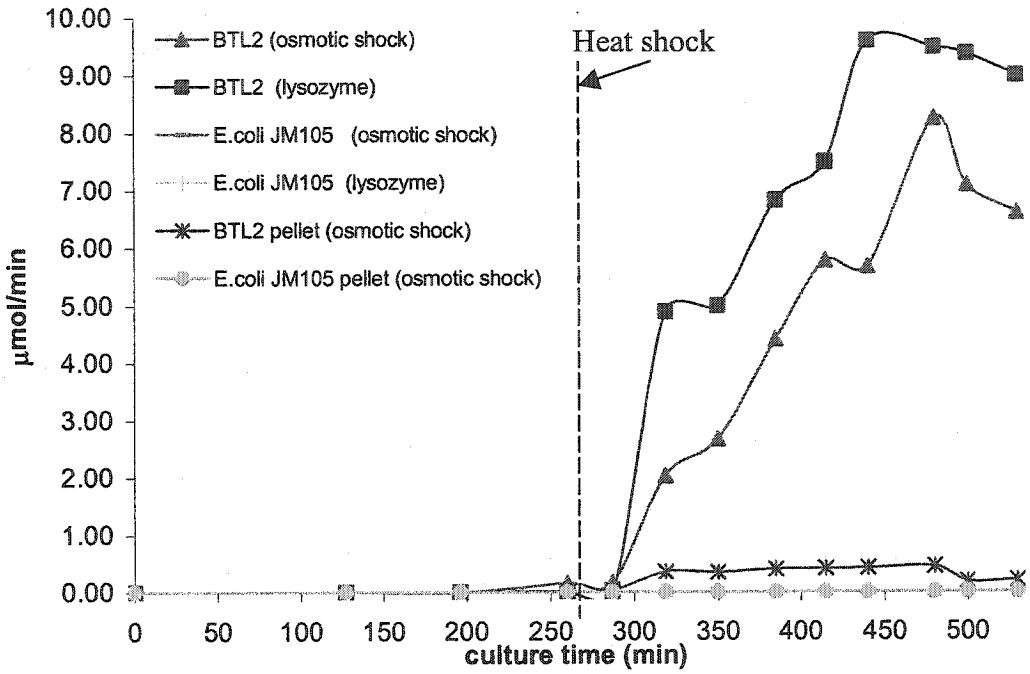

Figure 2 – Comparison of the hydrolytic activity of BTL2 produced from the transformed *E. coli* JM105 and extracted with the osmotic shock method, the BTL2 extracted with the lysozyme method, the extracts from *E. coli* JM105 and the cellular pellets remaining after the osmotic shock procedure. Heat shock was induced at 260 minutes.

An SDS-PAGE (Sodium Dodecyl Sulfate PolyAcrylamide Gel Electrophoresis) analysis of the protein extracts from samples prepared by either lysozyme or osmotic shock indicates a much purer protein extract in the latter case (lanes 3 and 4 versus lanes 9 and 10 in Figure 3). In the protein extracted from the peripasmic space by osmotic shock there are only two major components, one of which is due to *E. coli* itself (see control, lane 6 and 7 in Figure 3).

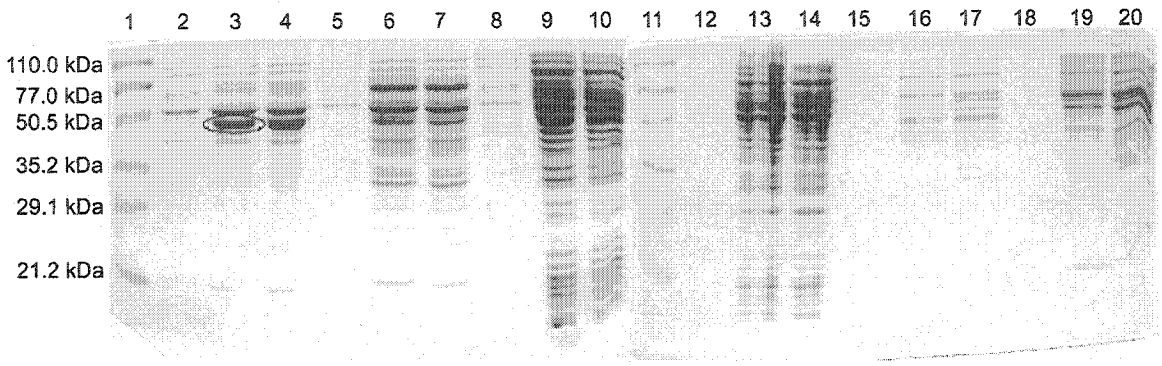

Figure 3 – SDS-PAGE of the protein extracts (control, lysozyme and osmotic lysis) of the samples collected during the protein expression in *E. coli* JM105. Lane 1: molecular weight marker; lane 2: BTL2 by osmotic shock at 196 min (heat shock was at 260 minutes); lane 3: BTL2 by osmotic shock at 480 min, the red oval indicates BTL2; lane 4: BTL2 by osmotic shock at 530 min; lane 5: *E. coli* (control) by osmotic shock at 196 min; lane 6: *E. coli* (control) by osmotic shock at 480 min; lane 7: *E. coli* (control) by osmotic shock at 530 min; lane 8: BTL2 by lysozyme method at 196 min; lane 9: BTL2 by lysozyme method at 480 min; lane 10: BTL2 by lysozyme method at 530 min; lane 11: molecular weight marker; lane 12: *E. coli* (control) by lysozyme method at 196 min; lane 13: *E. coli* (control) by lysozyme method at 480 min; lane 14: *E. coli* (control) by lysozyme method at 530 min; lane 15: BTL2 pellet after osmotic shock at 196 min; lane 16: BTL2 pellet after osmotic shock at 480 min; lane 17: BTL2 pellet after osmotic shock at 530 min; lane 18: *E. coli* (control) pellet after osmotic shock at 196 min; lane 19: *E. coli* (control) pellet after osmotic shock at 480 min; lane 20: *E. coli* (control) pellet after osmotic shock at 530 min.

Because of the simplicity and brevity of the osmotic shock method compared to the lysozyme one (see Materials and Methods), the cleaner protein obtained and the possibility of applying this method to the production of libraries of mutant proteins, all subsequent lyses used this procedure.

His tagging and purification of BTL2

The BTL2 gene was engineered with a His-tag to facilitate large-scale protein purification for carrying out scale-up reactions. Proteins that carry six to eight consecutive histidines at either the C or N terminus can be easily purified by metal affinity chromatography, also known as immobilisation affinity chromatography (IMAC)[44]. Eight histidines (His_8-tag) were introduced at the C terminus of BTL2, exploiting the presence of two cloning sites at the 3' end of the gene (*BamH I* and *EcoR*

I), before the bacteriophage fd transcriptional terminator (Scheme 1). We proceeded as shown in Scheme 2.

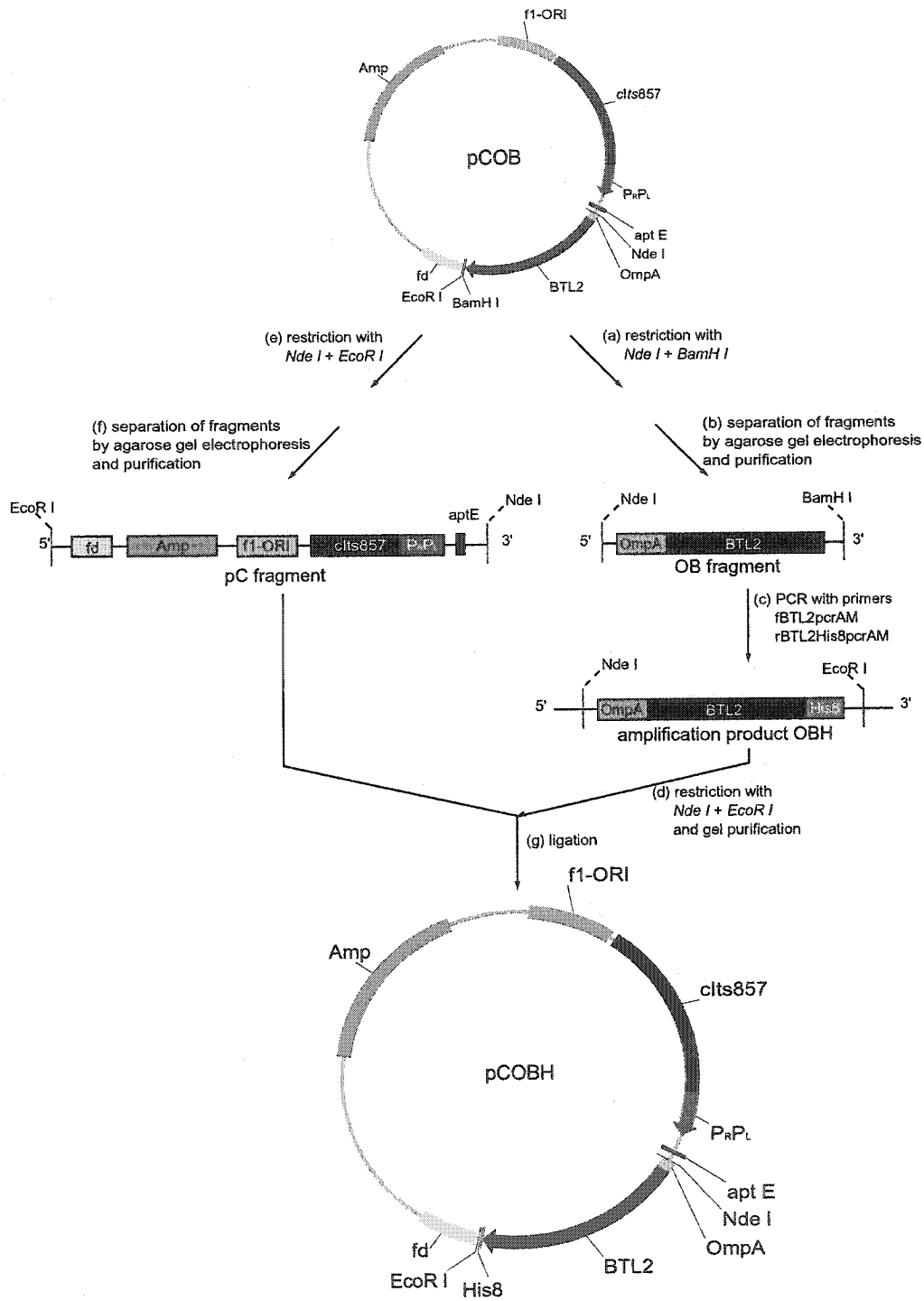

Scheme 2 – BTL2 his-tagging strategy. (a) The pCOB plasmid was digested with *BamH I and NdeI*; (b) the OB fragment was gel-purified; (c) the OB fragment was amplified with His_8-containing primer; (d) the amplification product was digested with *Nde I and EcoR I* and the resulting OBH fragment was purified by gel electrophoresis; (e) pCOB was also digested with *Nde I* and *EcoR I*; (f) the resulting pC fragment was purified and (g) the resulting pC and OBH fragments were ligated to obtain pCOBH.

DNA sequencing verified the introduction of the His_8-tag. Since a high fidelity polymerase enzyme had not been used to perform the amplification described above, there was some minor concern about the genetic integrity of the BTL2 gene. The sequencing confirmed the presence of 8 CAT codons, coding for 8 His residues, at the 3' terminus of the BTL2 gene, before the termination sequence TGA. There were four discrepancies between the His-tagged BTL2 gene (BTL2H) sequence and the sequence present in GenBank®[iii,45] (Accession Number X95309). The original BTL2 gene, a gift of Prof. Rolf Schmid (Institut für Technische Biochemie, University of Stuttgart, Germany) was verified. Both BTL2 and BTL2H had the same DNA sequence, indicating a mistake in the GenBank® submission.

The new His-tagged BTL2 protein was expressed and purified by affinity chromatography (Figure 4). The purified BTL2H retained its full activity towards PNPA (73.6 Umol/min*mg protein compared to 73.7 Umol/min*mg of the non tagged BTL2).

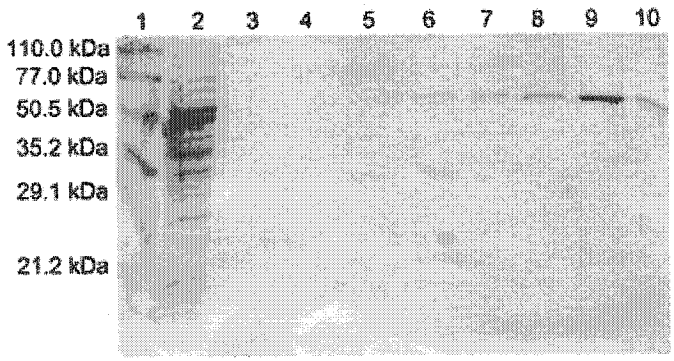

Figure 4 -SDS-PAGE of the fractions of the purification of BTL2H by affinity chromatography. Lane 1: molecular weight marker; lane 2: BTL2H after lysis (not purified); lane 3 to 10: fractions collected during the purification of BTL2H. Notice the clean samples of the protein in lanes 6 to 10.

[iii] GenBank® is the USA National Institutes of Health (NIH) genetic sequence database, an annotated collection of all publicly available DNA sequences. It is part of the International Nucleotide Sequence Database Collaboration that includes the DNA DataBank of Japan (DDBJ), the European Molecular Biology Laboratory (EMBL), and GenBank at the National Center for Biotechnonogy Information (NCBI) in the USA

The quest for the structure of BTL2

When this research was started there were no available X-ray or NMR structures for BTL2, nor there are now. When no X-ray or NMR structures are available, homology modelling represents an alternative to estimate a protein structure. Homology modelling is based on the fact that evolutionarily related proteins with similar sequences have similar structures.[46] The first attempts to obtain a homology-modelled structure for BTL2 consisted in submitting the enzyme sequence to SWISS-MODEL.[37] The attempt failed because of the poor homology of BTL2 with any protein of known structure present at that time (year 2000) in the database (homology < 25%).

Another approach was undertaken. A BLAST search[47] provided information on similar proteins. Among the lipases with the highest similarity (75-95%) there were *Bacillus stearothermophilus* lipase, *Staphilococcus aureus* and *hyicus* lipase. At that time none of them had a known 3D structure. PCL has low homology (16% identity) with BTL2 and its structure has been solved.[48,49] A suitable alignment was thus manually performed between BTL2 and PCL (Scheme 3). This alignment is consistent with the BTL2 primary amino acid sequence analysis by Schmid and co-workers[3]: S113, D317 and H358 form the catalytic triad. The consensus sequence Sm-X-Nu-X-Sm typical of lipases was found in BTL2, which is one example where Sm = A (A-H-S-Q-G). This sequence was aligned with the corresponding G-H-S-Q-G sequence of PCL. Thus the oxyanion hole residue Gln88 of PCL corresponds to BTL2 residue Gln114. Analogously, the consensus sequence relative to catalytic aspartate (G-N-D-G-I-V) was aligned with the corresponding Q-N-D-G-V-V of PCL and the consensus sequence relative to catalytic histidine (D-H-L-E) with the corresponding one in PCL (N-H-L-D). Significant homology was also found between PCL amino acid sequence relative to the oxyanion hole, P-I-I-L-V-H-G-L-T-G, and BTL2 sequence P-I-V-L-L-H-G-F-T-G. The oxyanion hole residue L17 of PCL corresponds to F16 of BTL2. Other areas showing some similarity, corresponding to strand β6 and helix α4 of PCL (residues 151 to 181 of BTL2) and to helices α5, α6, α7 and strand β3 of PCL (residues 210 to 299 of BTL2) were aligned as well to yield the result shown in Scheme 3. Lipases also possess calcium ion binding sites.[50] Using the alignment between *Pseudomonas glumae* lipase (PGL),

Staphylococcus hyicus lipase (SHL) and BTL2,[51] a possible calcium-binding site was identified between D365 and E360.

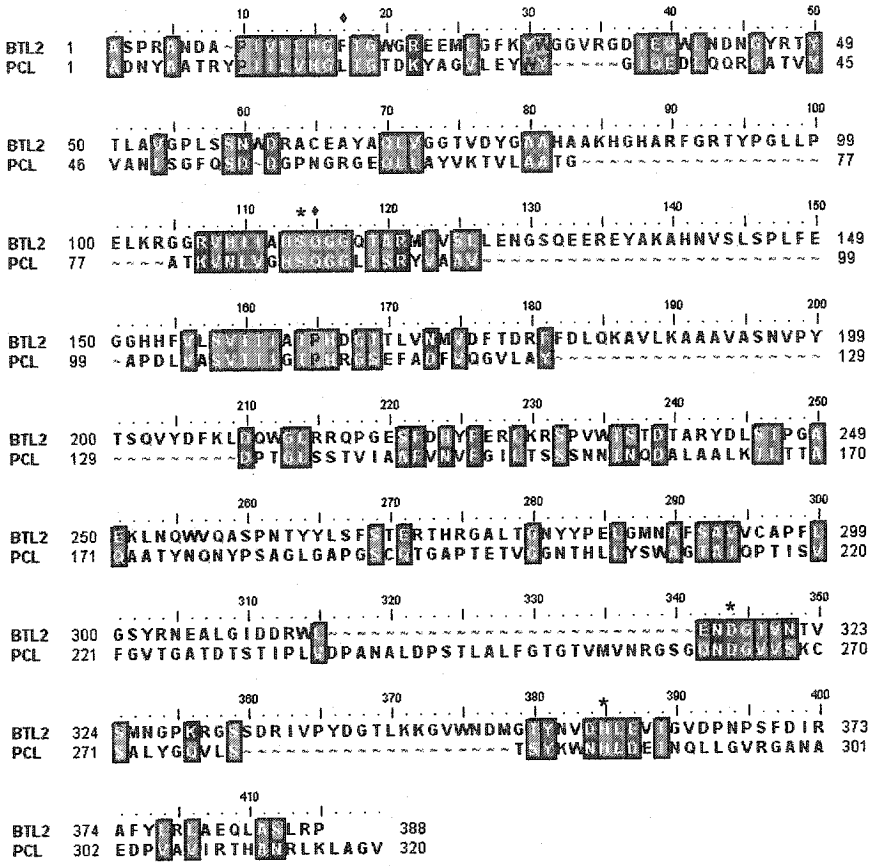

Scheme 3 - BTL2-PCL alignment. The coloured boxes show either identities or similarities between residues in the two sequences. *indicates BTL2 catalytic pocket residues S113, D317 and H358; ♦ indicates BTL2 oxyanion hole residues F16 and Q114.

A first homology model of the structure of BTL2 was obtained by submitting the alignment to Swiss Model – Optimised Mode.[36] The model contained several gaps matching the ones present in the alignment and due to the lower number of amino acids present in the template enzyme compared to BTL2 (320 versus 388). Despite the gaps in the structure and an imperfect position of one of the catalytic triad residues (Figure 5), the model was considered a good guess of what BTL2 could look like, especially in the area in and around the catalytic pocket.

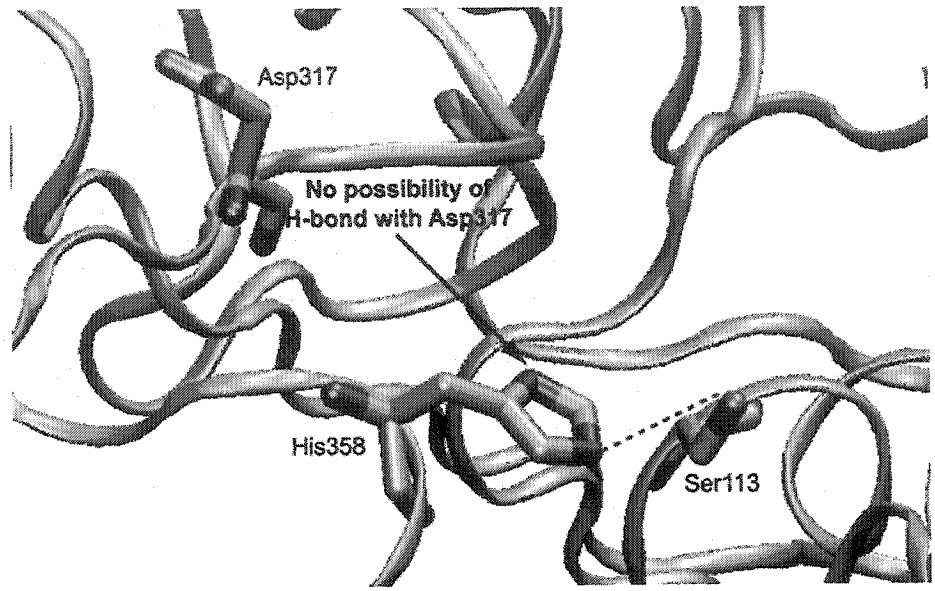

Figure 5 – BTL2 active site from the homology-modelled structure. The lack of H-bond between His358 (H358) and Asp317 (D317) is due to the wrong position of Asp317 (D317) side-chain in the model.

About one year after the first homology model of the structure of BTL2, a homology model of a lipase from *Bacillus stearothermophilus* P1 (Tlip) was published.[52] BTL2 and Tlip have 95% identity. Both possess a 29 amino acid long signal sequence, a mature lipase of 388 amino acids and a cleavage site of the signal sequence between A29 and A30. The catalytic triad residues S113, D317 and H358, identified by site-directed mutagenesis experiments by Sinchaikul *et al.*,[52] confirm Schmid *et al.*[3] assignments based on primary amino acid sequence analysis. Because of the high identity of BTL2 and Tlip, the fact that other researchers had used PCL as model structure for Tlip, with an alignment similar to the one used for BTL2, suggests that the BTL2 modelled structure was a good "guess".

In 2002 Tyndall *et al.*[53] published the crystal structure of Tlip (there called BSP) at 2.2 Å resolution (PDB ID: 1JI3). It was thus possible to submit the BTL2 sequence to SWISS-MODEL[37] and within a few minutes the new homology model of BTL2, now certainly very close to its real 3D structure (Figure 6), was received by e-mail.

Figure 6 – BTL2 closed[iv] structure based on homology model with BSP (cartoon representation). The active site residues are in space-fill: S113 in orange, D317 in green and H358 in ice-blue.

BTL2 catalyses the hydrolysis of solketal-*n*-octanoate and butyrate with modest E (E = 4.4 and 7.9).[8] In Chapter 3 the crystal structures of PCL-inhibitor complexes containing solketal as alcohol moiety are described and some residues that contribute to PCL enantioselectivity were located. To improve the enantioselectivity of BTL2 towards solketal by genetic engineering, the final BTL2 structure (closed form, the lid covers the active site) was overlapped with the structure of the open form of one of the PCL-inhibitor complexes containing (*S*)-solketal as alcohol moiety. The overlap showed that the catalytic pockets are very similar and likely a primary alcohol substrate would bind to BTL2 in a similar way than to PCL (Figure 7). The residues to mutate by saturation mutagenesis were chosen based on this overlap.

[iv] BTL2, as many lipases, has a lid that covers the active site.

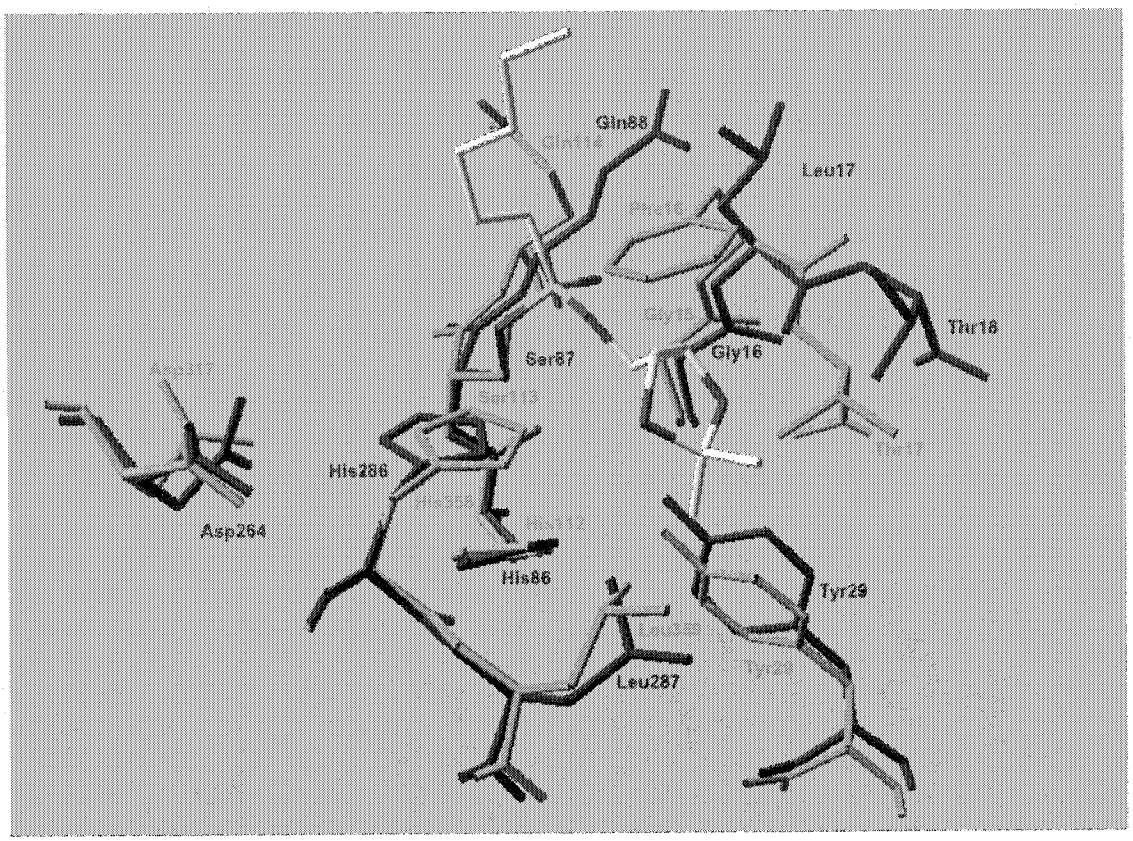

Figure 7 – Overlap of the BTL2 structure (closed form, green) with the PCL-inhibitor complex structure (open form, blue). The alcohol moiety of the inhibitor (CPK) is (*S*)-solketal.

Structure assisted site-saturation mutagenesis

Mutant libraries of positions G15, Y29, H112 and the double position F16-T17, corresponding to positions G16, Y29, H86 and L17-T18 of PCL, were created.

To have a 99% probability of sampling all possible codons (primers containing the degenerate NNN codon (single mutants) or NNK codon (double mutants) were used) for the single mutants 288 colonies (three 96 wells plates) were picked from the agar plates. For the double mutants (position F16 and T17), where each of the 32 possible codons relative to position 16 could be followed by one of 32 possible codons relative to position 17 (total of 1024 codons) a total of 4700 colonies should have been picked,[v,54] but a library containing only 672 colonies was prepared instead.

---

[v] The number of colonies N that have to be screened to have a probability P of taking all the possible n codons into consideration: $N\ln(1-1/n) = \ln(1-P)$.

Not all the colonies showed the same percentage of mutants active towards tributyrin, thus lipase activity (Figure 8).[38] The colonies showing lipase activity towards tributyrin were not all active towards PNPA (Figure 8). The mutants active towards PNPA were all screened, using the Quick E method,[41] towards solketal-*n*-octanoate, **1**. Other substrates used were 3-propyloxiranemethyl butanoate, **2** (wild-type Quick E = 2.2 ± 0.1 (*R*)), 3-bromo-2-methyl-1-propyl butanoate, **3** (wild-type Quick E = 1.9 ± 0.5 (*R*)), 2,3-epoxypropyl 4-nitrobenzoate, **4** (wild-type estimated E = 5.2 (*R*)[8]) and glycidyl butanoate, **5** (wild-type Quick E = 3.9 ± 0.2 (*R*)[9])(Figure 9).

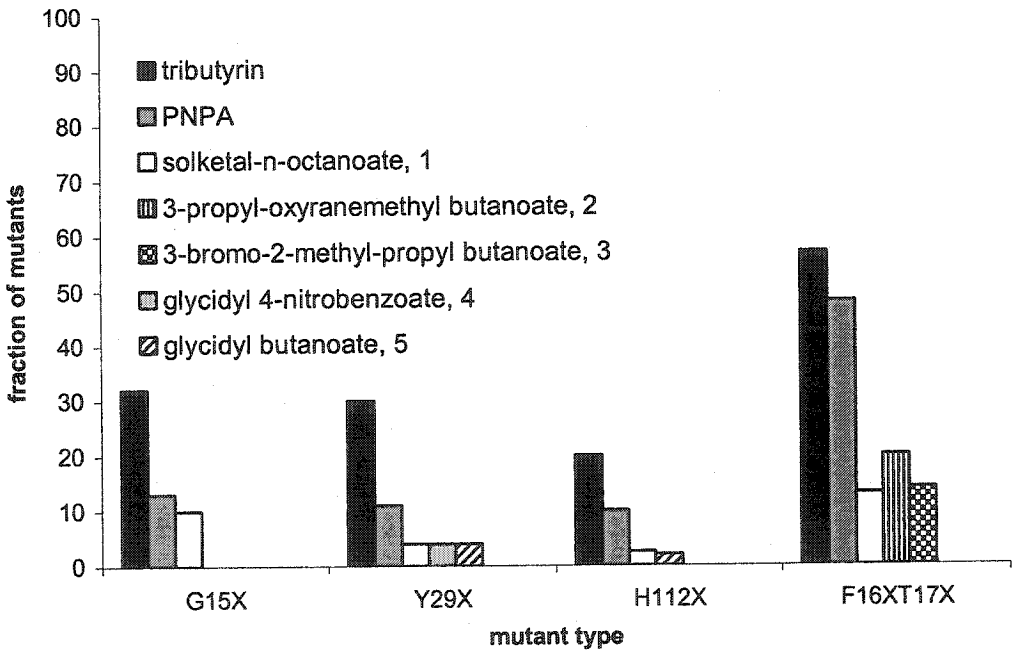

Figure 8 – Activity of the mutants present in the libraries towards tributyrin, PNPA and substrates **1** to **5**. All the mutants were checked for activity towards tributyrin. The ones that were active towards tributyrin were tested against PNPA. The mutants that showed activity towards PNPA were tested with substrates **1** to **5**. G15X were tested only with **1**; Y29X and H112X were tested with **1**, **4** and **5**; F16XG17X were tested with **1**, **2** and **3**.

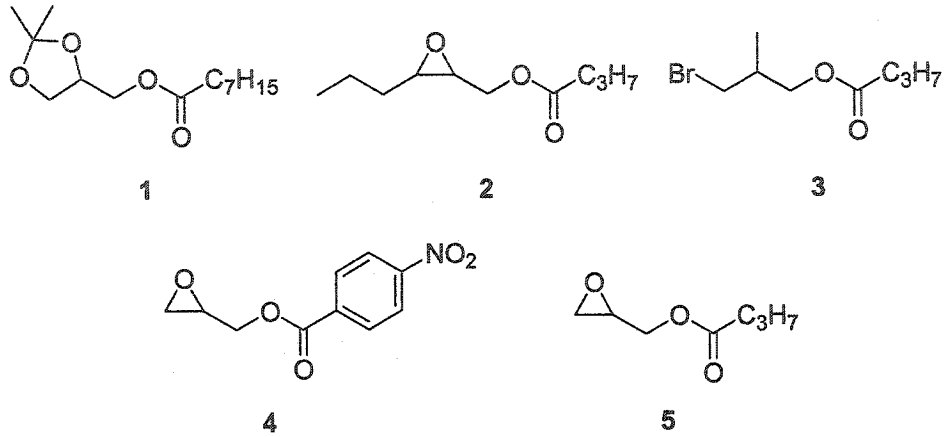

1 2 3

4 5

Figure 9 –Substrates used in the screening of the mutant libraries.

G15X mutants

Of the 288 enzymes present in the library of mutants at position 15, 32% hydrolysed tributyrin and only 13% (38 mutants) were active towards PNPA. Only 29 of them hydrolysed **1** (Figure 8). The screen of those 29 mutants towards substrate **1** did not identify any improved enzyme. The most enantioselective enzyme (Quick E = 3.1) was sequenced and found to be wild-type, Table 6.

Table 6 – Best screening results towards substrates **1-6**.

Mutation position	Library position	Enzyme[a]	Substrate	Quick E	End-point E
G15	195	wild-type	**1**	3.1 ± 0.1 (*R*)	4.5 (*R*)[8]
Y29	90	S29	**1**	5.6 ± 0.3 (*R*)	1.9 (*R*)
H112	12	wild-type	**1**	4.3 ± 0.5(*R*)	4.5 (*R*)[8]
H112	211	n.a.[b]	**5**	3.4 ± 0.5 (*R*)[9]	n.a.
F16T17	16	n.a.	**1**	3.6 ± 0.1 (*R*)	n.a.
F16T17	9	G16V17	**1**	3.4 ± 0.8 (*R*)	n.a.
F16T17	185	n.a.	**2**	2.5 ± 0.3 (*R*)	n.a.
F16T17	345	n.a.	**3**	2.3 ± 0.8 (*R*)	n.a.

[a] before screening the mutants libraries a few mutants were randomly sequenced to verify the success of the mutagenesis experiments; after screening sequencing and end-point E determinations were done only for mutants that showed Quick E at least 1 unit higher than the wild-type; [b] n.a. = not available.

Considering that only 29 enzymes, 10% of the total, hydrolysed substrate **1**, it is not surprising that the screen did not reveal any improved mutant. The library of 288 mutants should contain wild type BTL2 and 19 different mutants. Thus 5% of the enzymes in the library are wild-type. Finding only 10% of the mutants catalytically active towards **1** suggests that only two enzymes of the library can hydrolyse **1**. One is wild-type and the other is probably a mutant that was not identified because of its lower Quick E.

Y29X mutants

The library of mutants for position 29 contained only 30% of mutants active towards tributyrin and 11% (32 mutants) enzymes active towards PNPA. Using the reasoning above, half of them were wild-type and the other half one mutant. Of these 32 mutants, only 12 showed activity towards substrate **1** (Figure 8), although very low. The best mutant from the quick E screening (E = 5.5) was further characterised as a Ser variant. End-point E determination yielded E = 1.9. This library was also screened towards substrates **4** and **5**, but no improved enzymes were found.[9]

H112X mutants

Only 20% of the 288 mutants at position 112 present in the library showed activity towards tributyrin and 10% towards PNPA, thus again wild-type and one mutant. Of those 29 enzymes, only 7 hydrolysed substrate **1**, probably all wild-type. As for substrates **4** and **5**, 5 mutants hydrolysed substrate **5**, while none was active towards **4**.[9] None of those enzymes yielded any improvement compared to the wild type enzyme and they were not further characterised (Table 6). The change of this conserved residue among lipases, located next to the active site Ser113, may explain the very low percentage of active mutants.

F16XT17X mutants

Of the 672 mutants present in the library 57% hydrolysed tributyrin while 48% were active towards PNPA. 13% showed activity towards substrate **1**, 21% were active towards **2** and 15% towards **3**. Although the evaluation of 4700 mutants is theoretically required to maximise the probability of testing all possible mutants (footnote v, page 178) only 672 were considered. None of them showed improved E towards substrates **1**, **2** and **3** (Table 6) and it was decided not to pursue this route further.

Discussion

In Chapter 2, 3 and relative Appendices it has been shown that the molecular basis of PCL enantioselectivity rests on a few subtle interactions between enzyme and substrate. Here an attempt to increase the enantioselectivity of BTL2, a lipase structurally related to PCL, by structure-guided saturation mutagenesis, is reported. Saturation mutagenesis was chosen to avoid the tremendous amount of enzymes that need to be screened in random mutagenesis experiments (footnote i).

The very low fraction of active mutants present in the libraries of position 15, 29 and 112 suggests that only one amino acid substitution yields a mutant capable of catalysing the hydrolysis of solketal-*n*-octanoate, **1**. The mutant libraries should contain wild-type and 19 different mutants (19 different amino acid substitutions at the chosen position) for a total of twenty different enzymes. Each enzyme represents 5% of the mutants in the library. Finding only 10% or less of the mutants catalytically active towards **1** suggests that probably only two different enzymes can hydrolyse the substrate. One is wild-type and the other one is a mutant (Ser for the Y29 library; unidentified in the G15 and H112 libraries). Since only one mutant (or less) was catalytically active in each of these libraries, they yielded a total of only three mutants. This low fraction of active mutants may be due to the location of the mutations, very close to the active site, or to the thermostable nature of the lipase. All but one mutation is enough to alter the finely balanced structure for catalysis.

Given the very low fraction of active mutants, it is not surprising that a more enantioselective one was not found. In similar work using this approach with an esterase from *Pseudomonas fluorescens*, ~13% of the active mutants showed increased enantioselectivity.[55] To find a more enantioselective mutant among the three active ones would correspond to 33%, a much higher percentage.

The fraction of mutants in the F16T17 double mutants library that catalysed the hydrolysis of solketal-*n*-octanoate was higher, ~13%. The double mutation could yield 399 possible mutants (20 x 20 amino acids less one wild-type), so approximately 50 mutants (399 x 0.13) were active in the theoretical 4700 enzymes that should have been screened. Since only ~ 700 colonies were evaluated, less than 15% of what needed to be

screened, ~ 15% of the active mutants were found, that is, 8. This number is just on the edge of that where one would expect to find a more enantioselective mutant.

The low fraction of catalytically active mutants may be due to the position of the mutation sites in BTL2 three-dimensional structure. G15 is a conserved residue among lipases situated just before one of the oxyanion hole residues, here F16. Mutating it may disrupt the oxyanion hole structural integrity, which would result in loss of hydrolytic activity. The very low activity of the mutants at position 112 is probably due to the vicinity of this residue to catalytic S113. H112 is another conserved residue among lipases and is situated before the sharp turn where the catalytic S113 resides. Its mutation may inactivate the protein by changing the conformation of this sharp turn. This could modify the three dimensional arrangement of the catalytic triad, diminishing if not destroying its catalytic abilities.

In PCL L17, corresponding to F16 in BTL2, appears to have major interactions with solketal. It is the carbonyl of L17 that bumps into solketal in PCL, hence part of the protein main chain. Replacing the corresponding residue in BTL2 with another amino acid may not change the position of the carbonyl and may not affect the enzyme E. Although F16 and T17 in BTL2 do not overlap perfectly with PCL L17 and T18 (Figure 7), this is an artefact. A closed form model of BTL2 is overlapped with an open form crystal structure of a PCL-inhibitor complex. Upon lid opening the position of these two residues changes to yield the conformation of the oxyanion hole necessary for catalysis, as it is shown by the comparison between the closed form of PGL[vi] and the open form of PCL in Figure 10.

[vi] There is no available structure of the closed form of PCL. Scientists consider it to be analogous to the closed form of PGL due to the high identity between the two enzymes (83%).

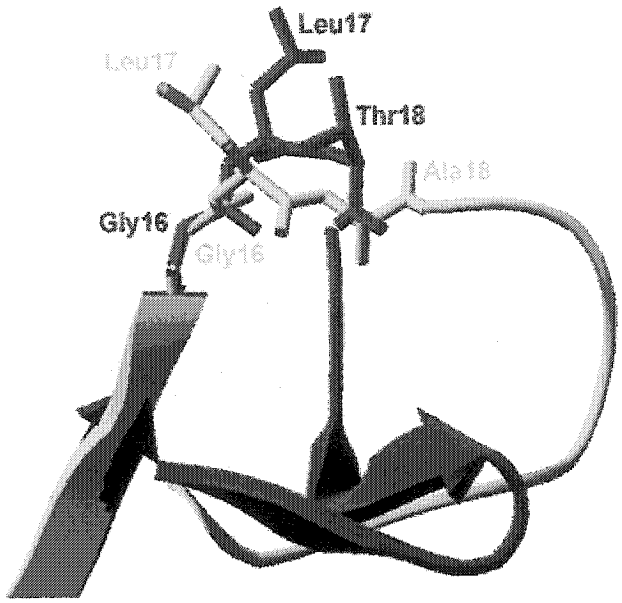

Figure 10 – Comparison between the position of residues 17-18 in the closed form of PGL (PDB ID[56]: 1QGE) (yellow) and in the open form of PCL (PDB ID: 3LIP[48]) (blue). The opening of the lid causes a rearrangement of the loop and places oxyanion hole residue Leu17 (L17) in the proper conformation for catalysis.

Despite a good homology model and a good strategy to improve the enantioselectivity of an interesting lipase such as BTL2, by mutating residues that were considered important for enantiorecognition of primary alcohols several inactive mutants were generated. The ones that retained a certain activity towards substrate 1 were often found to be wild type enzyme (Table 6). Residues too close to the catalytic machinery of the enzyme may have been chosen, causing a severe loss in activity when amino acids other than the original are introduced. Recently Pleiss *et al.*[57] genetically engineered PCL by introducing mutations at position L287 and Y29 *via* site-directed mutagenesis. The changes in enantioselectivity were small (3 to 6) and could be difficult to identify with our screening method.[vii] Also, lack of automated systems makes it extremely lengthy to express, screen and analyse the data relative to large numbers of enzymes, like it should have been done for the double mutants. Structure-guided saturation mutagenesis remains a valuable alternative to both directed evolution and site-directed mutagenesis. We cannot

[vii] Mr Geoffrey P. Horsman[55] used Quick E screening for identifying improved mutants of *Pseudomonas fluorescens* esterase (PFE) towards 2-bromo-3-methyl propionate. He reported Quick E values of 86, 95 and 123 for the same mutant W29L.

exclude that there could be an improved mutant within the 4300 enzymes we did not produce nor screen.

Acknowledgments

I wish to thank Prof. Karl Hult for his supervision at the Royal Institute of Technology (KTH), Stockholm, Sweden, Dr. Johanna C. Rotticci-Mulder for her help in the His-tagging of the BTL2 gene and Miss Agneta Eriksson for screening the mutants at position 29 and 112 towards substrates **4** and **5**.

References

[1]Hough, D.W.; Danson M.J.; *Curr. Opin. Chem. Biol.*, **1999**, *3*, 39-46.

[2]Schmidt-Dannert, C.; Rúa, M.L.; Atomi, H., Schmid, R.D. *Biochim. Biophys. Acta* **1996**, *1301*, 105-114.

[3]Schmidt-Dannert, C.; Rúa, M. L.; Schmid, R. D. *Methods Enzymol.* **1997**, *284*, 194-220.

[4]Schmidt-Dannert, C.; Rúa, M.L.; Wahl, S.; Schmid, R.D. *Biochemical Soc. Trans.* **1997**, 178-182

[5]Rúa, M. L.; Schmidt-Dannert, C.; Wahl, S.; Sprauer, A.; Schmid, R. D. *J. Biotechnol.* **1997**, *56*, 89-102.

[6]Belev, T. N.; Singh, M.; McCarthy, J. E. G. *Plasmid*, **1991**, *26*, 147-150.

[7]Rúa, M. L.; Atomi, H.; Schmidt-Dannert, C.; Schmid, R D. *Appl. Microbiol. Biotechnol.* **1998**, *49*, 405-410.

[8]Liu, A. M. F.; Somers, N. A.; Kazlauskas, R. J.; Brush, T. S.; Zocher, C.; Enzelberger, M. M.; Bornscheuer, U. T.; Horsman, G. P.; Mezzetti, A.; Schmidt-Dannert, C.; Schmid, R. D. *Tetrahedron: Asymmetry* **2001**, *12*, 545–556.

[9]Eriksson, A. *Diploma research project*, Royal Institute of Technology (KTH), Stockholm, Sweden, **2002**.

[10]Bornscheuer, U. T.; Kazlauskas, R. J. in *Hydrolases in Organic Synthesis*, Wiley-VCH, **1999**.

[11] Fischer, H.; Baer, E. *J. Am. Chem. Soc.* **1945**, *67*, 944-946.

[12]Weinstock, L. M.; Mulvey, D. M.; Tull, R. *J. Org. Chem.***1976**, *41*, 3121-3124.

[13]Kitahara T., Mori K., Matsui M. *Tetrahedron Lett.* **1979**, *32*, 3021-3024.

[14] Baer, E.; Fischer, H. O. L. *J. Biol. Chem.* **1939**, *128*, 463-473.

[15]Jung, M. E.; Shaw, T. J. *J. Am. Chem. Soc.* **1980**, *102*, 6304-6311.

[16]Baer, E.; Fischer, H. O. L. *J. Am. Chem. Soc.* **1939**, *61*, 761-765.

[17]Baer, E.; Fischer, H. O. L. *J. Am. Chem. Soc.* **1945**, *67*, 944-946.

[18]Lok, C. M.; Ward, J. P.; Van Dorp, D. A. *Chem. Phys. Lipids* **1976**, *16*, 115-122.

[19]Jurczak, J.; Pikul, S.; Bauer, T. *Tetrahedron*, **1986**, *42*, 447-488.

[20]Geerlof, A.; van Tol, B. A.; Jongejan, J. A.; Duine, J. A. *Biosci. Biotech. Biochem.* **1994**, *58*, 1028-1036.

[21]Vänttinen E., Kanerva L. T. *J. Chem. Soc., Perkin. Trans. 1* **1994**, 3459-3463.

[22]Sakai T., Kishimoto T., Tanaka Y., Ema T., Utaka M. *Tetrahedron Lett.* **1998**, 39, 7881-7884.

[23]Miyazawa T., Kurita S., Sakamoto H., Otomatsu T., Hirose K., Yamada T. *Biotech. Lett.* **1999**, 21, 447-450.

[24]Wang Y. F., Lalonde J. J., Momongan M., Bergbreiter D. E., Wong, C. H. *J. Am. Chem. Soc.* **1988**, *110*, 7200-7205.

[25] Phung A.N., Braun J., Le Goffic F. *Synth. Comm.* **1995**, 25, 1783-1788.

[26] Bosetti A., Bianchi D., Cesti P., Golini P. *Biocatalysis* **1994**, 9, 71-77.

[27] Partali V., Melbye A. G., Alvik T., Anthonsen T. *Tetrahedron: Asymmetry* **1992**, *3*, 65-72.

[28]Chen, C.-S.; Fujimoto, Y.; Girdaukas, G.; Sih, C. J. *J. Am. Chem. Soc.* **1982**, *104*, 7294–7299.

[29]Moore, J. C.; Jin, H.-M.; Kuchner, O.; Arnold, F. H. *J. Mol. Biol.* **1997**, *272*, 336-347.

[30]Reetz, M. T.; Wilensek, S.; Zha, D.; Jaeger, K.-E. *Angew. Chem. Int. Ed.* **2001**, *40*, 3589-3591.

[31]Cherry, J. R.; Lamsa, M. H.; Schneider, P.; Vind, J.; Svendson, A.; Jones, A.; Pedersen, A. H. *Nat. Biotechnol.* **1999**, *17*, 379-384.

[32]Guex, N.; Diemand, A.; Peitsch, M. C. *Trends Biochem. Sci.* **1999**, *24*, 364-367.

[33] Chapter 3 of this thesis.

[34] Humphrey, W.; Dalke, A.; Schulten, K. *J. Mol. Graphics* **1996**, *14*, 33-38.

[35]Guex N., Peitsch M.C. *Electrophoresis* **1997**, *18*, 2714-2723.

[36] http://swissmodel.expasy.org/

[37]http://www.expasy.ch/swissmod/SWISS-MODEL.html

[38]Liu A. M. F., *Master of science thesis*, McGill University, **2000**.

[39]Ausubel, F. M.; Brent, R.; Kingston, R. E.; Moore, D. D.; Seidman, J. G.; Smith, J. A.; Struhl, K. *Short Protocols in Molecular Biology*, 3rd edition, J. Wiley & Sons Inc. **1997**, 16-36.

[40]Papworth C., Bauer J. C., Braman J. *Strategies* **1996**, *9*, 3-4.

[41] Janes L.E., Kazlauskas R. J., *J. Org. Chem.* **1997**, *62*, 4560-4561.

[42] Nossal N. G., Heppel L. E. *J. Biol. Chem.* **1966**, *241*, 3055-3062.

[43]Bollag, D. M.; Edelstein, S. J. In *Protein Methods*, Wiley-Liss: New York, 1991; pp 27-43.

[44] Porath J., Carlsson J., Olsson I., Belfrage G. *Nature* **1975**, *258*, 598-599.

[45]Benson D. A., Karsch-Mizrachi I., Lipman D. J., Ostell J., Rapp B. A., Wheeler D. L. *Nucl. Acids Res.* **2002**, *30*, 17-20.

[46]Sander, C.; Schneider, R. *Proteins* **1991**, *9*, 56-68.

[47] Altschul, S. F.; Gish, W.; Miller, W.; Myers, E. W.; Lipman, D. J. *J. Mol. Biol.* **1990**, *215*, 403-410.

[48]Schrag, J.D.; Li, Y.; Cygler, M.; Lang, D.; Burgdorf, T.; Hecht, H.-J.; Schmid, R.; Schomburg, D.; Rydel, T.J.; Oliver, J.D.; Strickland, L.C.; Dunaway, C.M.; Larson, S.B.; Day, J.; McPherson, A. *Structure* **1997**, *5*, 187-202.

[49]Kim, K.K.; Song, H.K.; Shin, D.H.; Hwang, K.Y.; Suh, S.W. *Structure* **1997**, *5*, 173-185.

[50]Noble M.E.M., Cleasby A., Johnson L.N., Egmond M.R., Frenken L.G.J., *FEBS lett.* **1993**, *331*, 123.

[51]Simons J.W.F.A., van Kampen M.D., Ubarretxena-Belandia I., Cox R.C., Alves dos Santos C.M., Egmond M.R., Verheij H.M., *Biochemistry* **1999**, *38*, 2-10.

[52]Sinchaikul S., Sookkheo B., Phutrakul S., Wu Y.-T., Pan F.-M., Chen S.-T. *Biochem. Biophys. Res. Comm.* **2001,** 283, 868-875.

[53] Tyndall J. D. A., Sinchaikul S., Fothergill-Gilmore L. A., Taylor P., D. Walkinshaw M. D. *J. Mol. Biol.* **2002,** *323*, 859-569.

[54]Warren M. S., Benkovic S. J. *Protein Eng.* **1997,** *10*, 63-68.

[55]Horsman, G. P. *Master of science thesis*, McGill University, **2001.**

[56]http://www.pdb.org

[57]Gentner, C.; Schmid, R. D.; Pleiss, J. *Colloids and Surfaces B* **2002,** *26*, 57-66.

Summary, conclusions and future work

A few lipases catalyse the hydrolysis of esters of chiral primary alcohols with high enantioselectivity. The molecular basis of this enantioselectivity was controversial. It was unclear why the enantiopreference for primary alcohols is opposite to the one for secondary alcohols, why it is not possible to rationalise the enantiopreference towards primary alcohols with oxygen at the stereocentre with simple empirical rules[1] and why the enantioselectivity is usually lower for primary than for secondary alcohols.

To explain the molecular basis of lipases enantioselectivity towards primary alcohols we synthesised six phosphonate esters. They contained as alcohol moieties pure enantiomers of chiral primary alcohols. One pair of enantiomers did not have oxygen at the stereocentre while the other two pairs had oxygen at the stereocentre, only one behaving according to the empirical rule.[1] Phosphonates esters are lipase inhibitors and mimic the transition state in the lipase-catalysed hydrolysis of esters. We inhibited *Pseudomonas cepacia* lipase (PCL) with the synthesised phosphonates and solved the X-ray crystal structures of the complexes. The differences between the alcohol moieties in the complexes relative to each pair of enantiomers were subtle. To understand PCL enantioselectivity we then employed both kinetic and combined QM/MM modelling experiments based on the crystal structures.

We showed, by comparison of our crystal structures with the published crystal structure of PCL complexed with a chiral secondary alcohol,[2] that the opposite enantiopreference for primary and secondary alcohols depends on the different binding of such substrates within the catalytic pocket of the enzyme. Secondary alcohols bind the large group at the stereocentre in the large hydrophobic pocket HA, while our crystal structures reveal that the large group at the stereocentre of primary alcohols lays in a solvent exposed crevice and it is the acyl chain that binds in the HA pocket.

---

[1]Weissfloch, A. N. E.; Kazlauskas, R. J. *J. Org. Chem.*, **1995**, *60*, 6959-6969.

[2]Luić, M.; Tomić, S.; Leščić, I.; Ljubović, E.; Šepac, D.; Šunjić, V.; Vitale, L.; Saenger, W.; Kojić-Prodić, B. *Eur. J. Biochem.* **2001**, *268*, 3964-3973.

The subtlety of the interactions enzyme-substrate observed in our crystal structures and in the modelling demonstrates why the enantioselectivity of lipases towards primary alcohols is usually lower than for secondary alcohols.

For 2-methyl-3-phenyl-1-propanol, modelling of our crystal structures shows a better hydrogen bond between catalytic His286 Nε2 and the alcohol oxygen of the fast enantiomer. This is confirmed by the 100-times higher k_{cat} determined for this enantiomer. We thus propose that PCL enantioselectivity towards this alcohol arises from the better hydrogen bond of the fast enantiomer.

In the case of primary alcohols with oxygen at the stereocentre, the crystal structures reveal that the enantiomers can either undergo an "umbrella-like" inversion at the stereocentre or show "H-alignment". This may explain why the empirical rule[1] for primary alcohols is not reliable when oxygen is present at the stereocentre. Also, PCL enantioselectivity towards these substrates seems to depend on the interaction between the oxygen at the stereocentre and residues Leu17 and Thr18.

We then exploited PCL interfacial activation and the use of a solvent that stabilises the active open form of the enzyme, 30 vol% *n*-propanol in phosphate buffer (similar to the crystallisation solvent for the PCL-inhibitor complexes), to increase its enantioselectivity towards the acetates of 2-methyl-3-phenyl-1-propanol (E = 38) and 2-phenoxy-1-propanol (E = 52) compared to previously published values (16 and 17 respectively). We improved further this enantioselectivity by changing the acyl chain from acetyl to heptanoyl (E ≥190 and E = 70 respectively).

Last, we used protein engineering to increase the enantioselectivity of a lipase structurally related to PCL, *Bacillus thermocaltenuatus* lipase 2 (BTL2) towards solketal-*n*-octanoate. We built a homology-modelled structure of BTL2 and we chose the residues to mutate by comparison with our crystal structures of PCL-transition state analogues containing solketal as alcohol moiety. We did not find any improved mutant. On the contrary, we generated a large number of inactive enzymes. The residues that seem to be involved in the lipase enantiorecognition process and that we mutated were probably too close to the catalytic triad of the enzyme. Due to the lack of automated screening facilities we did not perform a complete screen of the double mutants (F16T17) library, which

showed the highest percentage of active enzymes. We cannot exclude the possibility that more enantioselective lipases could be present among the ones not expressed nor screened.

The complex architecture of enzymes renders it difficult to unravel their enantiorecognition mechanism. Although many prefer to tackle the problem from one point of view only, i.e. performing either molecular modelling or solving crystal structures, we used three different approaches: crystallography, modelling and kinetic studies. Basing our modelling on the crystal structures and with the support of the determined kinetic parameters, we proposed an explanation for the origins of PCL enantioselectivity towards primary alcohols. We also used some information from the crystallography to increase PCL enantioselectivity towards two of the three chiral primary alcohols used, 2-methyl-3-benzyl-1-propanol (from 16 to ≥ 190) and 2-phenoxy-1-propanol (from 17 to 70). We could not, however, generate more enantioselective enzymes by site-saturation mutagenesis of the residues that appear to be involved in the enantiorecognition mechanism.

While I am concluding my thesis, we are implementing the modelling approach adopted to explain lipases enantiorecognition of chiral primary alcohols. We still have to consider the effect of different acyl chain lengths and of the solvent, which we have shown in Chapter 4 to be relevant. Last, producing and screening the remaining 4000 BTL2 double mutants may permit finding an enzyme more enantioselective towards solketal.

Contributions to knowledge

1. For the first time we solved X-ray crystal structures of complexes PCL-transition state analogues for the lipase catalysed hydrolysis of esters of chiral primary alcohols. These transition state analogues contained as alcohol moieties pure enantiomers of chiral primary alcohols.

2. We showed with our X-ray crystal structures of complexes PCL-transition state analogues that the different enantiopreference of PCL for primary versus secondary alcohols arises from the different binding of primary and secondary alcohols in the catalytic pockets of the enzyme.

3. We proposed, combining structural, kinetic and modelling studies, that the molecular basis of PCL enantioselectivity towards primary alcohols without oxygen at the stereocentre rests on a better key hydrogen bond between catalytic histidine and alcohol oxygen.

4. We proposed that PCL enantioselectivity towards chiral primary alcohols with oxygen at the stereocentre depends on the interaction between this atom and PCL residues Leu17 and Thr18.

5. We demonstrated that the empirical rule for primary alcohols does not work when oxygen is present at the stereocentre due to the different binding of such alcohols within PCL catalytic pocket. 2-phenoxy-1-propanol enantiomers undergo an "umbrella-like" inversion at the stereocentre while solketal enantiomers show "H-alignment".

6. We increased PCL enantioselectivity towards esters of chiral primary alcohols by substrate engineering, changing the acyl chain from acetyl to heptanoyl, and by medium engineering.

7. We showed that it is difficult to increase the enantioselectivity of enzymes towards chiral primary alcohols by protein engineering. The residues involved in the enantiorecognition process are too close to the catalytic pocket of the enzyme and the enzyme-substrate interactions are too subtle.